UGR#259

DOE/ET/12138-1341(Vol.1)
(DE83008494)
Distribution Category UC-92a

FRACTURES IN ORIENTED DEVONIAN SHALE CORES FROM THE APPALACHIAN BASIN

BY

Mark A. Evans, Research Associate
Department of Geology & Geography
College of Arts & Sciences
Morgantown, West Virginia

January 1980

Prepared For

United States Department of Energy
Morgantown Energy Technology Center
Morgantown, West Virginia

Under Contract No. DE-AC21-76ET12138

TABLE OF CONTENTS

	page
LIST OF FIGURES	iii
LIST OF TABLES	iv
LIST OF PLATES	v
ACKNOWLEDGEMENTS	vi
ABSTRACT	1
INTRODUCTION	3
Purpose	3
Location	4
Regional Structure	4
Stratigraphy	8
Previous Investigations	8
METHODS OF ANALYSIS	11
Data Acquisition	11
Fractography	12
Fracture Types	23
Data Analysis	29
FRACTURE ANALYSIS	33
Reports on Fractures in Each Core	33
Regional Fracture Patterns	33
Core-induced Fractures	35
Natural Fractures	40
Slickensides and Slickenlines	43
Lincoln County, West Virginia, Cores	50
FRACTURE FREQUENCY	52
Core-induced Fractures	53
Natural Fractures	53
Slickensides	54
CONCLUSIONS	55
SUGGESTIONS FOR FUTURE WORK	58
REFERENCES	60

LIST OF FIGURES

figure page

16. Horizontal bedding plane slickenside mineralized with fibrous calcite, fibers are perpendicular to the fracture walls. From WV #6 (MERC #1) core 27

17. Inclined slickenside. From WV #4 (20402) core 28

18. Inclined slickensides in tendential view. From base of VA #1 (20338) core 28

19. Regional core-induced fracture patterns 37

20. Postulated maximum compressive stress trajectories..... 38

21. Regional natural fracture patterns 41

22. and 23. Regional slickenside patterns 44, 45

24. Regional slickenline patterns 46

25. Shear zones 48

LIST OF TABLES

table page

1. Core well data 6
2. Example of a fracture data sheet 13
3. Orientations of fracture orientation peaks of all fracture types for each core 34
4. Maximum compressive stress measurements in the Appalachian Plateau province 36

LIST OF PLATES

plate

1 and 2. Correlation of Middle and Upper Devonian rocks

3 and 4. Correlation of core-induced fracture frequencies

5 and 6. Correlation of natural fracture frequencies

7 and 8. Correlation of slickenside frequencies

ACKNOWLEDGEMENTS

The author would like to thank his committee members Dr. Robert C. Shumaker, Dr. Russell L. Wheeler, and Dr. Alan C. Donaldson for their guidance and assistance in the preparation of this thesis. He would also like to thank Dr. Byron Kulander for critically reviewing the manuscript, and John Wright for drafting the seemingly endless number of illustrations.

The author would like to extend his deep appreciation to his parents and his wife for their support and encouragement during the long hours spent taking classes and doing the research and writing associated with this degree.

ABSTRACT

Examination of thirteen oriented Devonian shale cores from the Appalachian Basin revealed considerable fracturing and shearing at depth. Fracture frequency and orientation measurements were made on the fractures in each core. Fractures and associated structures were differentiated (when possible) into core-induced fractures, unmineralized natural fractures, mineralized natural fractures, slickensided fractures, and slickenlines. Core-induced fractures exhibit a consistent northeast orientation both areally and with depth. This consistency indicates the presence of an anisotropy which is interpreted to be related to an east to northeast trending maximum compressive stress developed in eastern North America by the convective flow in the mantle associated with spreading along the Mid-Atlantic Ridge. Natural fracture, slickenside, and slickenline orientations are related to: 1) northwest directed tectonic compressive stresses associated with Alleghenian deformation, 2) stresses associated with local faulting, and 3) the same east to northeast maximum compressive stress responsible for the core-induced fractures. Higher frequencies of natural fractures and slickensides are associated primarily with incompetent, high-organic shales. Natural fractures occur most frequently in the Marcellus Shale, Tully Limestone, Geneseo Shale, West Falls Formation, and the Lower Huron Member of the Ohio Shale. Slickensided fractures occur most frequently in the Marcellus Shale, Tully Limestone, Geneseo Shale, West Falls Formation, base of the Java Formation, and Lower Huron and Cleveland Members of the Ohio Shale.

These observations are consistent with a fracture facies concept that proposes fracture development in shales that have acted as decollement zones during Alleghenian deformation. Detailed reports are included for each of the thirteen cores investigated.

INTRODUCTION

Purpose

Fractures in the Middle and Upper Devonian shale sequence of the Appalachian Basin are believed to provide the permeability needed for commercial gas production. If the nature, orientation, and intensity of the fractures can be determined, then the extent and location of potentially productive permeable zones can be predicted and better exploration programs planned for greater gas production.

Most studies of reservoirs with fracture permeability rely on surface joint data, photolineament data, and production studies to predict subsurface fracture patterns. However, the availability of numerous oriented cores from the Devonian shale sequence of the Appalachian Plateau province has allowed the characterization of subsurface fractures for parts of that sequence cored. The rock has not been exposed to weathering or long-term, near-surface tensile stresses which may add fracture patterns not found at depth. The cores present a unique opportunity to study natural fractures from a fractured reservoir and demonstrate that open fractures do exist at considerable depth in the earth's crust.

The purpose of this study is threefold: first, to document subsurface fractures in the Devonian shale by examining oriented cores; second, to determine relationships of subsurface fracture patterns to regional structure and stresses; and finally, to provide a basis for the evaluation of the utility of subsurface fracture patterns and possible highly fractured zones as an aid in gas exploration. Ultimately, the data collected in this study will be used by others for comparison

with additional production and geologic information.

Location

The study area comprises a large part of the Appalachian Plateau province, extending from eastern Ohio and southwestern Pennsylvania through West Virginia and into eastern Kentucky and western Virginia. Thirteen cores were examined from wells located throughout this area (figure 1, table 1).

Regional Structure

The Appalachian Plateau province lies between the relatively undisturbed rocks of the Central Stable Interior on the west and folded sedimentary rocks of the western Valley and Ridge province on the east. Surface rocks in the Plateau region appear to be flat-lying, but low-amplitude folds can be defined by detailed surface and subsurface mapping (figure 2). Decollement zones often separate undeformed or mildly deformed shallow rocks from those deformed by basement structures below. These decollement zones are the westward extensions of larger thrust zones in the adjacent Valley and Ridge Province. The Pine Mountain thrust, a large sheet detached in the Devonian shales, is found at the southeast boundary of the Plateau, at the common borders Kentucky, Virginia, and Tennessee. The Rome Trough, a large basement graben which formed during the early Cambrian, extends northeastward from eastern Kentucky through western West Virginia and possibly into Pennsylvania (figure 2). The Rome Trough is believed to be an extension of the Eastern Interior aulacogen (Harris, 1978), but it may be a back-arc or basin complex that formed at the inception of subduction

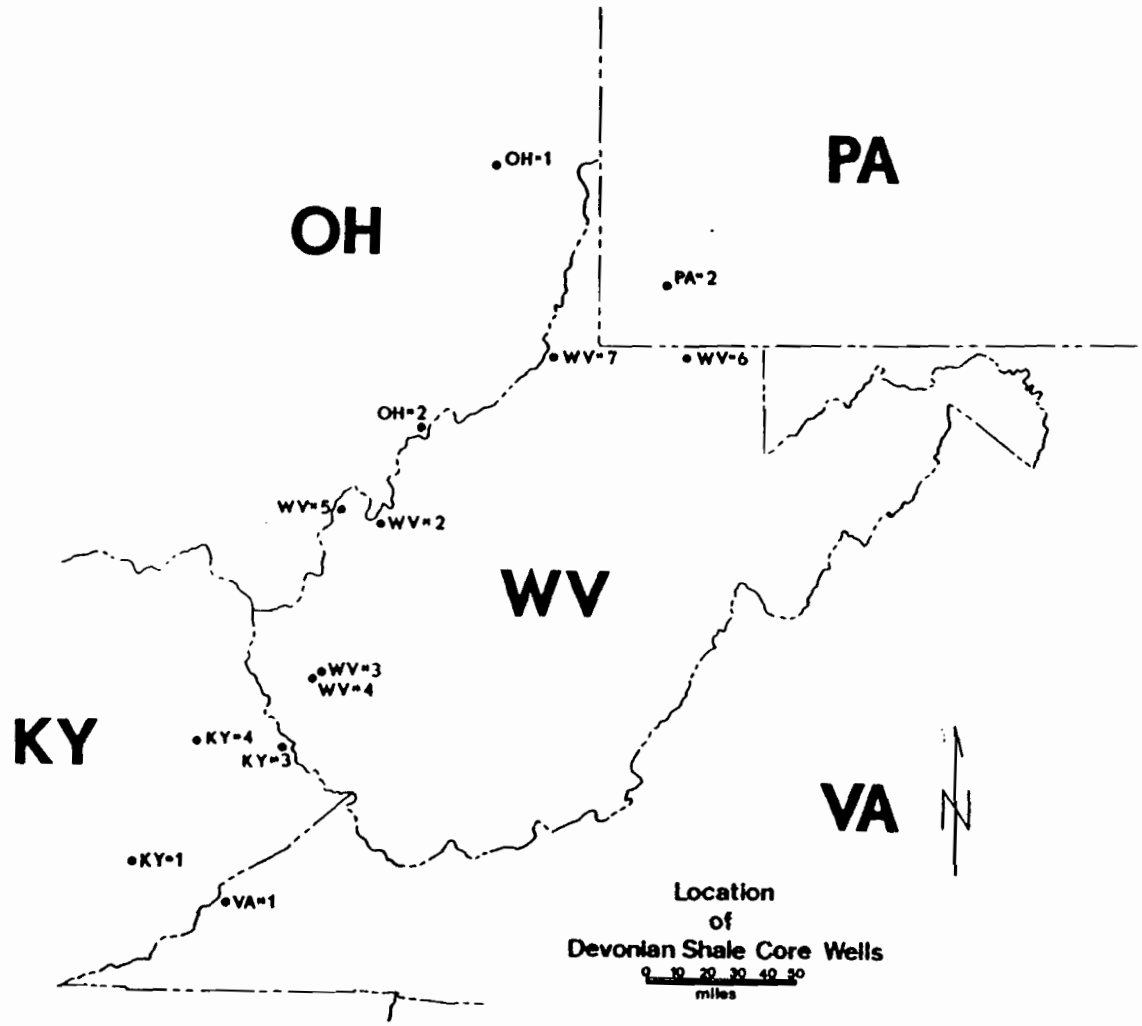

Figure 1. Location of core wells

EGSP Well No.	Company Well No.	State Well No. (if any)	Location	Latitude Longitude Carter Coordinates in KY & OH	Year Cored	Contractor	Cored Interval	Amt. of Core (in feet)	Total Depth	Elevation of KB (above sealevel)
OH #1	Glen Gery S-745	Permit No. 835	Carroll Co., OH	600 FSLX x 760 FWL SW ¼ sec. 29, T. 16N., R. 7W	1974	Belden and Blake, Inc.	2080 - 2200 3080 - 3200	240	5187	1045
KY #1	Nicholas-Combs 7239	Permit No. 20902	Perry Co., KY	1960 FNLX x 325 FWL 19-K-76	1975	Kentucky-West Virginia Gas Co.	2369 - 2700	330	2710	1000
WV #2	W.L. Pinnell 12041	Jac-1371	Jackson Co., WV	0.77 mi. W of 81° 50' 00"W 2.97 mi. S of 38°55' 00"N	1975	Consolidated Gas Co.	3220 - 3690	470	3742	[illegible]
WV #3	20403 Fee	LIN-1637	Lincoln Co., WV	3.1 mi. W of 82° 10' 00" 4.5 mi. S of 38° 10' 00"	1976	Columbia Gas Corp.	2720 - 4028	1308	4073	[illegible]
WV #4	20402 Fee	LIN-1636	Lincoln Co., WV	3.94 mi. W of 82° 10' 00" 4.83 mi. S of 38° 10' 00"	1976	Columbia Gas Corp.	2654 - 2770 3000 - 3118 3290 - 3588 3886 - 3968	614	4066	1153
OH #2	Florence L. House R-109	Permit No. 3521	Washington Co., OH	6200 ft. W of 81° 32' 30" 8400 ft. S of 39° 25' 00"	1976	River Gas Co.	3490 - 3714	224	6262	[illegible]
KY #3	20336 Fee	Permit No. 31020	Martin Co., KY	2750 FNL x 1650 FWL 16-P-85	1976	Columbia Gas Corp.	2429 - 3411	982	3456	[illegible]
VA #1	Penna.-Virginia Corp. 20338	Permit No. 253	Wise Co., VA	82° 41' 14"W 37° 00' 37"N	1977	Columbia Gas Corp.	4870 - 4985 5210 - 5475	380	5724	[illegible]
[illegible] #5	#3 D/K Farm	MAS-146	Mason Co. WV	82° 03' 45"W 38° 55' 30"N	1977	Reel Energy, Inc.	2673 - 3420	747	3422	[illegible]
[illegible] #6	MERC #1		Monongalia Co., WV	79° 58' 44"W 39° 40' 14"N	1978	U.S. Dept. of Energy	7168 - 7509	350	7520	[illegible]
[illegible] #7	Bach-Pyles UNIT #1	WET-645	Wetzel Co., WV	80° 49' 20"W 39° 40' 37"N	1978	Mobay Chemical Co.	6100 - 6650	550	6694	1355
[illegible] #4	Skaggs-Kelly UNIT #1 #3 R-S	Permit No.	Johnson Co., KY	82° 56' 20"W 37° 57' 40"N	1978	Ashland Exploration, Inc.	950 - 1500	550	1505	[illegible]
A #2	C.F.P.S. #1	ALL-20980	Allegheny Co., PA	79° 53' 30"W 40° 11' 30"N	1978	C.E. Power Systems	6950 - 7505	555	7520	760

Table 1. Core well data

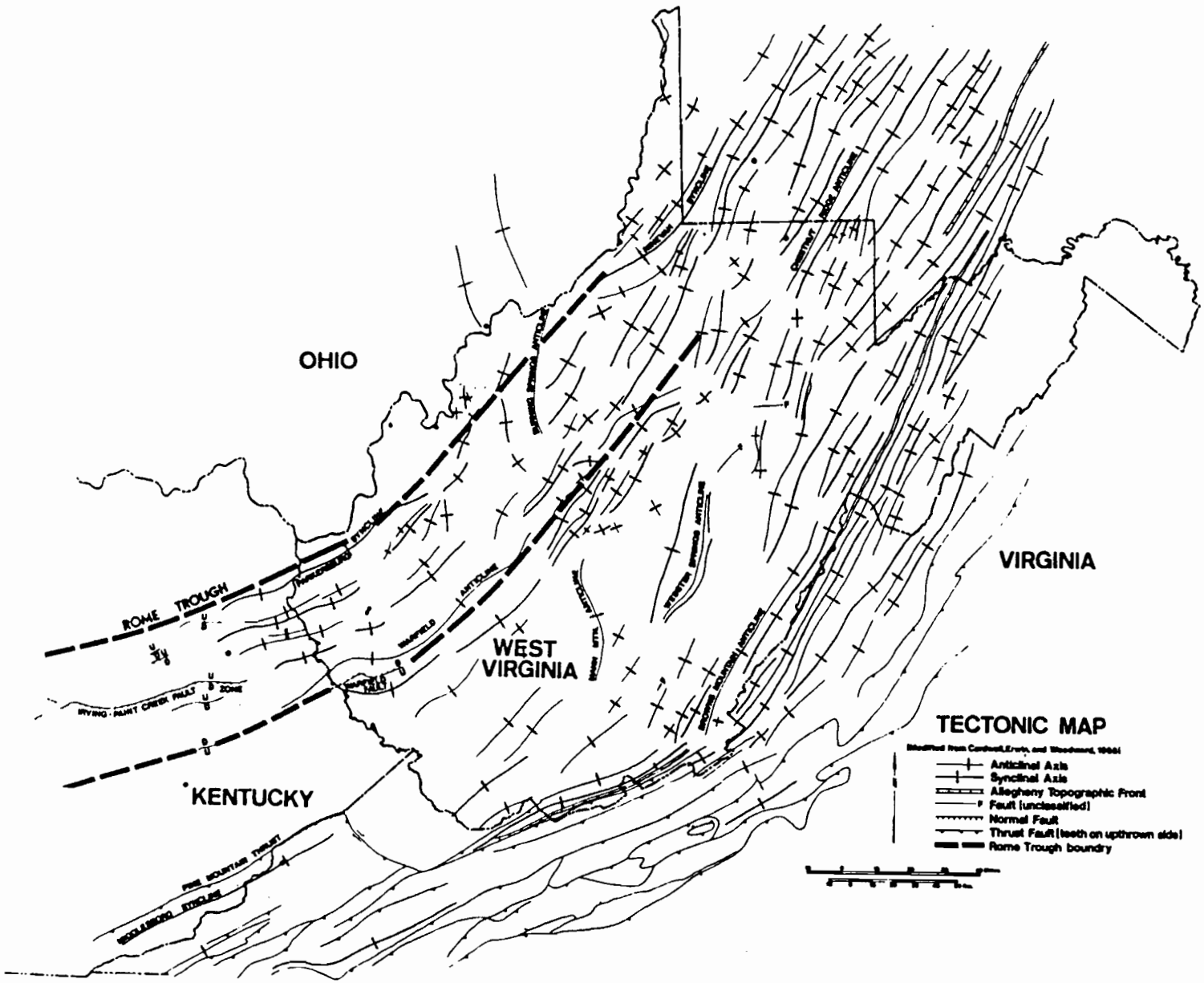

Figure 2. Tectonic map of the study area.

(Avalonian) along the Paleozoic North American continent (Shumaker, 1979). Low folds that are only visible in the subsurface in southwestern West Virginia and eastern Kentucky may be the result of reactivated Rome Trough faults which also affected sedimentation during the Devonian (Schaefer, 1979).

Stratigraphy

Surface rocks in the study area, which are primarily of Permian and Pennsylvanian age, consist of deltaic sequences of shale, sandstone, minor limestone, and coal. In the subsurface, the Mississippian system includes shales, sandstones, and a limestone which extends over most of the study area. Rocks of the Middle and Upper Devonian consist of siltstones, grey, brown, and black shales, and a few thin limestones. The rocks of the Lower Devonian are mainly limestones. Figure 3 shows the stratigraphic nomenclature for Middle and Upper Devonian rocks in the Appalachian Basin. More detailed discussions of the stratigraphy and structure in the vicinity of individual core wells are presented in the core well reports in the appendices.

Previous Investigations

One of the first studies of subsurface fractures in cores was made by Wilkinson (1953) who studied subsurface fractures in the Spraberry Field of west Texas and compared them with production trends. Friedman (1967) conducted a structural analysis of both macrofractures and microfractures in cores from the Santicoy Field in Ventura County, California. Stearns and Friedman (1972) present a method for core orientation and fracture measurment. They also give an identification

OHIO	VIRGINIA	PENNSYLVANIA / WEST VIRGINIA	NEW YORK		
BEREA SANDSTONE	POCONO FORMATION	POCONO FORMATION		MISSISSIPPIAN	
BEDFORD SHALE					
OHIO SHALE: CLEVELAND MEMBER	HAMPSHIRE FORMATION	HAMPSHIRE FORMATION	CONEWANGO GROUP	DEVONIAN	UPPER
OHIO SHALE: CHAGRIN SHALE	CHEMUNG FORMATION	CHEMUNG FORMATION	CONNEAUT GROUP		
OHIO SHALE: HURON MEMBER			CANADAWAY GROUP		
UPPER OLENTANGY SHALE	BRALLIER FORMATION	BRALLIER FORMATION	JAVA FORMATION		
			WEST FALLS FORMATION		
			SONYEA FORMATION		
	MILLBORO SHALE	HARRELL SHALE	GENESEE FORMATION		
LOWER OLENTANGY SHALE		TULLY LIMESTONE	TULLY LIMESTONE		MIDDLE
		MAHANTANGO FORMATION	MOSCOW FORMATION		
			LUDLOWVILLE FORMATION		
			SKANEATELES FORMATION		
		MARCELLUS SHALE	MARCELLUS SHALE		
DELAWARE LIMESTONE	ONONDAGA LIMESTONE / HUNTERSVILLE CHERT / NEEDMORE SHALE /	ONONDAGA FORMATION	ONONDAGA LIMESTONE		

Figure 3. Stratigraphic nomenclature for Middle and Upper Devonian rocks in the Appalachian Basin (from Neal, 1979).

system for distinguishing pre-core and core-induced fractures.

Two studies, Kulander, Dean, and Barton (1977) and Kulander, Barton, and Dean (1978), present an exhaustive treatment of core fractures and fracture characteristics as well as a system for classifying fracture types. It is this classification and the distinguishing characteristics of several fracture types described by Kulander et. al. (1977; 1978) that the author used in this study to distinguish natural (Kulander's pre-core fractures) and core-induced fractures.

The first studies of subsurface fracturing in the Appalachian Plateau province were conducted by the U. S. Bureau of Mines. Results of these studies are given by Overbey and Rough (1968), Overbey (1969), and Overbey and Rough (1971). Surface and subsurface fractures were investigated in the Bradford and Allegheny oilfields in northern Pennsylvania, southern New York state, and in Hocking County, Ohio.

A report by Wilson, Dixon, Shumaker, and Wheeler (1978) discusses fracture patterns observed in five cores from the Devonian shale of the Appalachian Basin. The cores: WV #3 (20403), WV #4 (20402), OH #2 (R-109), KY #3 (20336), and VA #1 (20338), were also investigated in this study.

Each well in this investigation has been previously logged and studied by personnel or representatives of the U. S. Department of Energy, including the author (Evans, 1978; 1979). However, this is the first comprehensive report that compiles, integrates, and analyzes all the data.

METHODS OF ANALYSIS

Data Acquisition

Each of the thirteen cores studied was oriented by one of three organizations: the U. S. Department of Energy - Morgantown Energy Technology Center (METC) (KY #1, OH #1, WV #2, WV #3, and WV #4); the West Virginia Geologic and Economic Survey (KY #3, OH #2, VA #1, WV #5, and WV #6); and Cliffs Minerals (PA #2, KY #4, and WV #7). Personnel of METC supplied core-induced fracture data to the author for four cores (WV #4, WV #5, VA #1, and KY #3) and undifferentiated fracture data for two cores (OH #1 and OH #2). Dr. Byron Kulander supplied fracture data for the KY #1 core. Thomas Wilson supplied fracture data for the KY #3 core. Nine cores were examined personally by the author (WV #2, WV #3, WV #4, WV #5, WV #6, WV #7, KY #4, PA #2, and VA #1) at the METC Core Lab and the Cliffs Minerals Core Lab.

Fractures in the cores were measured by using a 360° protractor and a ruler, or a goniometer (when available). The data recorded for each observed fracture includes (see table 2 for definitions):

1) Depth at which the fracture occurs (below Kelly bushing).
2) Strike.
3) Dip.
4) Upper extent.
5) Lower extent.
6) Total length.
7) Fracture type.
8) Whether the fracture is slickensided or not.

9, 10) If slickensided, trend and plunge of slickenlines (striations).

11) Slickenline intensity (based on arbitrary scale).

12) Type and amout of fracture mineralization (if any).

13) Type and extent of face markings, and fracture propagation direction (if determinable) (see fractography section below).

14) Lithology in which the fracture occurs.

15) Other comments.

A sample fracture data sheet is shown in table 2. Unsatisfactory core condition many times restricted the amount of data that could be collected. Either the core had been sampled to the extent that it was useless to collect quantitative data or the shale had disintegrated to a rubble. For example, the WV #2 and WV #3 cores were so badly broken and sampled to the extent that very few fractures could be measured, the author was forced to sample only five core-induced fractures per box. Accurate fracture lengths, and upper and lower extents of the fractures could not be determined for these two cores.

Fractography

During the study certain structural and surface features were observed on fractures, and these were used to interpret the type and origin of the fractures. For example, core-induced fractures posess a unique combination of fracture surface characteristics which distinguish them from natural fractures.

Kulander, Dean, and Barton (1977) and Kulander, Barton, and Dean (1978) have classified fracture surface characteristics into two groups:

Well WV #5 (#3 D/K)

Page 6 of 10

Depth	Strike	Dip	Upper Extent	Lower Extent	Total Length	Type	Slickensided ?	Slickenlines Trend	Slickenlines Plunge	Intensity	Mineral Fillings	Face Marks	Lithology Intersected	Comments
31501	N65E	40NW	IC	IC	8"	NAT. VERT	—	—	—	—	—	TH, HP E→W	Lam Sh	—
31503	—	horiz	—	—	—	SLICK	yes	N45W	00NW	3	—	—	Lam Sh	—
31510	N60E	50 SE	CB	BP	1"	IP	—	—	—	—	—	AL	Lam Sh	—
31526	N60E	50 SE	CB	BP	3'2"	PCL	—	—	—	—	—	AL	Lam Sh	—
31607	N40E	45 SE	CB	CB	5"	SLICK	yes	N50W	45 SE	1	—	—	Blk Sh	—
31613	N30W	60NE	CB	CB	1'3"	NAT INCL	—	—	—	—	calcite xls	HP NE→SW	Blk Sh	calc. cover 30% of surface

IC - UN. CORE
CB - CORE BOUNDARY
BP - BEDDING PLANE

IP - INDUCED PETAL
PCL - PETAL CENTERLINE
NAT VERT - NATURAL VERTICAL
NAT INCL - NATURAL INCLINED

TH - TWIST HACKLE
HP - HACKLE PLUME
E→W - PROPAGATION DIRECTION
AL - ARREST LINES

Slickenline Intensity

1 - GOUGED SURFACE
2 -
3 -
4 -
5 - POLISHED SURFACE

Lam Sh - LAMINATED SHALE
Blk Sh - BLACK SHALE

Table 2. Example of a fracture data sheet

transient features, which are structures on fracture surfaces, and tendential features, which are fracture trace changes (figure 4). Transient features are short range irregularities and perturbations of a fracture surface which can be attributed to:

1) Material inhomogeneities (fossils, pyrite nodules, pore space, etc.).
2) Sonic wave interference.
3) Local changes in stress directions and stress gradients in the dominant stress field.
4) Fracture velocity variations.

Among more common transient features are arrest lines or "rib marks" (figures 4A, 6, and 10), inclusion hackle (figure 4A), twist hackle (figures 4A, 10, and 13), and hackle plume or "feather fracture" (figures 4A, 9, 10, and 13).

Arrest lines record an instantaneous picture of the fracture front configuration at a particular time during fracture propagation. Inclusion hackle results from the interference with an advancing fracture front of an inclusion (pore space, weakly cemented area, grain of different composition or size, etc.) in its path. Twist hackle is generated at the fracture front when the direction of principle tension rotates in the plane containing the fracture front. Hackle plume is made up of twist hackle and inclusion hackle. It consists of a central axis that starts at the point of fracture origin and faint ridges that diverge outward from the axis in a plumose fashion toward the edge of the fracture plane (Kulander, Barton, and Dean, 1978). The presence of plumose markings on a fracture surface indicates that the

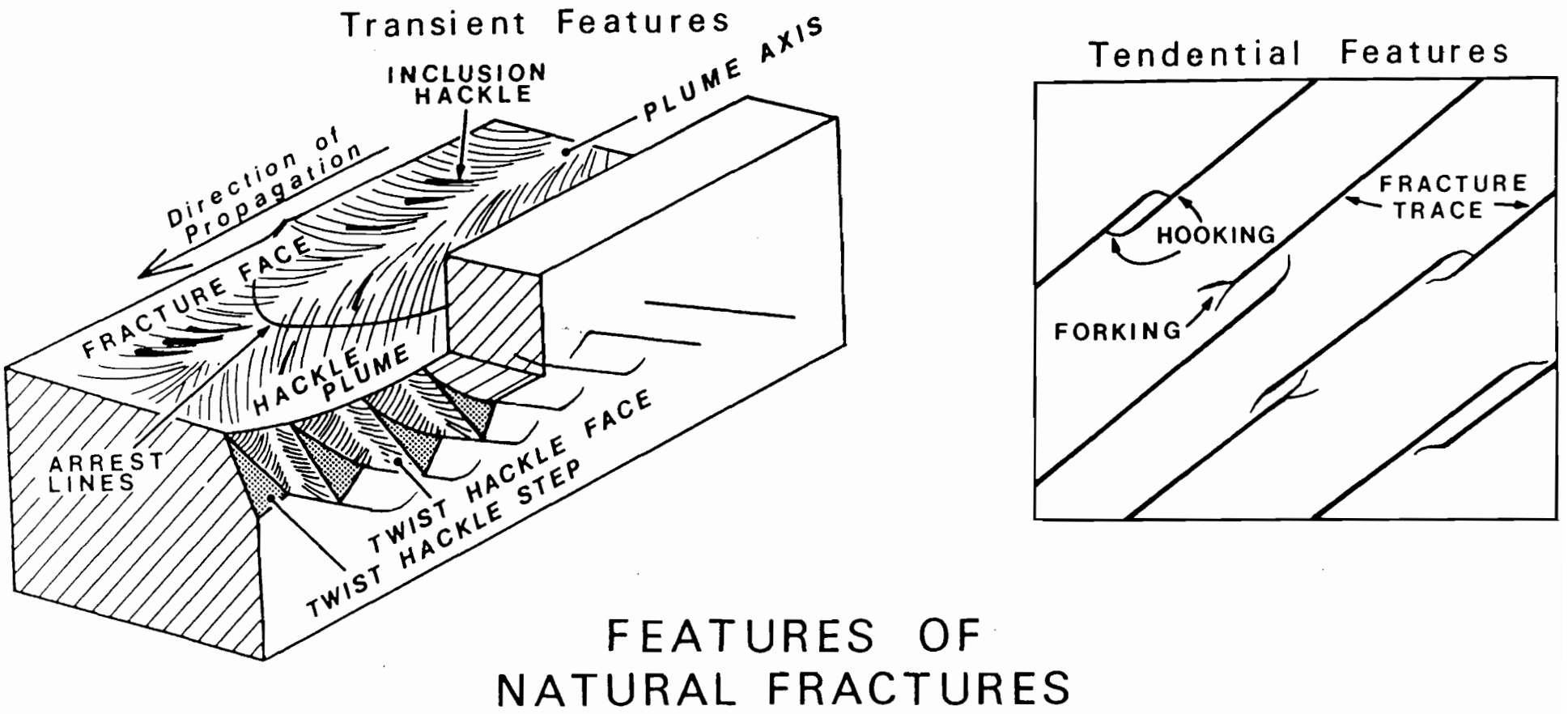

FEATURES OF NATURAL FRACTURES

Figure 4. Features of natural fractures: A) transient features, B) tendential features.

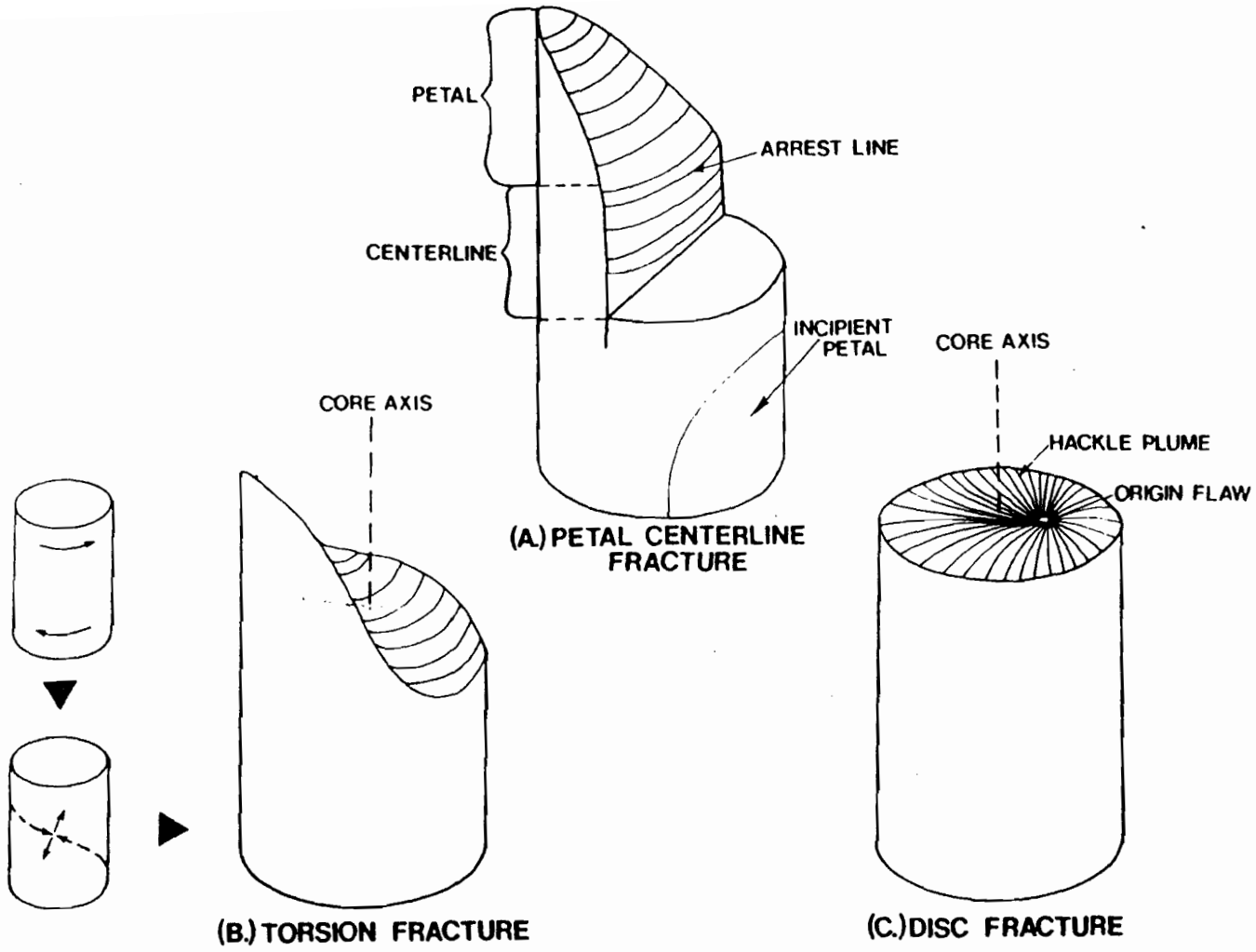

Figure 5. Idealized diagram of: A) petal-centerline fracture, B) torsion fracture, and C) disc fracture.

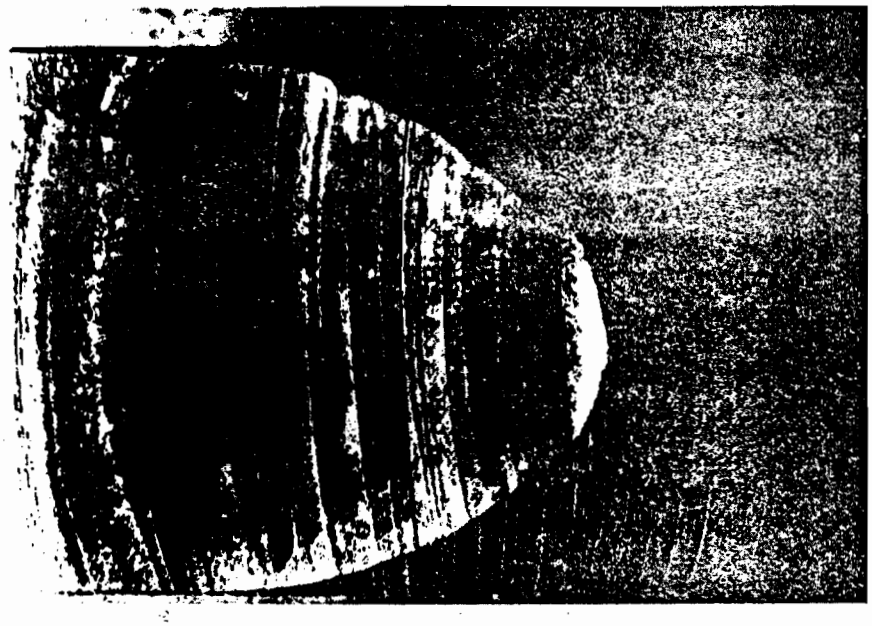

Figure 6. Petal-centerline fracture. Note symmetrical arrest lines downcore. From WV #5 (#3 D/K) core.

Figure 7. Three petal fractures, all with same strike and dip. From WV #5 (#3 D/K) core.

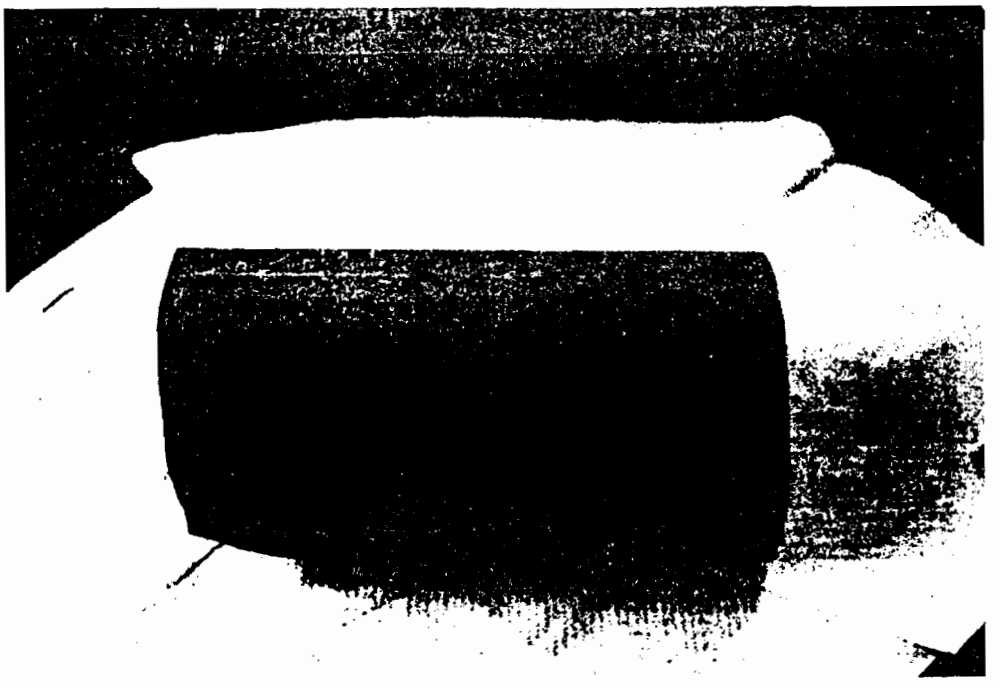

Figure 8. Two connected petal fractures forming a "scallop" fracture. Fracture C formed after A and B. From WV #5 (#3 D/K) core.

Figure 9. Disc fracture, and two petal fractures with same strike but opposing dips. Note hackle plume spreading from its origin, a fossil fragment, to meet the core boundary orthogonally. From WV #5 (#3 D/K) core.

Figure 10. Natural fracture termination, exhibiting: A) hackle plume, B) twist hackle, C) arrest line, and D) dolomite mineralization diminishing toward edge of fracture. From WV #5 (#3 D/K) core.

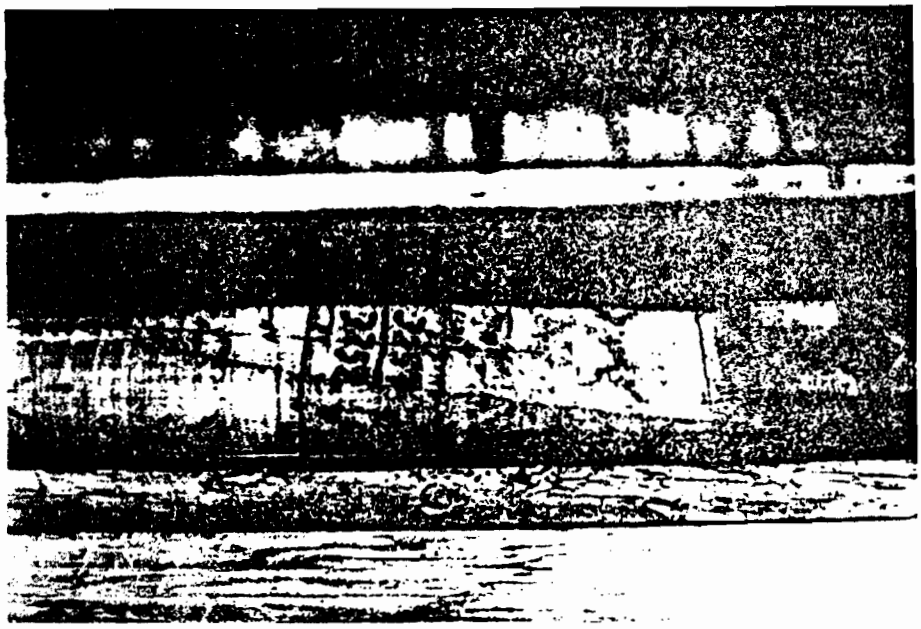

Figure 11. Three parallel subvertical natural fractures. From WV #5 (#3 D/K) core.

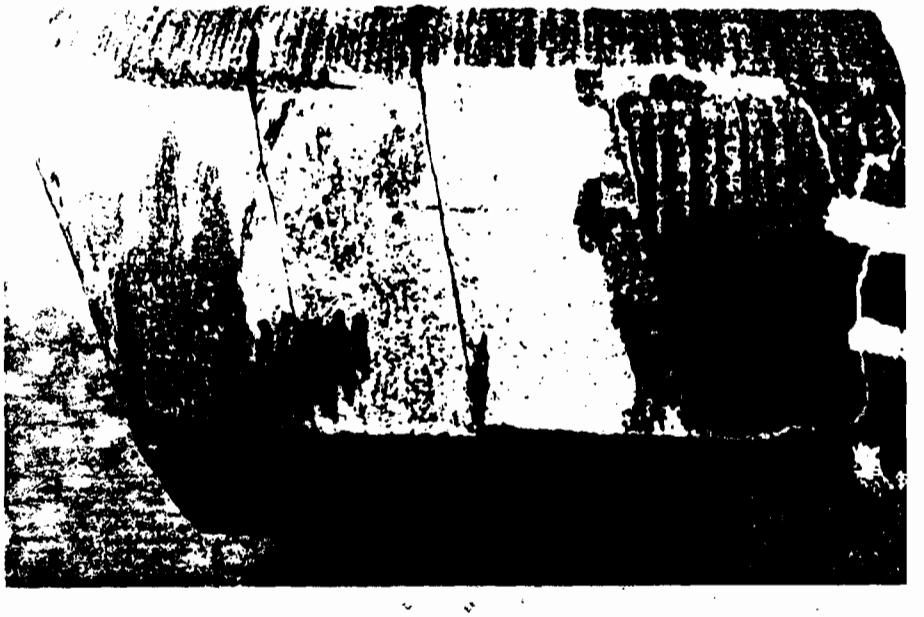

Figure 12. Natural fracture mineralized with calcite and pyrite. From WV #6 (MERC #1) core.

Figure 13. Two intersecting fractures of different strike and dip. Note: A) calcite mineralization, B) twist hackle, and C) hackle plume. From WV #4 (20402) core.

fracture walls have not ground against each other. However, high fluid pressure can permit preservation of plumes during relative slip of the walls.

Tendential features arise from long range changes in the stress field and are recorded as undulations in the fracture profile or trace line, generally at right angles to transient features. There are two basic types of tendential features; hooking and forking (figure 4B). The criteria used by the author to distinguish pre-core or natural fractures from core-induced fractures were set forth by Kulander, et. al. (1977; 1978) and are presented below.

Core-induced fractures have one or more of the following characteristics:

1) A fracture origin at the core boundary or within the core itself.
2) Hackle marks diverging and attempting to meet the core boundary or a pre-existing fracture surface orthogonally.
3) Hackle marks becoming coarse, the hackle steps increasing in relief in the immediate vicinity of the core boundary or pre-existing fracture surface.
4) Twist hackle originating near the core boundary or pre-existing fracture surfaces.
5) Hackle plumes on subhorizontal fractures that diverge from the central core area in a spiral pattern indicating a torque stress.
6) Closely spaced arrest lines on vertical and inclined fractures; arrest lines are convex downcore and symmet-

rical about the imaginary line down the fracture surface center.

7) Hackle marks on vertical or inclined fractures that diverge downcore symmetrically about an imaginary line down the fracture surface center.

8) Fractures that hook abruptly towards the core boundary or a pre-core (natural) fracture surface.

Natural fractures have one or more of the following characteristics:

1) Polished and slickensided fracture faces (almost always smooth and planar).

2) Fractures filled by fibrous or non-fibrous minerals.

3) Smooth fractures extending entirely across the core and against which later fractures usually terminate.

4) Inclines or vertical fracture faces displaying small, often conchoidal chips at the fracture-drilled core boundary intersection. The chips hook to meet the fracture orthogonally.

5) Conchoidal chips originating at the scribe marks on the core and curving to meet a pre-existing fracture face orthogonally.

6) Outsize transient markings or twist and inclusion hackle that do not curve to meet the core boundary orthogonally.

7) Several parallel to subparallel vertical or inclined fractures passing completely through the core.

8) General lack of any diagnostic symmetrical association

between fractographic markings, coring methods, and core geometry.

Fracture types

In the preceeding section on fractography we have been able to differentiate core-induced fractures and natural fractures. Core-induced fractures can be further subdivided. The common types include petal-centerline fractures, torsion fractures, and disc fractures.

Petal-centerline fractures (figures 5A, 6, 7, 8, and 9) form in response to a core-induced principal tension that rotates downward in a vertical plane from an inclined orientation to horizontal. The petal section of these fractures is that portion that curves in a downcore direction from a dip angle generally between 30° and 70° at the core boundary to a vertical dip within the core. A petal fracture may form without the vertical centerline portion (figures 7, 8, and 9). Very often these fractures show a remarkably consistent strike orientation throughout a core even though they may have opposing dips (figure 9). This strike consistency indicates that these fractures follow a stres or rock fabric anisotropy throughout the drilled section (Kulander et. al., 1978).

Torsion fractures (figure 5B) are formed by a torsion induced stress generated behind the drill bit. They are distinguished by a helical fracture trace on the core surface.

Disc fractures (figures 5C and 9) are horizontal to subhorizontal and form in response to vertically acting principal tensile stress. This stress is attributed to unloading and bit pressure along with vibrations and torques inherent to the drilling process.

The orientation or frequency of torsion fractures and disc fractures were not measured, and these fractures will not be discussed further, except to indicate their presence or absence in a particular core.

Natural or pre-core fractures are formed as a result of the failure of the rock under natural stresses in the earth's crust. Natural fractures are subdivided into unmineralized fractures, mineralized fractures, and slickensides. In this study, natural fractures, exclusive of slickensides, are referred to simply as "natural fractures" and they are joints. Natural fractures in the cores are generally subvertical to vertical (figure 11).

Natural tension fractures may form near the earth's surface where tensile total principal stresses are possible or they may form at depth where only effective tension is possible and where pore fluid is important in fracture genesis. The coring process samples those natural fractures which, in most cases, formed at depth and thus probably in a different stress system than did fractures near the surface. According to Secor (1969, p. 41):

> When natural tension fracturing occurs at depth in the earth's crust, in the presence of high pore pressures, macroscopic fracture growth is a slow process consisting in detail of numerous short, quick episodes of fracture propagation interspersed with longer periods of quiescence during which pore fluid from the surrounding rock percolates into the crack and wedges it open.

The formation of these fractures requires a ratio of fluid pressure to overburden weight which approaches one (Secor, 1965). Natural fractures often occur as two or more distinct sets intersec-

ting acutely or orthogonally. These sets may have originated at different times under different stress conditions.

Many of the natural fractures in the shale cores are mineralized (figures 10, 12, and 13). The most common fillings are calcite, dolomite, barite, pyrite, anhydrite, or some combination of these. The fillings may be massive, crystalline, or fibrous. The fibrous fillings consist of mineral fibers, usually calcite, that are perpendicular to, or at a slight angle to, the fracture walls. The fibers grew parallel to the principal acting tension as the fracture opened (Durney and Ramsay, 1973).

Slickensides are small faults which are distinguished and studied separately from other natural fractures. The orientations of the striations or slickenlines on the slickensides were measured. These striae form when the fracture surfaces are forced past one another during slippage. It is presumed that the slickenlines are oriented in the direction of movement. Figure 14 illustrates the use of the terms slickenside and slickenline, for the common case of slickenlines trending up- or down-dip on the slickenside.

Slickensides are divided into two classes: subhorizontal to horizontal (dip $< 10^{\circ}$) (figures 15 and 16), and inclined (dip $\geq 10^{\circ}$) (figures 17 and 18). This distinction was made to separate low dipping fracture surfaces that generally are slickensided bedding planes from more inclined shear fractures. The strike orientations of subhorizontal to horizontal slickensides were not measured because strike lines are too difficult to determine on fractures dipping less than 10°. It was felt that measuring only slickenline trends on the low

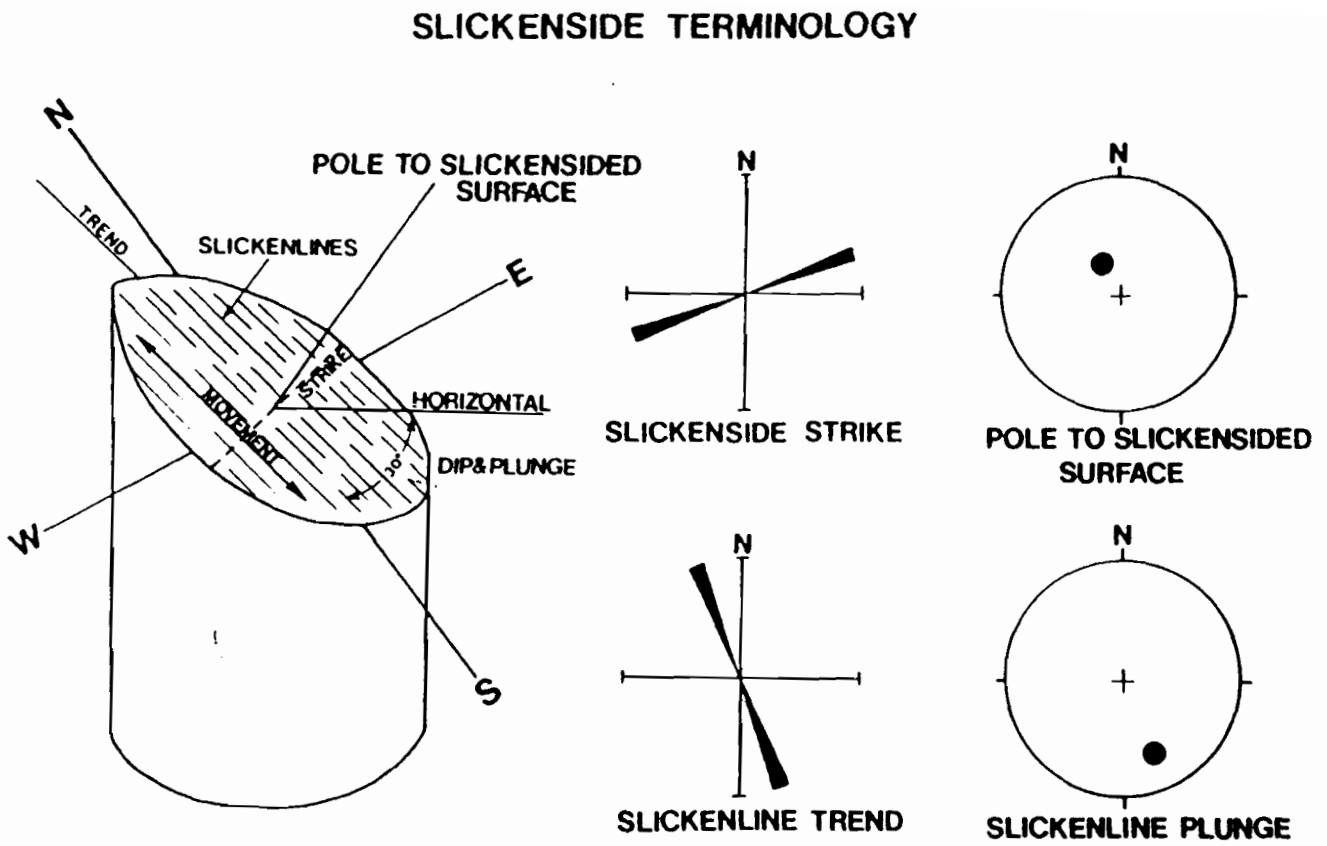
SLICKENSIDE TERMINOLOGY
N
TREND
POLE TO SLICKENSIDED SURFACE
SLICKENLINES
E
STRIKE
HORIZONTAL
MOVEMENT
20°
DIP& PLUNGE
W
S
N
SLICKENSIDE STRIKE
N
POLE TO SLICKENSIDED SURFACE
N
SLICKENLINE TREND
N
SLICKENLINE PLUNGE

Figure 14.

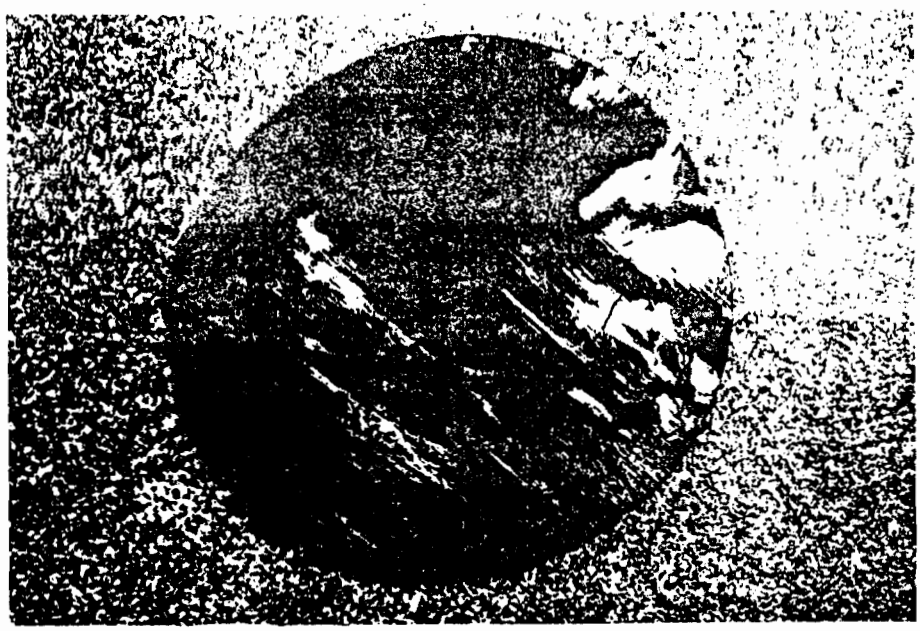

Figure 15. Horizontal bedding plane slickenside. Note irregular surface. From WV #6 (MERC #1) core.

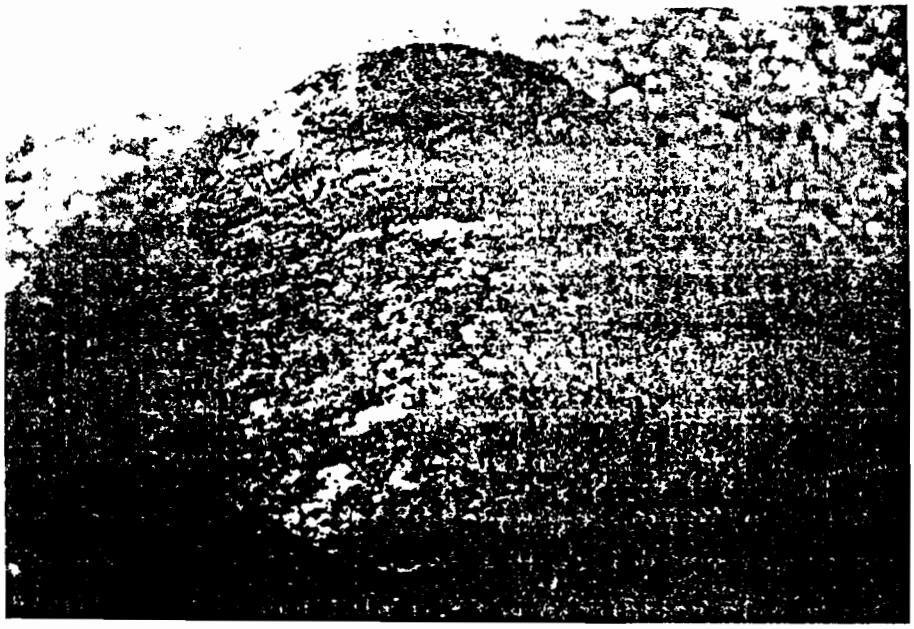

Figure 16. Horizontal bedding plane slickenside mineralized with fibrous calcite, fibers are perpendicular to the fracture walls. From WV #6 (MERC #1) core.

Figure 17. Inclined slickenside. From WV #4 (20402) core.

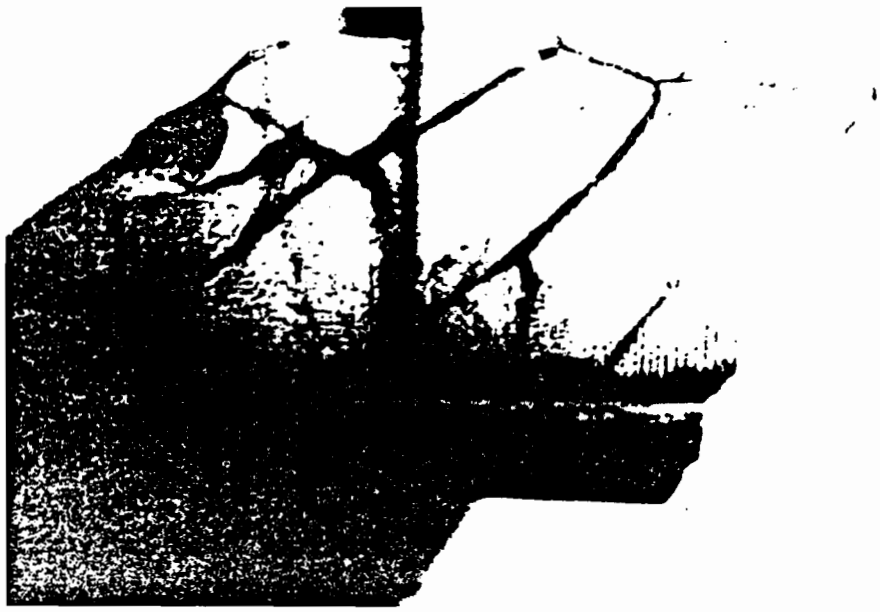

Figure 18. Inclined slickensides in tendential view. From base of VA #1 (20338) core.

dipping fractures would be more accurate and meaningful. Slickensides were found to be mineralized with either calcite, dolomite, barite, pyrite, or some combination of these. The fillings are usually fibrous and found on horizontal and low dipping slickensides (figure 16). This indicates that the fracture was open, and that fluid under high pressure was passing along the bedding planes separating the fracture.

Data Analysis

Core fracture data were analyzed by several methods: 1) composite rose diagrams and lower hemisphere equal area projections for all fractures of each fracture type (core-induced, natural, and slickensided) and slickenlines in each core, 2) rose diagrams and equal area projections for each fracture type and slickenlines in approximately equal core-length intervals in each core, 3) fracture frequency vs. depth plots for each fracture type in each core, 4) statistical testing to determine peaks in composite rose plots, and 5) statistical comparisons of core-length interval core-induced fracture orientation distributions.

To further aid in data analysis the core-length interval rose diagrams and equal area projections were plotted next to a gamma-ray log of the cored interval. This was done so that changes in fracture orientation with depth and stratigraphy could be observed. Composite fracture data sheets of all fracture types and slickenlines were made for each core to compare differences in fracture orientation and frequency with fracture type, depth, and stratigraphy. The composite rose diagrams for each core were plotted on maps to determine regional

subsurface fracture trends. Histograms of strikes of core-induced fractures, in approximately equal core-length intervals of each core, were plotted so that subtle differences in strike could be observed. The Upper and Middle Devonian units of each core well were correlated across the study area. Fracture frequencies in each shale unit were then compared between wells. This was done for each fracture type in order to determine if certain units are characteristically more fractured.

Plotting of fracture strikes and slickenline trends as rose diagrams was accomplished using a CALCOMP plotter and program (Werner, Program to plot orientation data, unpublished manuscript) on the IBM 360/75-370/148 of West Virginia Network for Educational Telecomputing. Except where noted, a 5° class interval was used in all rose diagrams and histograms. Plotting of fracture strikes and dips, and slickenline trends and plunges was accomplished using a computer program (Wheeler, unpublished program) which plots a Mellis-contoured equal area projection of fracture strike and dip or slickenline trend and plunge.

Data analysis was accomplished by visual inspection and interpretation. This analysis involved choosing peaks from the rose diagrams and clusters from the equal area projections as well as trends from regional maps. Also, visual comparisons of fracture frequencies were made between cores by examining the cross sections. Since personal bias tends to color this form of interpretation, statistical testing has also been performed to provide an impartial assessment of the data.

A statistical test discussed by Abdel-Rahman and Hay (1978) was

used to determine if individual peaks and troughs found visually on the composite rose plots are significant statistically. Identification of peaks and troughs uses the Poisson method for calculating the minimum and maximum numbers of fractures, respectively, needed to fill in any one orientational class in order to reject the assumption of random distribution of the data.

The differences between core-length interval core-induced fracture orientation distributions were determined by using a modification of the Kolomogorov-Smirnov (K-S) test. This modification, suggested by Kuiper (1960), takes into consideration the circular nature of the data. The hypothesis tested was that the two distributions compared were equal. The test was accomplished using a computer program (Werner, Program to plot orientation data, unpublished manuscript). Statistics generated by the program include; N (number of fractures) in each interval; VN, the test statistic; and alpha (α), the significance level. The test results are in the appendices.

A bias, introduced by the coring method, exists in the sampling of natural fractures at depth by the core bit. Two factors are involved. These are the spacing of the fractures relative to the diameter of the core and the orientation of the fractures relative to the core axis. For example, natural vertical fractures which are spaced one foot apart are poorly sampled by a six inch core bit in a vertical hole. The sampling improves, however, as the angle between the fractures and the core axis increases. According to Stearns and Friedman (1972) the distribution of dip angles between the fracture

and the core axis follows a Gaussian distribution. They present a method to weight observed fracture frequencies of differently dipping fracture sets in cores in order to determine their relative order of abundance. The weighting procedure was not used in this study, because the author felt that, in most cases, the natural fracture and slickenside orientations did not show enough variability to warrant its use.

FRACTURE ANALYSIS

Reports on Fractures in Each Core

Individual reports on each of the cored wells studied are presented in the appendices. Each report discusses, in detail, the fractures and fracture patterns in that particular core and their relationships to local structures and regional tectonics. A brief discussion of gas production from the shale section of the well is also included in these reports. The reader may wish to refer to these reports for detailed information to evaluate conclusions drawn by the author. However, for easy reference the dominant fracture peaks and their statistical significance, for each core, are summarized in table 3.

Regional Fracture Patterns

Distinct, statistically significant fracture orientation peaks, dominant fracture trends, or both, were found in all of the cores studied. Certain of these trends are unique to a particular core and show little or no relationship to trends in other cores. Such unique trends are probably related to stresses associated with local structures or local stress anomalies. Certain other fracture trends, however, can be found in several cores throughout the Appalachian Plateau province with only minor, and usually predictable, variations in trend between cores. Because of their regional extent, these trends seem related to stresses associated with regional deformation. Of course, some variation in regional fracture trends are found which resulted from the interaction of both local and regional stresses. Fracture trends resulting from local influences are discussed primarily

Well No.	Natural Fracture Peaks				Slickenside Peaks				Slickenline Peaks				Core-Induced Fracture Peaks		
OR #1	Undiff. N20°-30°E N25°E 0.05	Undiff. N63°W not sig.	—	—	—	—	—	—	—	—	—	—	—	—	—
ET #1	Undiff. N5°-15°W N10°W 0.05	Undiff. N3°E 0.05	Undiff. N39°W 0.10	Undiff. N33°E 0.10	N3°E 0.01	—	—	—	N87°W 0.01	N83°E 0.01	N27°E 0.01	N33°W 0.05	—	—	—
WV #2	N57°E 0.01	—	—	—	N5°-20°W N13°W 0.01	—	—	—	N70°-85°E N77°E 0.01	—	—	—	N50°-70°E N60°E 0.01	N17°W 0.05	—
WV #3	N40°-70°E N45°E 0.01	N27°W 0.01	N83°E 0.01	—	N70°-85°E N77°E 0.01	N75°W not sig.	N27°E not sig.	N63°E not sig.	N5°-20°W N13°W 0.01	N65°W not sig.	—	—	N35°-75°E N65°E 0.01	N83°E 0.01	—
WV #4	N20°-35°E N27°E 0.01	N67°E not sig.	N63°W not sig.	N3°W not sig.	N33°-45°E N40°E 0.01	—	—	—	N40°-50°W N45°W 0.01	N33°E not sig.	N27°W not sig.	—	N20°-45°E N33°E 0.01	—	—
OR #2	Undiff. N60°-75°E N67°E 0.01	—	—	—	—	—	—	—	—	—	—	—	—	—	—
ET #3	N67°W not sig.	N47°W not sig.	N37°E not sig.	—	N17°W 0.05	N47°E 0.05	N83°E 0.05	—	N7°W 0.05	N73°E 0.10	N43°W not sig.	—	N40°-55°E N47°E 0.01	N63°E 0.01	N13°E 0.01
VA #1	N7°W 0.01	N37°W 0.01	N83°W not sig.	N13°E not sig.	N40°-55°E N47°E 0.01	N27°E not sig.	—	—	N35°-55°W N45°W 0.01	—	—	—	N45°-70°E N57°E 0.01	—	—
WV #5	N70°-90°E N75°E 0.01	N33°E 0.05	N45°-60°W 0.05	—	N17°W 0.01	—	—	—	N67°E 0.01	—	—	—	N65°-85°E N75°E 0.01	—	—
WV #6	N83°E 0.01	N67°W 0.05	N47°W not sig.	—	N0°-30°E N15°E 0.05	N20°-30°W N25°W 0.05	—	—	N65°-73°W N70°W 0.01	—	—	—	—	—	—
WV #7	N37°W 0.01	N43°W 0.05	—	—	N15°-30°E N23°E 0.05	N43°W 0.10	—	—	N67°W 0.05	—	—	—	N67°E 0.01	—	—
ET #4	N40°-70°E N65°E 0.01	N47°E 0.10	—	—	N7°W not sig.	N53°E not sig.	N85°E not sig	—	N43°W not sig.	N3°W not sig.	N85°E not sig.	N55°W not sig.	N35°-65°E N50°E 0.01	N73°E 0.01	—
VA #2	N17°E not sig.	N37°E not sig.	N85°E not sig.	N47°W not sig.	N47°E 0.01	—	—	—	N40°-60°W N50°W 0.01	—	—	—	—	—	—

Key: N5°-15°W / N13°W / 0.01 — --- peak range; --- average peak orientation; --- value, significance

Table 3. Fracture orientation peaks for all fracture types for each core

in the individual core reports. This analysis will concentrate on coherent regional patterns of each structure studied: Core-induced fractures; natural fractures; slickensided fractures, and their associated slickenlines.

Core-induced Fractures

Composite rose diagrams of core-induced fractures for each core were plotted on a map of the study area to evaluate the consistency of trends from well to well. Core-induced fracture orientations show a remarkable preference for a northeast trend in nearly all cores in which they occur (figure 19). Minor, yet significant, variations in trend do exist locally. The consistent orientation indicates the presence of a stress or rock fabric anisotropy in the rocks throughout the Appalachian Plateau province. This anisotropy probably relates to the present day horizontal maximum compressive stress which exists in eastern North America (Sbar and Sykes, 1973). The present day stress was delimited from a combination of fault plane solutions of earthquakes, in-situ stress measurements, and observations of postglacial deformation (pop-ups). Voight (1969) suggests that the stress relates to convective flow in the mantle associated with the spreading of the crust, including North America, away from the Mid-Atlantic Ridge. This stress would be Mesozoic in origin, and it would probably have nullified any previous residual stress in the crust. Figure 20 shows dominant core-induced fracture orientations along with postulated maximum compressive stress trajectories, based on data in table 4. The core-induced fracture trends closely follow the stress trajectories.

The anisotropy may also be related to the rock fabric. Peng and

TABLE 4

COMPRESSIVE STRESS MEASURMENTS IN THE APPALACHIAN PLATEAU

Location	Trend of	Method	Reference
1) Alma Twp., N.Y.	N77°E	HYDRO	2
2) Falls Twp., Ohio	N64°E	HYDRO	4
3) Falls Twp., Ohio	N63°E	HYDRO	4
4) Bradford, Pa.	N70°E	HYDRO	5
5) Barberton, Ohio	N90°E	SR	3
6) Gibsonville, Ohio	N78°E	SR	7
7) Logan, Ohio	N75°E	BHD	6
8) Laural Twp., Hocking Co., Oh.	N73°E	BHD & IP	6
9) Scherrodsville, Ohio	N88°E	BHD	6
10) Loudenville, Ohio	N83°W	BHD	6
11) Allegheny Co., N.Y.	N62°E	IP	6
12) Logan Co., W.Va.	N87°W	BHD	6
13) Lincoln Co., W.Va.	N37°E	IP	6
14) Roan Co., W.Va.	N87°W	TS	6
15) Roan Co., W.Va.	N83°E	TS	6
16) Jackson Co., W.Va.	N82°W	BHD	6
17) Doddridge Co., W.Va.	N87°E	TS	6
18) Monongalia Co., W.Va.	N84°W	IP	6
19) Monongalia Co., W.Va.	N66°E	BHD	6
20) Buchanan, Va.	N71°E	BHD	6
21) Perry Co., Ky.	N67°E	BHD	6
22) Wetzel Co., W.Va.	N40°E ?	BHD	6
23) Lincoln Co., W.Va.	N40°-50°E	IP	1

References: 1- Brechtel, Abou-Sayed, and Clifton (1977); 2- Hamison and Stahl (1969); 3- Obert (1962); 4- Overbey and Rough (1968); 5- Overbey and Rough (1971); 6- Overbey (1976); 7- Rough and Lambert (1971)

HYDRO - Hydrofracture
SR - Strain Relief
BHD - Borehole deformation gauge
IP - Impression packer survey
TS - Televiewer survey

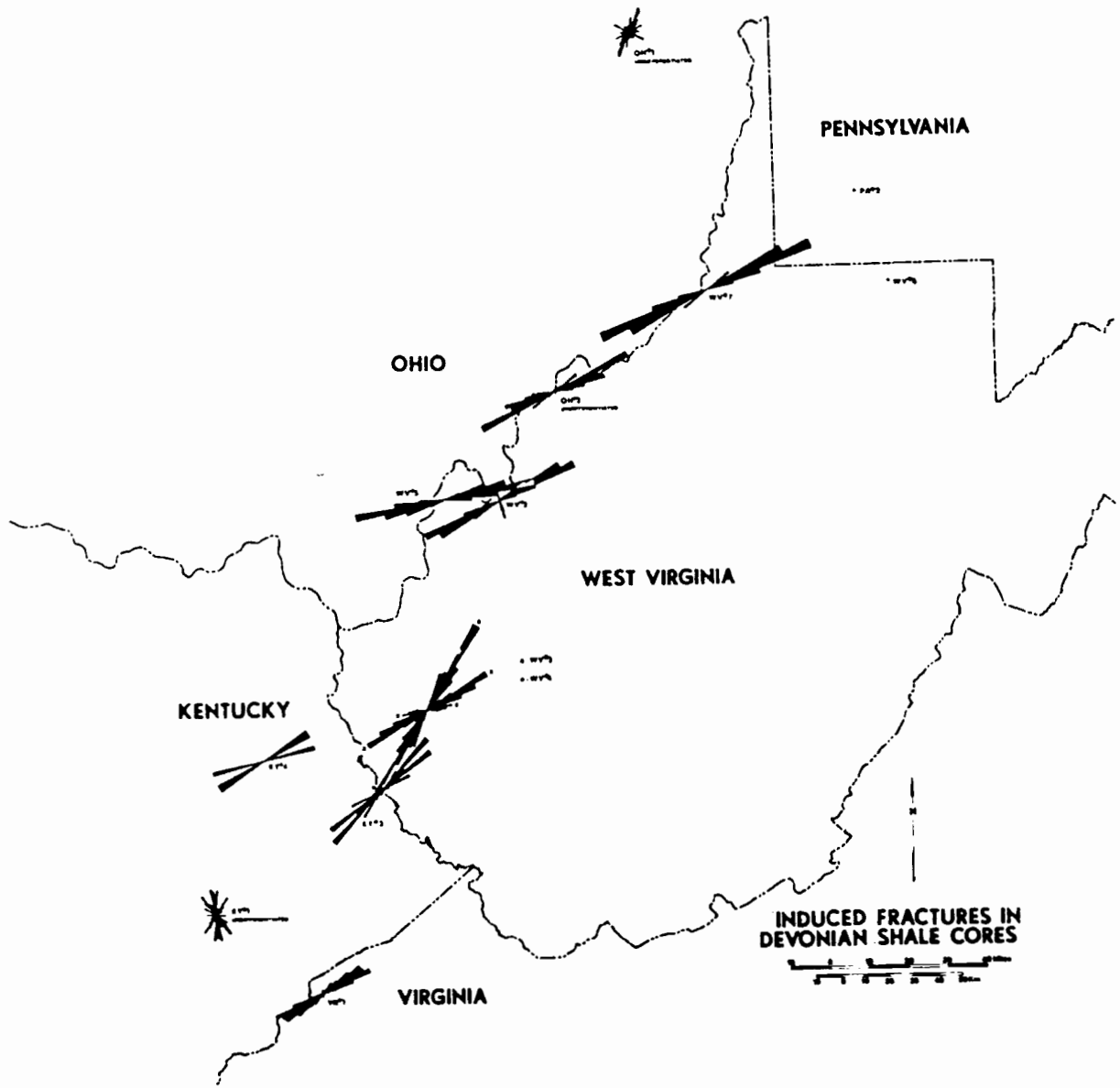

Figure 19. Regional core-induced fracture patterns.

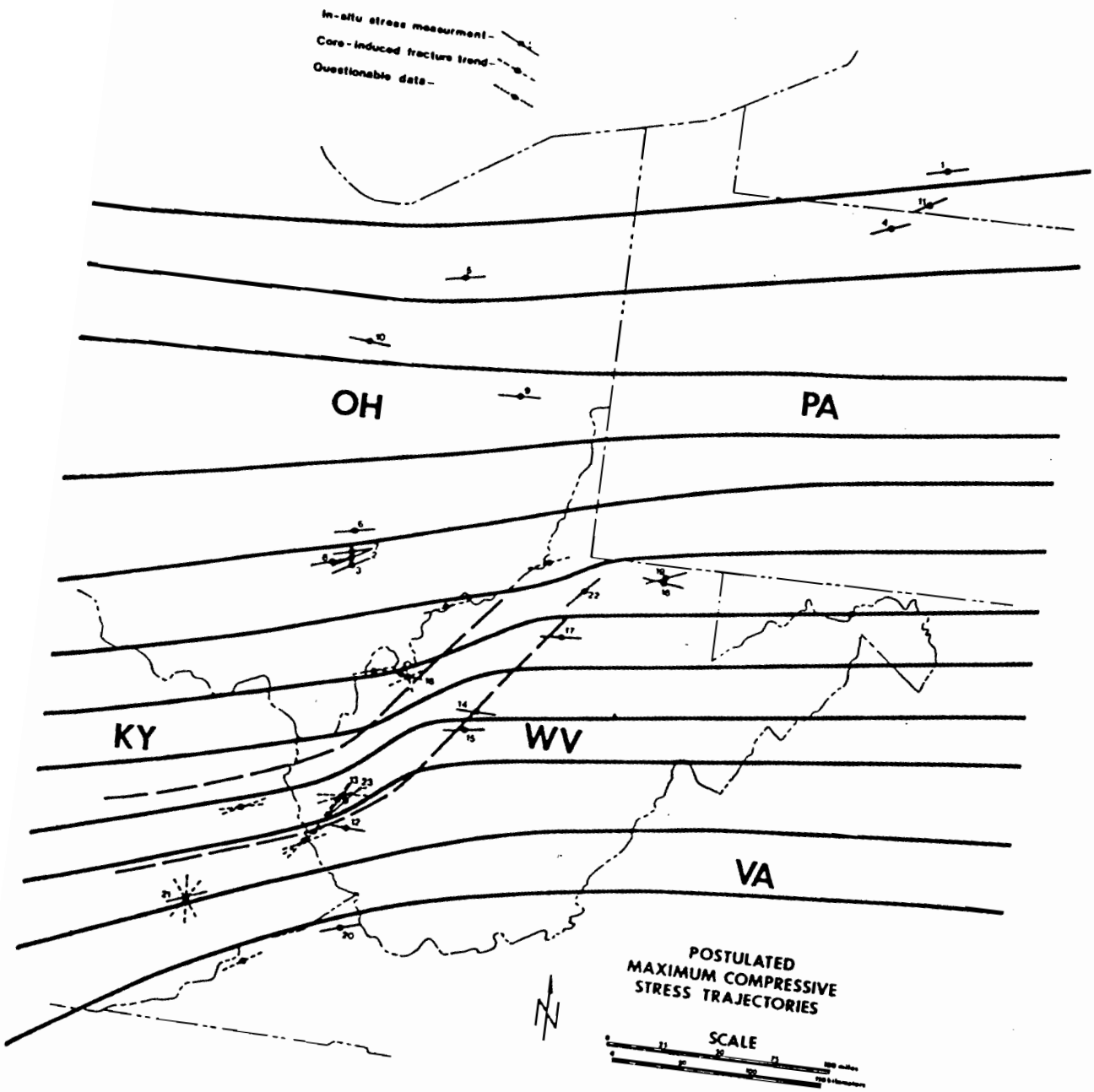
In-situ stress measurment
Core-induced fracture trend
Questionable data
OH
PA
KY
WV
VA
POSTULATED
MAXIMUM COMPRESSIVE
STRESS TRAJECTORIES
SCALE
N

Figure 20.

Okubo (1978) propose that the Devonian shale in the WV #3 (20403) core contains lenticular microcracks lying in the horizontal plane with their long axes predominatly parallel to N60°E (the core-induced fracture trend), intermediate axes parallel to N30°W, and their short axes vertical. However in a petrographic study, Vinopal, Nuhfer, and Klanderman (1979) found no evidence for a microcrack system in the WV #3 (20403) core. Microcracks in an oriented core from Hocking County, Ohio, were found to strike N67°E, nearly paralleling the measured in-situ stress of N73°E (Overbey and Rough, 1971). If a microcrack system exists, it probably formed as an extension feature under the influence of the post-Paleozoic east to northeast trending maximum compressive stress. If microcracks are present throughout the entire Plateau they may serve as Griffith cracks in the formation of the core-induced fractures, as well as planes of weakness in which the fractures propagate. Microcracks may also serve as the origins of northeast striking natural fractures which parallel the core-induced fractures.

Local fracture trends in the Appalachian Plateau province which do not follow the dominant northeast trend, may be the result of stress distributions which are modified by remnant stress, uplift, movement associated with decollement zones, and basement structures. One large basement structure which modifies the stress system is the Rome Trough, over which stress trajectories change abruptly (figure 20) and fracture patterns become quite variable. Advani, et. al. (1977) has shown through finite element analysis that stress distributions are altered over the Rome Trough basement fault zones. Core-induced fracture orientations were found to differ by 30° between the WV #3 (20403) and WV #4 (20402)

cores which are located over the Rome Trough in Lincoln County, West Virginia. These core wells are only 0.9 miles apart and have average core-induced fracture orientations of N63°E and N33°E, respectively. To the southwest, just south of a Rome Trough fault, The KY #3 (20336) core has core-induced fracture orientations ranging from N33°E to N63°E, with a large peak at N47°E. The KY #1 (7239) core, which is also just south of a Rome Trough fault, and near other proposed basement faults, has several undifferentiated fracture trends: N33°E, N3°E, N5°-15°W, and N37°W. Throughout the rest of the Appalachian Plateau province, core-induced fracture strikes range from N50°E to N85°E.

Natural Fractures

Composite rose diagrams of natural fracture orientations for each core were plotted on a map of the study area so that regional relationships could be observed. Natural fracturea are positively identified in most of the cores studied, and they probably constitute a portion of the undifferentiated fractures logged in the OH #1 (S-745), OH #2 (R-109), and KY #1 (7239) cores. Natural fracture trends throughout the Appalachian Plateau province are the result of regional and local stress conditions. Two regional natural fracture systems predominate (figure 21). One system consists of northwest striking extension fractures. These fractures are orthogonal to central Appalachian trends in West Virginia, southeastern Ohio, and southwestern Pennsylvania, and probably formed under compressive stresses during Alleghenian deformation. Natural fractures of this system strike more northerly, and are orthogonal to the southern Appalachian trend, in southern West Virginia, eastern Kentucky, and western Virginia. Dolomite mineral-

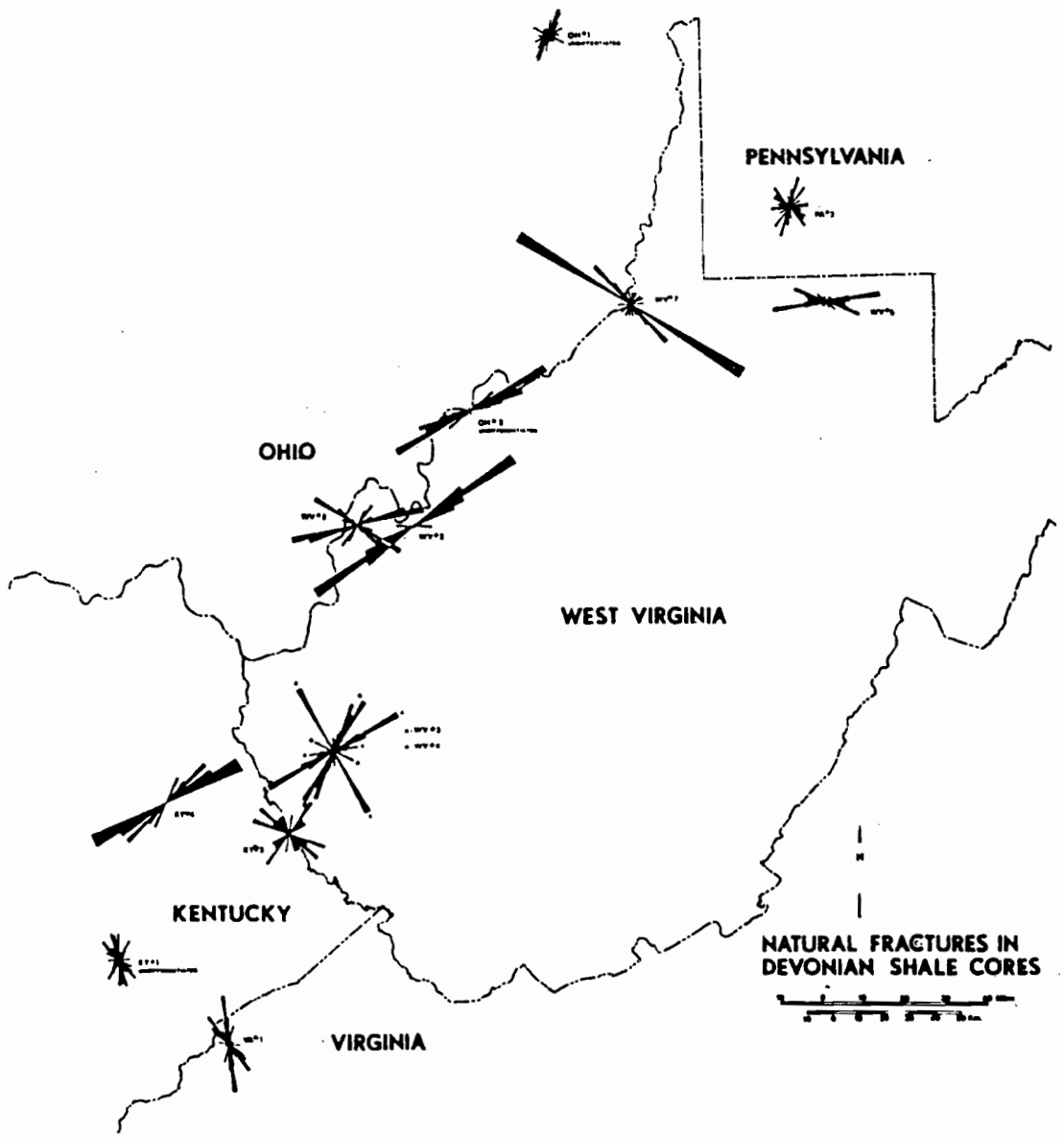

Figure 21. Regional natural fracture patterns.

ization found primarily within the northwest set in the WV #3 (20403) and WV #5 (#3 D/K) cores, suggests a preferential mineralization of this system.

The second natural fracture system found in the cores from the Appalachian Plateau province is one that generally strikes northeast, parallelling the core-induced fractures and maximum compressive stress present in most of eastern North America (Sbar and Sykes, 1973). This system may have originated from stress created during post-Paleozoic plate spreading. It is possible that these natural fractures formed when the stress was considerably greater than the present day in-situ stress, or that they are presently in the process of forming. If the former is true, an early Mesozoic age seems likely. The fractures of this system are often mineralized with calcite.

Local structures many times affect fracture trends in an area. In eastern Kentucky and southwestern West Virginia, for example, numerous surface faults of the eastern Kentucky fault system and subsurface faults of the Rome Trough, probably contributed to the formation of a wide variety of natural fracture patterns. Natural fractures in this area formed by the several stress fields described above, that is local faulting, regional stress, and the interaction of these stress fields. The chaotically fractured nature of this area probably contributes to the success of the Eastern Kentucky Gas Field. Long (1979) found that surface fracture patterns in eastern Kentucky are also more complex than in surrounding areas.

Fractures in the PA #2 (C.E.P.S. #1) core from Allegheny County, Pennsylvania, exhibit a great diversity in trend. The core well is

located on the perimeter of a line of structural discontinuity (Wagner and Lytle, 1976), upon which structural strike and folds of the Appalachian trend are interrupted or terminated. This zone may be one of several that have been interpreted as basement transcurrent faults (Cardwell, Erwin, and Woodward, 1968). The variety in fracture orientation cannot be explained by a simple northwest directed compressive stress, as during Alleghenian deformation, and probably relates to movement or stress along the discontinuity. Wagner and Lytle (1976) have found that oil and gas fields in southwestern Pennsylvania terminate against lines of structural discontinuity. Possibly, the highly fractures nature of these zones allows the hydrocarbon to escape.

The well is also located near the proposed Lat. 40°N basement fault zone (Root and Hoskins, 1977). Altered stress fields above this zone may have also contributed to the chaotic fracture pattern.

Slickensides and Slickenlines

Composite rose diagrams of slickenside strikes and slickenline trends, and equal area projections of poles to slickensided surfaces, were plotted on maps of the study area so that regional relationships could be observed. Slickensides are found in all but one of the cores investigated (figures 22 and 23). Their presence throughout the Appalachian Plateau province can be related to décollement tectonics, local faulting, and compaction. One dominant slickenside strike and the associated slickenlines (figure 24) have formed as a result of Alleghenian compressive stresses. The slickenside strikes parallel the Appalachian trend whereas the slickenlines are orthogonal to it. During Alleghenian deformation, large blocks of the detached sedimentary section

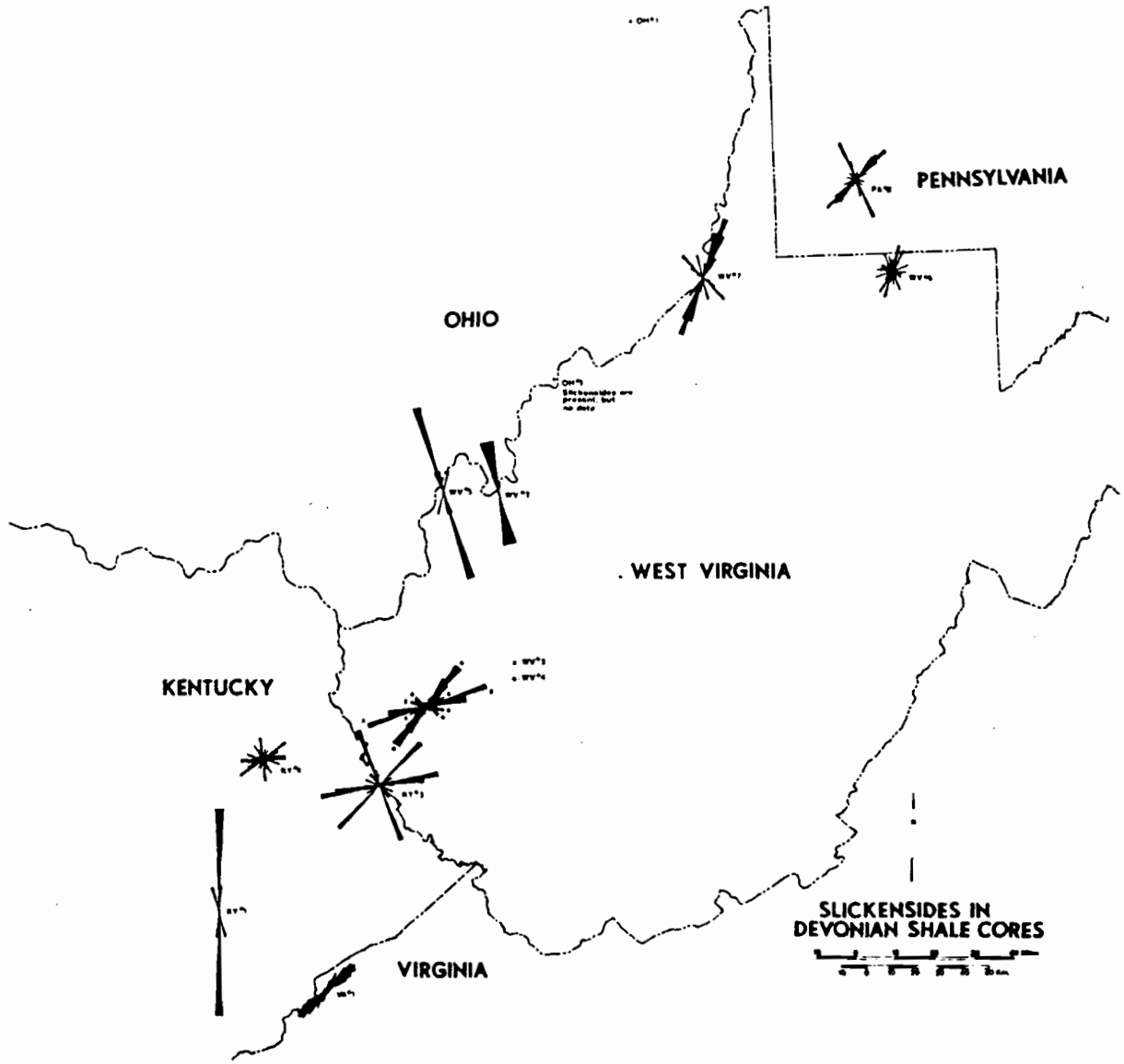

Figure 22. Regional slickenside patterns.

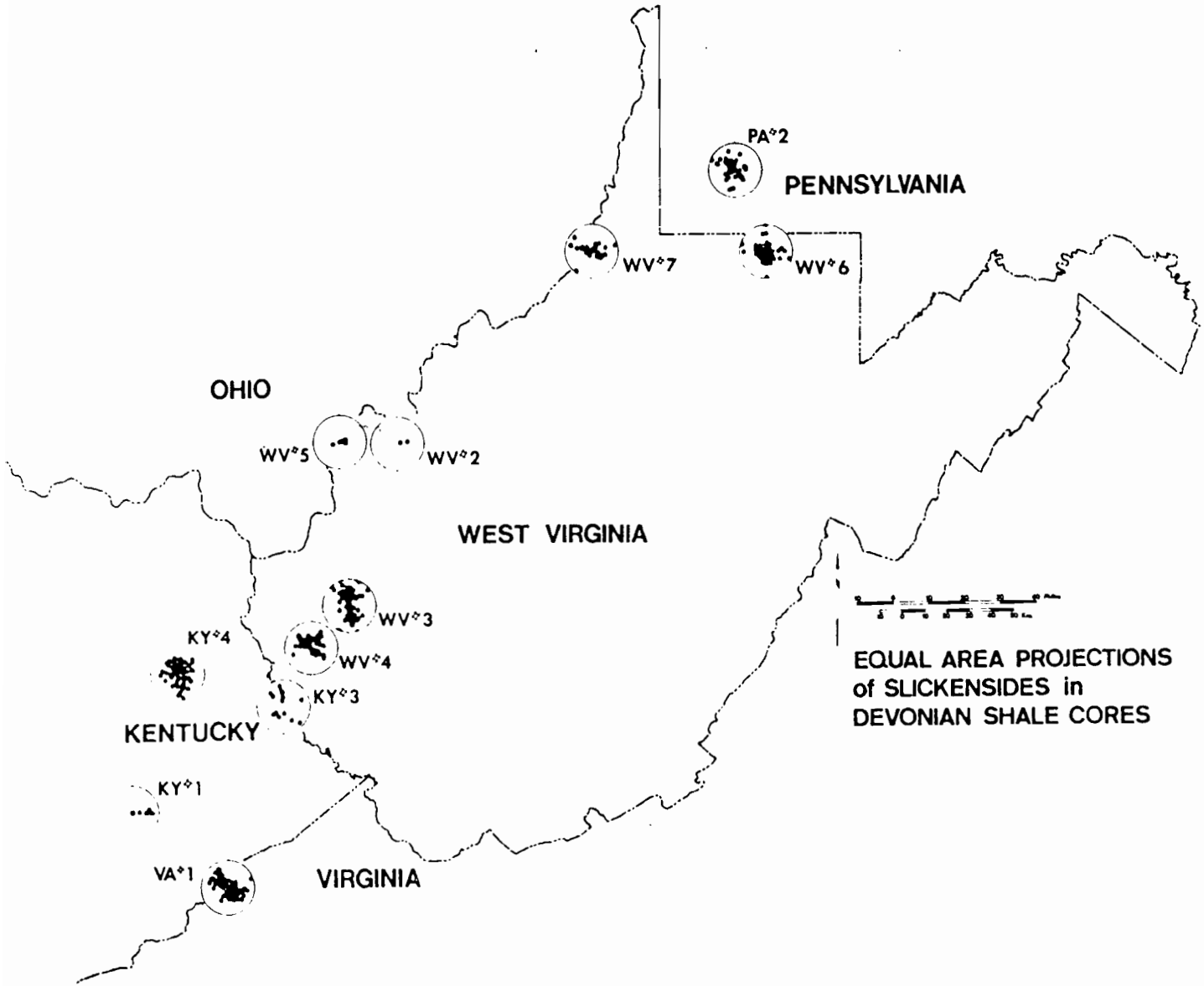

Figure 23. Regional slickenside patterns.

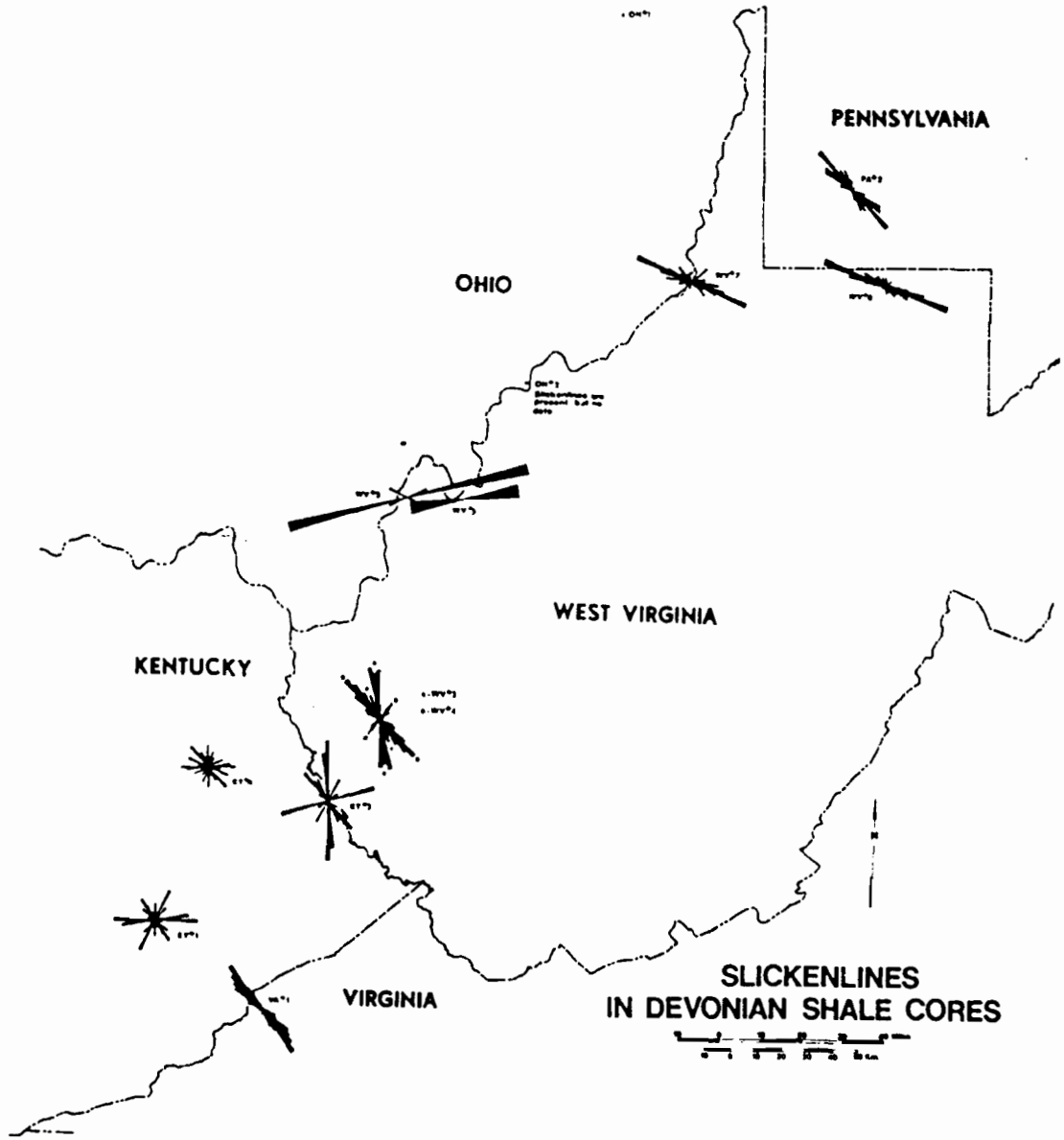

Figure 24. Regional slickenline patterns.

were moved to the west along several decollements in the Silurian Salina salt and Devonian shales. Several of the cores investigated in this study pass through the decollement zones in the Devonian shales. Décollement zones are characterized by intense deformation in the form of numerous slickensides and natural fractures throughout. They are usually found in the lowest viscosity (softest, least competent) strata, the black high organic shales, but may extend into higher viscosity (stiffer, more competent) rock. Décollement zones result from deformation, primarily simple (rectilinear) shear, being distributed across infinitely narrow faults. Distributing the shear markedly reduces the stresses associated with moving thrusts and the work expended in the process. This distributed shear is a natural consequence of the loading process thought to be responsible for gravity sliding and subhorizontal orogenic transport (Kehle, 1970). Deformation interpreted to be décollement zones was identified in southwestern Pennsylvania (PA #2), northern West Virginia (WV #6, WV #7), southwestern West Virginia (WV #3, WV #4), on the Pine Mountain overthrust sheet (VA #1), and possibly in eastern Kentucky (KY #4).

A model which seems to best describe the shear fracture (slickenside) orientations found in the décollement zones of the cores in this study is presented by Skempton (1966). It is the classic shear zone model that he describes which allows for three types of shear fractures: displacement shears, Riedel shears, and thrust shears. Displacement shears (D in figure 25) lie parallel or subparallel to the ab plane (figure 25). Riedel shears (R in figure 25) lie en echelon, and are inclined 10° to 30° to the ab plane, with the acute angle

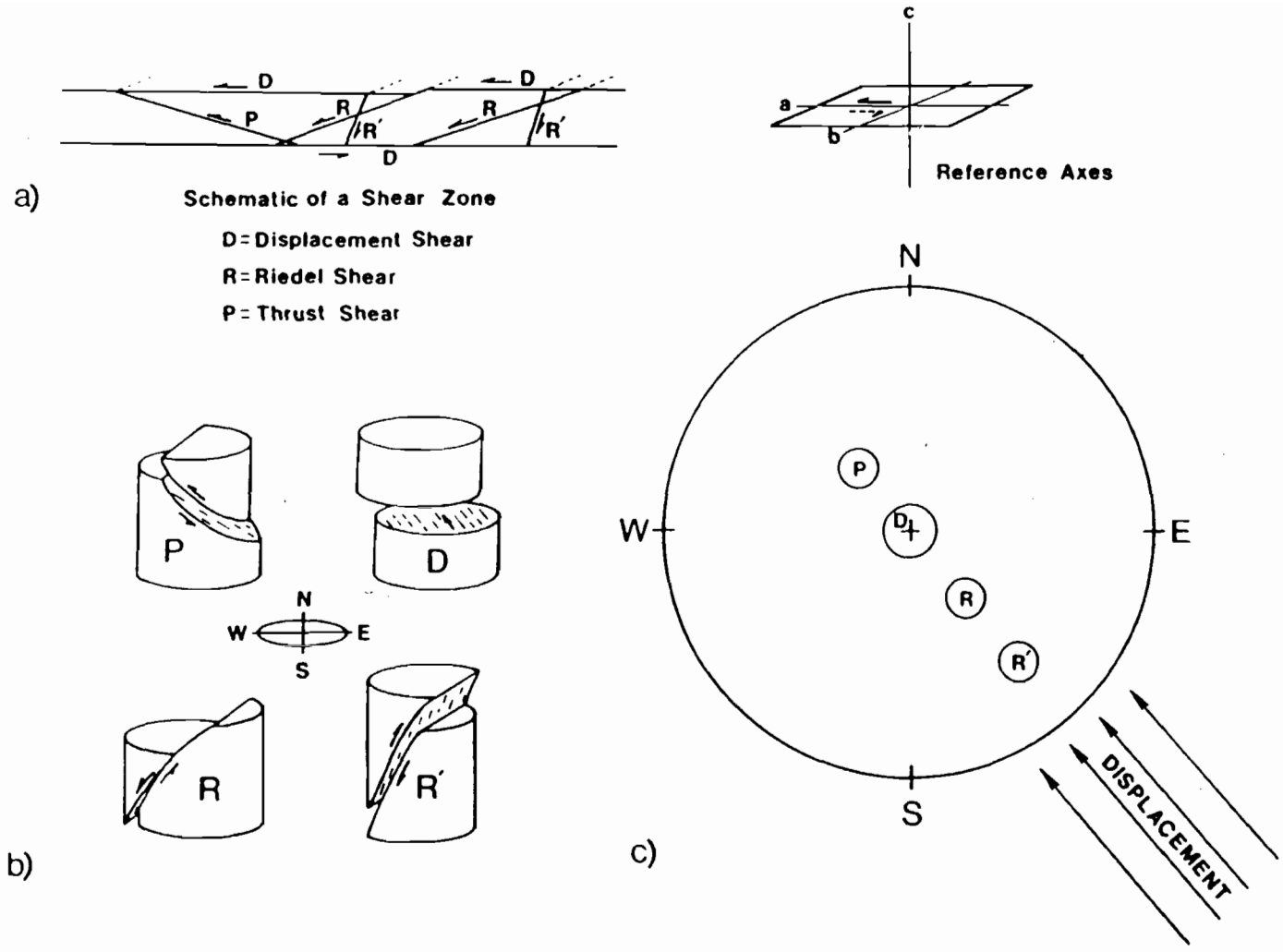

Figure 25. Shear zones

always pointing against the direction of relative movement. Ideally these shears are accompanied by a conjugate set R' (R' in figure 25) which should make an acute dihedral angle with the main R shears. Thrust shears (P in figure 25) have a dip opposite to the Riedel shears. The acute angle with the ab plane points in the direction of relative movement. The slickensided fractures, as they would appear in a vertical core cutting through a décollement zone, are shown in figure 25b. An equal area projection of poles to slickensided surfaces in a décollement zone would ideally exhibit four clusters (figure 25c). The sense of displacement in both illustrations is to the northwest. After formation, and with continuous shearing, the slip planes may rotate, altering the geometric relationships accordingly.

In several of the décollement zones, subhorizontal to horizontal slickensides, and at times inclined slickensides, were found to be mineralized with fibrous calcite. This is indicative of a very high fluid pressure in the shales and a vertical principal effective tension during mineralization (Durney and Ramsay, 1973). Such abnormally pressured rocks are preferred sites for décollement because they are probably less viscous than their normally pressured counterparts (Kehle, 1970). Fiber growth may have occured during or after décollement movement. The fibers are usually vertical, but they may be curved indicating movement during fiber growth.

As with natural fractures, slickensides and slickenlines exhibit a wide variety of orientations in eastern Kentucky. Most of the orientations can be related to fault movements in the area, either directly or through adjustment and compaction of the rocks after

faulting. Slickensides in the WV #2 (12041) and WV #5 (#3 D/K) cores from Jackson and Mason Counties, West Virginia, respectively, strike approximately N20°W. Slickenlines trend approximately N70°E. These trends may be related to the detached Burning Springs Anticline which is northeast of the wells.

The Lincoln County, West Virginia, Cores

The WV #3 (20403) and WV #4 (20402) core wells in Lincoln County, West Virginia, require a special discussion as they exhibit dramatic differences in orientations of all fracture types and slickenlines. This is true even though the wells are only 0.9 miles apart. Dominant fracture and slickenline patterns differ by approximately 30° between cores. There are, however, some fracture sets in each core that are unique to that core. The differences between the two cores may be the result of one or more of the following:

1) One, or both of the cores may not be oriented correctly. A problem in alignment could have arisen through misalignment of the orienting camera with the scribe marks on the core. The author checked core orientations, as marked after coring, and they agreed with the orientation logs. The alignment is therefore assumed to be correct.

2) One, or both of the cores may overlie a basement fault of the Rome Trough. The difference in fracture and slickenline patterns between the two cores may be related to altered stress distributions over a fault zone (Advani, 1977). In adjoining Mingo, Logan, Boone, and Kanawha Counties Kulander and Dean (1978a; 1978b) found chaotic fracturing in coals over a basement fault zone. Altered stress fields also could have affected the sense of movement in décollement zones

(Kulander and Dean, 1978).

3) Slickensides present in both cores suggest that the Devonian shales contain décollement zones. Movement within the décollement zones may have altered stress distributions in the shales, resulting in the formation of spatially variable fracture orientations.

4) The area in which the two wells are located is in the transition zone between the central and southern Appalachians. The intersection of the stress fields of both provinces may have resulted in altered stress distributions in the shales and, consequently, spatially variable fracture orientations. However, Dean and Kulander (1978) found no change in regional fracture trends from the southern Appalachians to the central Appalacians in southeastern West Virginia.

The second explanation in itself is most likely. However, the others may have contributed to some extent and should not be ignored, but checked in future investigations.

FRACTURE FREQUENCY

During the course of this study it was found that the occurrence and frequency of fractures in the cores is, in many cases, dependent on stratigraphy. This is true of all fracture types, but certain fracture types reflect this more so than others. Spacing changes from one lithology to another are expected. However, the occurrence of natural vertical unmineralized fractures, mineralized fractures, and slickensides together may create a permeability that is important to shale gas production. The occurrence of associated porosity within a highly fractured lithology has been called a porous fracture facies (Shumaker, 1978).

In order to investigate the stratigraphic position of the zones of intense fracturing in the 13 core wells, several stratigraphic cross sections were constructed in which the Middle and Upper Devonian units are correlated across the study area (plates 1 and 2). The Middle and Upper Devonian constitutes that portion of the Devonian between the Mississippian Berea Sandstone and the Devonian Onondaga Limestone. By examining the cross sections, one notices that the Middle and Upper Devonian section has its greatest thickness (nearly 6000 feet) in the PA #2 (C.E.P.S. #1) core well which is located near the center of the Appalachian Basin. To the south and to the west the thickness decreases, until, in eastern Kentucky, the section is only 600 feet thick. An unconformity on top of the Onondaga Limestone extends throughout the study area. Several units of the Middle Devonian are terminated against this unconformity just west of the center of the basin.

After correlating stratigraphic units, fracture frequency plots from the composite data sheets were placed on the cross sections. Three separate correlations were made, one each for core-induced fractures, natural fractures, and slickensides. Visual comparisons of the fracture frequencies were then made to determine which units had an abundance of, or lacked fractures.

Core-induced Fractures

Core-induced fracture frequencies remain quite consistent throughout the cored intervals and show very little similarity from core to core (plates 3 and 4). However, a general lack of core-induced fractures was found to be characteristic of the Java Formation and the West Falls Formation, particularly the Rhinestreet Member. It is also worth noting that it is near the base of the Java Formation that the core-induced fracture orientations generally deviate. The Sonyea Formation in the WV #7 (E-P #1) core and the Upper Huron Member in the KY #4 (#3 R-S) core are the only units in those cores in which core-induced fractures are found.

Natural Fractures

Unlike the core-induced fractures, natural fracture frequencies show distinct relationships to stratigraphic units (plates 5 and 6). The units which usually contain an abundance of natural fractures are the Marcellus Shale, Tully Limestone, Geneseo Shale, West Falls Formation, and the Lower Huron Member. Other units in the cores have natural fractures, but not in as great abundance. The Java Formation, on the other hand, generally lacks natural fractures.

Slickensides

Slickensides are generally found most frequently in those units which also have a high frequency of natural fractures (plates 7 and 8). The units which usually contain an abundance of slickensides are the Marcellus Shale, Tully Limestone, Geneseo Shale, West Falls Formation, base of the Java Formation, Lower Huron Member and Cleveland Member. Presumably, several of these units act as décollement zones in the Appalachian Plateau province.

This study has found the Lower Huron Member to be most important in that at least one slickenside has been found near the base of the Lower Huron Member in all cores which have sampled that interval (WV #3, WV #4, WV #5, KY #1, KY #3, and VA #1). The trend of the slickenlines on the slickensides are usually northeast-southwest. The slickensides are all very low dipping. The author has termed this the "Lower Huron slip plane" as it seems to be of regional extent throughout southwestern West Virginia and eastern Kentucky.

With exception of the Tully Limestone, the highly fractured units are in the softer, less competent organic shales. This is probably because the less competent strata absorbed a great proportion of the stresses associated with local and regional deformation and faulting.

The porous fracture facies concept is generally supported by this study. Units which are highly fractured may serve as conduits for the flow of gas in the subsurface, in which case, if an appropriate seal is present, these intervals may prove to be excellent producers. If, however, no seal is present, these highly fractured units may allow the gas to escape and abnormally low production would result.

CONCLUSIONS

Subsurface fractures in the Appalachian Plateau province can be related to Alleghenian deformation, local faulting, and crustal spreading along the Mid-Atlantic Ridge. Northwest directed tectonic compressive stresses present during Alleghenian deformation have resulted in a system of vertical, northwest striking natural fractures, and a system of northeast striking slickensides with northwest trending slickenlines. Anomalous fracture patterns have resulted from altered stress fields within the Rome Trough area, above basement fault zones in eastern Kentucky, southwestern West Virginia, and possibly southwestern Pennsylvania. Crustal spreading along the Mid-Atlantic Ridge is believed to result in an east to northeast trending maximum compressive stress throughout most of eastern North America. This stress is interpreted to have created a regional system of northeast striking natural fractures and an in-situ stress or rock fabric anisotropy which causes the formation of northeast striking core-induced fractures. The stress probably originated during the Mesozoic. In two of the cores studied, calcite mineralization was found primarily on the northeast striking natural fractures, and dolomite mineralization was found on the northwest striking fractures. This preferential mineralization suggests that the fractures of each trend formed, or were open, at different times.

Several of the cores investigated in this study pass through décollement zones in the Devonian shales. These zones are characterized by intense deformation in the form of numerous natural fractures and slickensides. The zones are found primarily in the lowest vis-

cosity strata and result from shear being distributed across the interval. Décollement zones are noted in cores from southwestern Pennsylvania, northern West Virginia, southwestern West Virginia, within the Pine Mountain thrust sheet in western Virginia, and possibly in eastern Kentucky, suggesting several detachments of regional extent. Slickensides in several of the décollement zones are mineralized with fibrous calcite, indicating the existence of a high fluid pressure in the shales. A model which seems to best describe the slickenside orientations found in décollement zones is the classic shear zone model.

Increased frequency of natural fractures and slickensides within less competent, and primarily shale units such as the Marcellus Shale, Tully Limestone, Geneseo Shale, West River Shale, West Falls Formation, base of the Java Formation, Lower Huron Member, and Cleveland Member support the concept of porous fracture facies for shale gas production (Shumaker, 1978). A porous fracture facies serves as a passageway for the gas in the subsurface. If a seal is present, the zone may prove to be an excellent producer. However, without a seal, the fractures may serve as escape routes for the gas. Several of the aforementioned units served as décollement zones. At least one slickenside is found at the base of the Lower Huron Member in each of the cores which intersect that unit. This is the most extensive slip plane found in the section studied.

The Devonian shale sequence in the western half of the Appalachian Basin contains large amounts of natural gas, but commercial gas production is limited to areas where natural fracture systems increase

the otherwise insignificant permeability. Delineation of zones of more intense fracturing, especially mineralized fractures, and understanding the nature of the fractures in the shale in terms of origin, orientation, and frequency, is crucial to an accurate apprasial of shale gas potential.

SUGGESTIONS FOR FUTURE WORK

1. Surface fracture orientation data for the Appalachian Plateau province needs to be examined to determine relationships with subsurface natural and core-induced fracture patterns. In some areas surface fracture patterns may be useful in predicting subsuface fracture patterns, and thus help in determining well stimulation strategies.

2. Linear features (lineaments) picked on high and low altitude photographs, and satellite images of areas around oriented-core wells may prove useful in predicting both subsurface and surface fracture patterns.

3. The regional subsurface fracture patterns found in this study may extend throughout the entire Appalachian Plateau province. The study area needs to by extended into eastern Tennessee, central West Virginia, northern Pennsylvania, and southern New York state. Oriented cores are available from eastern Tennessee, northern Pennsylvania, and southern New York state.

4. Four of the cores used in this study were not examined personally by the author. The cores (KY #1, KY #3, OH #1, and OH #2), which are in very poor condition, need to be examined in detail to differentiate fracture types, fracture orientations, and mineral fillings.

5. The two cores from Lincoln County, West Virginia, are only 0.9 miles apart and yet have such different fracture patterns. More work needs to be done to determine why these cores are so different.

6. Very little is known about conditions in decollement zones

during décollement movement. Since several of the cores investigated in this study intersect décollement zones, a unique opportunity is presented to study their formation and effects. Among the structures which may be used are slickenside and slickenline orientations, natural fracture orientations, shale microfabric, microstructures, mineral filling types, and mineral fibers.

7. The consistent core-induced fracture orientations found in the cores may be related to some type of stress or rock fabric anisotropy. An extensive petrographic study of all shale types could determine whether or not a microcrack system, or other type of rock fabric anisotropy, exists.

8. The three cored wells in eastern Kentucky indicate that the area is chaotically fractured. More work needs to be done to determine the cause for this, and if it is related to basement faulting and resultant stresses. Also, the chaotic fracturing should be examined in relation to the high shale gas production in the area.

REFERENCES

Abdel-Rahman, M. A., and Hay, A. M., 1978, ms, Statistical analysis of multi-modal orientation data: in review for 3rd International Conference on Basement Tectonics Proceedings, 24 ms p.

Advani, S. H., GangaRao. H. V. S., Chang, H. Y., Dean, C. S., and Overbey, W. K., Jr., 1977, Stress trajectory simulations across the Appalachian Plateau province in West Virginia, in Proceedings: First Eastern Gas Shales Symposium: USERDA-Morgantown Energy Research Center, MERC/SP-77/5, p. 442-448.

Cardwell, D. H., 1974, Oriskany and Huntersville Gas Fields of West Virginia: W. Va. Geol. and Econ. Surv. Min. Res. Series No. 5, map, scale 1:250,000, 2 sheets.

Cardwell, D. H., Erwin, R. B., and Woodward, H. P., 1968, Geologic Map of West Virginia: W. Va. Geol. and Econ. Surv., scale 1:250,000, 2 sheets.

Dean, S. C., and Kulander, B. R., 1978, Chronology of fold development between the central and southern Appalachians, southern West Virginia, in Abstracts with programs, Southeast Section, Geol. Soc. Am., v. 10, No. 3, p. 166-167.

deWys, J. N., and Renton, J. J., 1979, Inorganic geochemistry studies of the eastern Kentucky gas field, in Proceedings: Third Eastern Gas Shales Symposium, H. Barlow, ed.: USDOE-Morgantown Energy Technology Center, METC/SP-79/6, p. 165-209.

Dixon, J. M., 1979, A method to identify zones of intense jointing with application to the Parsons Lineament, West Virginia: Open-file Report, USDOE-Morgantown Energy Technology Center, 46 p.

Durney, D. W., and Ramsay, J. G., 1973, Incremental strains measured by syntectonic crystal growth, in Gravity and Tectonics, K. Dejong and R. Scholten, eds.: John Wiley, New York, p. 67-96.

Engelder, T., 1979, Mechanisms for strain within the Upper Devonian clastic sequence of the Appalachian Plateau, western New York: Am. Jour. Sci., v. 279, p. 527-542.

Evans, M. A., 1978, Fracture density and orientation of the Reel Energy #3 D/K core from Mason County, West Virginia: Open-file Report No. 52, USDOE-Morgantown Energy Technology Center, 48 p.

_____. 1979, Fracture density and orientation study of the MERC #1 core from Monongalia County, West Virginia: Open-file Report, USDOE-Morgantown Energy Technology Center, 38 p.

Friedman, M., 1967, Structural analysis of fractures in cores from the Santicoy Field, Ventura County, California: Am. Assoc. Petrol. Geologists Bull., v. 53, p. 367-389.

Frone, K. H., 1978, Deep Devonian shale gas test in northern West Virginia, in Pre-prints for: Second Eastern Gas Shales Symposium, Vol. 2: USDOE-Morgantown Energy Technology Center, METC/SP-78/6, p. 89-99.

Hamison, B., and Stahl, E. J., 1969, Hydraulic fracturing and the extraction of minerals through wells, in Third Symposium on Salt: Northern Ohio Geol. Surv., p. 421-432.

Harris, L. D., 1978, The Eastern Interior Aulacogen and its relation to Devonian shale-gas production, in Pre-prints for: Second Eastern Gas Shales Symposium: USDOE-Morgantown Energy Technology Center, METC/SP-78/6, p. 55-72.

Harris, L. D., and Milici, R. C., 1977, Characteristics of thin-skinned style of deformation in the southern Appalachians and potential hydrocarbon traps: U. S. Geol. Surv. Prof. Paper 1018, 40 p.

Kehle, R. O., 1970, Analysis of gravity sliding and orogenic translation: Geol. Soc. Am. Bull., v. 18, p. 1641-1664.

Komar, C. A., Frone, K. H., and Yost, A. B., 1978, Stimulation technology: a progress review: Open-file Report, USDOE-Morgantown Energy Technology Center, 68 p.

Kuiper, N. H., 1960, Test concerning random points on a circle: Indag. Math, v. 22, p. 38-47.

Kulander, B. R., Barton, C. C., and Dean, S. L., 1979, The application of fractography to core and outcrop fracture investigations: USDOE-Morgantown Energy Technology Center, 167 p.

Kulander, B. R., and Dean, S. L., 1978a, ms, Rome Trough relationship to fracture domains, regional stress history, and decollement structures: in review for Proc. Southeast Section Geological Soc. Am. Symposium on western limits of detachment and related structures in the Appalachian foreland, 7 ms p.

_____. 1978b, Fracture domain correlation with Rome Trough structure, geophysical anomalies, and regional stress configuration, south central West Virginia, in Abstracts with Programs, Southeastern Section, Geol. Soc. Am., v. 10, No. 3, p. 173.

Kulander, B. R., Dean, S. L., and Barton, C. C., 1977, Fractographic logging for determination of pre-core and core-induced fractures-Nicholas Combs No. 7239 well, Hazard, Kentucky: USERDA-Morgantown Energy Research Center, MERC-77/3, 44 p.

Larese, R. E., and Heald, M. T., 1977, Petrography of selected Devonian shale core samples from the CGTC 20403 and CGSC 11940 wells, Lincoln and Jackson Counties, West Virginia: USERDA-Morgantown Energy Research Center, MERC/CR-77/6, 22 p.

Long, B. R., 1979, Regional survey of surface fractures in eastern Kentucky: Masters thesis, West Virginia University, Morgantown, W. Va., 66 p.

Neal, D. W., 1979, Subsurface stratigraphy of the Middle and Upper Devonian clastic sequence in southern West Virginia and its relation to gas production: Ph.D. dissertation, West Virginia University, Morgantown, W. Va., 144 p.

Obert, L., 1962, In-situ determination of stress in rock: Mining Engineer, v. 14, p. 51-58.

Overbey, W. K., Jr., 1969, Stress fields as indicated by fracture orientations - potential applications to petroleum production: Paper presented at the U. N. Forth Symposium on the Development of Petroleum Resources of Asia and the Far East, Canberra, Australia, Oct. 27-Nov. 10, 1968, 18 p.

_____. 1976, Effect of in-situ stresses on induced fractures, in Devonian ShaleProduction and Potential: Proc. Seventh Appalachian Petroleum Geology Symposium, Morgantown, W. Va., March 1-4, 1976, USERDA-Morgantown Energy Researcg Center, MERC/SP-76/2, p. 182-211.

Overbey, W. K., Jr., and Rough, R. L., 1968, Surface studies predict orientation of induced formation fractures: Producers Monthly, v. 32, p. 16-19.

_____. 1971, Prediction of oil-and-gas-bearing rock fractures from surface structural features: U. S. Bureau Mines Rept. Inv. 7500, 14 p.

Peng, S. S., and Okubo, S., 1978, Prediction of in-situ stresses from directional properties of rock cores for field development of Devonian shales: Open-file Report No. 108, USDOE-Morgantown Energy Technology Center, 72 p.

Root, S. I., and Hoskins, D. M., 1977, Lat. 40°N fault zone, Pennsylvania: a new interpretation: Geology, v. 5, p. 719-723.

Rough, R. L., and Lambert, W. G., 1971, In-situ strain orientations: a comparison of three measuring techniques: U. S. Bureau Mines Rept. Inv. 7575, 17 p.

Sbar, M. L., and Sykes, L. R., 1973, Contemporary compressive stress and siesmicity in eastern North America: an example of intraplate tectonics: Geol. Soc. Am. Bull., v. 84, p. 1861-1882.

Schaefer, W. M., 1979, Geology and producing characteristics of the Devonian brown shale, Midway-Extra Field, Putnam County, West Virginia: Masters thesis, West Virginia University, Morgantown, West Virginia, 67 p.

Secor, D. T., Jr., 1965, Role of fluid pressure in jointing: Am. Jour. Sci., v. 263, p. 633-646.

_____. 1969, Mechanics of natural extension fracturing at depth in the earth's crust, in Research in Tectonics: Canada Geol. Surv. Paper 68-52, 48 p.

Shumaker, R. C., 1978, Porous fracture facies in the Devonian shales of eastern Kentucky and West Virginia, in Preprints for: Second Eastern Gas Shales Symposium, vol. 1: USDOE- Morgantown Energy Technology Center, METC/SP-78/6, p. 360-369.

_____. 1979, Paleozoic disruptive deformation in North American Continent and its relation to formation and development of interior basins and deformation within orogenic core: abstract, Am. Assoc. Petrol. Geol. Bull., v. 63, p. 1588.

Skempton, A. W., 1966, Some observations on tectonic shear zones, in Proc. First Congress of the International Society of Rock Mechanics, p. 329-335.

Stearns, D. W., and Friedman, M., 1972, Reservoirs in fractured rock, in Stratigraphic Oil and Gas Fields: Am. Assoc. Petrol. Geol. Memoir 16, p. 82-106.

Vickers, M. K., 1976, Marietta: unpublished manuscript, W. Va. Geol. Surv., 10 ms p.

Vinopal, R. J., Nuhfer, E. B., and Klanderman, D. S., 1979, A petrologic evaluation of the significance of natural fractures in low porosity shale reservoirs - results of investigation in the Upper Devonian of West Virginia and Virginia, in Proceedings: Third Eastern Gas Shales Symposium: USDOE- Morgantown Energy Technology Center, METC/SP-79/6, p. 63-78.

Voight, B., 1969, Evolution of North Atlantic Ocean: revelence of rock pressure measurements, in North Atlantic - Geology and Continental Drift: Am. Assoc. Petrol. Geol. Memoir 12, p. 955-962.

Wagner, W. R., and Lytle, W. S., 1976, Greater Pittsburgh region revised surface structure and its relation to oil and gas fields: Penn. Geol. Surv. Info. Circ. 80, 20 p.

Werner, E. W., 1977, ms, Program to plot orientation data: unpublished manuscript, West Virginia University, Morgantown, West Virginia, 23 ms p.

Wilkinson, W. M., 1953, Fracturing in Spraberry Reservoir, West Texas: Am. Assoc. Petrol. Geol. Bull., v. 37, p. 250-265.

Wilson, T. H., Dixon, J. M., Shumaker, R. C., and Wheeler, R. L., 1978, ms, Fracture patterns observerd in cores from the Devonian shale of the Appalachian Basin: in review for Proc. Southeast Section Geol. Soc. Am. Symposium on Western Limits of Detachment and Related Structurs in the Appalachian Foreland, 19 ms p.

Young, D. M., 1957, Deep drilling through Cumberland overthrust block in southwest West Virginia: Am. Assoc. Petrol. Geol. Bull., v. 41, p. 2567-2573.

☆ U S GOVERNMENT PRINTING OFFICE 1983-646-069/772

PLATE I

UPPER AND MIDDLE DEVONIAN

Sheet 1

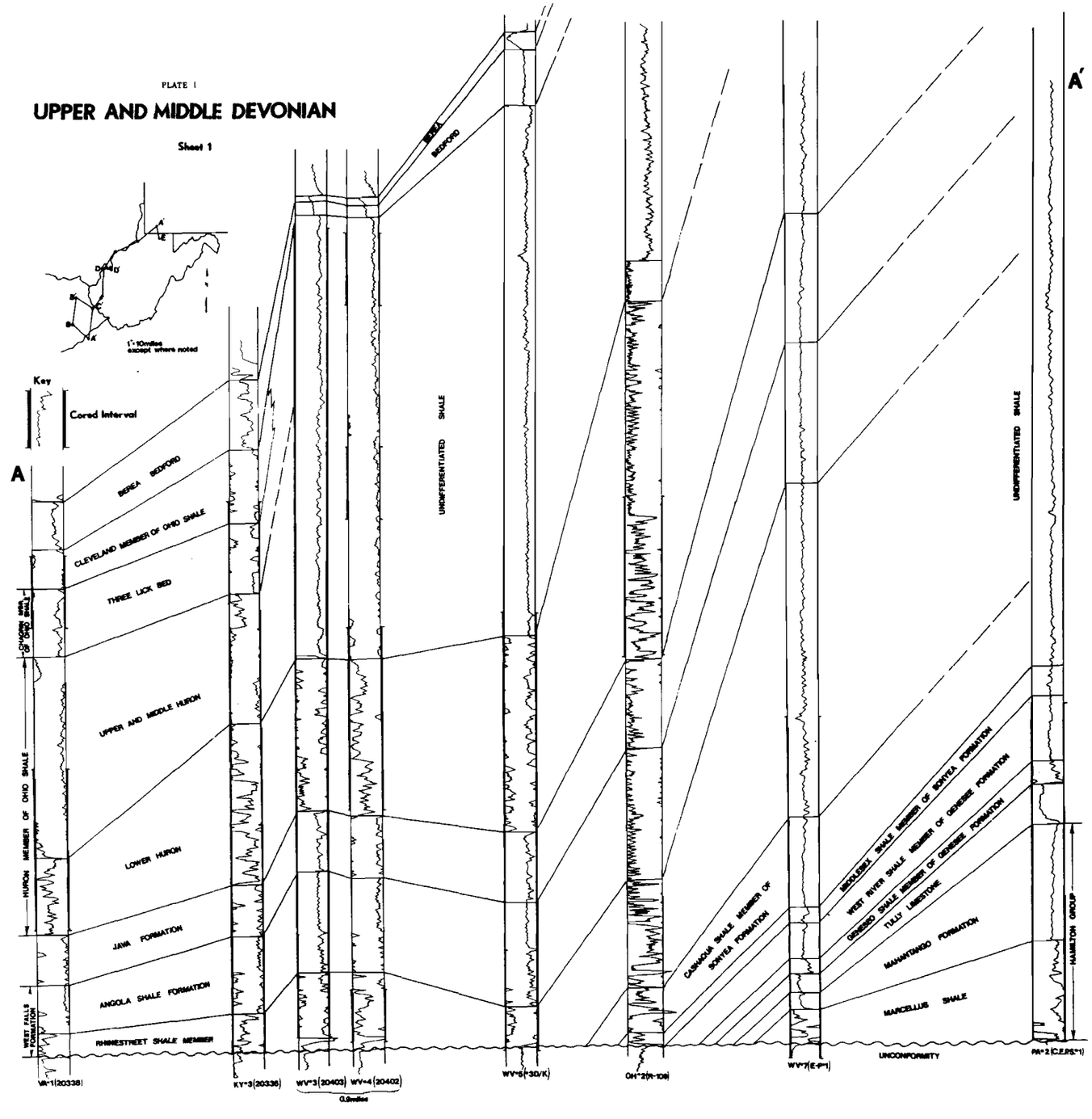

PLATE 2

UPPER AND MIDDLE DEVONIAN

Sheet 2

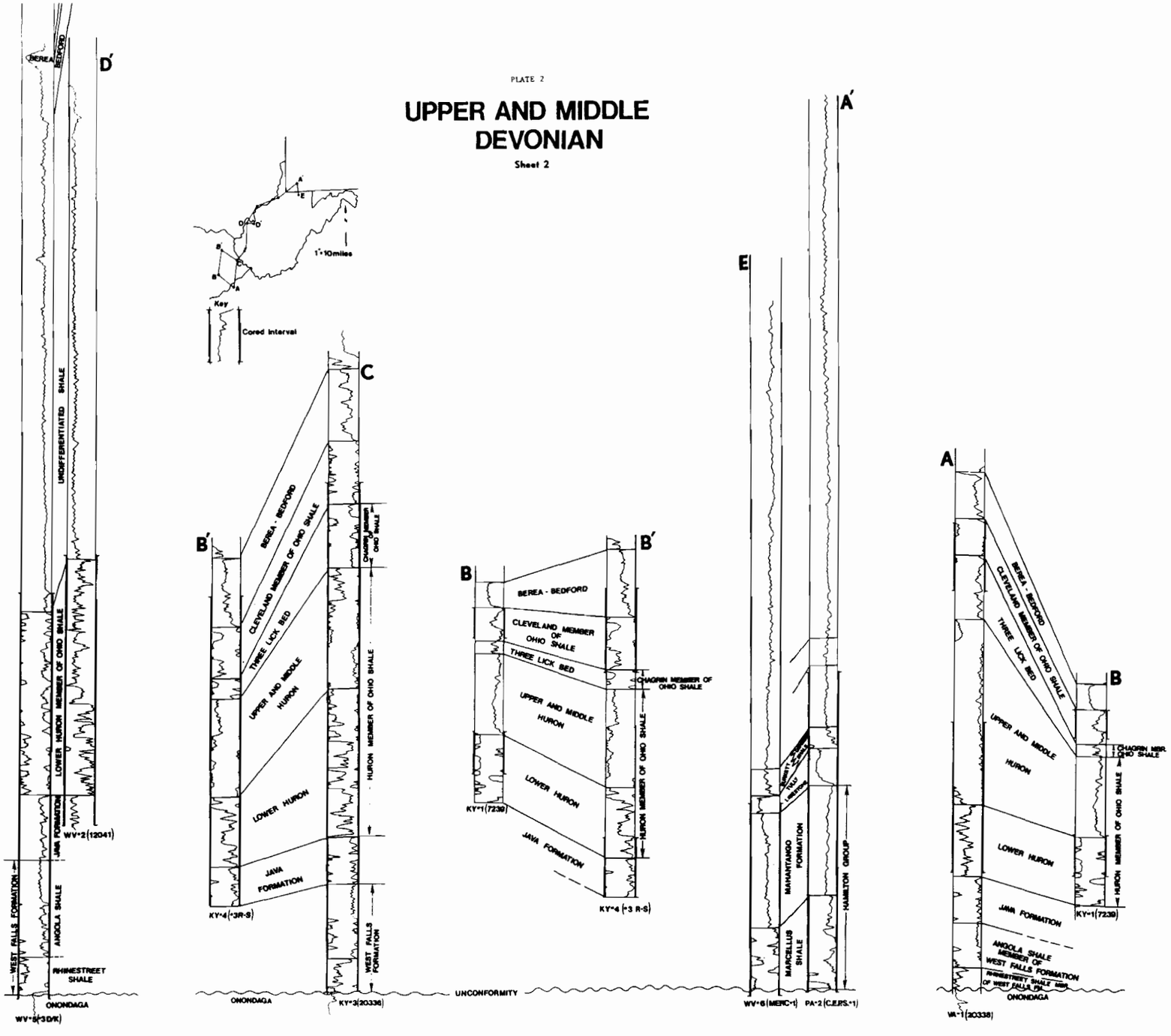

PLATE 3

UPPER AND MIDDLE DEVONIAN CORE-INDUCED FRACTURES

Sheet 1

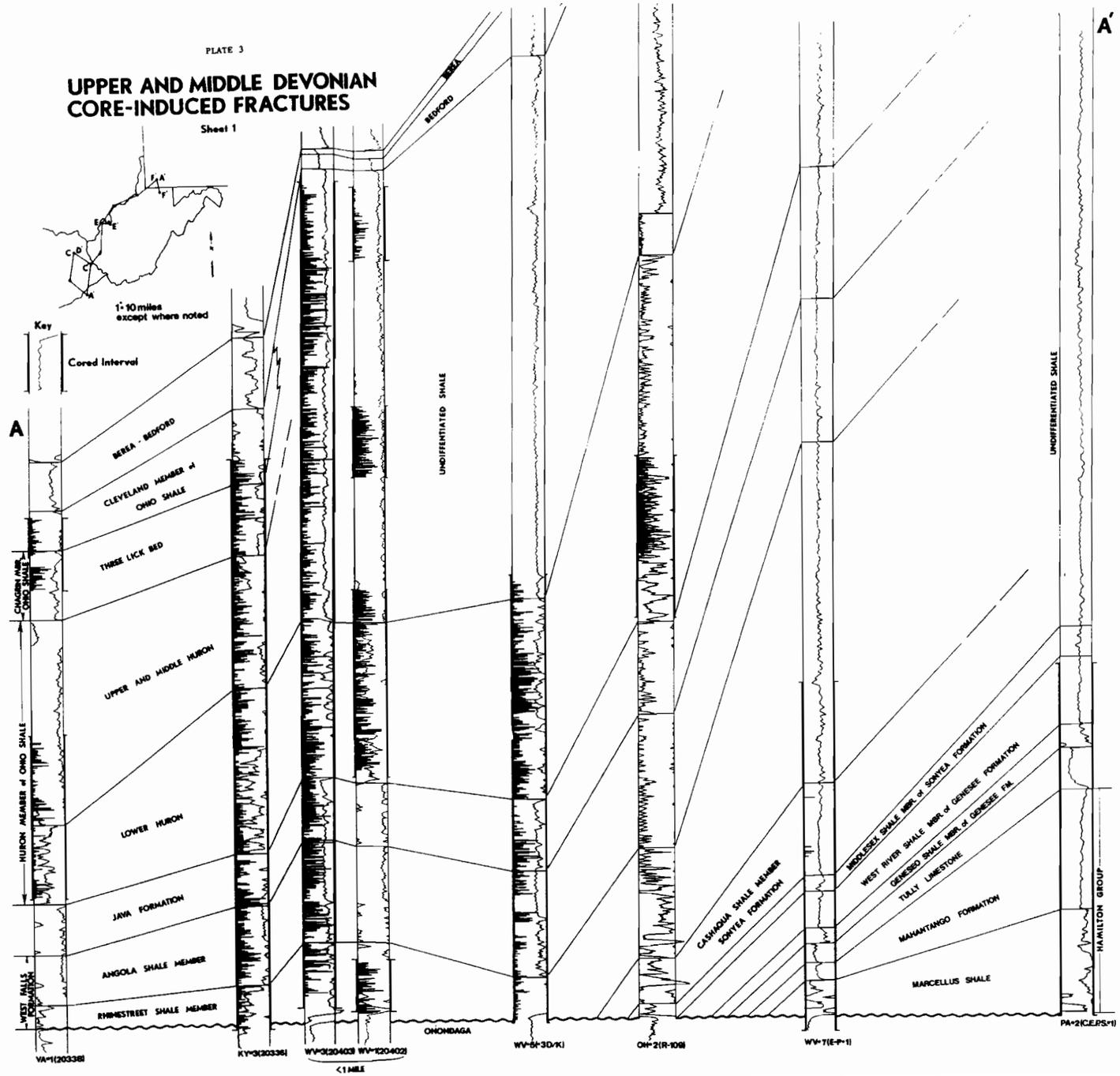

UPPER AND MIDDLE DEVONIAN CORE-INDUCED FRACTURES

Sheet 2

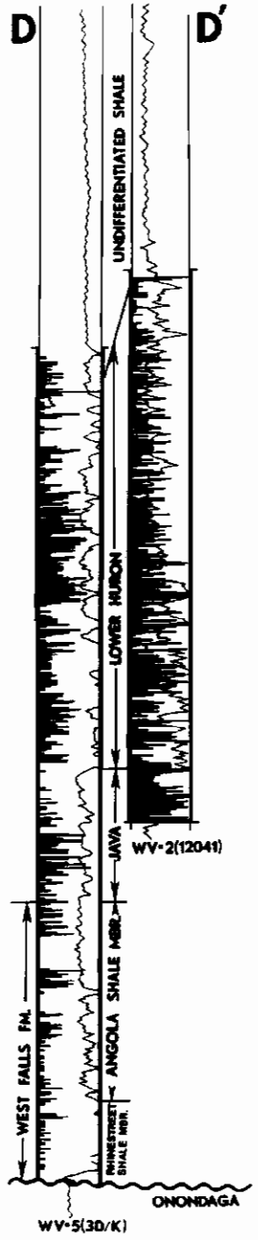

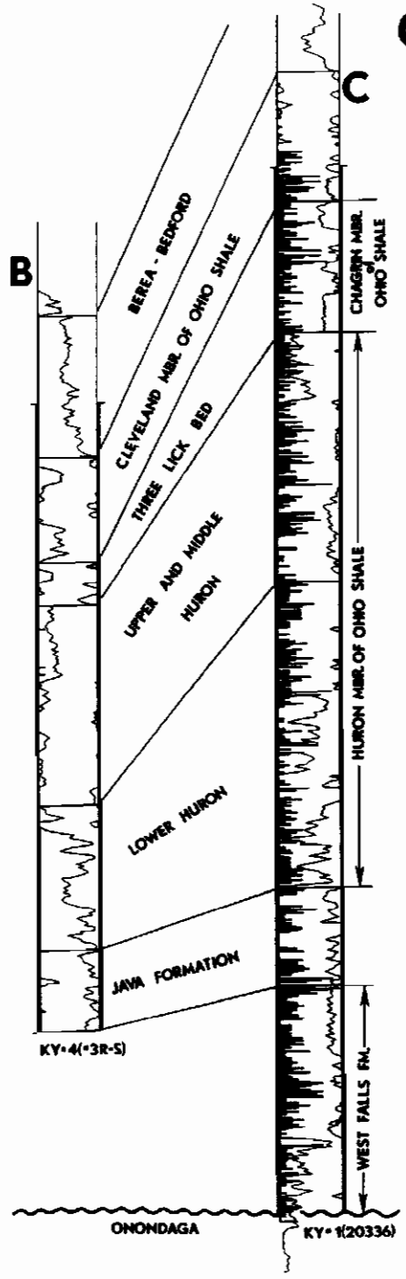

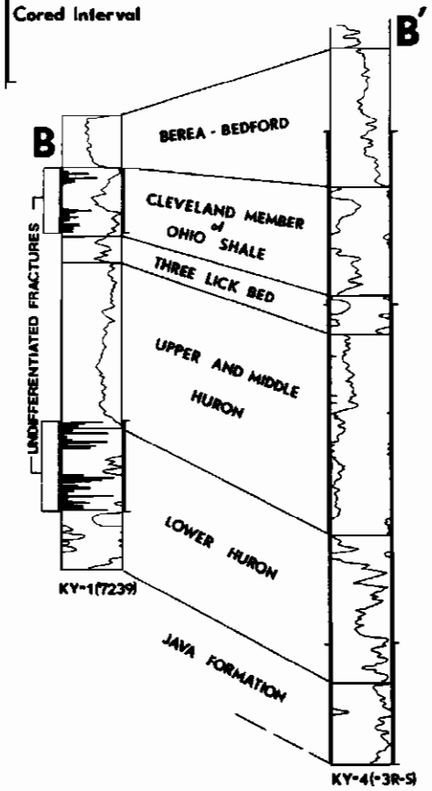

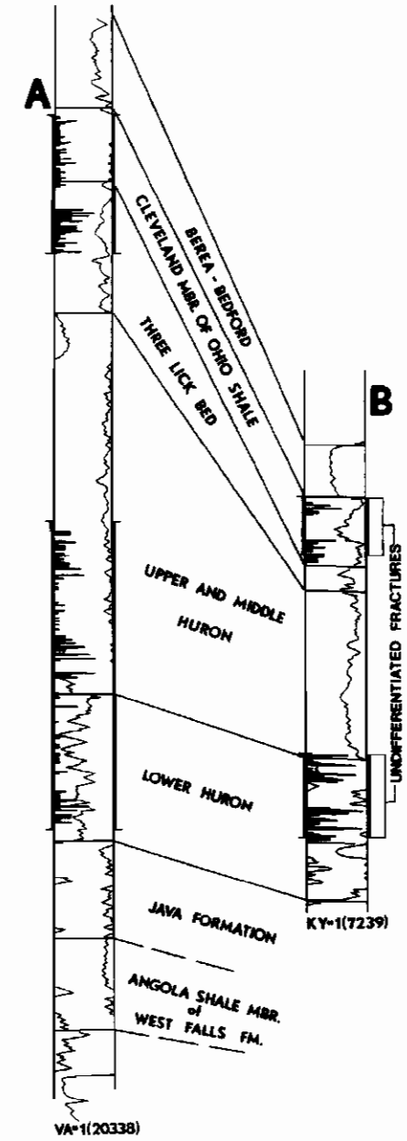

PLATE 5

UPPER AND MIDDLE DEVONIAN NATURAL FRACTURES

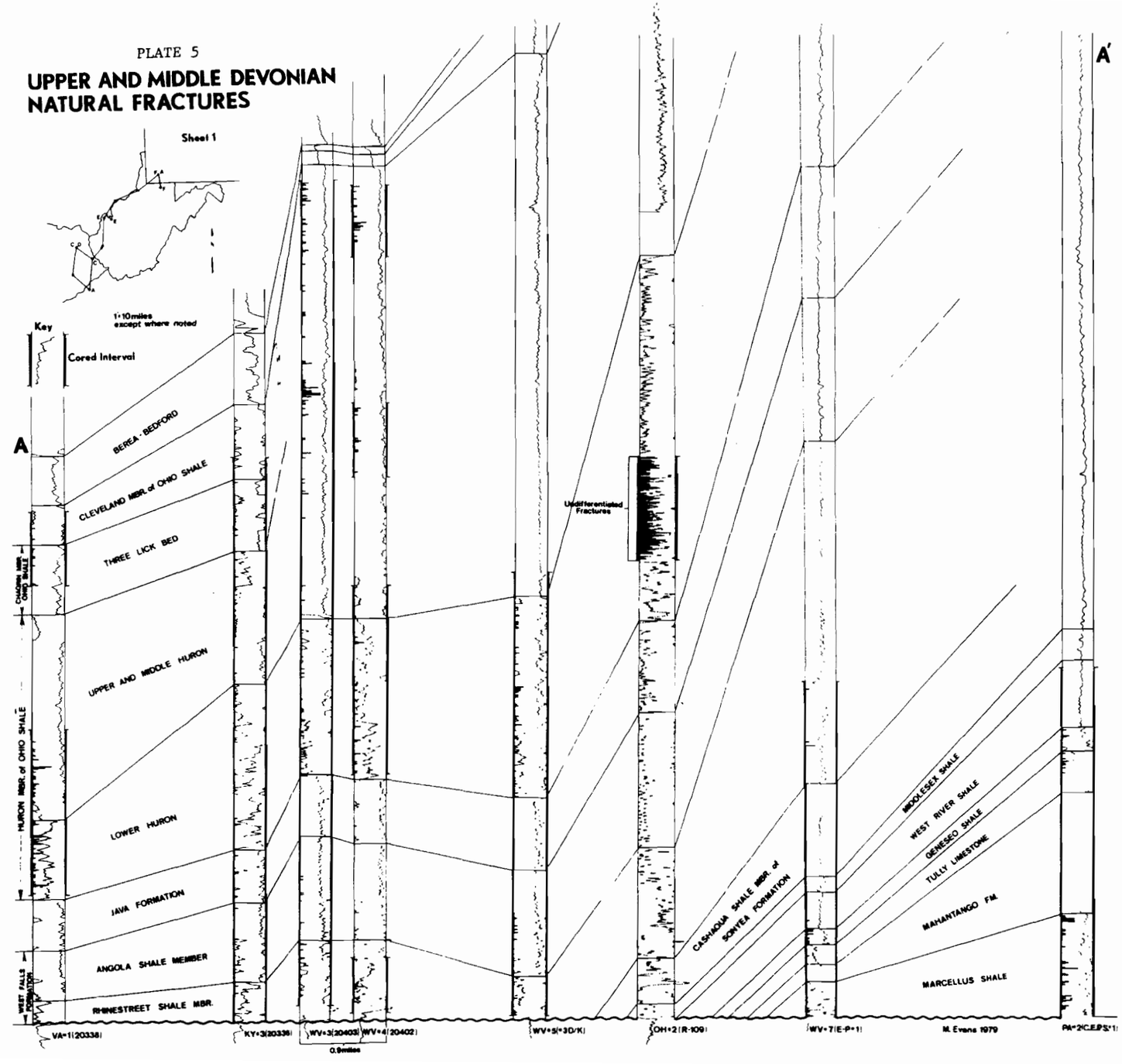

PLATE 6

UPPER AND MIDDLE DEVONIAN NATURAL FRACTURES

Sheet 2

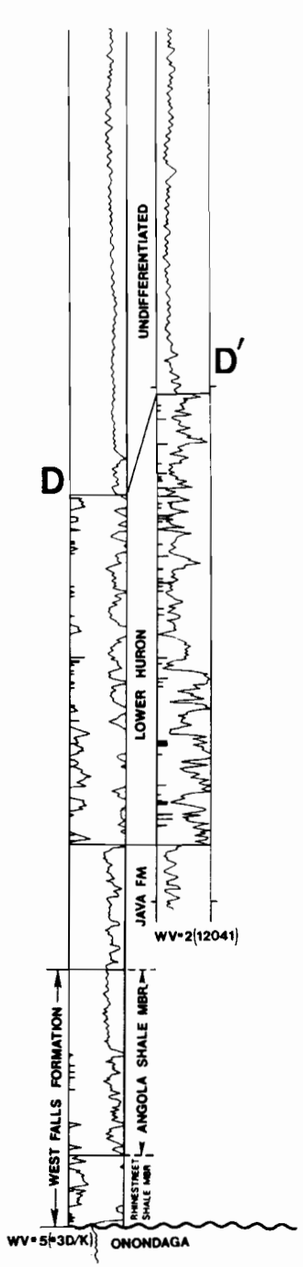

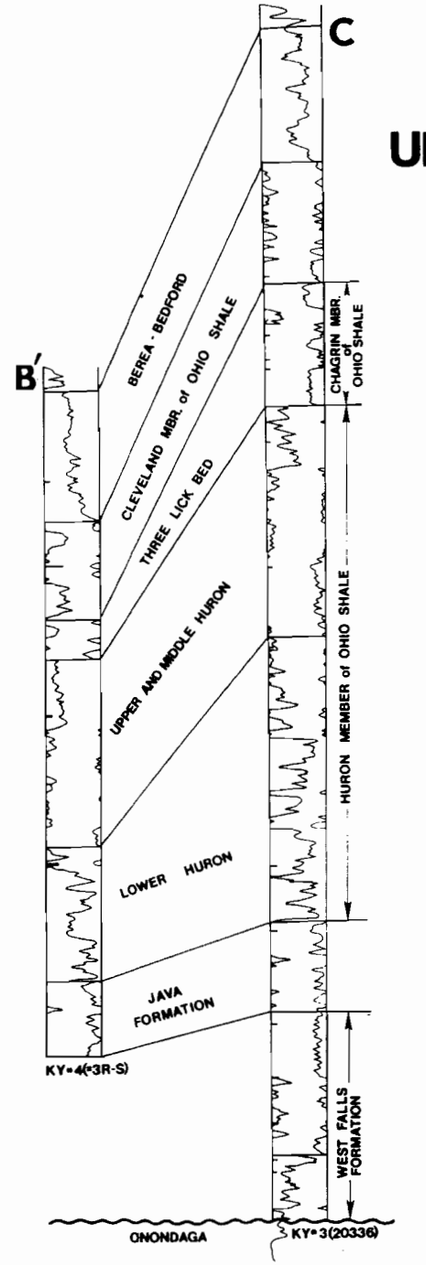

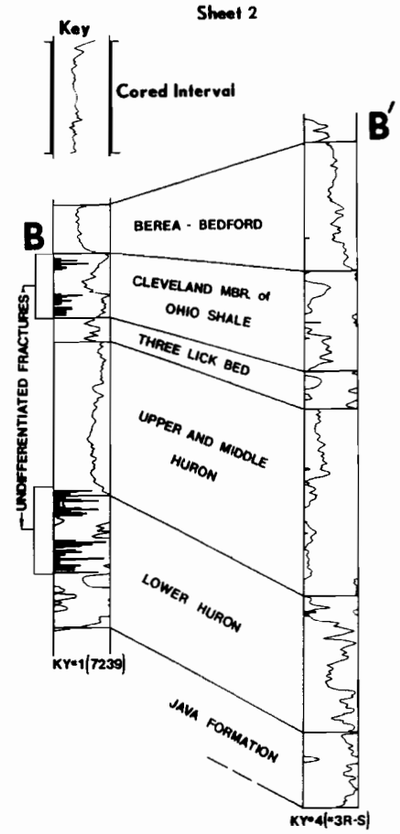

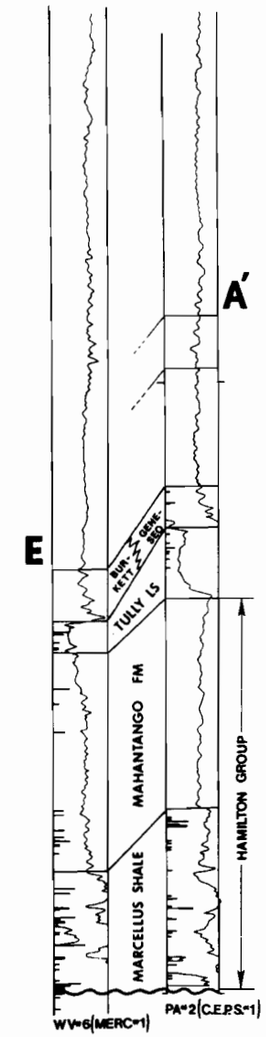

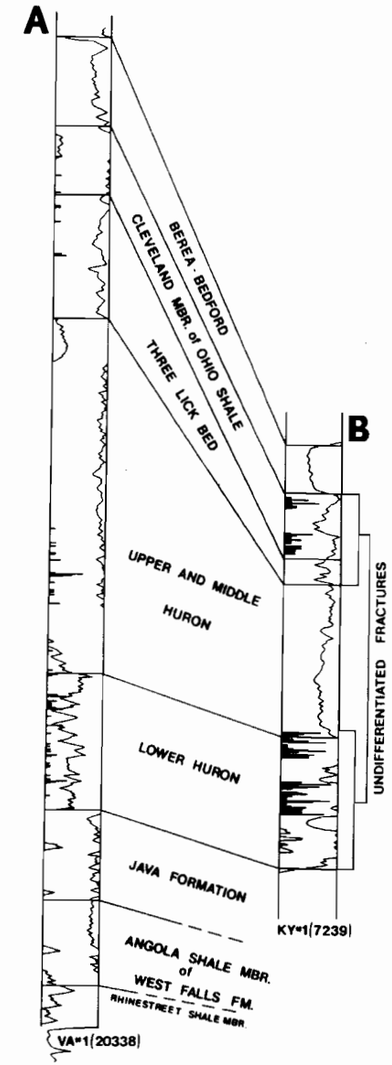

PLATE 7

UPPER AND MIDDLE DEVONIAN SLICKENSIDES

Sheet 1

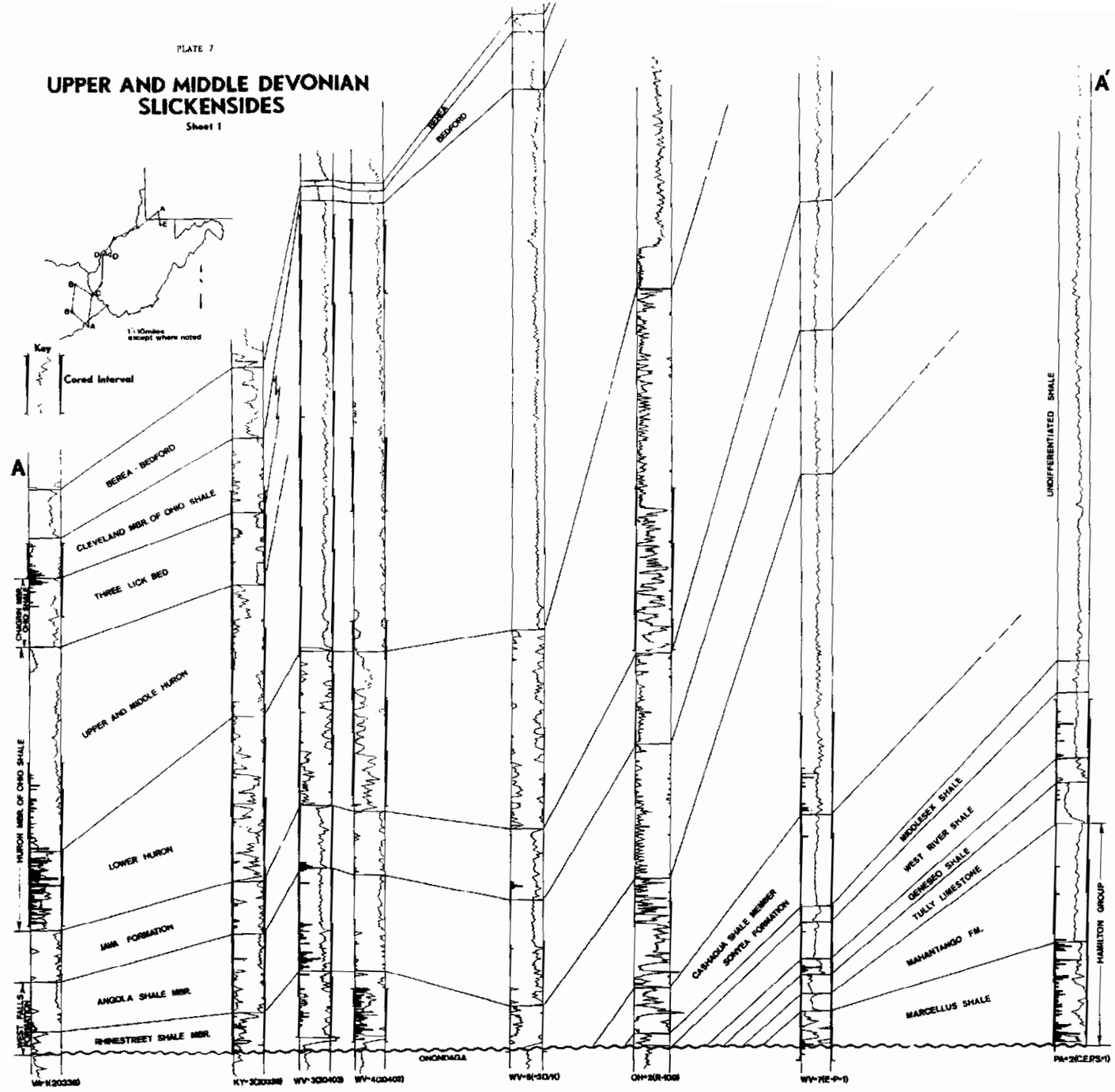

UPPER AND MIDDLE DEVONIAN SLICKENSIDES

Sheet 2

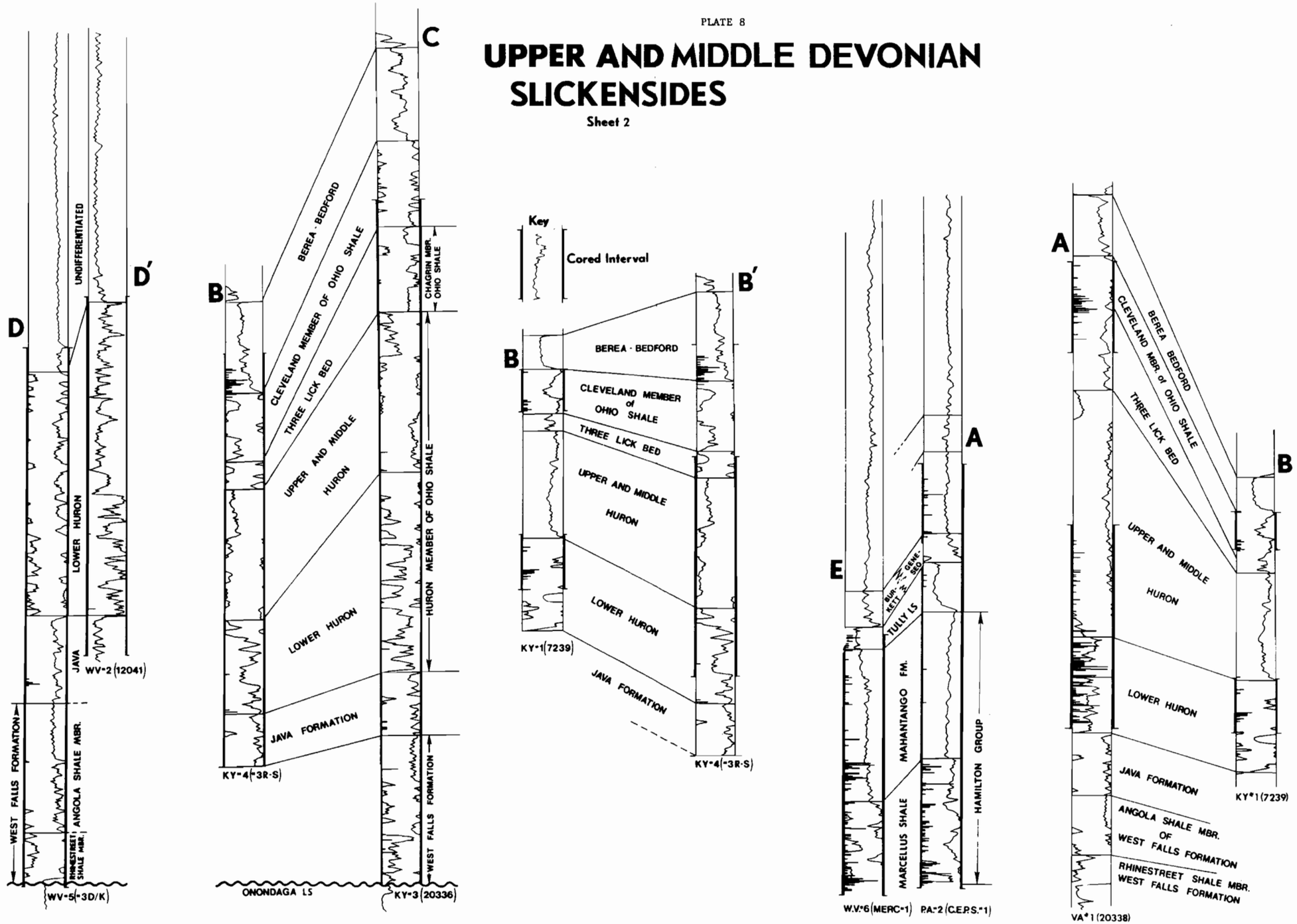

UGR #259

DOE/ET/12138-1341(Vol.2)
(DE83008483)
Distribution Category UC-92a

FRACTURES IN ORIENTED DEVONIAN SHALE CORES FROM THE APPALACHIAN BASIN
VOLUME II (Appendices)

BY

Mark A. Evans, Research Associate
Department of Geology & Geography
College of Arts & Sciences
West Virginia University
Morgantown, W.V. 26506

January 1980

Prepared For

United States Department of Energy
Morgantown Energy Technology Center
Morgantown, West Virginia

Under Contract No. DE-AC21-76ET12138

DOE/ET/12138-1341(Vol.2)
(DE83008483)
Distribution Category UC-92a

FRACTURES IN ORIENTED DEVONIAN SHALE CORES FROM THE APPALACHIAN BASIN
VOLUME II (Appendices)

BY

Mark A. Evans, Research Associate
Department of Geology & Geography
College of Arts & Sciences
West Virginia University
Morgantown, W.V. 26506

January 1980

Prepared For

United States Department of Energy
Morgantown Energy Technology Center
Morgantown, West Virginia

Under Contract No. DE-AC21-76ET12138

TABLE OF CONTENTS

page

LIST OF FIGURES..... iii

LIST OF TABLES..... xiii

INTRODUCTION TO APPENDICES..... 66

APPENDIX A: WV #2 (12041) CORE WELL..... 67

APPENDIX B: WV #3 (20403) CORE WELL..... 85

APPENDIX C: WV #4 (20402) CORE WELL..... 106

APPENDIX D: WV #5 (#3 D/K) CORE WELL..... 125

APPENDIX E: WV #6 (MERC #1) CORE WELL..... 147

APPENDIX F: WV #7 (E-P #1) CORE WELL..... 161

APPENDIX G: OH #1 (S-745) CORE WELL..... 177

APPENDIX H: OH #2 (R-109) CORE WELL..... 185

APPENDIX I: VA #1 (20338) CORE WELL..... 195

APPENDIX J: PA #2 (C.E.P.S. #1) CORE WELL..... 214

APPENDIX K: KY #1 (7239) CORE WELL..... 228

APPENDIX L: KY #3 (20336) CORE WELL..... 244

APPENDIX M: KY #4 (#3 R-S) CORE WELL..... 261

LIST OF FIGURES

figure page

A-1. Index map for the WV #2 (12041) core well 72

A-2. Gamma-ray log, Middle and Upper Devonian - WV #2 (12041) core well 73

A-3. (A) composite rose diagram of core-induced fracture strikes, and (B) equal area projection of poles to core-induced fracture surfaces - WV #2 (12041) core 74

A-4. Equal area projections of poles to core-induced fracture surfaces and rose diagrams of core-induced fracture strikes for approximately equal length intervals of the WV #2 (12041) core 75

A-5. Histograms of core-induced fracture orientations - WV #2 (12041) core 76

A-6. (A) composite rose diagram of natural fracture strikes, and (B) equal area projection of poles to natural fracture surfaces - WV #2 (12041) core 78

A-7. Equal area projections of poles to natural fracture surfaces and rose diagrams of natural fracture strikes for approximately equal length intervals of the WV #2 (12041) core 79

A-8. (A) composite rose diagram of slickenside strikes, and (B) equal area projection of poles to slickensided surfaces - WV #2 (12041) core 80

A-9. Equal area projection of poles to slickensides surfaces and rose diagrams of slickenside strikes for approximately equal depth intervals of the WV #2 (12041) core . 81

A-10. (A) composite rose diagram of slickenline trends, and (B) equal area projection of slickenlines - WV #2 (12041) core 82

A-11. Equal area projections of slickenlines and rose diagrams of slickenline trends for approximately equal length intervals of the WV #2 (12041) core 83

A-12. Composite data sheet of fracture frequencies and orientations for all fracture types 84

B-1. Index map of the WV #3 (20403) core well 92

B-2. Gamma-ray log, Middle and Upper Devonian - WV #3 (20403) core well 93

B-3. (A) composite rose diagram of core-induced fracture strikes, and (B) equal area projection of poles to core-induced fracture surfaces - WV #3 (20403) core 94

LIST OF FIGURES (CONT.)

figure page

B-4. Equal area projections of poles to core-induced fracture surfaces and rose diagrams of core-induced fracture strikes for approximately equal length intervals of the WV #3 (20403) core 95

B-5. Histograms of core-induced fracture orientations - WV #3 (20403) core 96

B-6. (A) composite rose diagram of natural fracture strikes, and (B) equal area projection of poles to natural fracture surfaces - WV #3 (20403) core 98

B-7. Equal area projections of poles to natural fracture surfaces and rose diagrams of natural fracture strikes for approximately equal length intervals of the WV #3 (20403) core 99

B-8. N30°W striking dolomite filled natural fracture from interval 3030'-3070' - WV #3 (20403) core 100

B-9. (A) composite rose diagram of slickenside strikes, and (B) equal area projection of poles to slickensided surfaces - WV #3 (20403) core 101

B-10. Equal area projections of poles to slickensided surfaces and rose diagrams of slickenside strikes for approximately equal length intervals of the WV #3 (20403) core 102

B-11. (A) composite rose diagram of slickenline trends, and (B) equal area projection of slickenlines - WV #3 (20403) core 103

B-12. Equal area projections of slickenlines and rose diagrams of slickenline trends for approximately equal length intervals of the WV #3 (20403) core 104

B-13. Composite data sheet of fracture frequencies and orientations for all fracture types - WV #3 (20403) core 105

C-1. Index map for the WV #4 (20402) core well 112

C-2. Gamma-ray log, Middle and Upper Devonian - WV #4 (20402) core well 113

C-3. (A) composite rose diagram of core-induced fracture strikes, and (B) equal area projection of poles to core-induced fracture surfaces - WV #4 (20402) core 114

C-4. Equal area projections of poles to core-induced fracture surfaces and rose diagrams of core-induced fracture strikes for approximately equal length intervals of the WV #4 (20402) core 115

LIST OF FIGURES (CONT.)

figure page

C-5. Histograms of core-induced fracture orientations - WV #4 (20402) core 116

C-6. (A) composite rose diagram of natural fracture strikes, and (B) equal area projection of poles to natural fracture surfaces - WV #4 (20402) core 118

C-7. Equal area projections of poles to natural fracture surfaces and rose diagrams of natural fracture strikes for approximately equal length intervals of the WV #4 (20402) core 119

C-8. (A) composite rose diagram of slickenside strikes, and (B) equal area projection of poles to slickensided surfaces - WV #4 (20402) core 120

C-9. Equal area projections of poles to slickensided surfaces and rose diagrams of slickenside strikes for approximately equal length intervals of the WV #4 (20402) core 121

C-10. (A) composite rose diagram of slickenline trends, and (B) equal area projection of slickenlines - WV #4 (20402) core 122

C-11. equal area projections of slickenlines and rose diagrams of slickenlines for approximately equal length intervals of the WV #4 (20402) core 123

C-12. Composite data sheet of fracture frequencies and orientations for all fracture types - WV #4 (20402) core 124

D-1. Index map for the WV #5 (#3 D/K) core well 131

D-2. Gamma-ray log, Middle and Upper Devonian - WV #5 (#3 D/K) core well 132

D-3. (A) composite rose diagram of core-induced fracture strikes, and (B) equal area projection of poles to core-induced fracture surfaces - WV #5 (#3 D/K) core 133

D-4 - D-6. Equal area projections of poles to core-induced fracture surfaces and rose diagrams of core-induced fracture strikes for approximately equal length intervals of the WV #5 (#3 D/K) core 134, 135, 136

D-7. Histograms of core-induced fracture orientations - WV #5 (#3 D/K) core 137

D-8. (A) composite rose diagram of natural fracture strikes, and (B) euqla area projection of poles to natural fracture surfaces - WV #5 (#3 D/K) core 139

LIST OF FIGURES (CONT.)

figure page

D-9 - D-11. Equal area projections of poles to natural fracture surfaces and rose diagrams of natural fracture strikes for approximately equal depth intervals of the WV #5 (#3 D/K) core 140, 141, 142

D-12. Natural fracture mineralized with euhedral calcite crystals - WV #5 (#3 D/K) core 143

D-13. Natural fracture mineralized with massive dolomite - WV #5 (#3 D/K) core 143

D-14. (A) composite rose diagram of slickenside strikes, and (B) equal area projection of poles to slickensided surfaces - WV #5 (#3 D/K) core 144

D-15. (A) composite rose diagram of slickenline trends, and (B) equal area projection of slickenlines - WV #5 (#3 D/K) core 145

D-16. Composite data sheet of fracture frequencies and orientations for all fracture types - WV #5 (#3 D/K) core ... 146

E-1. Index map of the WV #6 (MERC #1) core well 152

E-2. Gamma-ray log, Middle and Upper Devonian - WV #6 (MERC #1) core well 153

E-3. (A) composite rose diagram of natural fracture strikes, and (B) equal area projection of poles to natural fracture surfaces - WV #6 (MERC #1) core 154

E-4. Equal area projections of poles to natural fracture surfaces and rose diagrams of natural fracture strikes for approximately equal length intervals of the WV #6 (MERC #1) core 155

E-5. (A) composite rose diagram of slickenside strikes, and (B) equal area projection of poles to slickensided surfaces - WV #6 (MERC #1) core 156

E-6. Equal area projections of poles to slickensided surfaces and rose diagrams of slickenside strikes for approximately equal length intervals of the WV #6 (MERC #1) core 157

E-7. (A) composite rose diagram of slickenline trends, and (B) equal area projection of slickenlines - WV #6 (MERC #1) core 158

E-8. Equal area projections of slickenlines and rose diagrams of slickenline trends for approximately equal length intervals of the WV #6 (MERC #1) core 159

LIST OF FIGURES (CONT.)

figure page

E-9. Composite data sheet of fracture frequencies and orientations for all fracture types - WV #6 (MERC #1) core... 160

F-1. Index map of the WV #7 (E-P #1) core well 166

F-2. Gamma-ray log, Middle and Upper Devonian - WV #7 (E-P #1) core well 167

F-3. (A) composite rose diagram of core-induced fracture strikes, and (B) equal area projection of poles to core-induced fracture surfaces - WV #7 (E-P #1) core well ... 168

F-4. Equal area projections of poles to core-induced fracture surfaces and rose diagrams of core-induced fracture strikes for approximately equal length intervals of the WV #7 (E-P #1) core 169

F-5. (A) composite rose diagram of natural fracture strikes, and (B) equal area projection of poles to natural fracture surfaces - WV #7 (E-P #1) core 170

F-6. Equal area projections of poles to natural fracture surfaces and rose diagrams of natural fracture strikes for approximately equal length intervals of the WV #7 (E-P #1) core 171

F-7. (A) composite rose diagram of slickenside strikes, and (B) equal area projection of poles to slickensided surfaces - WV #7 (E-P #1) core 172

F-8. Equal area projections of poles to slickensided surfaces and rose diagrams of slickenside strikes for approximately equal length intervals of the WV #7 (E-P #1) core 173

F-9. (A) composite rose diagram of slickenline trends, and (B) equal area projection of slickenlines - WV #7 (E-P #1) core 174

F-10. Equal area projections of slickenlines and rose diagrams of slickenline trends for approximately equal length intervals of the WV #7 (E-P #1) core 175

F-11. Composite data sheet of fracture frequencies and orientations for all fracture types - WV #7 (E-P #1) core ... 176

G-1. Index map for the OH #1 (S-745) core well..... 180

G-2. Rose diagram of undifferentiated fracture strikes - OH #1 (S-745) core 181

G-3. Histograms of undifferentiated fracture orientations - OH #1 (S-745) core..... 182

LIST OF FIGURES (CONT.)

figure page

G-4. Composite data sheet of undifferentiated fracture frequencies and orientations - OH #1 (S-745) core 184

H-1. Index map for the OH #2 (R-109) core well 188

H-2. Gamma-ray log, Middle and Upper Devonian - OH #2 (R-109) core well 189

H-3. (A) composite rose diagram of undifferentiated fracture strikes, and (B) equal area projection of poles to undifferentiated fracture surfaces - OH #2 (R-109) core 190

H-4. Equal area projections of poles to undifferentiated fracture surfaces and rose diagrams of undifferentiated fracture strikes for approximately equal length intervals of the OH #2 (R-109) core 191

H-5. Histograms of undifferentiated fracture orientations - OH #2 (R-109) core 192

H-6. Composite data sheet of undifferentiated fracture frequencies and orientations - OH #2 (R-109) core 194

I-1. Index map for the VA #1 (20338) core well showing surface structure on the Pine Mountain thrust sheet, and a cross section through the thrust sheet 201

I-2. Gamma-ray log, Middle and Upper Devonian - VA #1 (20338) core well 202

I-3. (A) composite rose diagram of core-induced fracture strikes, and (B) equal area projection of poles to core-induced fracture surfaces - VA #1 (20338) core 203

I-4. Equal area projections of poles to core-induced fracture surfaces and rose diagrams of core-induced fracture strikes for approximately equal length intervals of the VA #1 (20338) core 204

I-5. Histograms of core-induced fracture orientations - VA #1 (20338) core 205

I-6. (A) composite rose diagram of natural fracture strikes, and (B) equal area projection of poles to natural fracture surfaces - VA #1 (20338) core 207

I-7. Equal area projections of poles to natural fracture surfaces and rose diagrams of natural fracture strikes for approximately equal length intervals of the VA #1 (20338) core 208

LIST OF FIGURES (CONT.)

figure page

I-8. (A) composite rose diagram of slickenside strikes, and (B) equal area projection of poles to slickensided fracture surfaces - VA #1 (20338) 209

I-9. Equal area projections of poles to slickensided surfaces and rose diagrams of slickenside strikes for approximately equal length intervals of the VA #1 (20338) core 210

I-10. (A) composite rose diagram of slickenline trends, and (B) equal area projection of slickenlines - VA #1 (20338) core 211

I-11. Equal area projections of slickenlines and rose diagrams of slickenline trends for approximately equal length intervals of the VA #1 (20338) core 212

I-12. Composite data sheet of fracture frequencies and orientations for all fracture types - VA #1 (20338) core 213

J-1. Index map for the PA #2 (C.E.P.S. #1) core well with major structures and lines of structural discontinuity in the Pittsburgh, Pennsylvania region. Also, the location of the proposed Lat. 40°N Fault Zone 219

J-2. Gamma-ray log, Middle and Upper Devonian - PA #2 (C.E.P.S. #1) core well..... 220

J-3. (A) composite rose diagram of natural fracture strikes, and (B) equal area projection of poles to natural fracture surfaces - PA #2 (C.E.P.S. #1) core 221

J-4. Equal area projections of poles to natural fracture surfaces and rose diagrams of natural fracture strikes for approximately equal length intervals of the PA #2 (C.E.P.S. #1) core 222

J-5. (A) composite rose diagram of slickenside strikes, and (B) equal area projection of poles to slickensided surfaces - PA #2 (C.E.P.S. #1) core 223

J-6. Equal area projections of poles to slickensided surfaces and rose diagrams of slickenside strikes for approximately equal length intervals of the PA #2 (C.E.P.S. #1) core ..... [illegible]

J-7. (A) composite rose diagram of slickenline trends, and (B) equal area projection of slickenlines - PA #2 (C.E.P.S. #1) core ..... [illegible]

J-8. Equal area projections of slickenlines and rose diagrams of slickenline trends for approximately equal length intervals of the PA #2 (C.E.P.S. #1) core 226

LIST OF FIGURES (CONT.)

figure page

J-9. Composite data sheet of fracture frequencies and orientations for all fracture types - PA #2 (C.E.P.S. #1) core 227

K-1. Index map for the KY #1 (7239) core well 233

K-2. Gamma-ray log, Middle and Upper Devonian - KY #1 (7239) core well 234

K-3. (A) composite rose diagram of undifferentiated fracture strikes, and (B) equal area projection of poles to undifferentiated fracture surfaces - KY #1 (7239) core... 235

K-4. Equal area projections of poles to undifferentiated fracture surfaces and rose diagrams of undifferentiated fracture strikes for approximately equal length intervals of the KY #1 (7239) core 236

K-5. Histograms of undifferentiated fracture orientations - KY #1 (7239) core 237

K-6. (A) composite rose diagram of slickenside strikes, and (B) equal area projection of poles to slickensided surfaces - KY #1 (7239) core 239

K-7. Equal area projections of poles to slickensided surfaces and rose diagrams of slickenside strikes for approximately equal length intervals of the KY #1 (7239) core 240

K-8. (A) composite rose diagram of slickenline trends, and (B) equal area projection of slickenlines - KY #1 (7239) core 241

K-9. Equal area projections of slickenlines and rose diagrams of slickenline trends for approximately equal length intervals of the KY #1 (7239) core 242

K-10. Composite data sheet of fracture frequencies and orientations for all fracture types - KY #1 (7239) core 243

L-1. Index map for the KY #3 (20336) core well 248

L-2. Gamma-ray log, Middle and Upper Devonian - KY #3 (20336) core well 249

L-3. (A) composite rose diagram of core-induced fracture strikes, and (B) equal area projection of poles to core-induced fracture surfaces - KY #3 (20336) core 250

LIST OF FIGURES (CONT.)

figure page

L-4. Equal area projections of poles to core-induced fracture surfaces and rose diagrams of core-induced fracture strikes for approximately equal length intervals of the KY #3 (20336) core 251

L-5. Histograms of core-induced fracture orientations - KY #3 (20336) core 252

L-6. (A) composite rose diagram of natural fracture strikes, and (B) equal area projections of poles to natural fracture surfaces - KY #3 (20336) core 254

L-7. Equal area projections of poles to natural fracture surfaces and rose diagrams of natural fracture strikes for approximately equal length intervals of the KY #3 (20336) core 255

L-8. (A) composite rose diagram of slickenside strikes, and (B) equal area projection of poles to slickensided surfaces - KY #3 (20336) core 256

L-9. Equal area projections of poles to slickensided surfaces and rose diagrams of slickenside strikes for approximately equal length intervals of the KY #3 (20336) core. 257

L-10. (A) composite rose diagram of slickenline trends, and (B) equal area projection of slickenlines - KY #3 (20336) core 258

L-11. Equal area projection of slickenlines and rose diagrams of slickenline trends for approximately equal length intervals of the KY #3 (20336) core 259

L-12. Composite data sheet of fracture frequencies and orientations for all fracture types - KY #3 (20336) core 260

M-1. Index map for the KY #4 (#3 R-S) core well 266

M-2. (A) composite rose diagram of core-induced fracture strikes, and (B) equal area projection of poles to core-induced fracture surfaces - KY #4 (#3 R-S) core 267

M-3. Equal area projections of poles to core-induced fracture surfaces and rose diagrams of core-induced fracture strikes for approximately equal length intervals of the KY #4 (#3 R-S) core 268

M-4. Class 1 fracture - KY #4 (#3 R-S) core 269

LIST OF FIGURES (CONT.)

Figure page

M-5. Class 2 fracture - KY #4 (#3 R-S) core 269

M-6. (A) composite rose diagram of natural fracture strikes, and (B) equal area projection of poles to natural fracture surfaces - KY #4 (#3 R-S) core 270

M-7. Equal area projections of poles to natural fracture surfaces and rose diagrams of natural fracture strikes for approximately equal length intervals of the KY #4 (#3 R-S) core 271

M-8. (A) composite rose diagram of slickenside strikes, and (B) equal area projection of poles to slickensided surfaces - KY #4 (#3 R-S) core 272

M-9. Equal area projections of poles to slickensided surfaces and rose diagrams of slickenside strikes for approximately equal length intervals of the KY #4 (#3 R-S) core 273

M-10. (A) composite rose diagram of slickenline trends, and (B) equal area projection of slickenlines - KY #4 (#3 R-S) core 274

M-11. Equal area projections of slickenlines and rose diagrams of slickenline trends for approximately equal length intervals of the KY #4 (#3 R-S) core 275

M-12. Composite data sheet of fracture frequencies and orientations for all fracture types - KY #4 (#3 R-S) core 276

LIST OF TABLES

table		page
A-1.	Core-induced fracture orientation statistics - WV #2 (12041) core	77
B-1.	Core-induced fracture orientation statistics - WV #3 (20403) core	97
C-1.	Core-induced fracture orientation statistics - WV #4 (20402) core	117
D-1.	Core-induced fracture orientation statistics - WV #5 (#3 D/K) core	138
G-1.	Undifferentiated fracture orientation statistics - OH #1 (S-745) core	183
H-1.	Undifferentiated fracture orientation statistics - OH #2 (R-109) core	193
I-1.	Core-induced fracture orientation statistics - VA #1 (20338) core	206
K-1.	Undifferentiated fracture orientation statistics - KY #1 (7239) core	228
L-1.	Core-induced fracture orientation statistics - KY #3 (20336) core	253

APPENDICES

INTRODUCTION TO APPENDICES

Thirteen cores from wells located throughout the Appalachian Basin were examined (figure 1, table 1). The following are separate, self-contained reports summarizing fracture data obtained on each of the cores. Each report discusses, in detail, the fracture types and fracture patterns described in that particular core, and it relates the fractures to local structure and regional tectonics. A brief discussion of gas production from the Devonian shale in the well is also included in each report.

APPENDIX A: WV #2 (12041) CORE WELL

WV #2 (12041) CORE WELL

Location

The WV #2 (12041) core well is located in Jackson County, West Virginia, approximately three miles west of the town of Cottageville (figures 1 and A-1, table 1). The wellsite is on the western flank of the N60°E trending Parkersburg Syncline. Regional structure of the Devonian shales shows a monoclinal dip of less than 1° to the southeast. A total of 490 feet of the Devonian was cored, from 3220'-3690' (figure A-2).

Production Data

One interval of the well (3400'-3560') was stimulated by foam fracturing resulting in an initial open flow of 180 mcf/day (Komar, Frone, and Yost, 1978).

Core-induced fractures

Core-induced fractures are the most common fracture type in the core. The lower portion of the Lower Huron Member of the Ohio Shale and the Java Formation tend to have a greater abundance of core-induced fractures than the other units (figure A-12). The orientations of only a portion of the core-induced fractures were measured due to the poor condition of the core. The frequency distribution diagram does, however, indicate the presence of all core-induced fractures. The composite rose diagram of core-induced fracture strikes (figure A-3) has two peaks. There is a 1.0% chance that the peak at N50°-70°E does not exist, and a 5.0% chance that the peak at N17°W does not exist. The equal area projection of poles to core-induced fracture surfaces

(figure A-3) has four clusters corresponding to the opposing dips of the two fracture sets. Core-induced fracture orientations change dramatically from a N50°-70°E trend to a N17°W trend at 3679', which is 10 feet above the top of the Java Formation (figures A-4 and A-5, table A-1). Two subhorizontal slickensides are also found at this point. This change in orientation indicates an almost 90° swing in a stress or rock fabric anisotropy. The swing may be the effect of altered stres fields in the Java Formation caused by differential movement below the slip plane, which has also been noted in other wells. The consistent N50°-70°E orientation may be related to the general east to northeast trending maximum compressive stress present in most of eastern North America (Sbar and Sykes, 1973).

Natural Fractures

Natural fractures are found only in the Lower Huron Member of the Ohio Shale, above the slickenside zone. Below that point, in the Java Formation, no natural fractures were found (figure A-12), again probably resulting from altered stress fields in the Java Formation. The natural fracture composite rose diagram (figure A-6) has a single peak at N57°E. There is a 1.0% chance that this peak does not exist. The equal area projection of poles to natural fracture surfaces (figure A-6) has two peripheral clusters corresponding to the subvertical to vertical fracture dips. There is very little scatter in natural fracture orientation (figure A-7). None of the natural fractures in the WV #2 (12041) core are mineralized.

The N57°E natural fracture set parallels the dominant core-nduced fracture trend and may have formed under the same stress

conditions which formed the core-induced fractures. The fractures in this set are also subparallel to slickenline trends in this core and may have fored as extension fractures under compression from the northeast during formation of the Buring Springs Anticline.

Slickensides and Slickenlines

Slickensides are found in only two distinct zones, both of which are located near viscosity boundaries in the shale (figure A-12). The upper zone, at 3544', is in a thin high-organic shale layer immediately below a harder shale layer. The lower zone, at 3641', is in a high organic shale near the base of the Lower Huron Member of the Ohio Shale, immediately above the harder grey shles of the Java Formation. The slickenside composite rose diagram (figure A-8) has a single peak at N5°-20°W. There is a 1.0% chance that this peak does not exist. The equal area projection of poles to slickensided surfaces (figure A-8) has two clusters; one, dipping 10°SW, another, dipping 30°SW. Slickenside orientations do not change with depth or stratigraphy (figure A-9). None of the slickensides in this core are mineralized.

The slickenline composite rose diagram (figure A-10) has a single peak at N77°E. There is a 1.0% chance that this peak does not exist. The equal area projection of slickenlines (figure A-10) has two low-dipping clusters corresponding to the N77°E trend. Slickenline orientations do not change with depth or stratigraphy (figure A-11).

The two slickenside occurences, because of their limited number and extent, cannot be considered décollement zones. However, they may be slip planes which formed as the rock absorbed the remaining stresses of dying out detachments to the east. The N77°E displacement trend

suggests a relationship to the detached Burning Springs Anticline to the northeast.

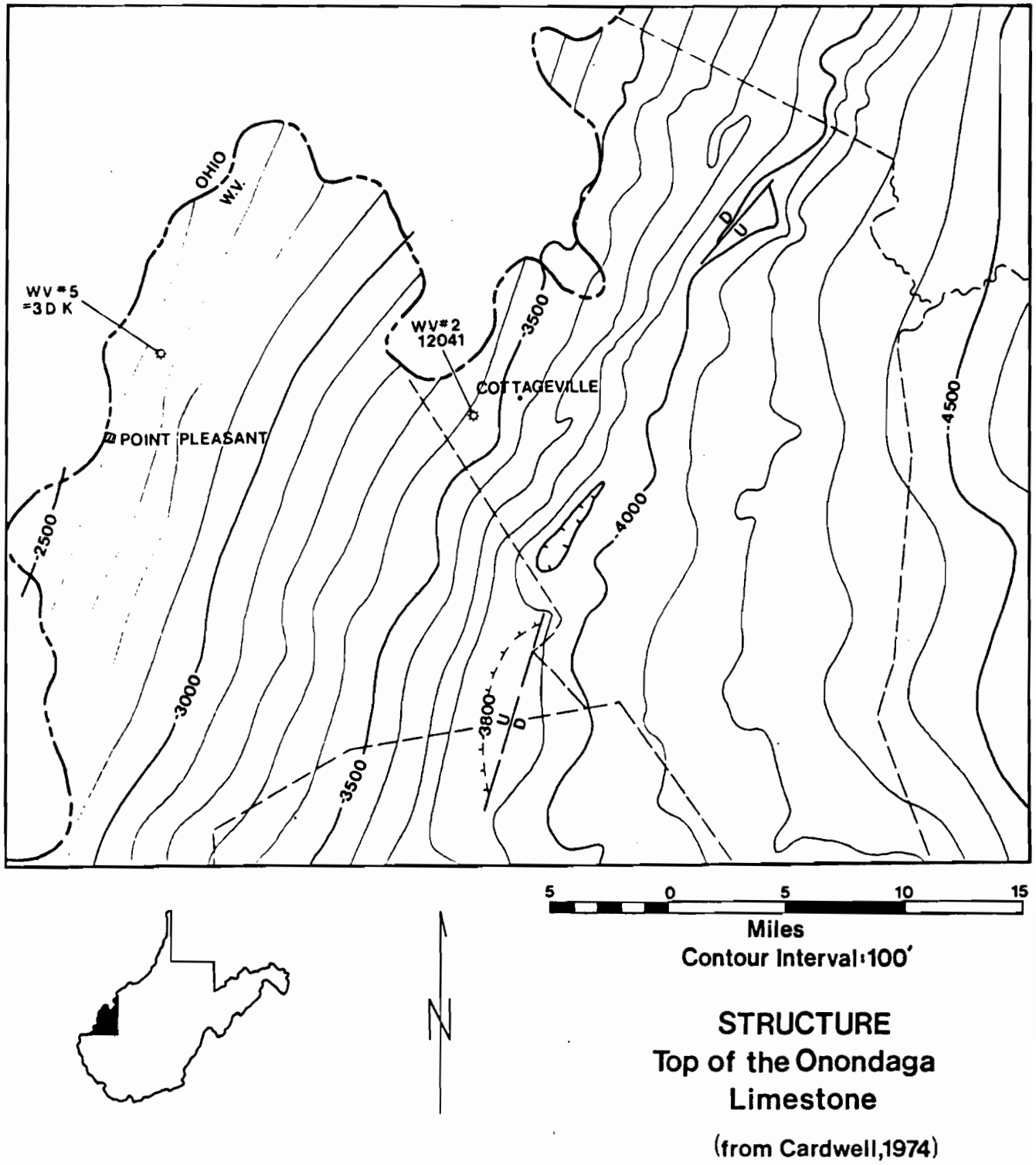

Figure A-1. Index map for the WV #2 (12041) core well

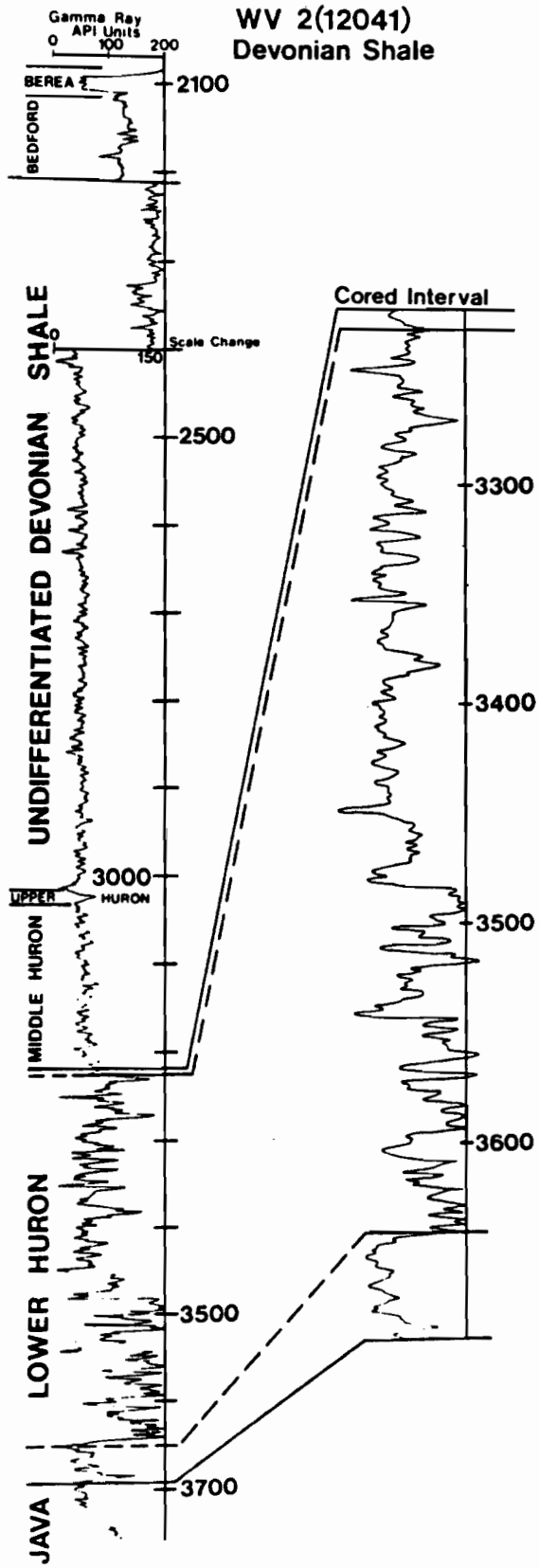

Figure A-2. Gamma-ray log, Middle and Upper Devonian

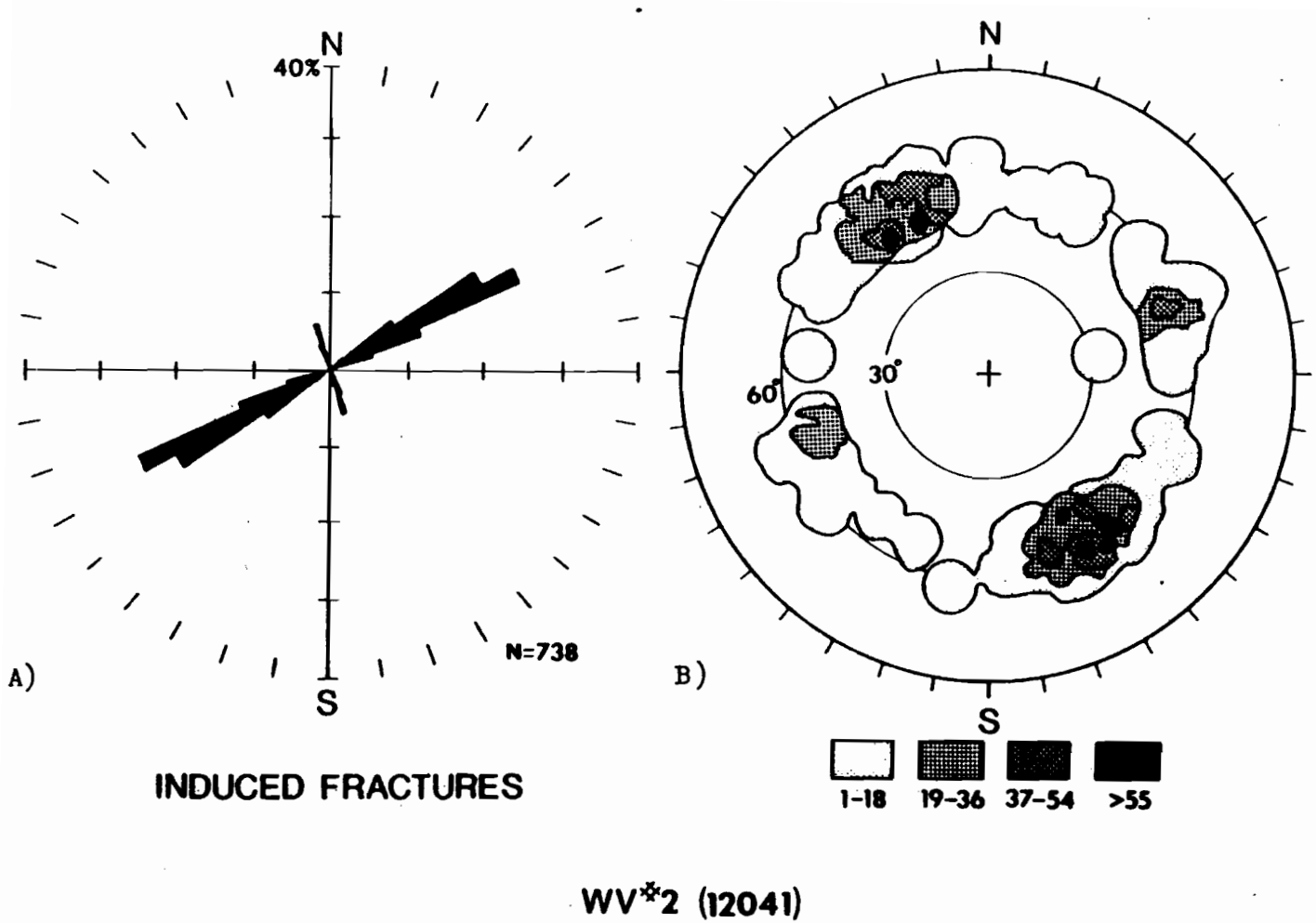

Figure A-3. (A) composite rose diagram of core-induced fracture strikes, and (B) equal area projection of poles to core-induced fracture surfaces

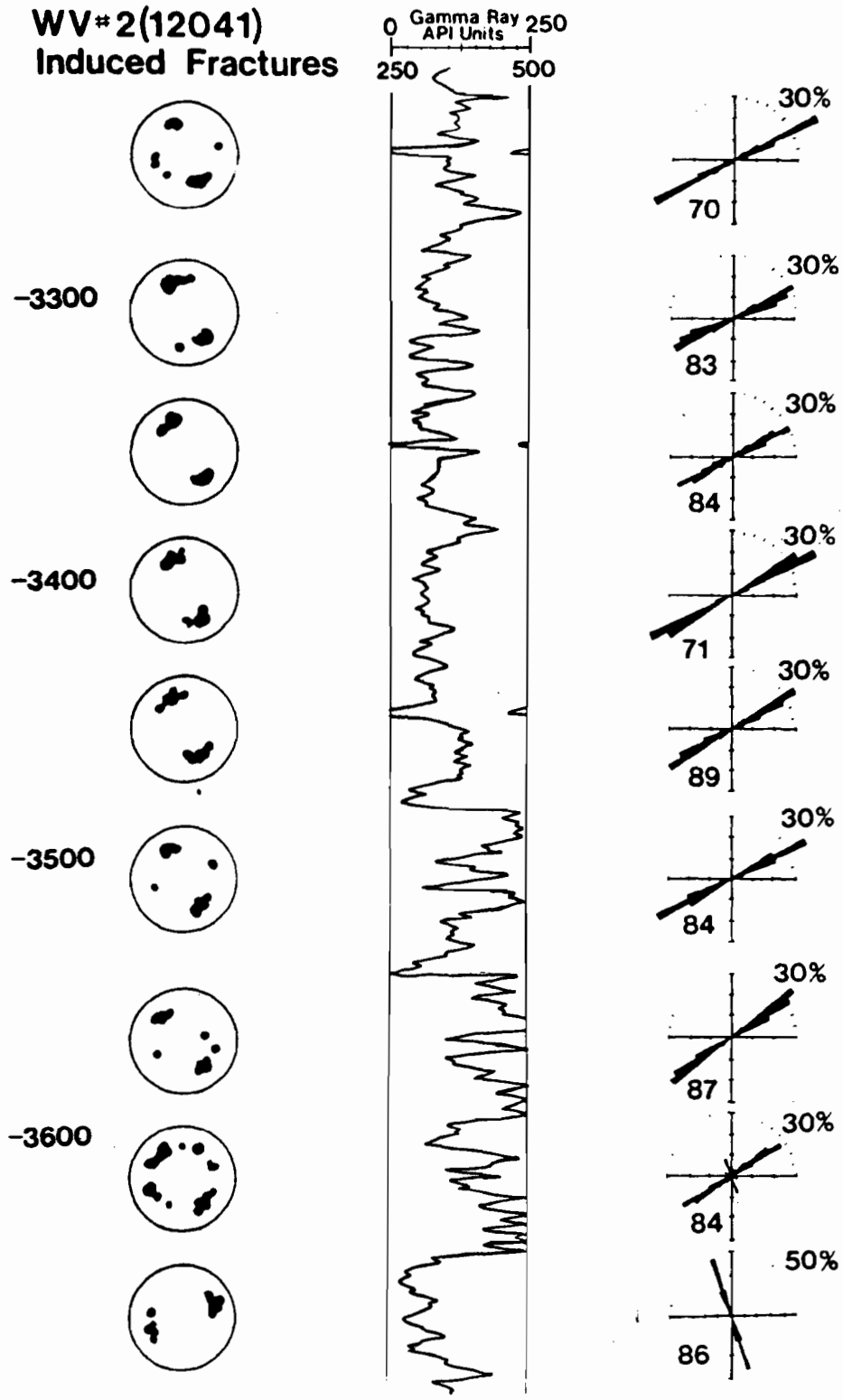

Figure A-4. Equal area projections of poles to core-induced fracture surfaces and rose diagrams of core-induced fracture strikes for approximately equal length intervals of the WV #2 (12041) core.

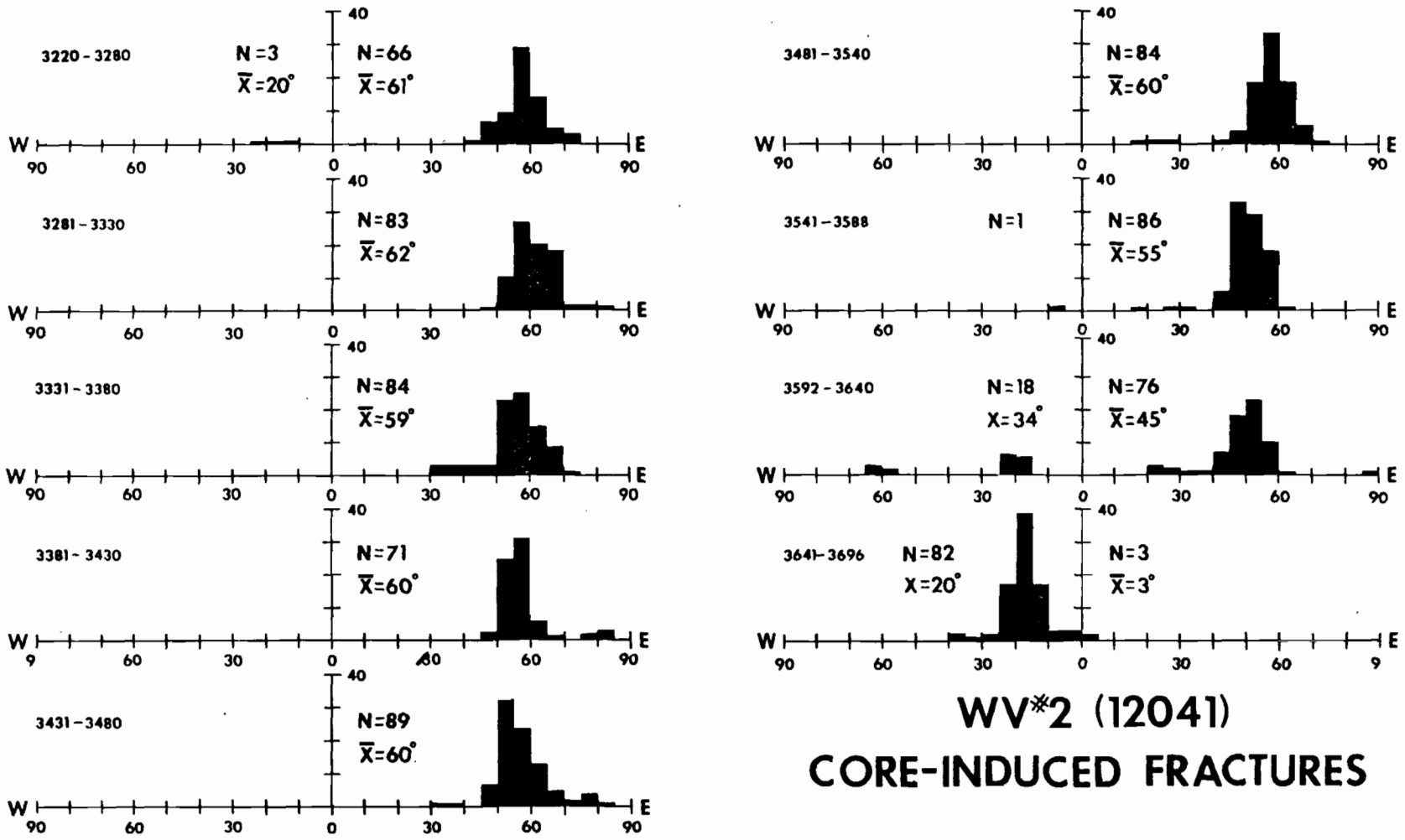

WV#2 (12041)
CORE-INDUCED FRACTURES

Figure A-5. Histograms of core-induced fracture orientations.

TABLE A-1

WV #2 (12041) INDUCED FRACTURES

Interval	N	VN	α
3220-3280	69		
		2.2395	≤1.00
3281-3330	83		
		2.5886	≤0.05
3331-3380	84		
		2.3425	≤0.10
3381-3430	71		
		1.5828	≤1.00
3431-3480	89		
		1.9002	≤1.00
3481-3540	84		
		4.6540	≤0.01
3541-3590	87		
		2.5095	≤0.05
3591-3640	84		
		7.6401	≤0.01
3641-3690	86		

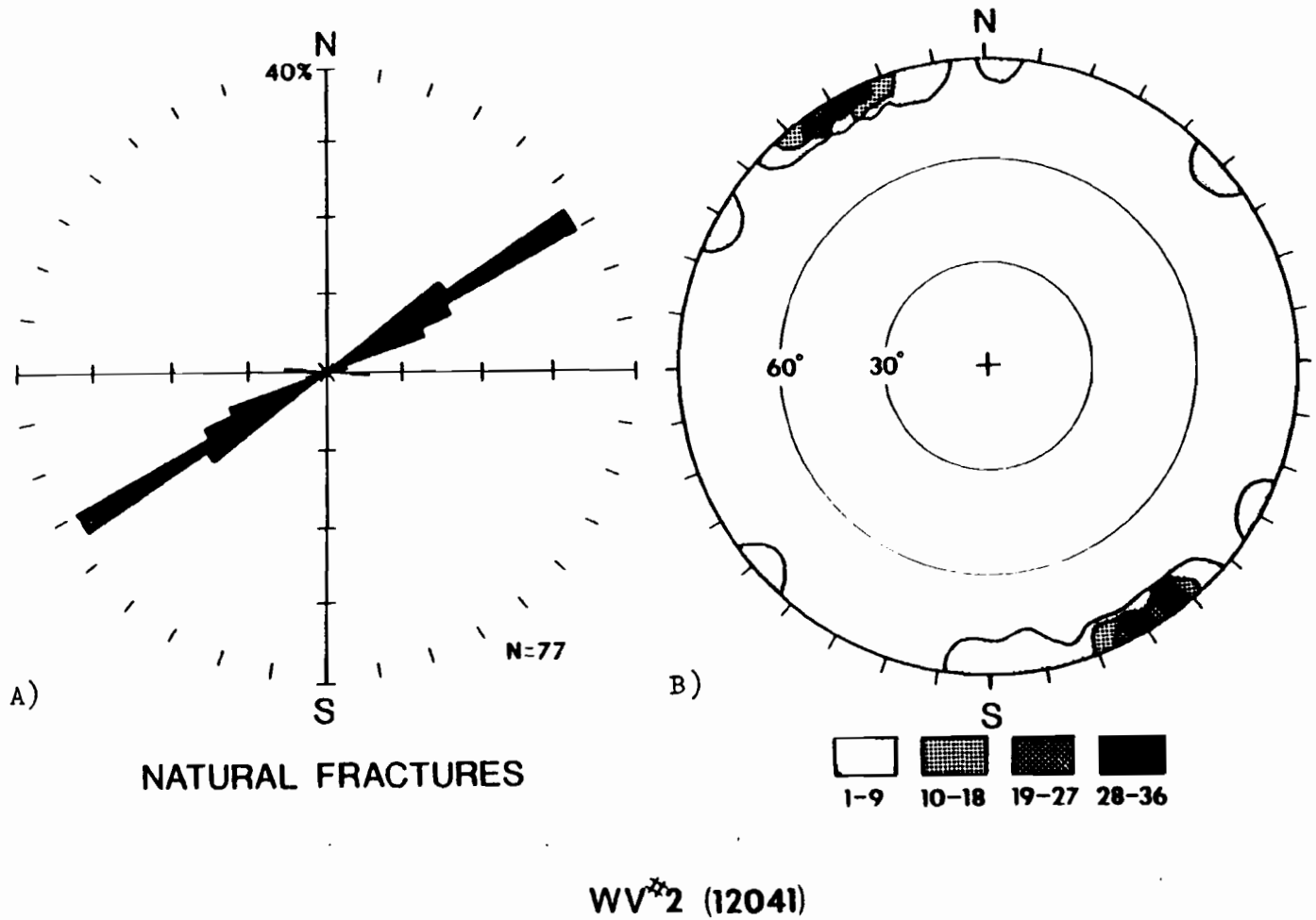

Figure A-6. (A) composite rose diagram of natural fracture strikes, and (B) equal area projection of poles to natural fracture surfaces

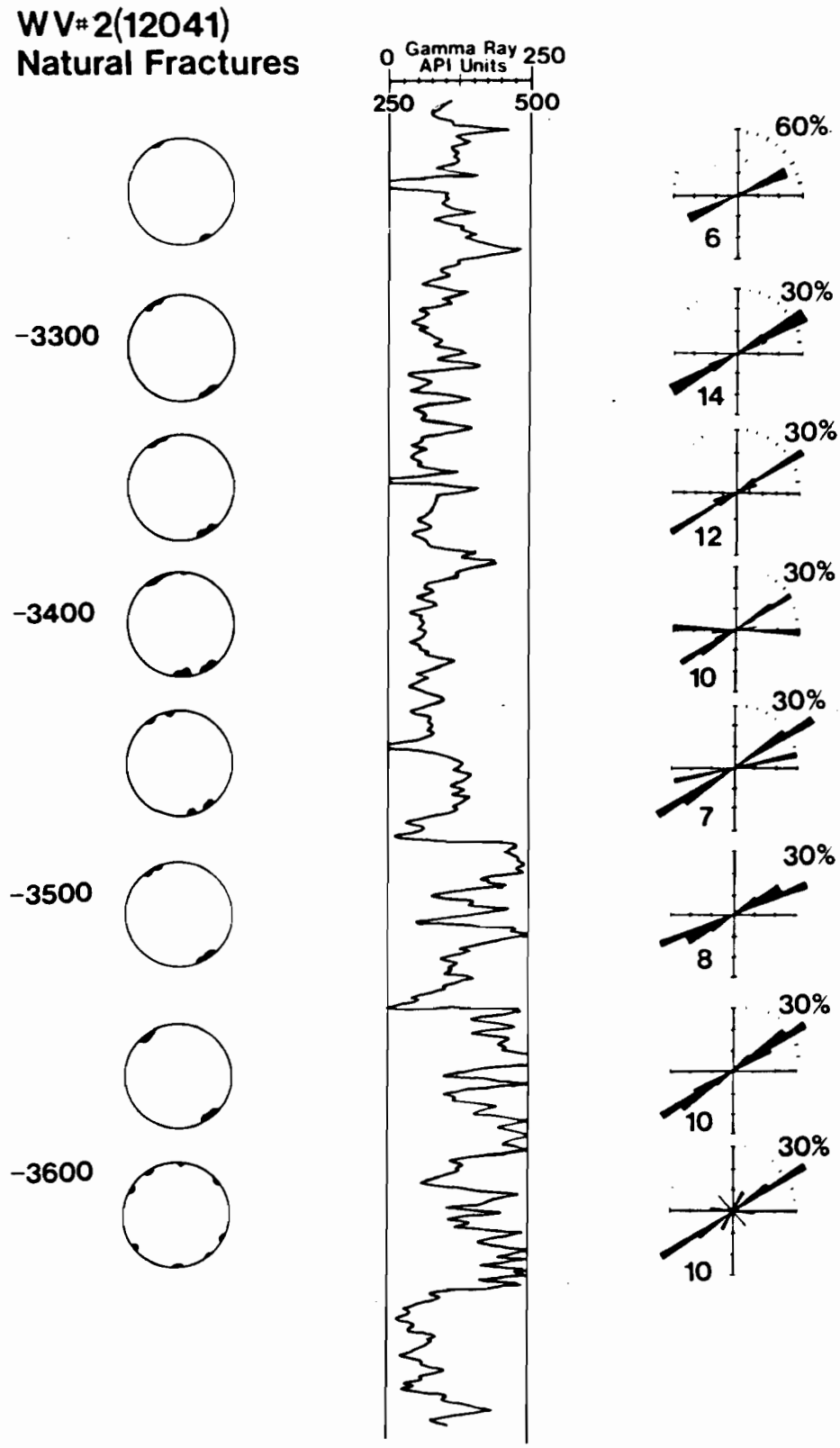

Figure A-7. Equal area projections of poles to natural fracture surfaces and rose diagrams of natural fracture strikes for approximately equal length intervals of the WV #2 (12041) core.

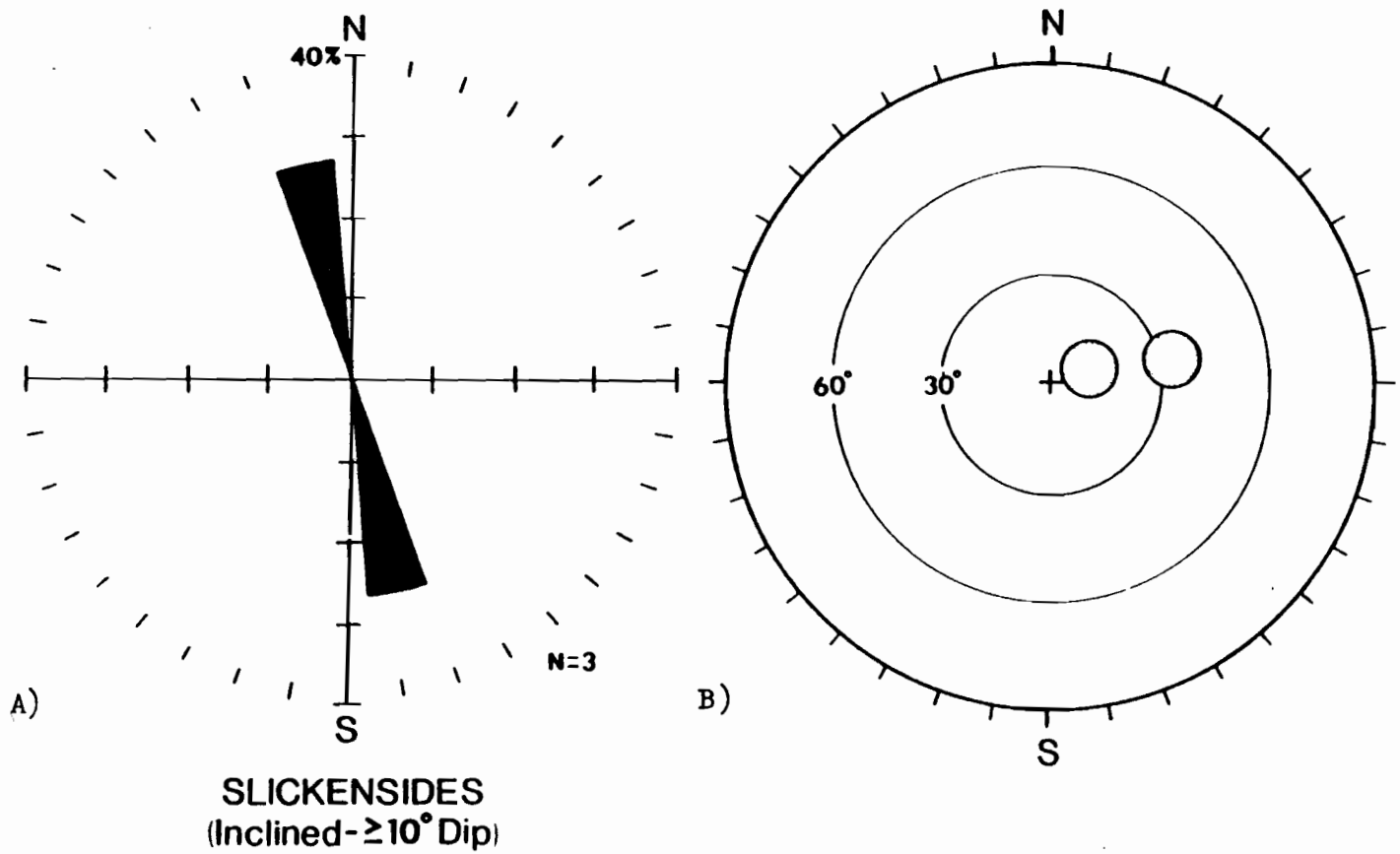

WV*2 (12041)

Figure A-8. (A) composite rose diagram of slickenside strikes, and (B) equal area projection of poles to slickensided surfaces

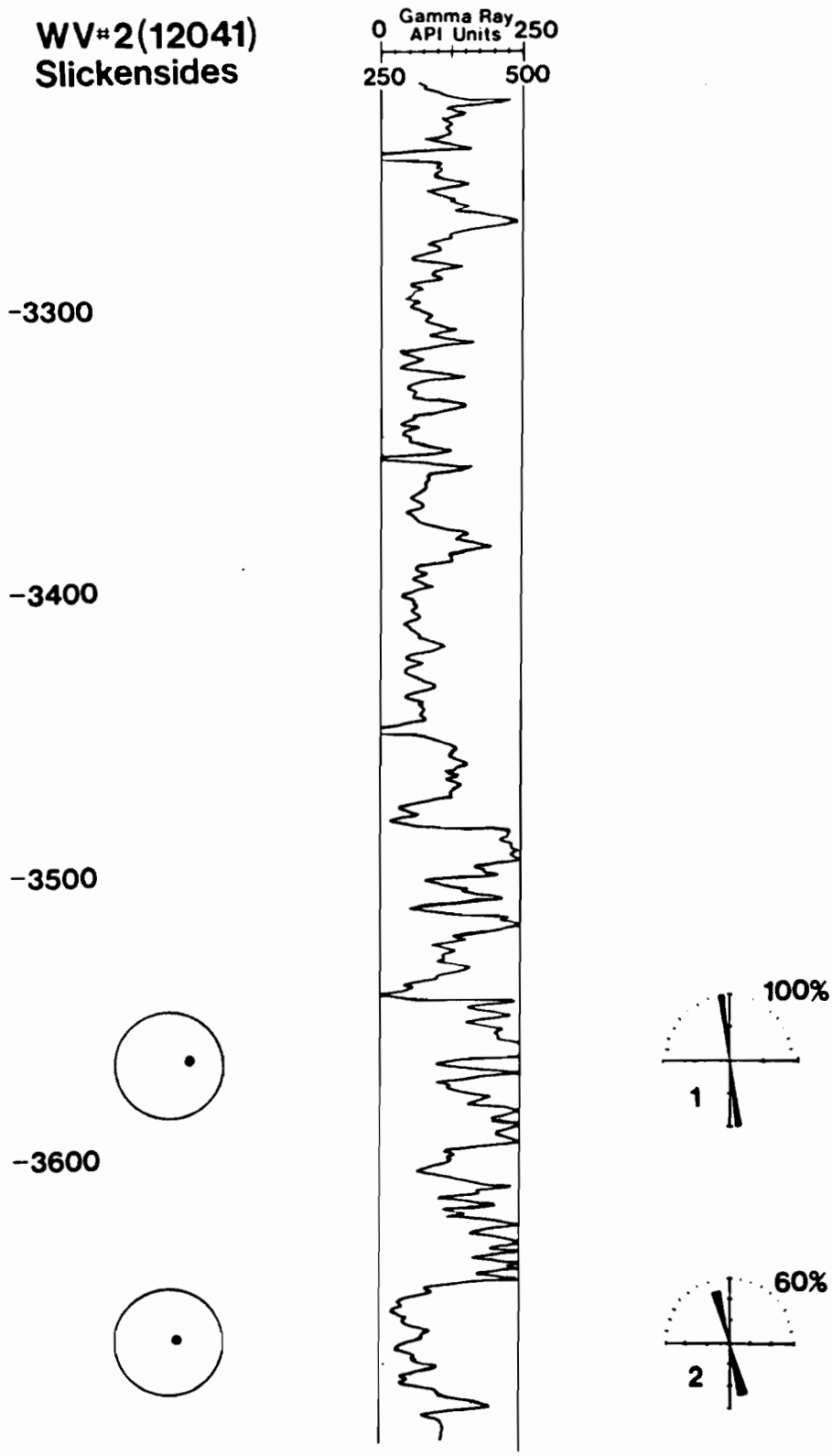

Figure A-9. Equal area projections of poles to slickensided surfaces and rose diagrams of slickenside strikes for approximately equal length intervals of the WV #2 (12041) core.

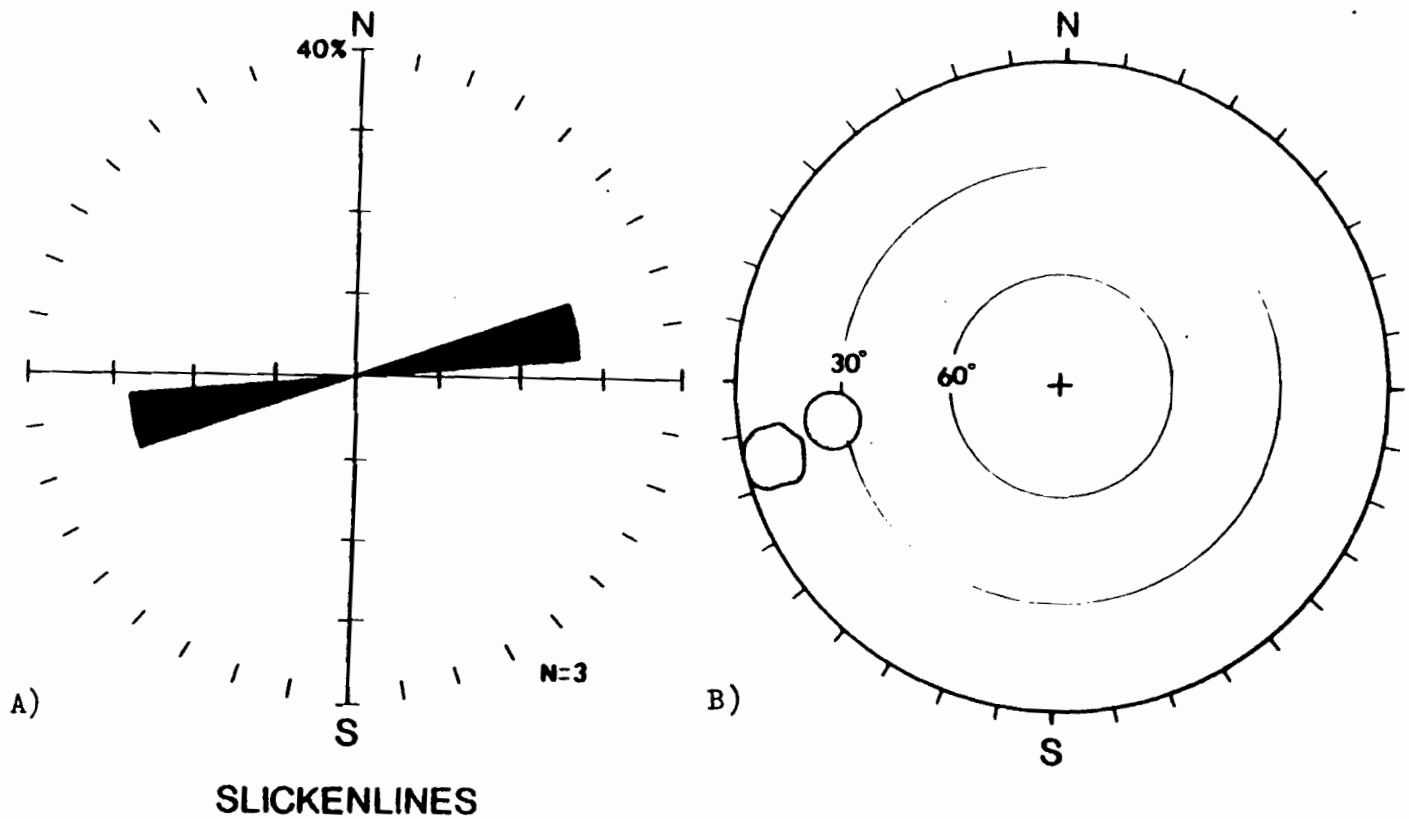

WV*2 (12041)

Figure A-10. (A) composite rose diagram of slickenline trends, and (B) equal area projection of slickenlines

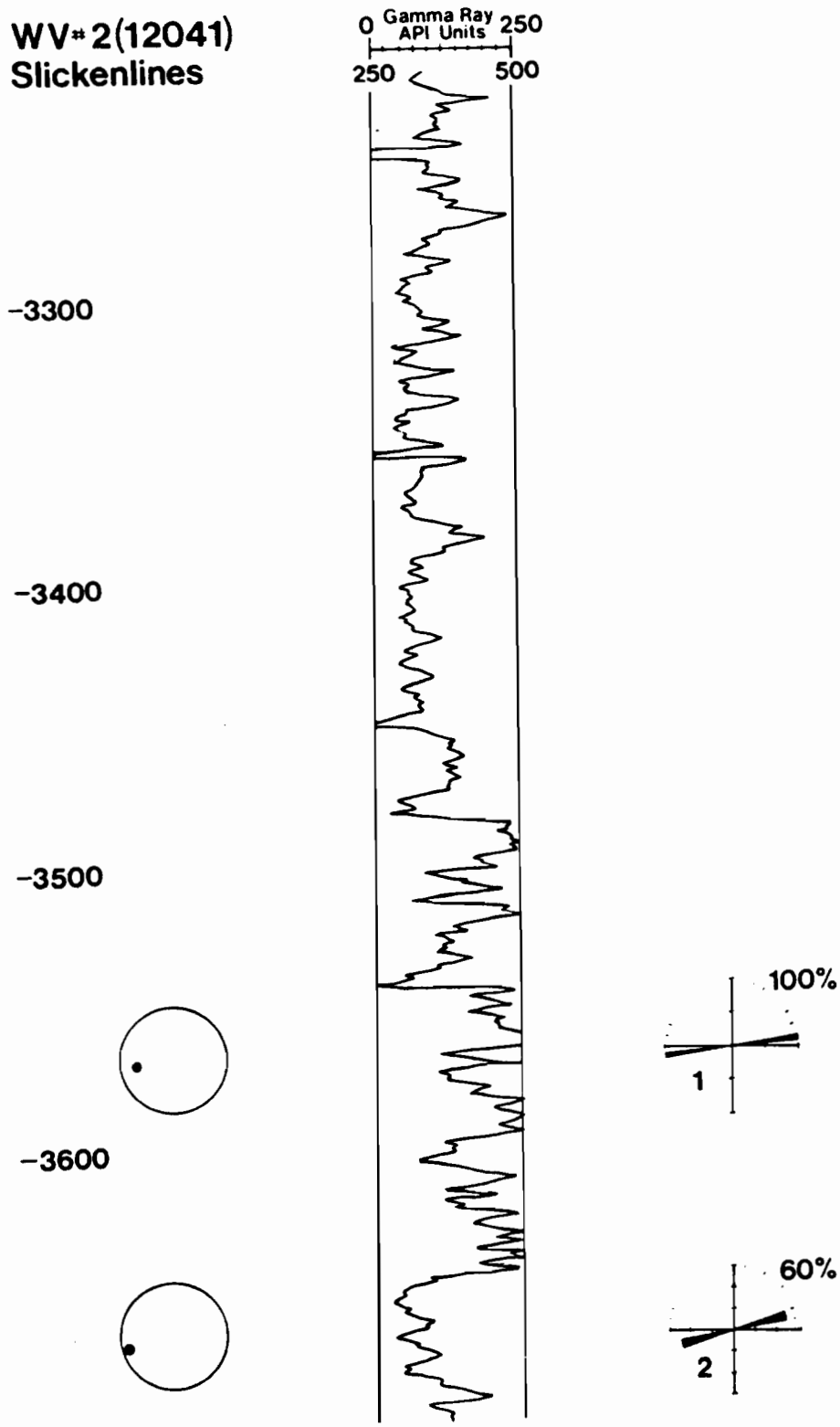

Figure A-11. Equal area projections of slickenlines and rose diagrams of slickenline trends for approximately equal length intervals of the WV #2 (12041) core.

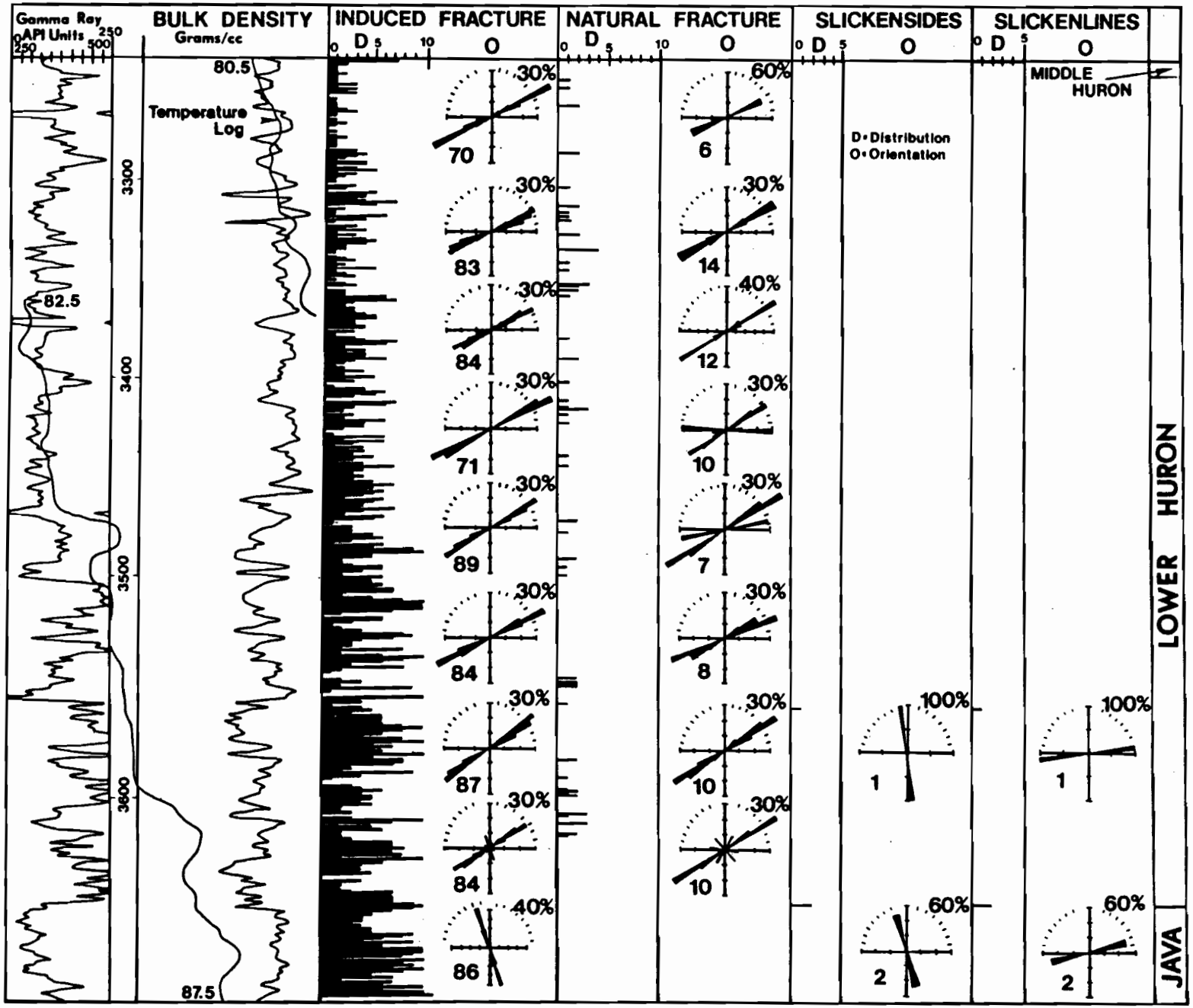

Figure A-12. Composite data sheet of fracture frequencies and orientations for all fracture types.

APPENDIX B: WV #3 (20403) CORE WELL

WV #3 (20403) CORE WELL

Location

The WV #3 (20403) core well is located in Lincoln County, West Virginia, three miles southwest of the town of Ranger (figures 1 and B-1, table 1). The wellsite is directly over the Rome Trough, 15 miles north of the northeast trending Warfield Fault. Fold axes in the area generally trend N65°E. Regional structure of the Devonian shales is a monoclinal dip of less than 1° to the east. This is the longest core studied with 1308 feet of the Devonian cored, from 2720'-4025' (figure B-2).

Production Data

Four intervals of the well had gas shows: 2775'-2825' (381 mcf/day, 160 mcf/day after fracturing), 2950'-3225' (103 mcf/day, 107 mcf/day after fracturing), 3400'-3650' (95 mcf/day, 200 mcf/day after fracturing), and 3850'-4025' (show, 110 mcf/day after fracturing) (Komar, Frone, and Yost, 1978).

Core-induced Fractures

Core-induced fractures are the most common fracture type in the core and are well distributed throughout the cored interval (figure B-13). The orientations of only a portion of the core-induced fractures were measured due to the poor condition of the core. The frequency distribution diagram does, however, indicate the presence of all core-induced fractures. The core-induced fracture composite rose diagram (figure B-3) has two peaks, N55°-75°E with an average strike of N65°E,

and N83°E. There is a 1.0% chance that each of these peaks do not exist. The equal area projection of poles to core-induced fracture surfaces (figure B-3) has two wide clusters corresponding to the merging of opposing dips of the two fracture sets. Core-induced fracture strikes are consistent down through the Lower Huron Member where they swing from an orientation at the base of the Java Formation (figures B-4 and B-5, table B-1). This swing may be the effect of altered stress fields in the Java Formation, resulting from the unit being bounded by slip planes.

The generally consistent fracture orientations suggest that a stress or fabric anisotropy exists in the rock. This anisotropy may be related to the general east to northeast trending maximum compressive stress present in most of eastern North America (Sbar and Sykes, 1973).

Natural Fractures

Natural fractures are found throughout the core except in the Java Formation. A concentration of fractures exists in the interval 3030'-3070' (figure B-13). The natural fracture composite rose diagram (figure B-6) has three peaks. There is a 1.0% chance that the peaks at N60°-70°W and N27°W do not exist, and a 10% chance that the peak at N83°E does not exist. The equal area projection of poles to natural fracture surfaces (figure B-6) has six clusters: two wide clusters resulting from the merging subvertical to vertical northeast trending fracture sets; two smaller clusters which correspond to the vertical N27°E set; and two clusters dipping 35°NW abd 35°SE, resulting from inclined N75°E striking fractures.

The northeast striking natural fracture sets are found throughout the core and they parallel the core-induced fracture strikes to the point of swinging from N65°E to N83°E near the base of the Lower Huron Member of the Ohio Shale, and then back to N65°E at the base of the Java Formation (figure B-7). This also suggests that there may have been, and still may be, altered stress fields in the Java Formation and that these natural fractures formed in relation to the same stresses responsible for the core-induced fractures. The two trends also generally parallel fold axes in the area. This suggests the possibility that these fractures formed as release fractures when tectonic stresses were relaxed. Some of the fractures in the two northeast striking sets are mineralized, primarily with massive or crystalline calcite.

The N27°W fracture set is vertically limited, occurring only in the interval 3030'-3070'. This set is mineralized exclusively with massive or crystalline dolomite or barite (Larese and Heald, 1977) (figure B-8). In this section of shale there are also several inclined N75°E striking dolomite filled fractures. This interval is one of the gas producing intervals of the well. The N27°W set is orthogonal to the southern Appalachian trend and probably formed as an extension fracture set under tectonic compressive stresses directed from the southeast. This is supported by the occurrence, in this interval, of a single slickenside having slickenlines trending N7°W, and by the inclined N75°E striking fractures which are interpreted to be mineral filled shear fractures. This fracture zone may have formed in relation to slip movement.

The difference in mineralization between the northeast striking fractures and the northwest striking fractures may indicate different times of formation. Since the northeast striking sets parallel the core-induced fractures it seems likely that they formed later than the northwest set.

Slickensides and Slickenlines

Slickensides are confined to several distinct zones. One slickenside, as mentioned above, is at 3050' in the interval of N27°W striking natural fractures. Slickensides are also found at the base of the Lower Huron Member of the Ohio Shale (one horizontal slickenside), base of the Java Formation, and throughout the entire West Falls Formation (figure B-13). The Lower Huron and Java zones occur near viscosity boundaries, and the West Falls zone occurs in a low-viscosity dark shale unit immediately above the much stiffer Onondaga Limestone. Only the West Falls slickenside zone and the zone at the base of the Java Formation are vertically extensive enough to be considered décollement zones. The slickenside composite rose diagram (figure B-9) has a single statistically significant peak at N70°-85°E with an average strike of N77°E. There is a 1.0% chance that this peak does not exist. Three smaller peaks that are not statistically significant are N75°W, N27°E, and N63°E. Poles to slickensided surfaces form an incomplete girdle across the equal area projection (figure B-9). The pattern of clusters is close to that expected for a shear zone, but dips of the Riedel and thrust shear clusters exceed the 30° maximum. This may be explained by rotation of the slickensides during shearing. The 0° dipping cluster in the center is the

displacement shear cluster, the 40°NW dipping cluster is the Riedel shear cluster, and the 40°SE dipping cluster is the thrust shear cluster. R' shears may be present in the scatter in the southeast quadrant of the plot. Two small clusters corresponding to the vertical fractures of the N75°W set are found on the perimeter of the plot in the northeast and southwest quadrants. The slickensides of this set occur only in the Java Formation and in the Rhinestreet Member of the West Falls Formation (figure B-10).

The slickenline composite rose diagram (figure B-11) has a single significant peak at N5°-20°W with an average trend of N13°W. There is a 1.0% chance that this peak does not exist. Two peaks which are not statistically significant occur at N27°W and N65°W. The equal area projection of slickenlines (figure B-11) has four clusters: two, at 30°SE and 30°NW which result from the merging of the N5°-20°W set and the N27°W set; and two, on the perimeter of the plot, corresponding to the subhorizontal slickenlines of the N65°W set. The N5°-20°W set occurs primarily in the Angola Shale Member of the West Falls Formation. The N65°W set occurs primarily in the Rhinestreet Shale Member of the West Falls Formation and consists of nearly horizontal slickenlines on the vertical N75°W striking slickensides. The N27°W set is found only in the Rhinestreet Member of the West Falls Formation and in the lower portion of the Java Formation (figure B-12). Very few slickensides in the core are mineralized. Massive calcite is the most common filling.

The N5°-20°W and N27°W trending slickenlines parallel the N27°W natural fracture set and are orthogonal to the dominant slickenside

orientation. These three fracture sets are related in that they probably formed under the same tectonic compressive stresses that existed during the formation of the southern Appalachians. The N75^{o}W slickenside set, with its N65^{o}W trending slickenlines, shows no relationship to any known nearby structures.

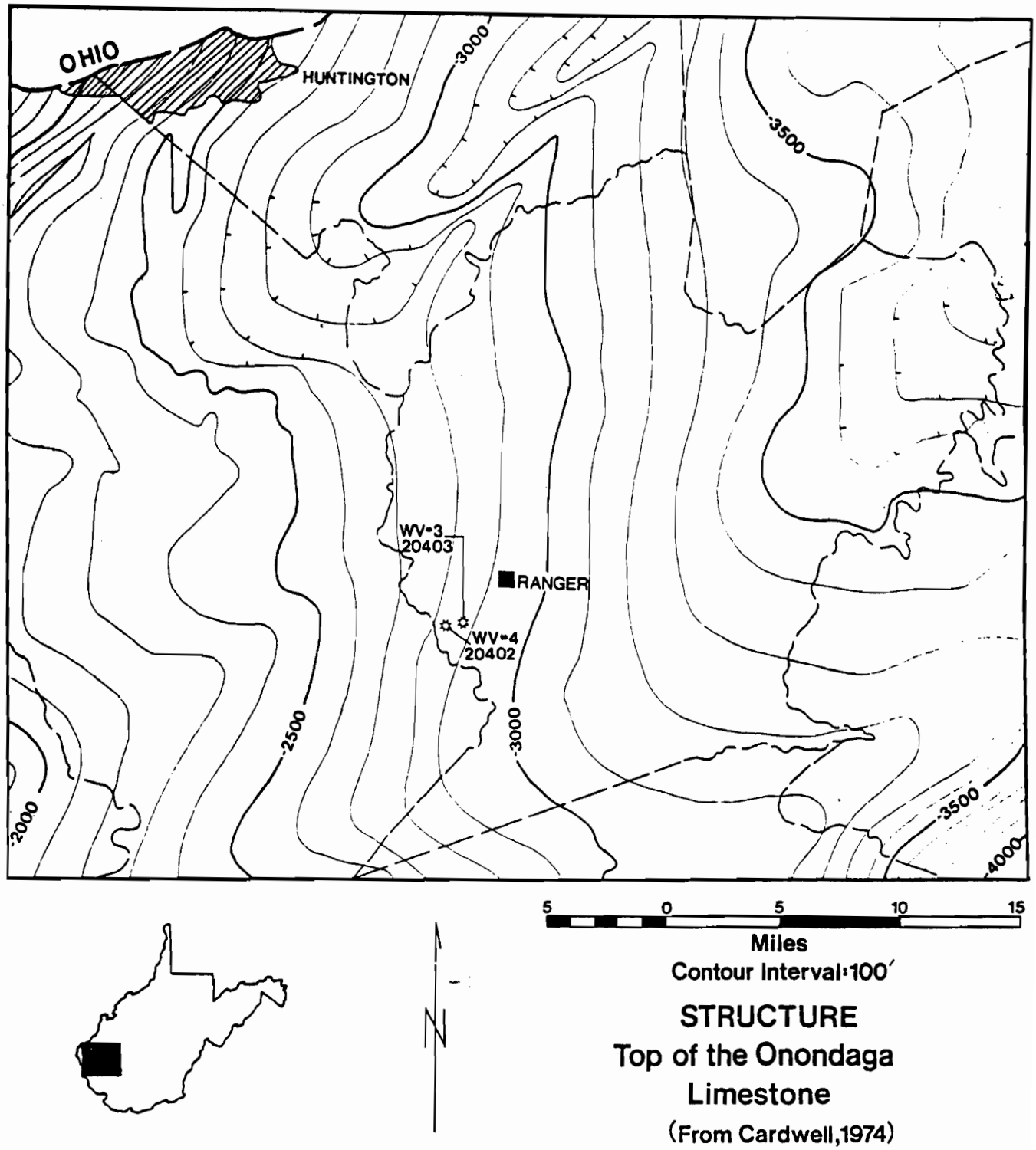

Figure B-1. Index map of the WV #3 (20403) core well

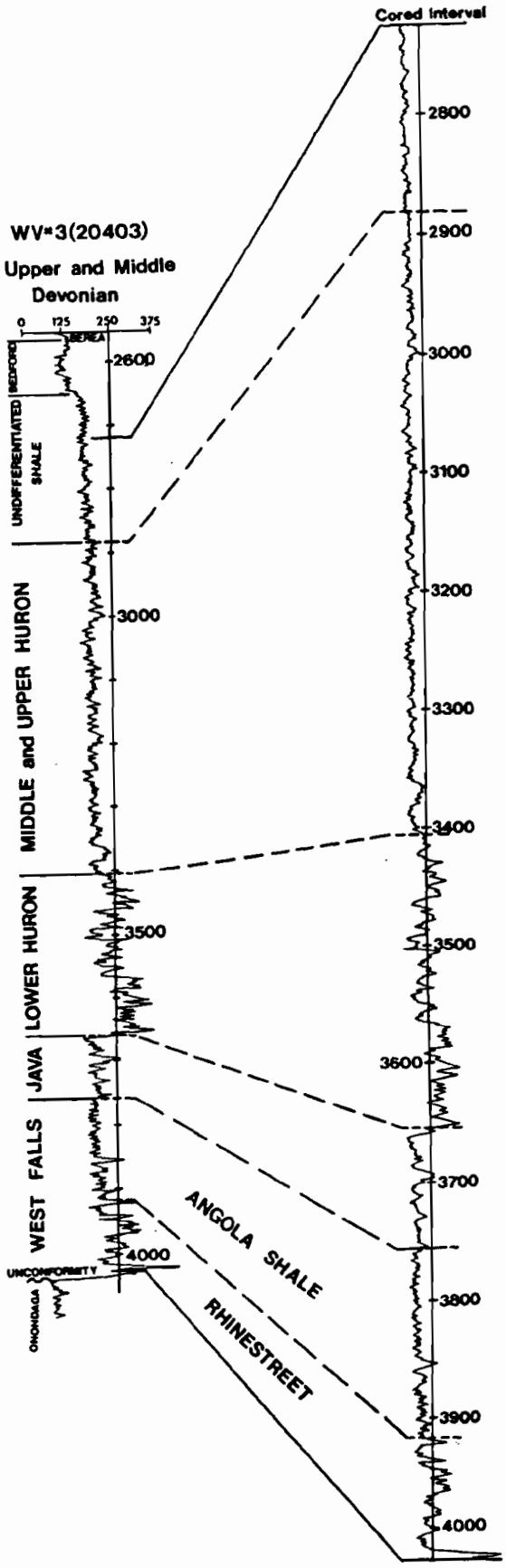

Figure B-2. Gamma-ray log, Middle and Upper Devonian.

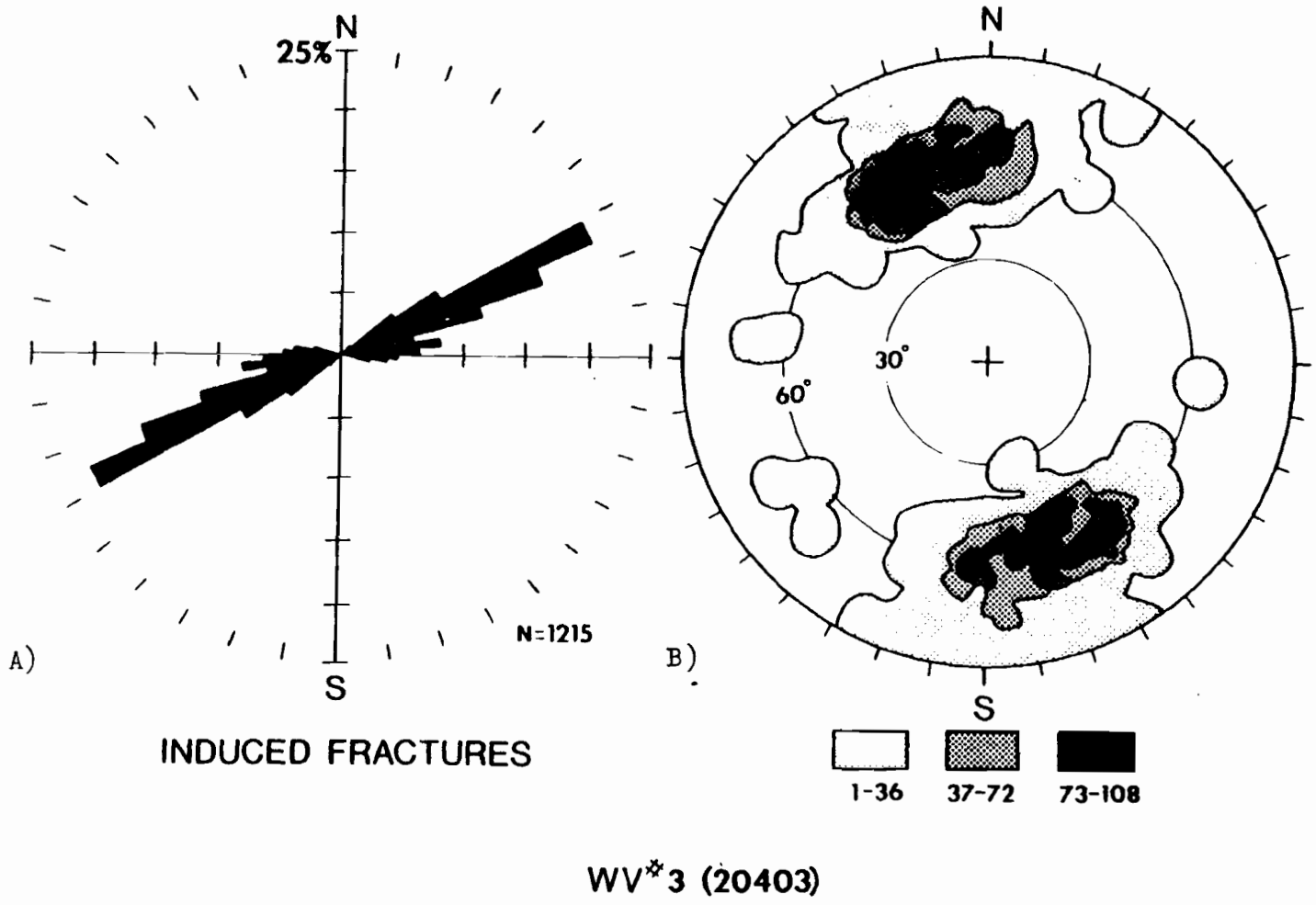

Figure B-3. (A) composite rose diagram of core-induced fracture strikes, and (B) equal area projection of poles to core-induced fracture surfaces

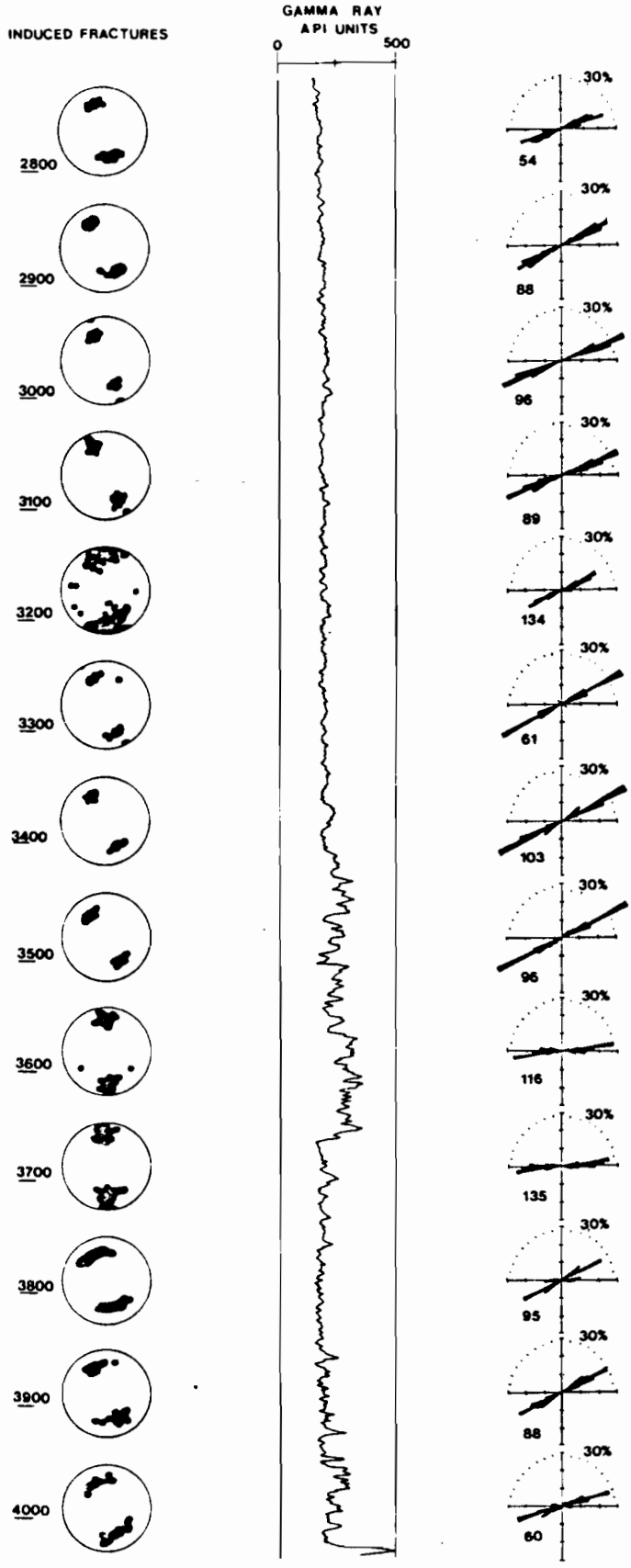

Figure B-4. Equal area projections of poles to core-induced fracture surfaces and rose diagrams of core-induced fracture strikes for approximately equal length intervals of the WV #3 (20403) core.

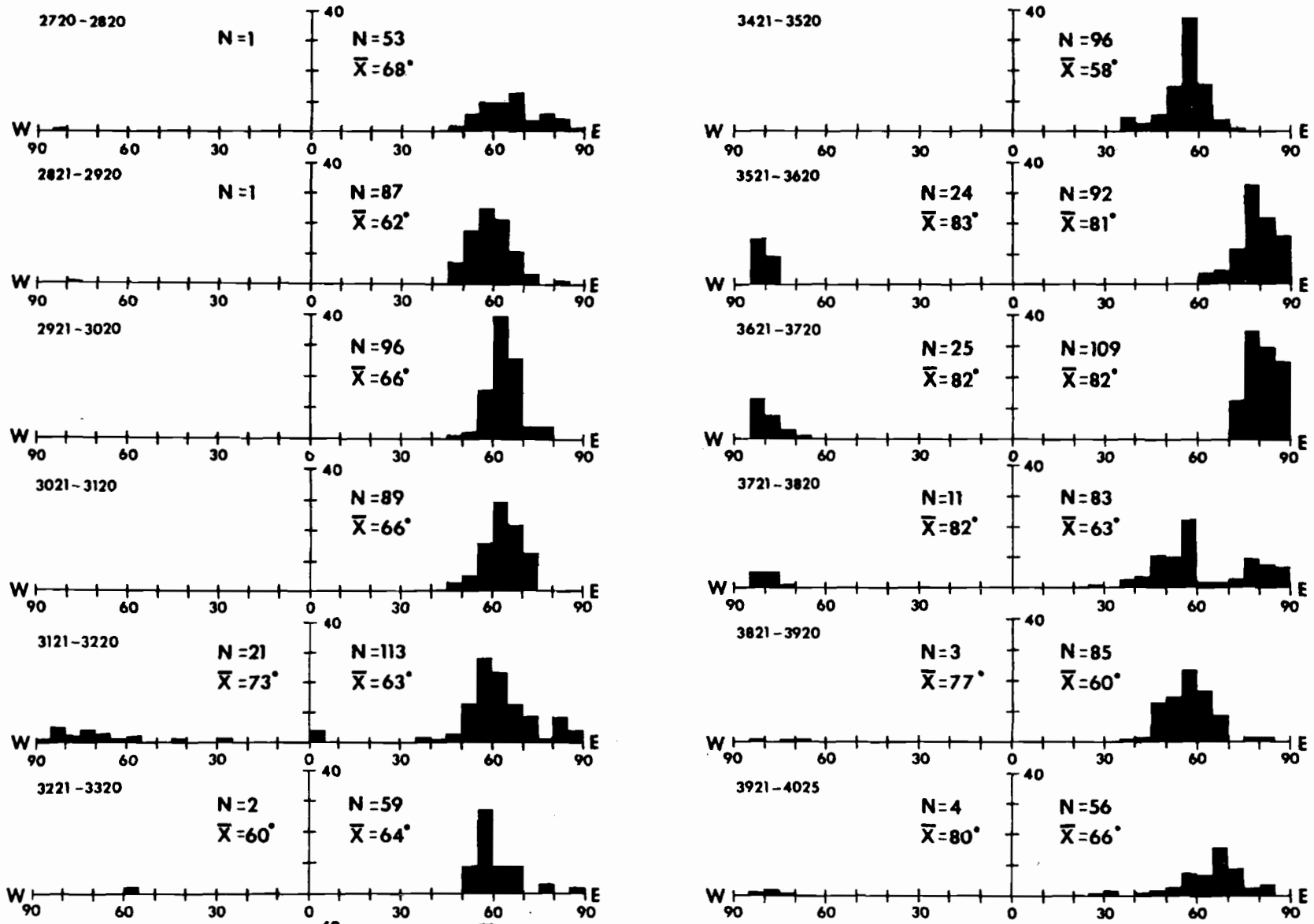

WV#3 (20403)

CORE-INDUCED FRACTURES

Figure B-5. Histograms of core-induced fracture orientations.

TABLE B-1

WV #3 (20403) INDUCED FRACTURES

Interval	N	VN	α
2720-2820	54		
		2.6938	≤0.05
2821-2920	88		
		3.6866	≤0.01
2921-3020	96		
		1.3117	≤1.00
3021-3120	89		
		3.5455	≤0.01
3121-3220	134		
		2.8474	≤0.01
3221-3320	61		
		1.8808	≤1.00
3321-3420	103		
		1.4943	≤1.00
3421-3520	96		
		9.0201	≤0.01
3521-3620	116		
		1.4204	≤1.00
3621-3720	134		
		5.4656	≤0.01
3721-3820	96		
		3.5267	≤0.01
3821-3920	88		
		3.6265	≤0.01
3921-4025	60		

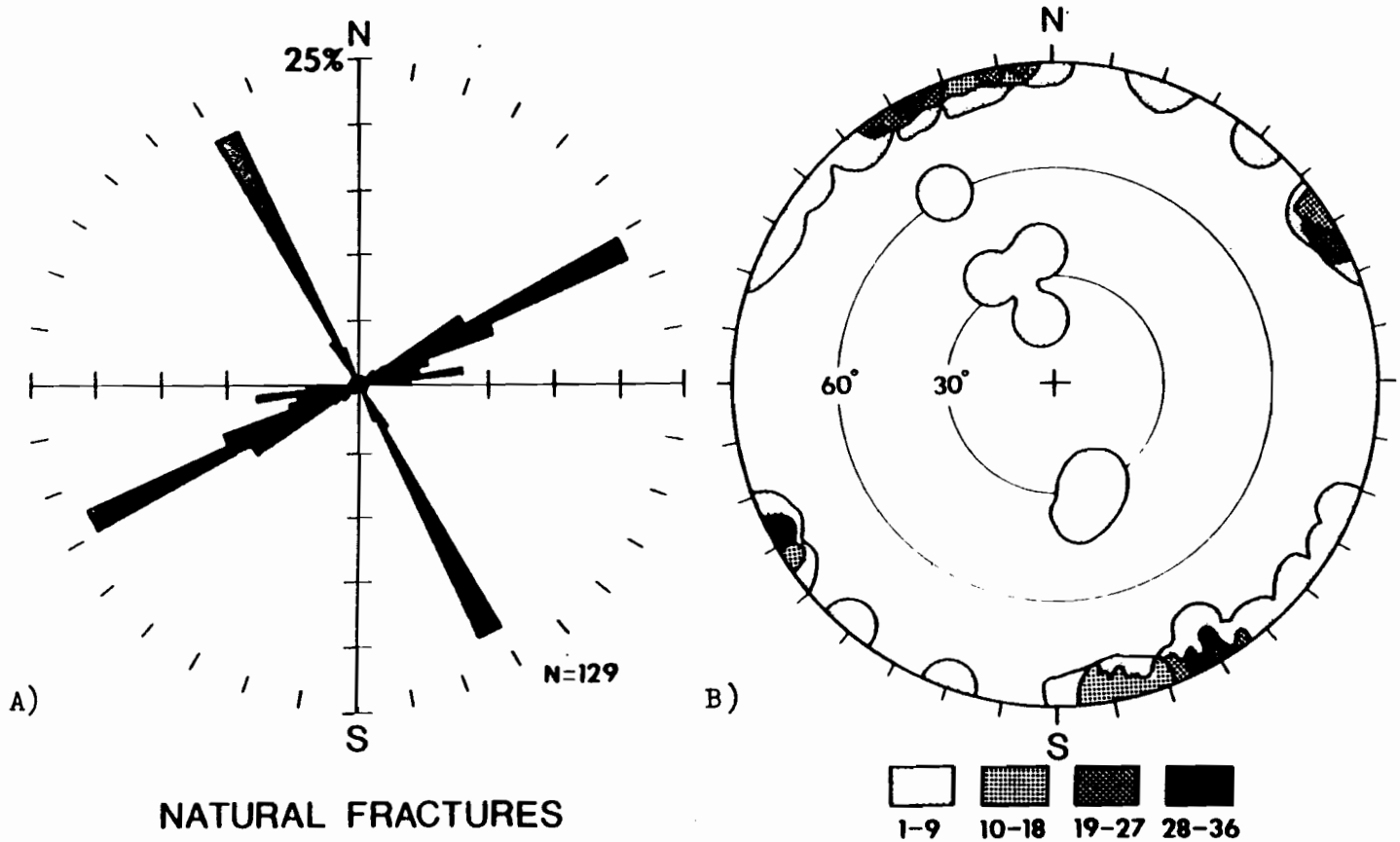

WV*3 (20403)

Figure B-6. (A) composite rose diagram of natural fracture strikes, and (B) equal area projections of poles to natural fracture surfaces

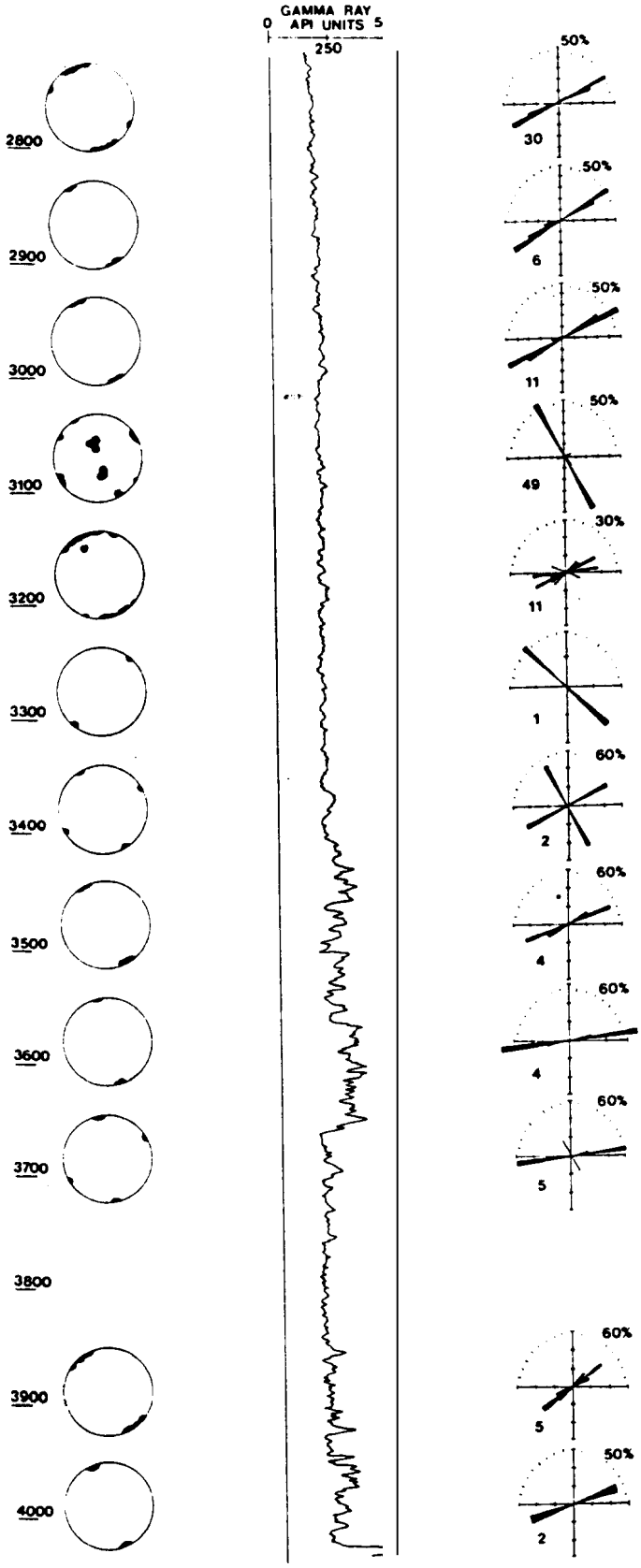

Figure B-7. Equal area projections of poles to natural fracture surfaces and rose diagrams *of* natural fracture strikes for approximately equal length intervals of the WV #3 (20403) core.

Figure B-8. N30°W striking dolomite filled natural fracture from interval 3030'-3070' - WV #3 (20403) core.

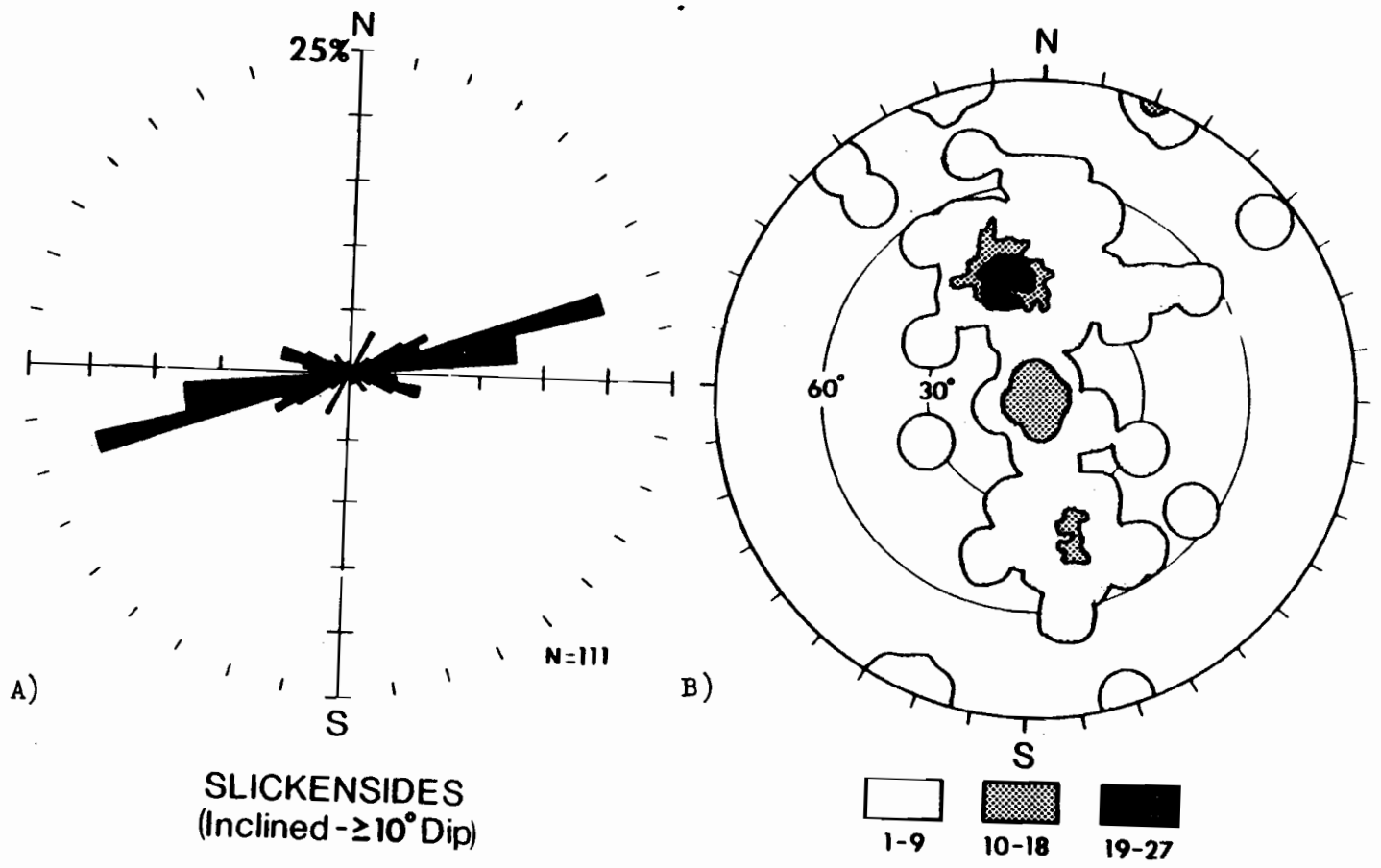

WV*3 (20403)

Figure B-9. (A) composite rose diagram of slickenside strikes, and (B) equal area projection of poles to slickensided surfaces

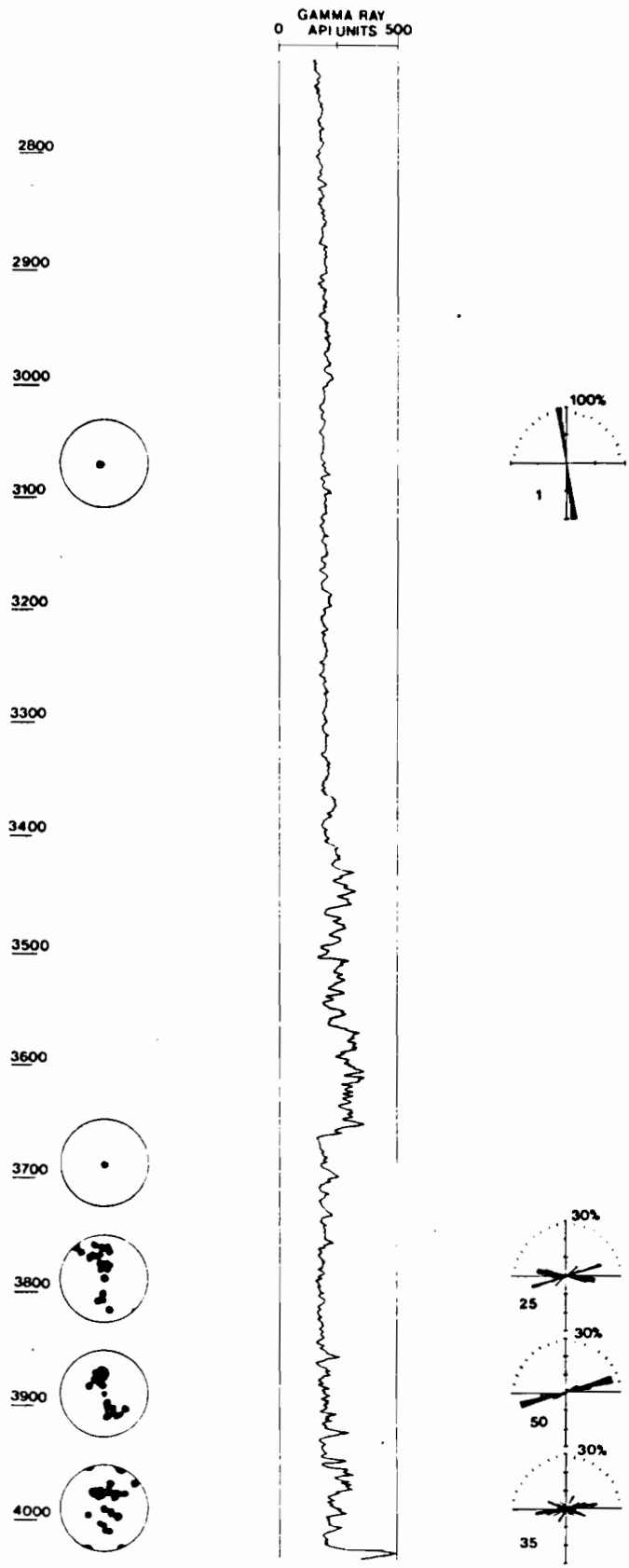

Figure B-10. Equal area projections of poles to slickensided surfaces and rose diagrams of slickenside strikes for approximately equal length intervals of the WV #3 (20403) core.

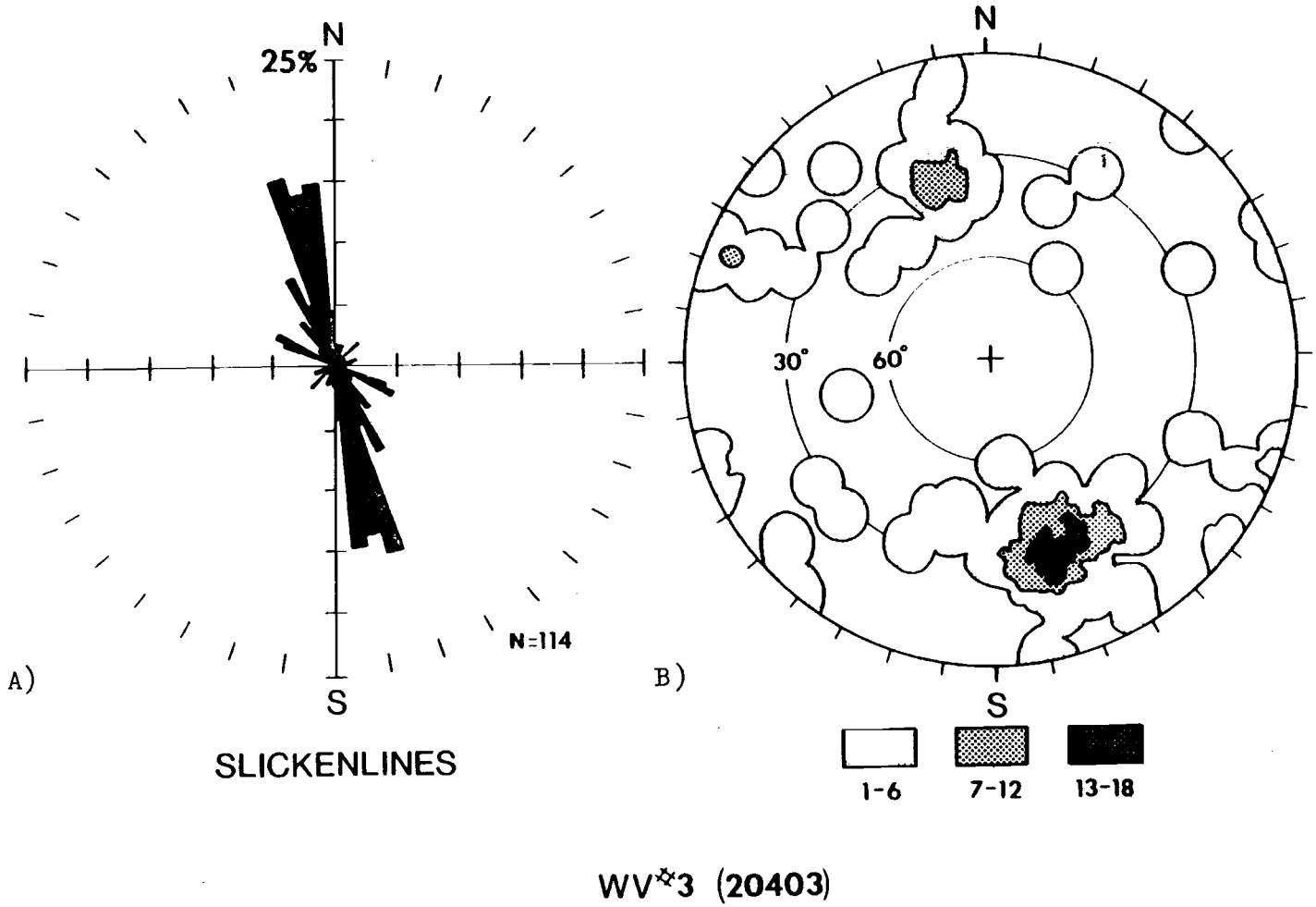

Figure B-11. (A) composite rose diagram of slickenline trends, and (B) equal area projection of slickenlines

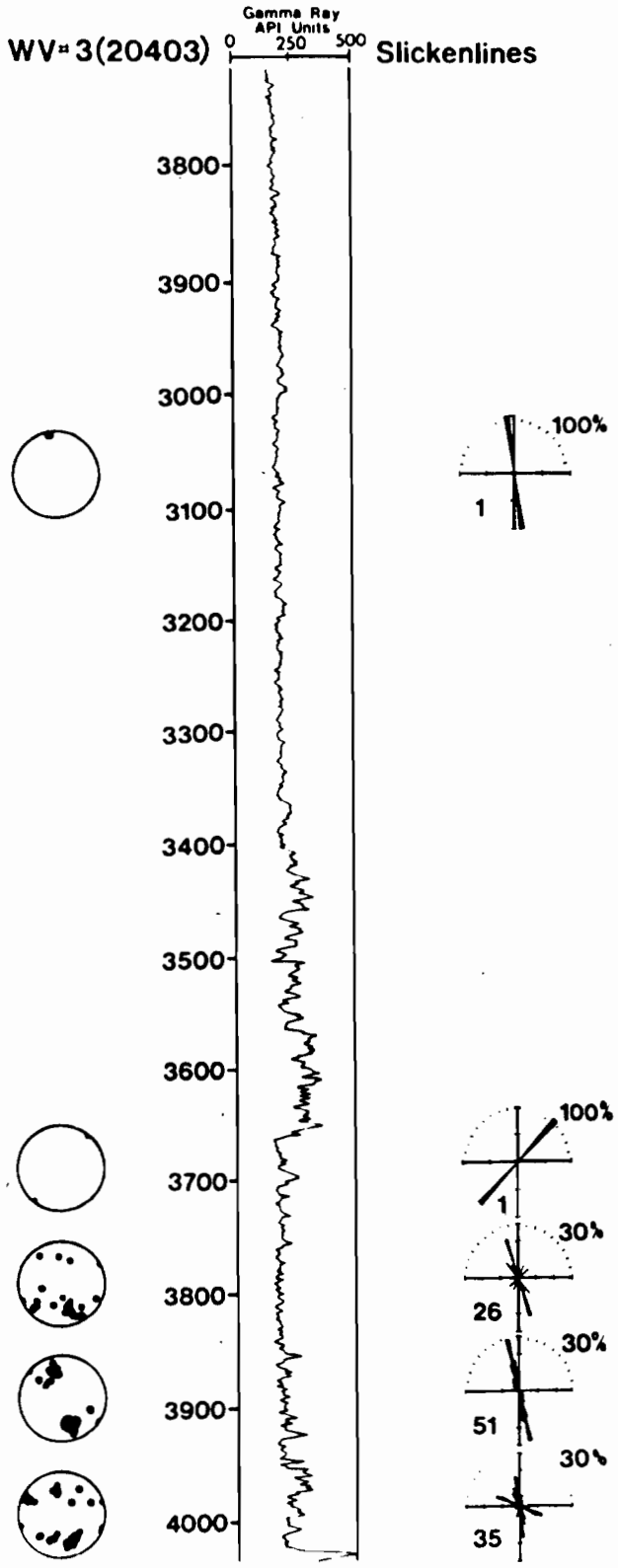

Figure B-12. Equal area projections of slickenlines and rose diagrams of slickenline trends for approximately equal length intervals of the WV #3 (20403) core.

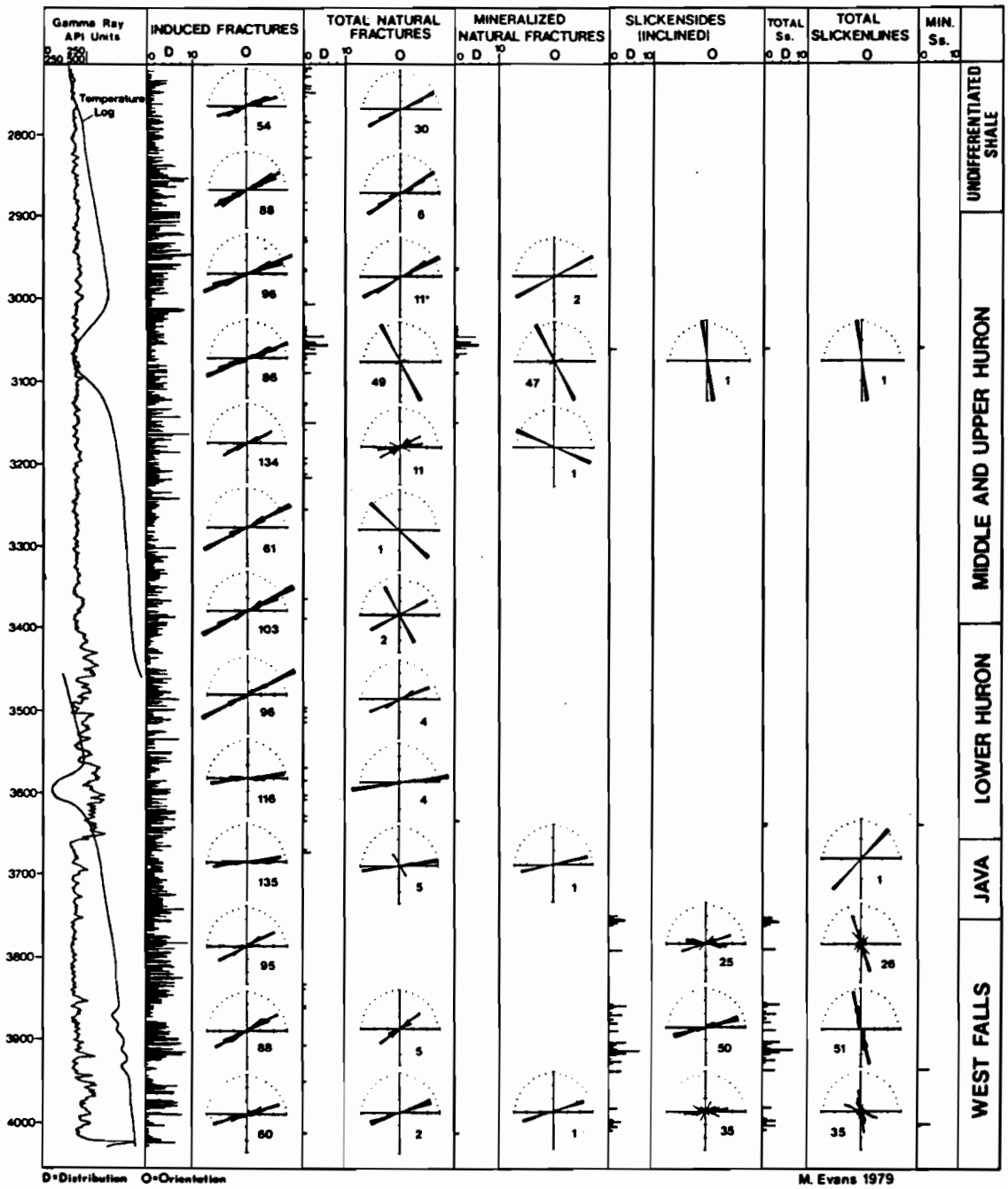

Figure B-13. Composite data sheet of fracture frequencies and orientations for all fracture types.

APPENDIX C: WV #4 (20402) CORE WELL

WV #4 (20402) CORE WELL

Location

The WV #4 (20402) core well is located 0.9 miles southwest of the WV #3 (20403) core well and approximately four miles southwest of the town of Ranger, Lincoln County, West Virginia (figures 1 and C-1, table 1). The wellsite is within the Rome Trough, 15 miles north of the northeast trending Warfield Fault. Fold axes in the area generally trend N65°E. Regional structure of the Devonian shales is a monoclinal dip of less than 1° to the east. A total of 614 feet of the Devonian was cored from four separate intervals: 2654'-2770', 3000'-3118', 3280'-3588', and 3886'-3968' (figure C-2).

Production Data

No production data was available.

Core-induced Fractures

Core-induced fractures are the most common fracture type in the core and are well distributed throughout the cored intervals (figure C-12). There is, however, a notable drop off in frequency in the 2654'-2770' interval in the undifferentiated shales. The core-induced fracture composite rose diagram (figure C-3) has a single peak at N20°-45°E with an average strike of N33°E. There is a 1.0% chance that this peak does not exist. The equal area projection of poles to core-induced fracture surfaces (figure C-3) has four clusters corresponding to the petal and centerline portions of the fractures. Core-induced fracture orientation distributions show only minor variations throughout the core. The greatest amount of scatter occurs in the

undifferentiated shales (figures C-4 and C-5, table C-1).

The generally consistent fracture orientations suggest the presence of a stress or rock fabric anisotropy. The N33°E trending anisotropy may be related to the general east to northeast maximum compressive stress present in most of eastern North America (Sbar and Sykes, 1973). This trend is 30° more northerly than the dominant core-induced fracture trend in the nearby WV #3 (20403) core well.

Natural Fractures

Natural fractures occur throughout the cored intervals. A concentration of fractures is found in the interval 2723'-2733' (figure C-12). The natural fracture composite rose diagram (figure C-6) has a single statistically significant peak at N20°-35°E with an average strike of N27°E. There is a 1.0% chance that this peak does not exist. Four peaks that are not statistically significant occur at N67°E, N3°W, N17°W, and N63°W. The equal area projection of poles to natural fracture surfaces (figure C-6) has eight periferal clusters corresponding to four of the five subvertical to vertical fracture sets. Natural fracture orientations are quite variable and show no pattern or systematic variation with depth or stratigraphy (figure C-7). Several of the natural fracture sets are mineralized, generally with massive or crystalline calcite. A greater proportion of natural fractures are mineralized in the West Falls Formation than in any other unit in the core.

The N20°-35°E natural fracture set parallels the core-induced fractures and may have formed under the same stress conditions. The set also parallels the central Appalachian trend and may have formed

as a release fracture set when Alleghenian tectonic stresses were relaxed. The N67°E set parallels the southern Appalachian trend and also may have formed when tectonic stresses were relaxed. This set also parallels the core-induced fractures, natural fractures, and slickensides in the WV #3 (20403) core. The N63°W set is orthogonal to the central Appalachian trend and probably formed as extension fractures when tectonic compressive stresses were oriented N60°-70°W during Alleghenian deformation. The N3°W and N17°W sets may actually be part of the same set. They are nearly orthogonal to the southern Appalachian trend and also probably formed as extension fractures. These two sets are subparallel to the N27°W natural fracture set in the WV #3 (20403) core.

Slickensides and Slickenlines

Slickensides are found in three zones: at 3400', in the Middle Huron Member of the Ohio Shale; at 3582', 10 feet above the base of the Lower Huron Member of the Ohio Shale; and throughout the entire cored portion of the West Falls Formation (figure C-12). The Lower Huron zone occurs in a soft dark shale unit immediately above the contact with the stiffer shales of the Java Formation. The West Falls zone occurs in a low-viscosity dark shale unit immediately above the much stiffer Onondaga Limestone. Only the West Falls zone is vertically extensive enough to be classified as a decollement zone. The Lower Huron zone correlates with a similar zone in the WV #3 (20403) core.

The slickenside composite rose diagram (figure C-8) has a single peak at N35°-45°E with an average strike of N40°E. There is a 1.0%

chance that this peak does not exist. A smaller peak which is not statistically significant occurs at N55°W. The slickensided surfaces in this set are gouged and intensely slickenlined, more so than the dominant set. Also, this set only occurs in the West Falls Formation. The poles to slickensided surfaces form an incomplete girdle across the equal area projection (figure C-8). The cluster pattern follows that expected for a shear zone. The 0° dipping cluster in the center is the displacement shear cluster, the Riedel shear cluster dips 20°NW, and the thrust shear cluster dips 30°SE. R' shears are not present in this core. A 50°SW dipping cluster results from the N55°W slickenside set. Very few of the slickensides in this core are mineralized, and those occur only in the West Falls Formation. Massive calcite is the dominant filling. Slickenside orientations show very little scatter or systematic variation with depth or stratigraphy (figure C-9).

The slickenline composite rose diagram (figure C-10) has a single statistically significant peak at N40°-50°W. There is a 1.0% chance that this peak does not exist. A smaller peak, at N33°E, is not statistically significant. This orientation is found only on the N55°W slickenside set. The equal area projection of slickenlines (figure C-10) has three clusters: two of which correspond to the low-dipping N40°-50°W trending slickenlines, and a 50°SW dipping cluster resulting from the N33°E trending set. Slickenlines show very little variation from a northwest trend, except in the Lower Huron Member of the the Ohio Shale and West Falls Formation (figure C-11).

The N40°-50°W slickenlines are subparallel to the N63°W natural fractures and are orthogonal to the N35°-45°E slickenside set. These

three trends are related in that they all probably formed under the same tectonic compressive stresses. The N55^{o}W slickenside set may indicate a splay off of a basement fault, or compaction and settling of the shales resulting from basin subsidence or movement along a Rome Trough fault.

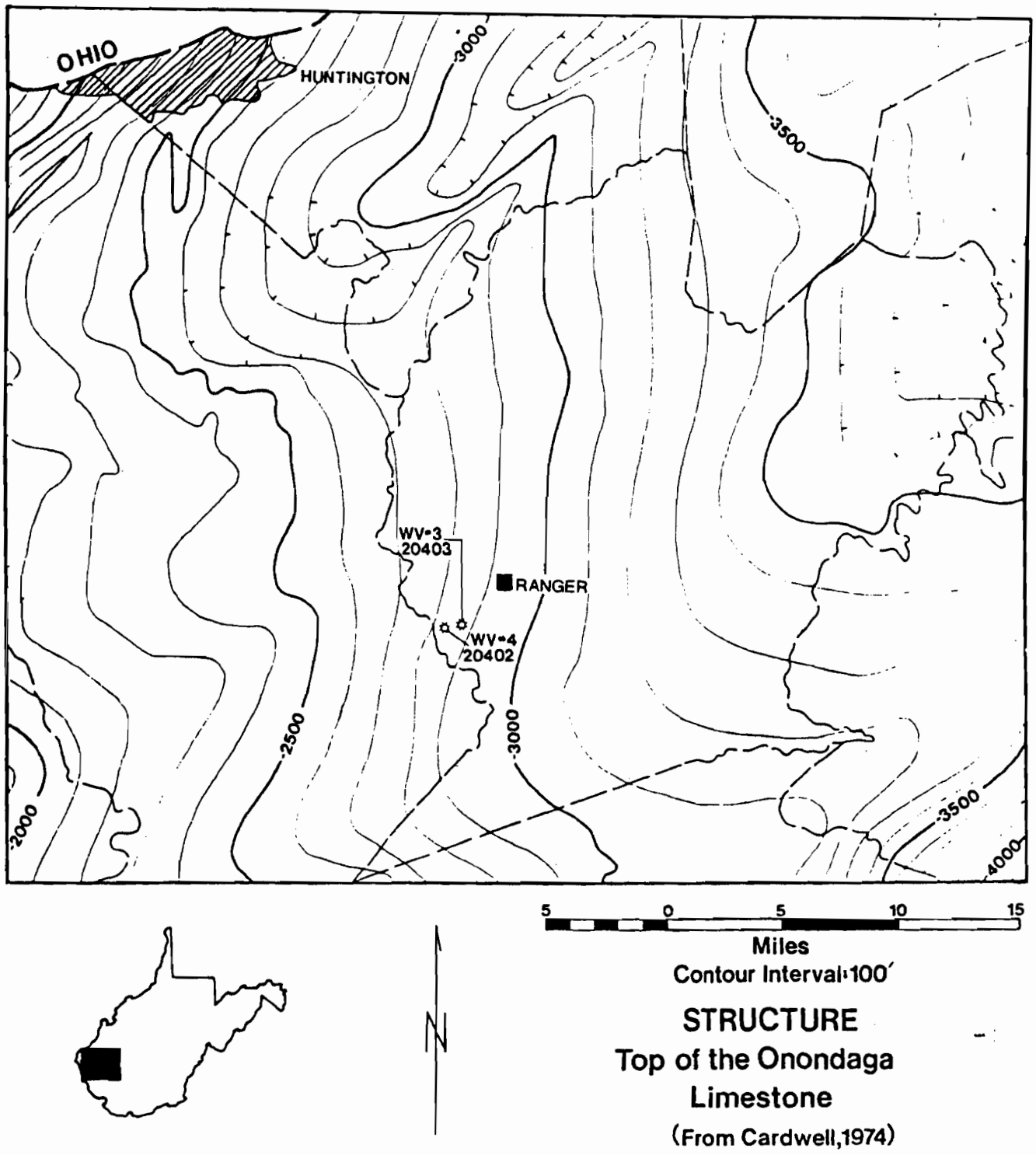

Figure C-1. Index map for the WV #4 (20402) core well

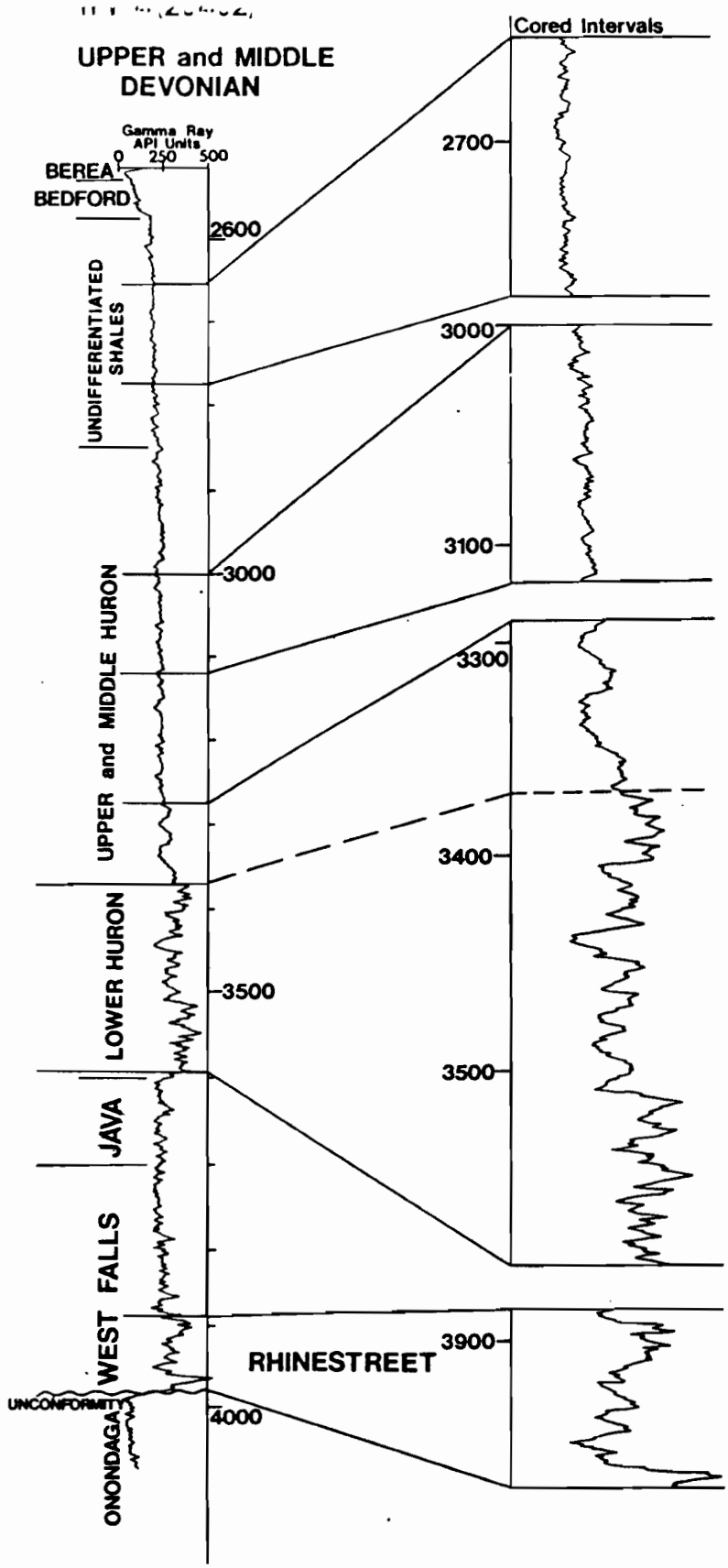

Figure C-2. Gamma-ray log, Middle and Upper Devonian.

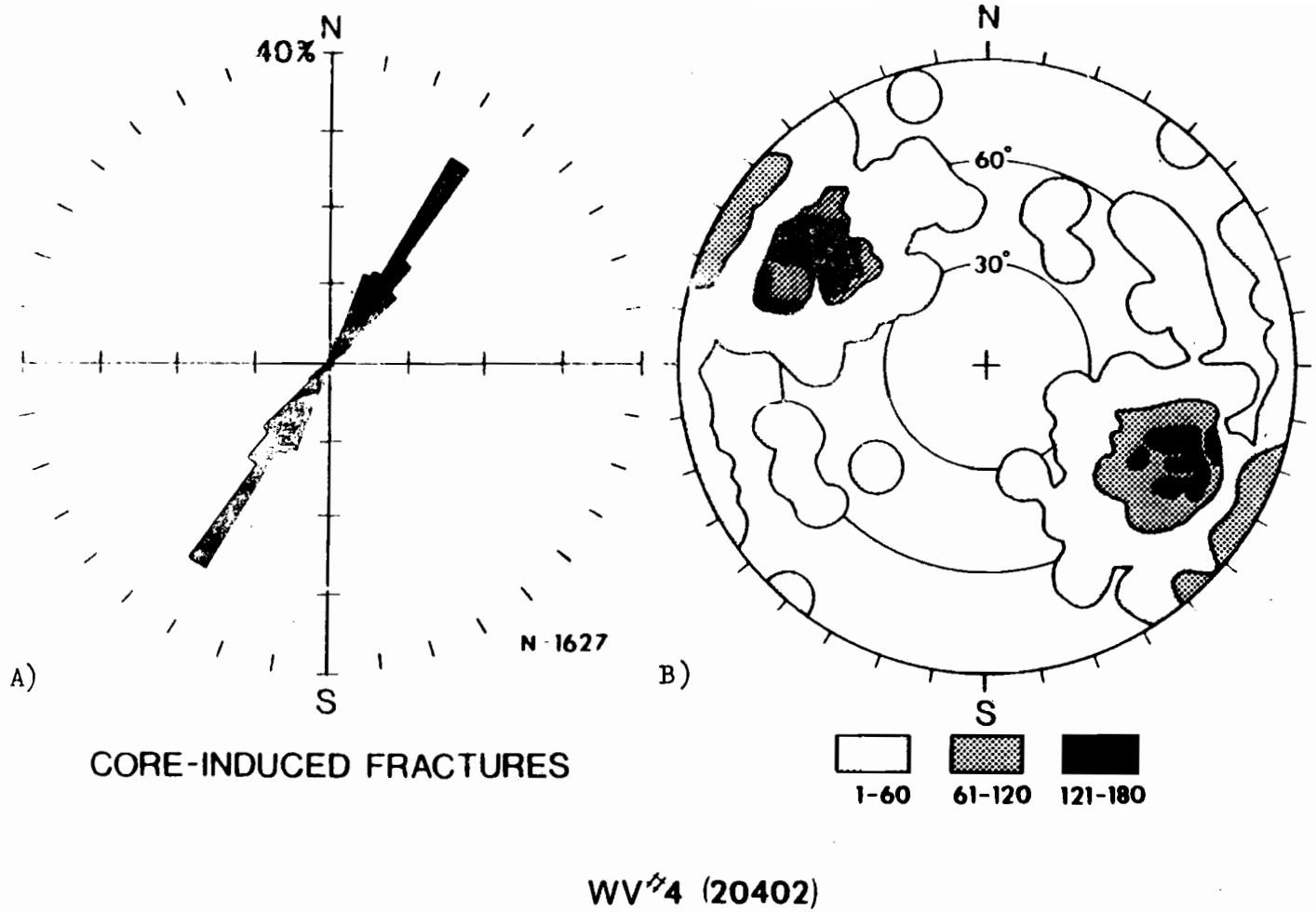

Figure C-3. (A) composite rose diagram of core-induced fracture strikes, and (B) equal area projection of poles to core-induced fracture surfaces

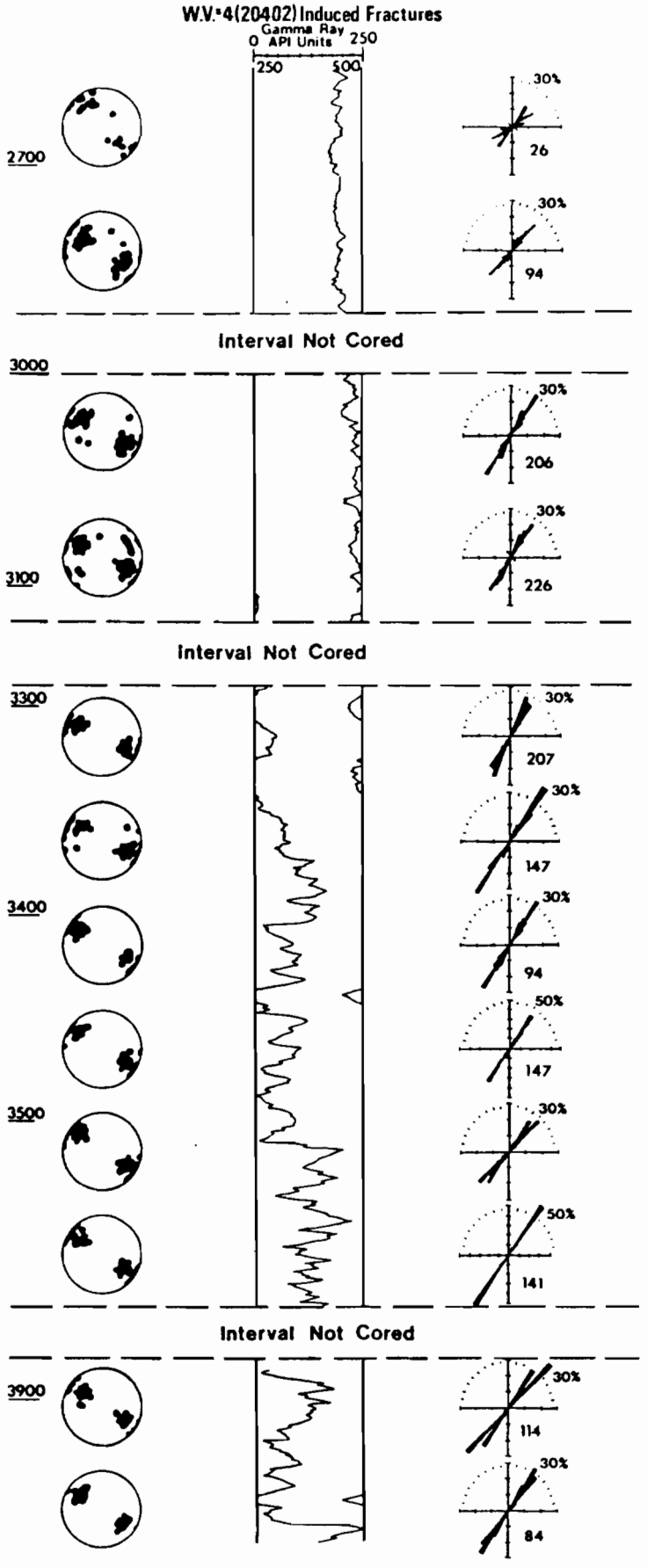

Figure C-4. Equal area projections of poles to core-induced fracture surfaces and rose diagrams of core-induced fracture strikes for approximately equal length intervals of the WV #4 (20402) core.

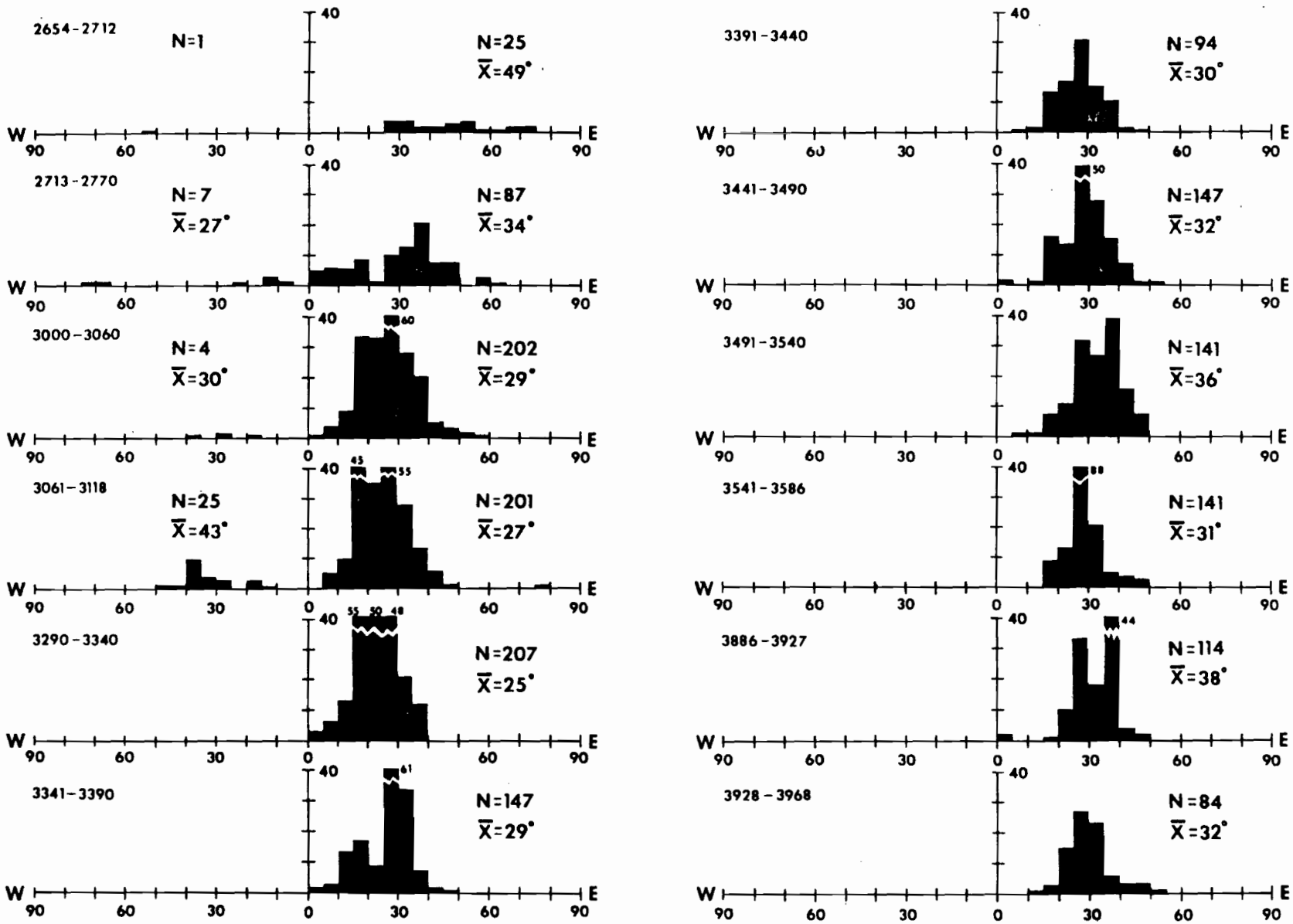

WV※4 (20402) CORE-INDUCED FRACTURES

Figure C-5. Histograms of core-induced fracture orientations.

TABLE C-1

WV #4 (20402) INDUCED FRACTURES

Interval	N	VN	α
2654-2712	26		
2713-2770	94	2.0503	≤1.00
3000-3060	206	4.5132	≤0.01
3061-3118	226	1.7621	≤1.00
3290-3340	207	3.2234	≤0.01
3341-3390	147	4.3534	≤0.01
3391-3440	94	2.5982	≤0.05
3441-3490	147	2.5579	≤0.05
3491-3540	141	3.1142	≤0.01
3541-3588	141	4.7160	≤0.01
3886-3927	114	4.3561	≤0.01
3928-3968	84	3.1239	≤0.01

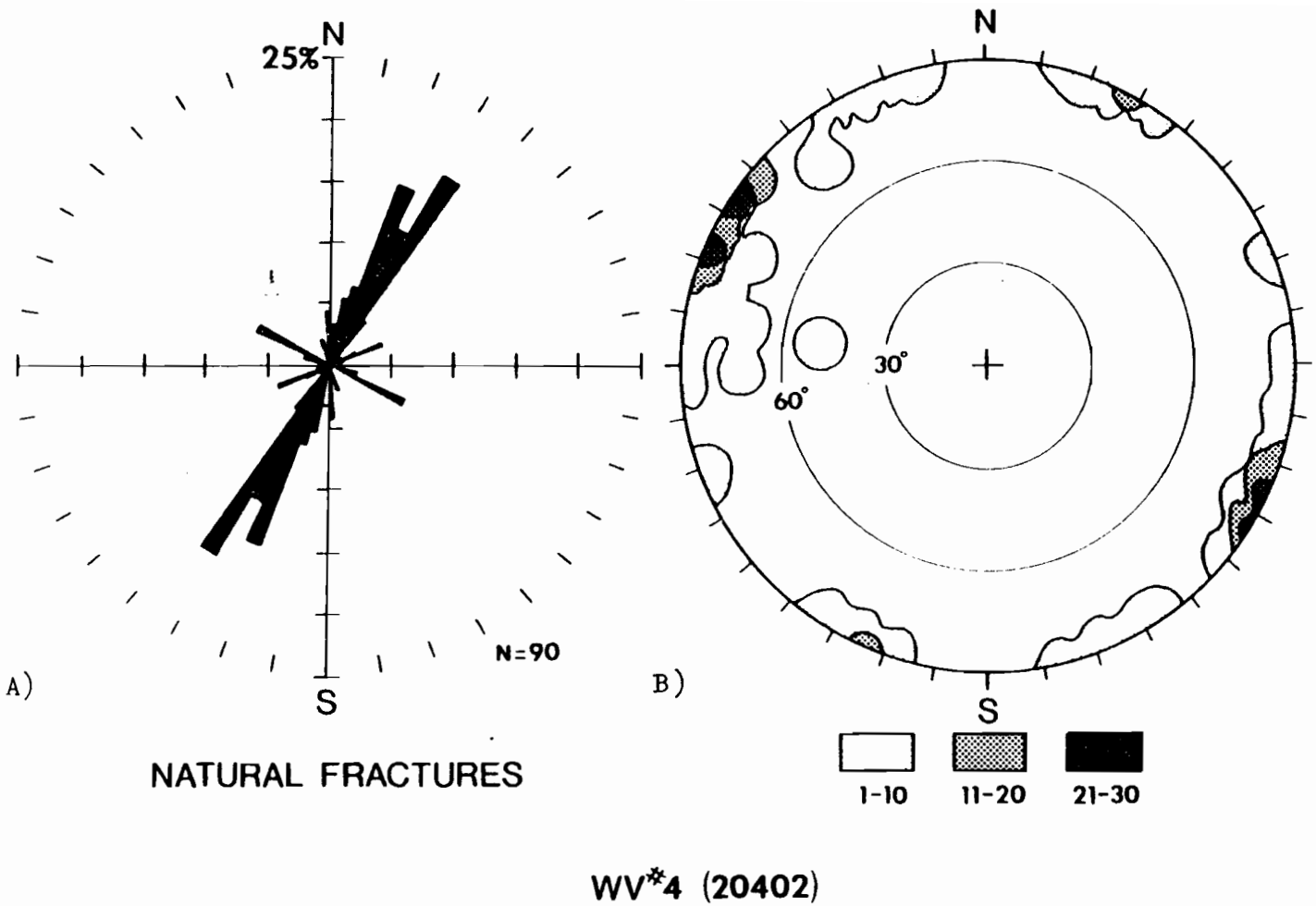

Figure C-6. (A) composite rose diagram of natural fracture strikes, and (B) equal area projection of poles to natural fracture surfaces

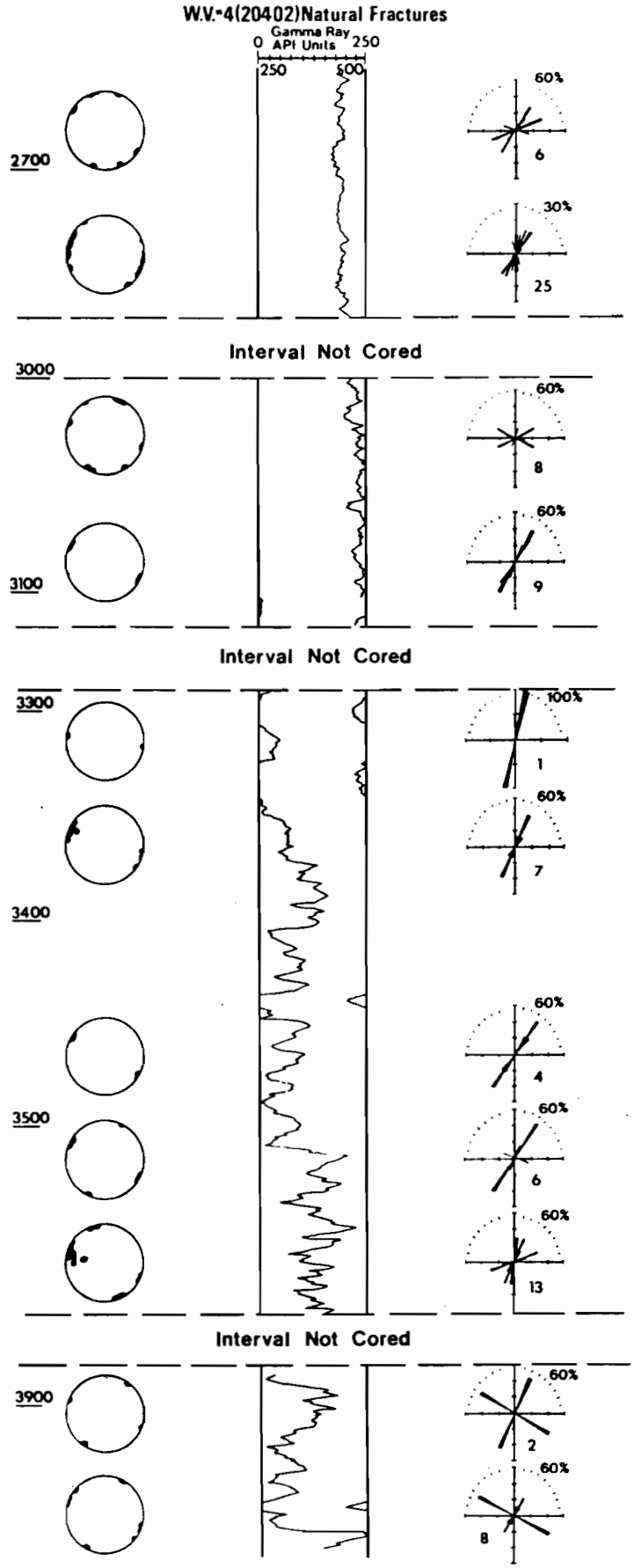

Figure C-7. Equal area projections of poles to natural fracture surfaces and rose diagrams for approximately equal length intervals of the WV #4 (20402) core.

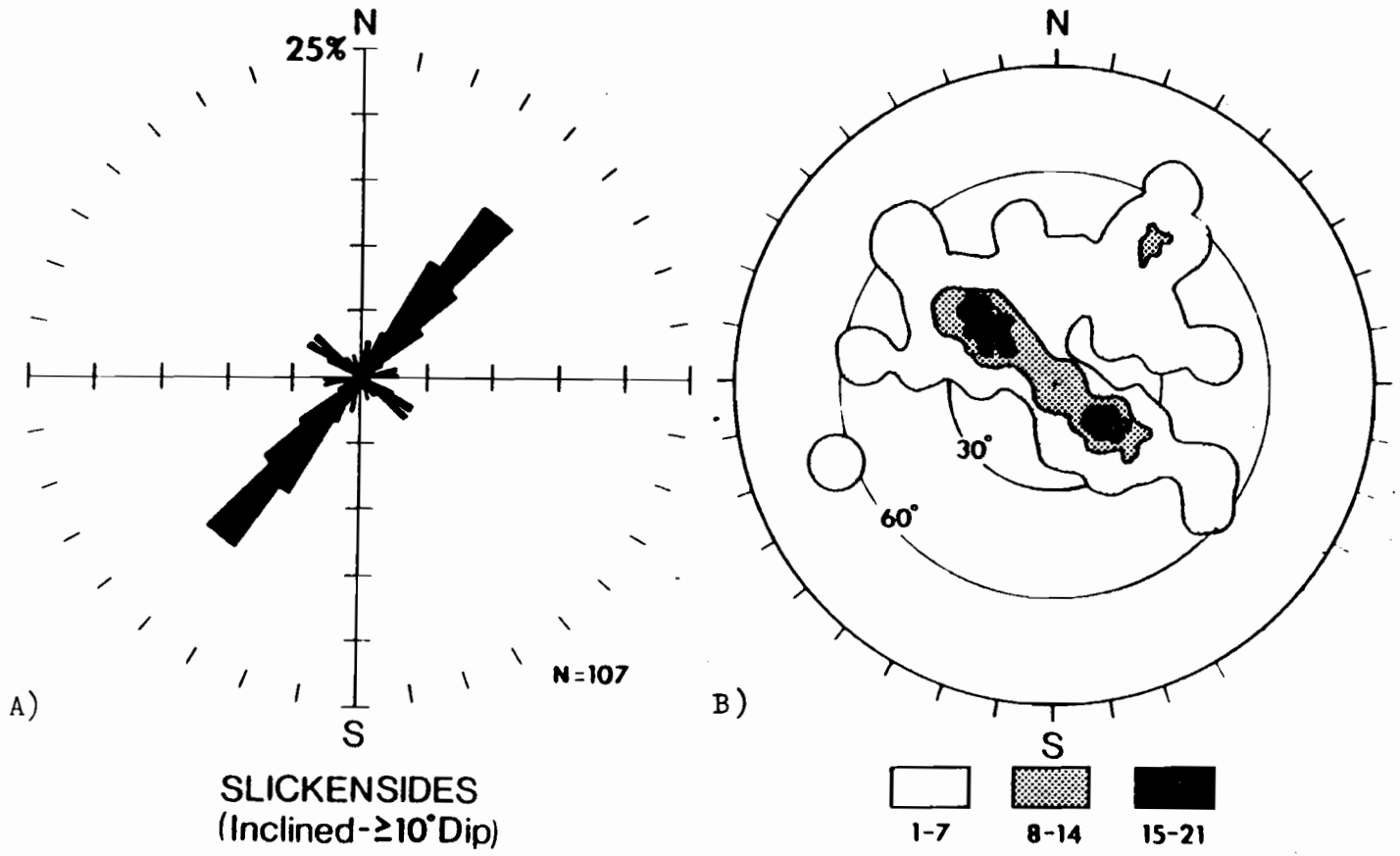

WV*4 (20402)

Figure C-8. (A) composite rose diagram of slickenside strikes, and (B) equal area projection of poles to slickensided surfaces

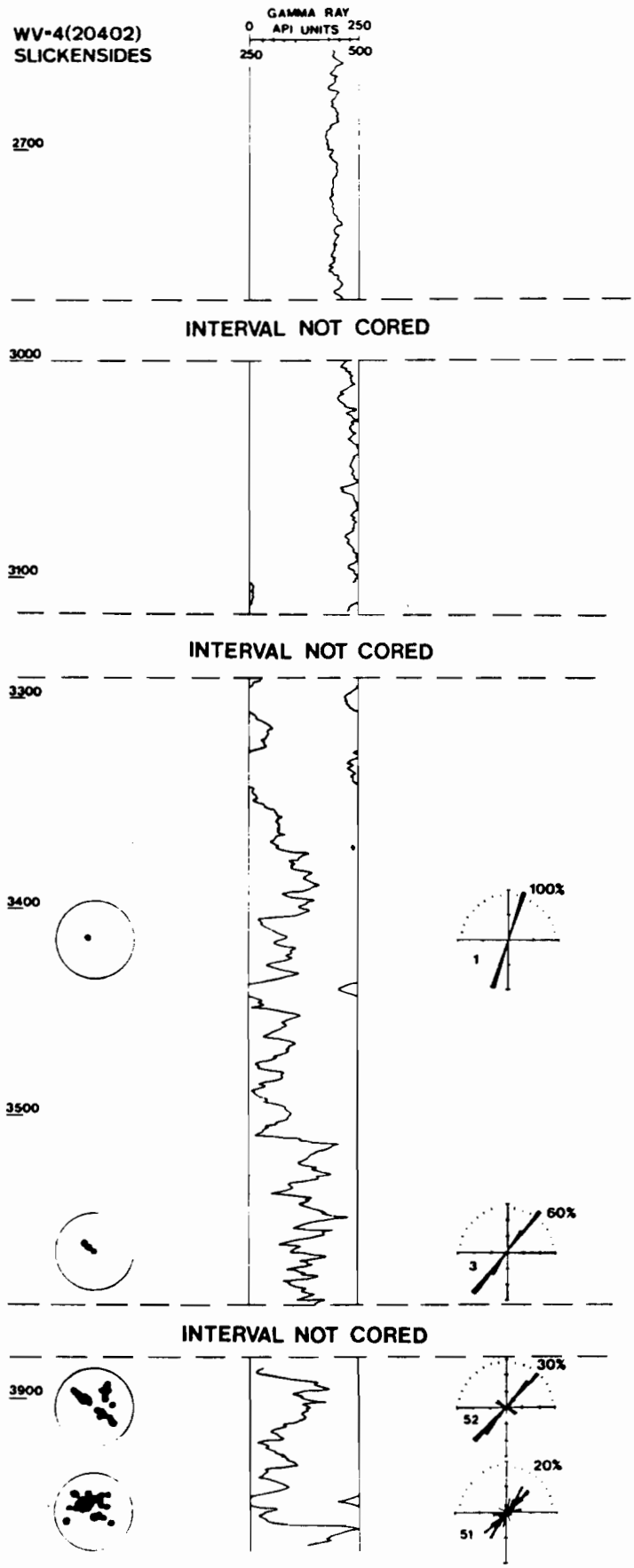

Figure C-9. Equal area projections of poles to slickensided surfaces and rose diagrams of slickenside strikes for approximately equal length intervals of the WV #4 (20402) core.

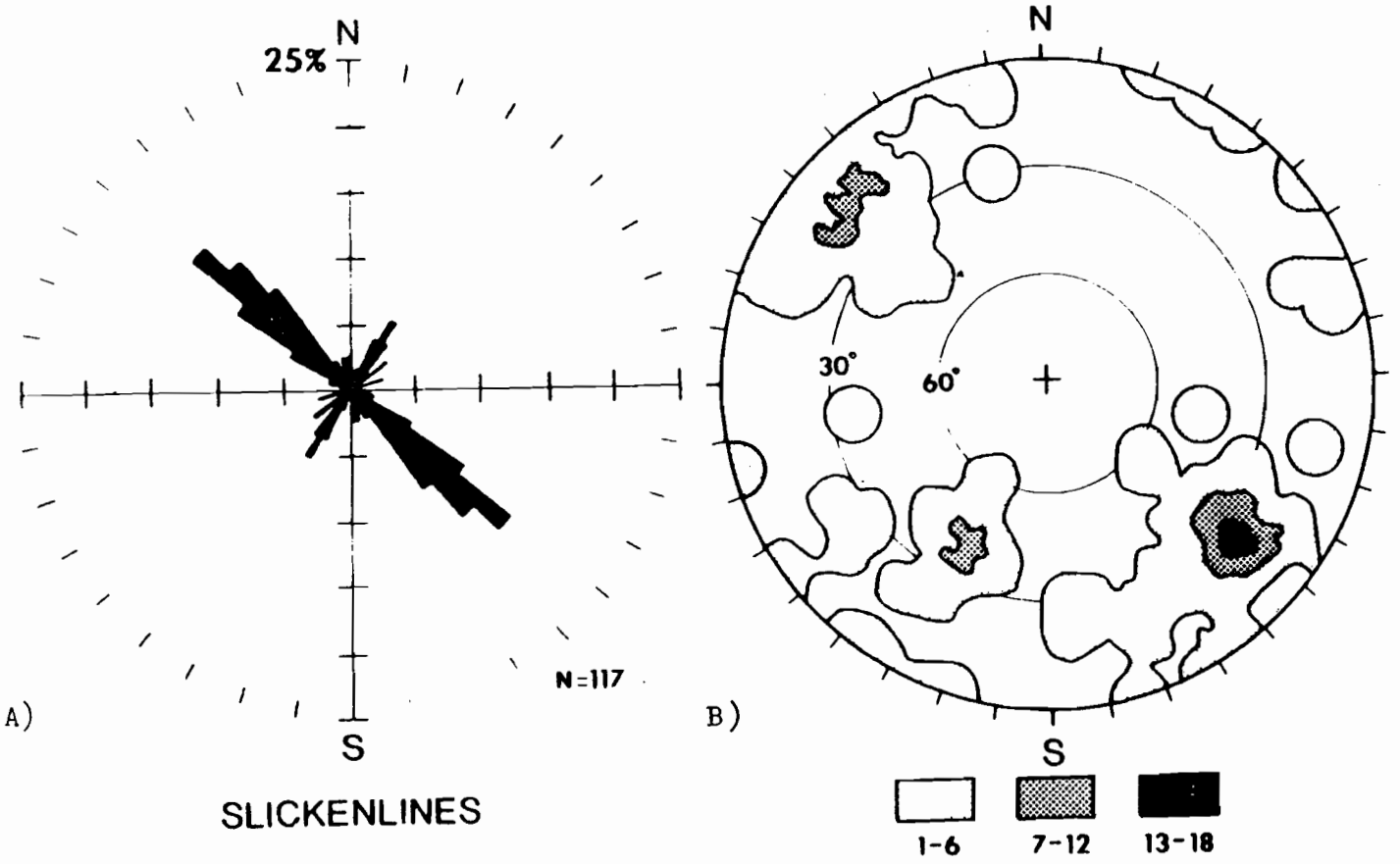

WV*4 (20402)

Figure C-10. (A) composite rose diagram of slickenline trends, and (B) equal area projection of slickenlines

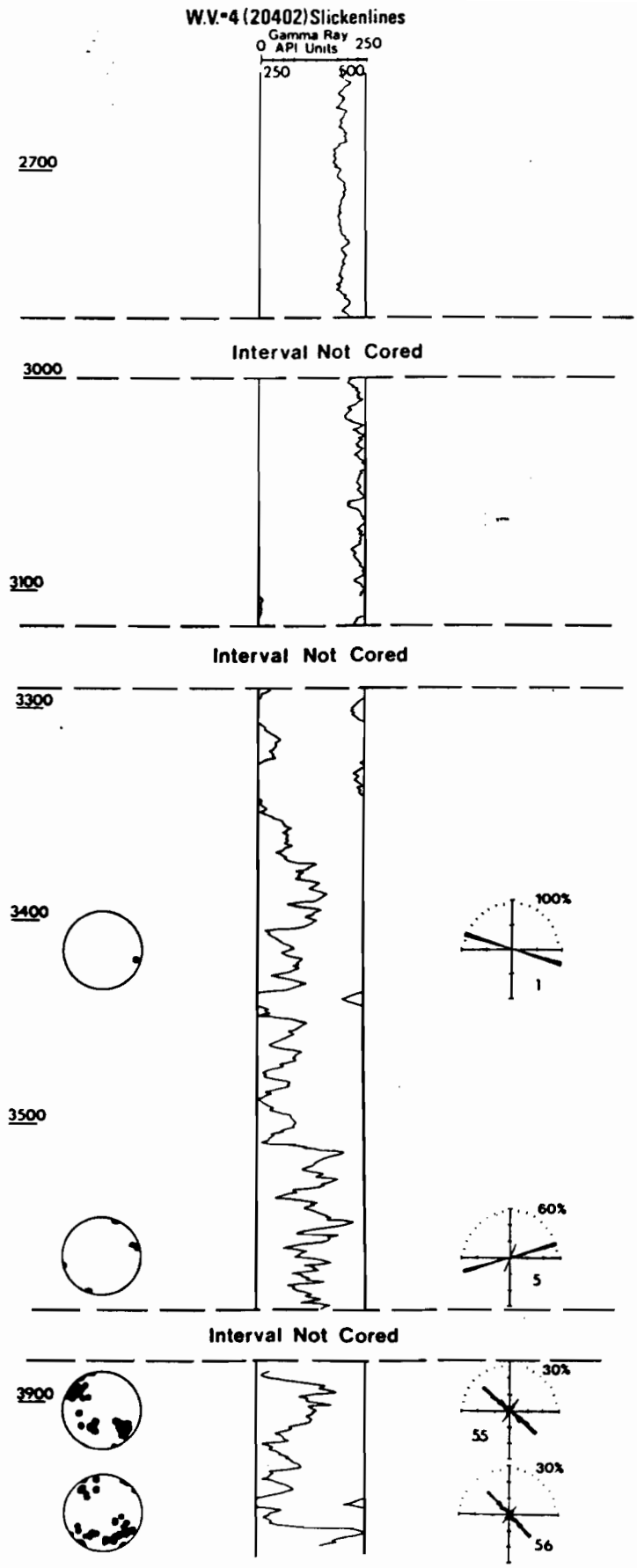

Figure C-11. Equal area projections of slickenlines and rose diagrams of slickenline trends for approximately equal length intervals of the WV #4 (20402) core.

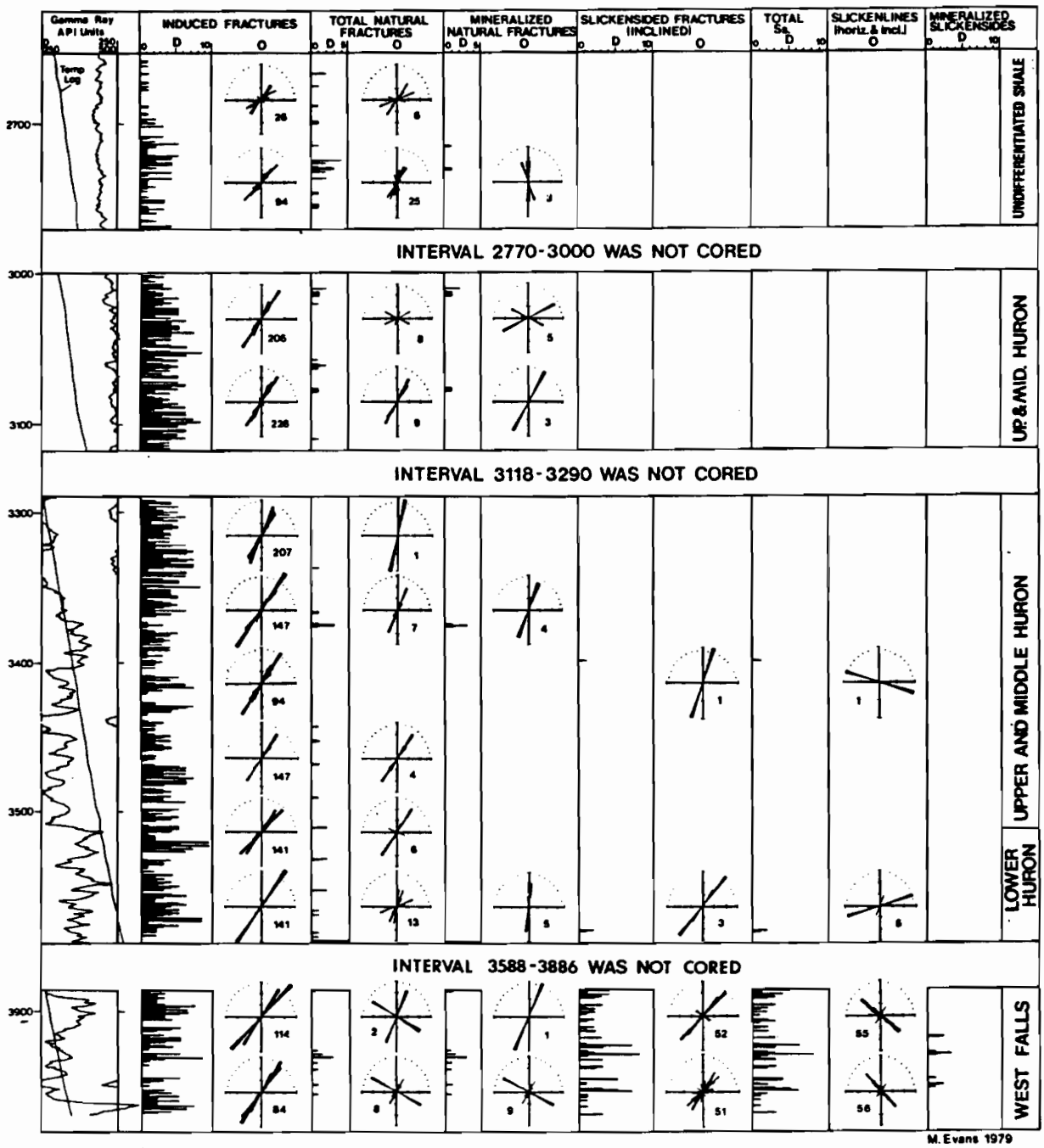

Figure C-12. Composite data sheet of fracture frequencies and orientations for all fracture types.

APPENDIX D: WV #5 (#3 D/K) CORE WELL

WV #5 (#3 D/K) CORE WELL

Location

The WV #5 (#3D/K) core well is located in Mason County, West Virginia, approximately five miles northeast of the town of Point Pleasant (figures 1 and D-1, table 1). The wellsite is on the western flank of the N60°E trending Parkersburg Syncline. Regional structure of the Devonian shales shows a monoclinal dip of less than 1° to the southeast. A total of 747 feet of the Devonian was cored, from 2673'-3420' (figure D-2). The first 38 feet of the core could not be oriented because it was severely broken during coring. This interval was not used in this study, and data collection began at 2711'.

Production Data

Two intervals of the WV #5 (#3 D/K) well were stimulated. Interval 2730'-3042' in the Huron Member of the Ohio Shale was stimulated with a cryogenic type treatment resulting in an initial open flow of 456 mcf/day. Interval 3348'-3374' in the Rhinestreet Member of the West Falls Formation was stimulated by foam fracturing and the resulting initial open flow was 50 mcf/day. This interval was immediately flooded out, presumably with salt water from the underlying Onondaga Limestone (Overbey, personal communication).

Core-induced fractures

Core-induced fractures are the most abundant fracture type in the core. The Huron Member of the Ohio Shale has the greatest freqency of core-induced fractures with abundance dropping off in the Java Formation and West Falls Formation (figure D-16). The composite

rose diagram of core-induced fracture strikes (figure D-3) has one peak at N65°-85°E with an average orientation of N75°E. There is a 1.0% chance that this peak does not exist. The equal area projection of poles to core-induced fracture surfaces (figure D-3) has two clusters corresponding to the opposing dips of the fractures. Core-induced fracture strike distributions change subtly downcore with the greatest difference occurring between intervals 3201'-3250' and 3251'-3300'. Average orientations for these intervals are N71°E and N85°E respectively (figures D-4, D-5, D-6, and D-7, table D-1). The change occurs near the base of the Angola Shale Member of the West Falls Formation.

The consistency in core-induced fracture strike indicates that a stress or rock fabric anisotropy may be present in the rock around this well. This anisotropy may be related to the east to northeast trending maximum compressive stress present in most of eastern North America (Sbar and Sykes, 1973).

Natural Fractures

Natural fractures are found primarily in the Huron Member of the Ohio Shale, but a few are also found in the West Falls Formation (figure D-16). The natural fracture composite rose diagram (figure D-8) has three peaks. There is a 1.0% chance that the peak at N65°-80°E does not exist and a 5.0% chance that the peaks at N45°-60°W and N33°E do not exist. The equal area projection of poles to natural fracture surfaces (figure D-8) has six peripheral clusters corresponding to the three subvertical to vertical fracture sets. Fractures of the N65°-80°E set are found throughout the core, whereas

fractures of the N45°-60°W set are restricted only to the lower portion of the Huron Member of the Ohio Shale (figures D-9, D-10, and D-11).

Over one third of the natural fractures in the core are mineralized, with either calcite, dolomite, anhydrite, or barite, in the crystallized form or as massive coatings sparsely covering the fracture surface (figure D-12). All of the mineralized fractures are found in the Huron Member of the Ohio Shale. The fractures with calcite mineralization generally strike N65°-80°E, whereas the fractures with dolomite mineralization (figure D-13) generally strike N45°-60°W and are concentrated in a zone between 2870' and 2890'. The N33°E set is not mineralized. This preference in fracture mineralization suggests that one fracture set formed, or was open, at a time different from that of the other fracture set. If this is the case, each set would have been exposed to fluid pressure and temperature conditions, and groundwater chemistries different from that of the other set, resulting in the formation of different minerals. No abutting relationships were found in the core to conferm this idea.

The calcite mineralized N65°-80°E set has nearly the same orientation as the core-induced fractures. Therefore, it is possible that these natural fractures formed under the same stress conditions responsible for the core-induced fractures. This would make the N65°-80°E set the most recent because it follows the current stress or rock fabric anisotropy. The fractures in this set also parallel slickenline trends in this core, suggesting that they may have formed as extension fractures under compression from the northeast during formation of the Burning Springs Anticline. The N45°-60°W natural

fracture set is nearly orthogonal to the trend of the central Appalachians and probably formed as an extension fracture set under tectonic compressive stresses during Alleghenian deformation. The N33°E set parallels the central Appalachians and may have formed as a release fracture set as Paleozoic tectonic stresses were relaxed.

Slickensides and Slickenlines

In the WV #5 (#3 D/K) core, slickensides are found in only two distinct zones, both of which are located near viscosity boundaries in the shales (figure D-16). The upper zone, at 3036', is the soft high-organic black shales of the Huron Member, 10 feet above the contact with the stiffer shales of the Java Formation. The lower zone, 3128'-3136', is in the Java Formation, 13 feet above the contact with the slightly softer shales in the Angola Shale Member. The slickenside composite rose diagram (figure D-14) has a single peak at N17°W. There is a 1.0% chance that this peak does not exist. The equal area projection of poles to slickensided surfaces (figure D-14) has two clusters dipping 20°SW and 20°NE. The slickensides in the Java Formation show more scatter in strike than those in the Huron Member and are less well developed.

The slickenline composite rose diagram (figure D-15) has a single peak trending N67°E. There is a 1.0% chance that this peak does not exist. The equal area projection of slickenlines (figure D-15) has tow peripheral clusters that correspond to the low dipping slickenlines. The two slickenside zones, because of their limited vertical extent and limited number of readings, cannot be considered decollement

zones. However they may be slip planes which formed as the rock absorbed the remaining stresses of dying out detachments to the east. The N67°E displacement trend suggests a relationship to the detached Burning Springs Anticline located forty miles to the northeast.

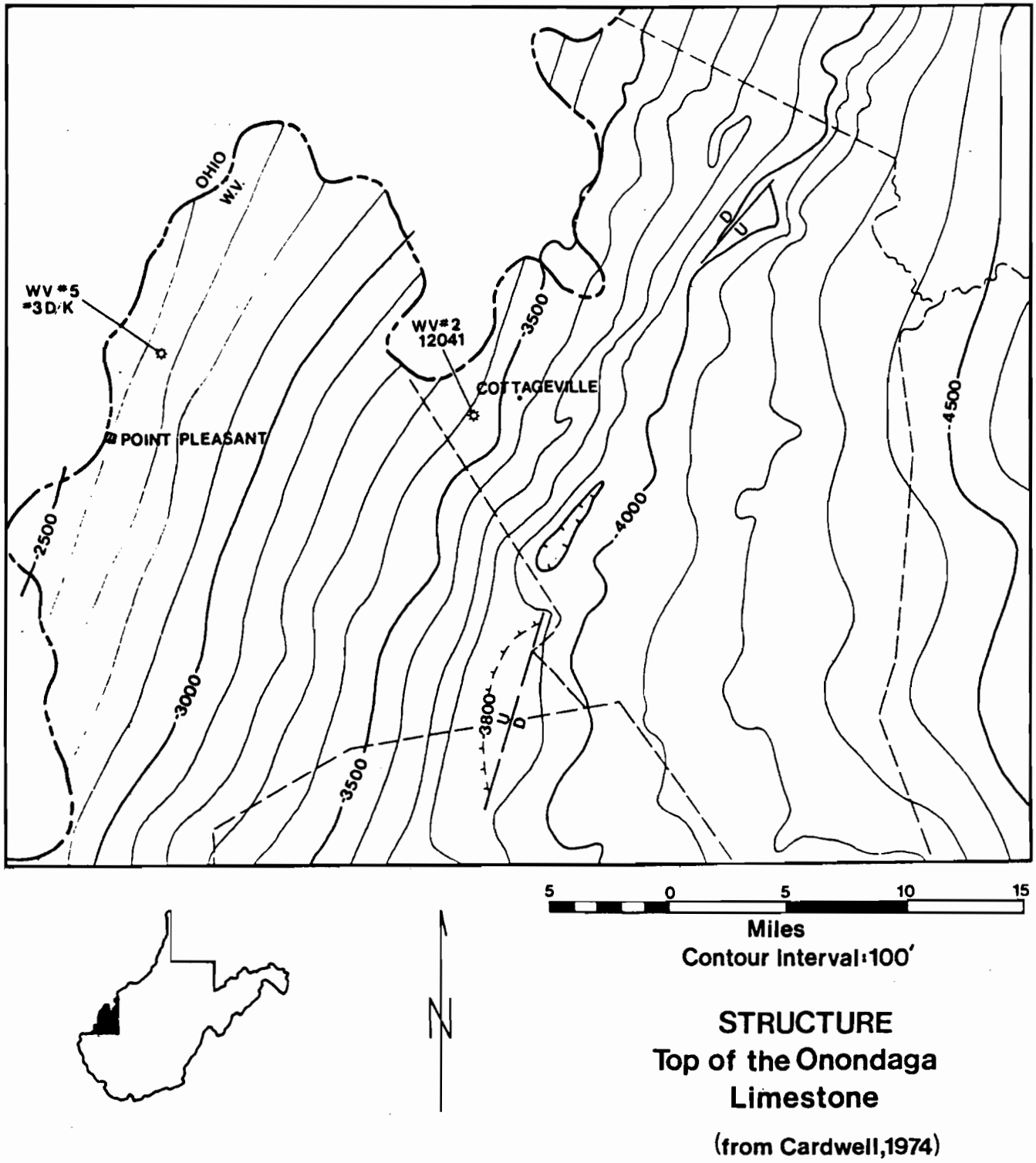

Figure D-1. Index map for the WV #5 (#3 D/K) core well

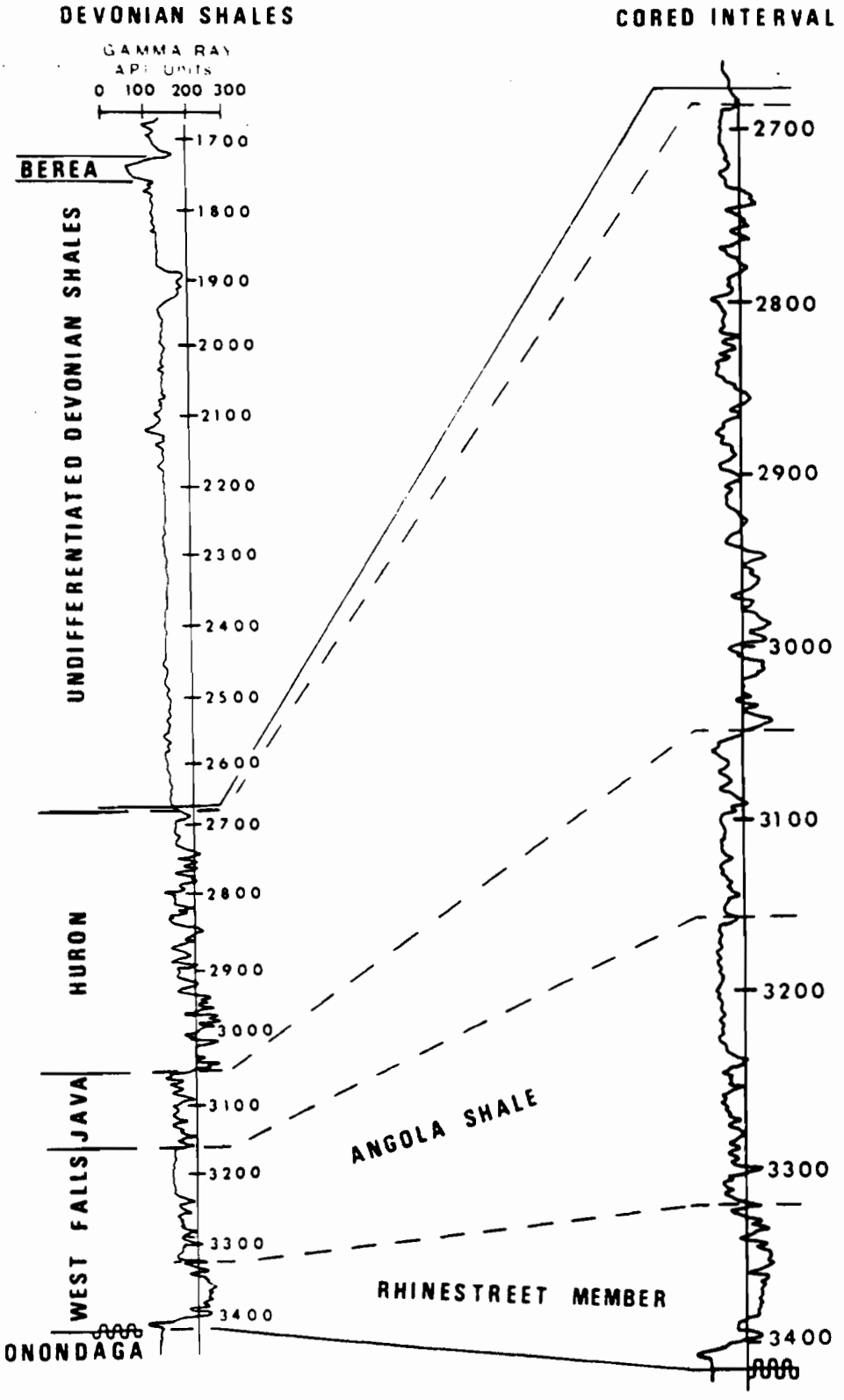

Figure D-2. Gamma-ray log, Middle and Upper Devonian

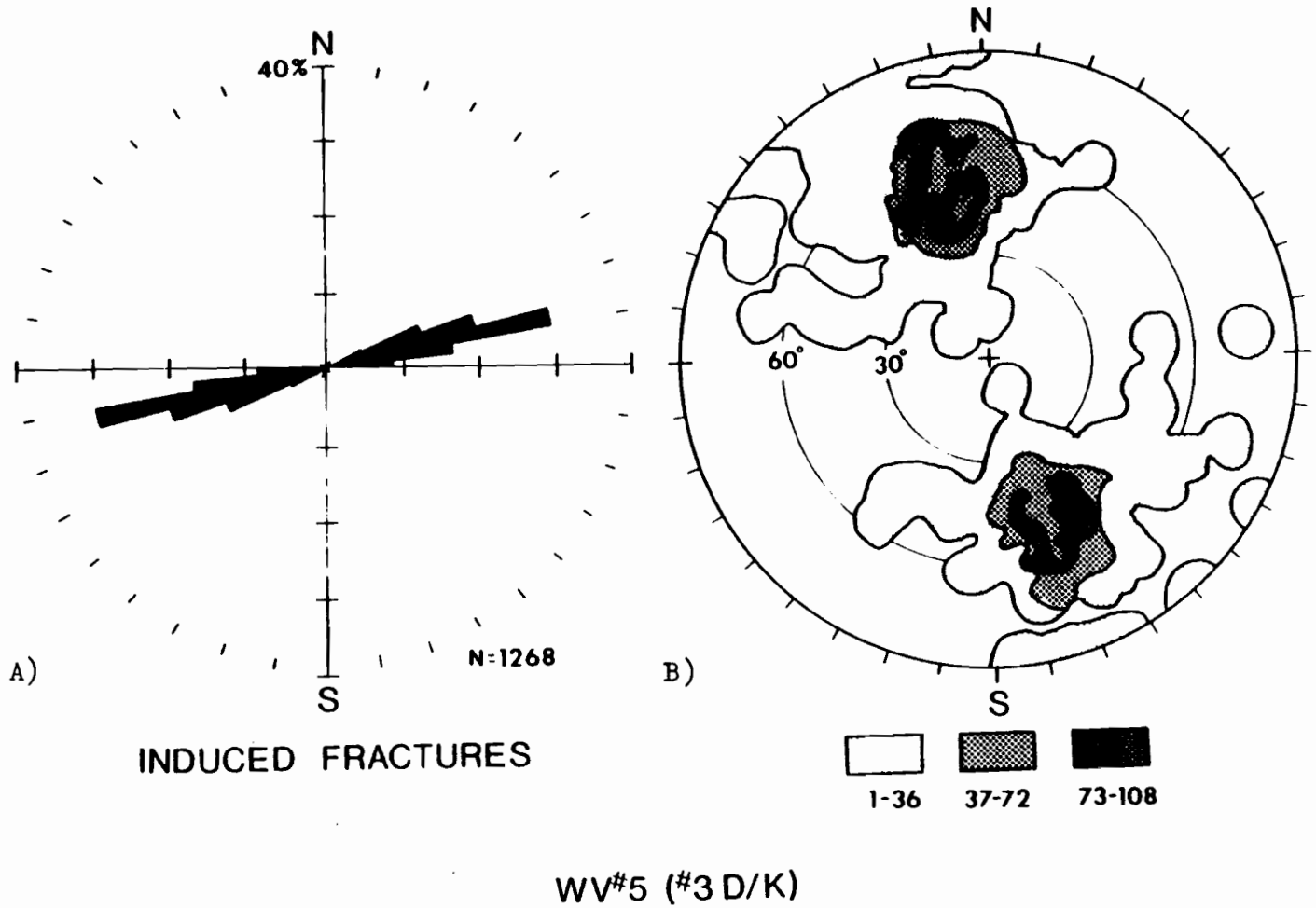

Figure D-3. (A) composite rose diagram of core-induced fracture strikes, and (B) equal area projection of poles to core-induced fracture surfaces

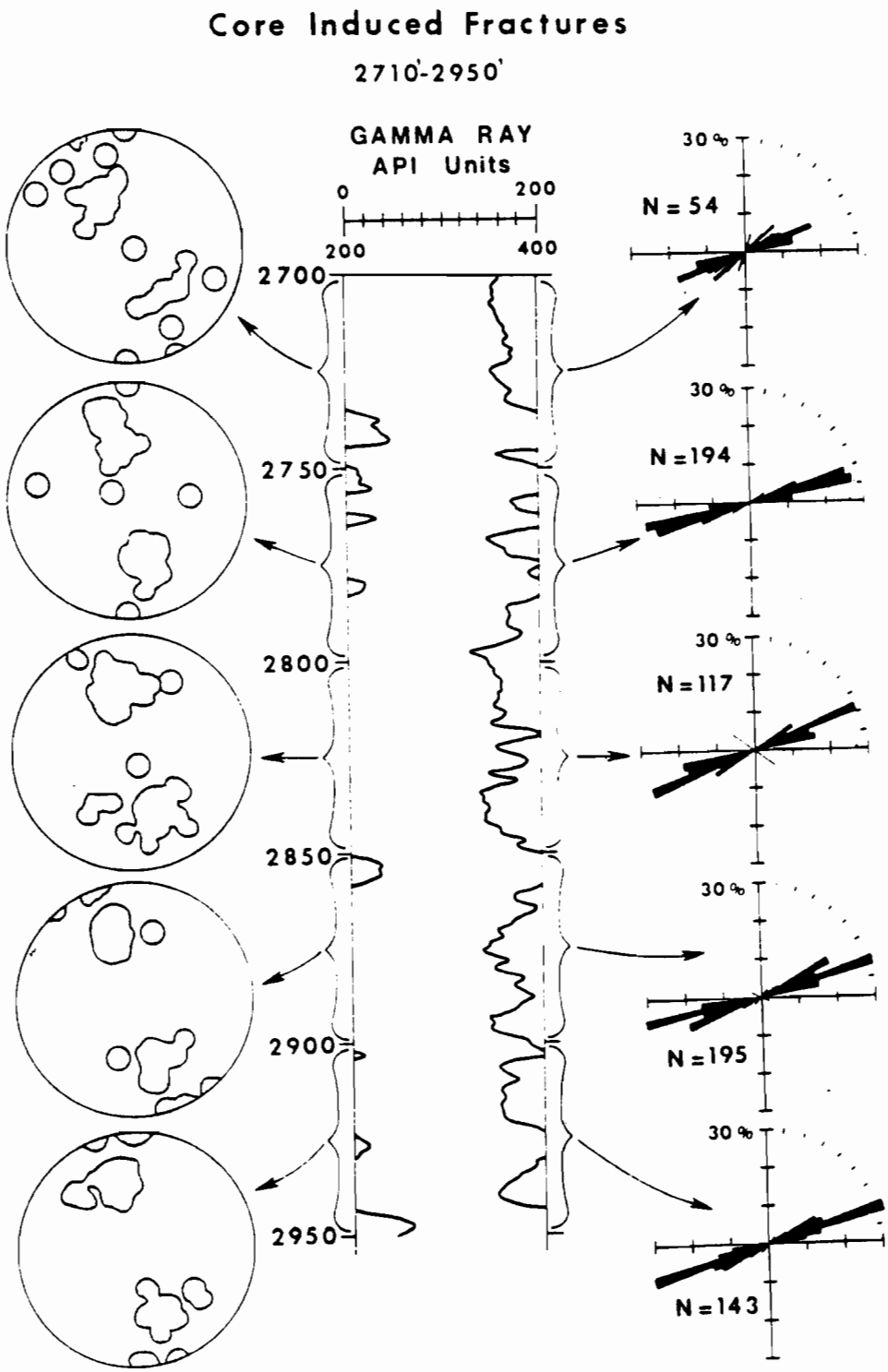

Figure D-4. Equal area projections of poles to core-induced fracture surfaces and rose diagrams of core-induced fracture strikes for approximately equal length intervals of the WV #5 (#3 D/K) core. Also figures D-5 and D-6.

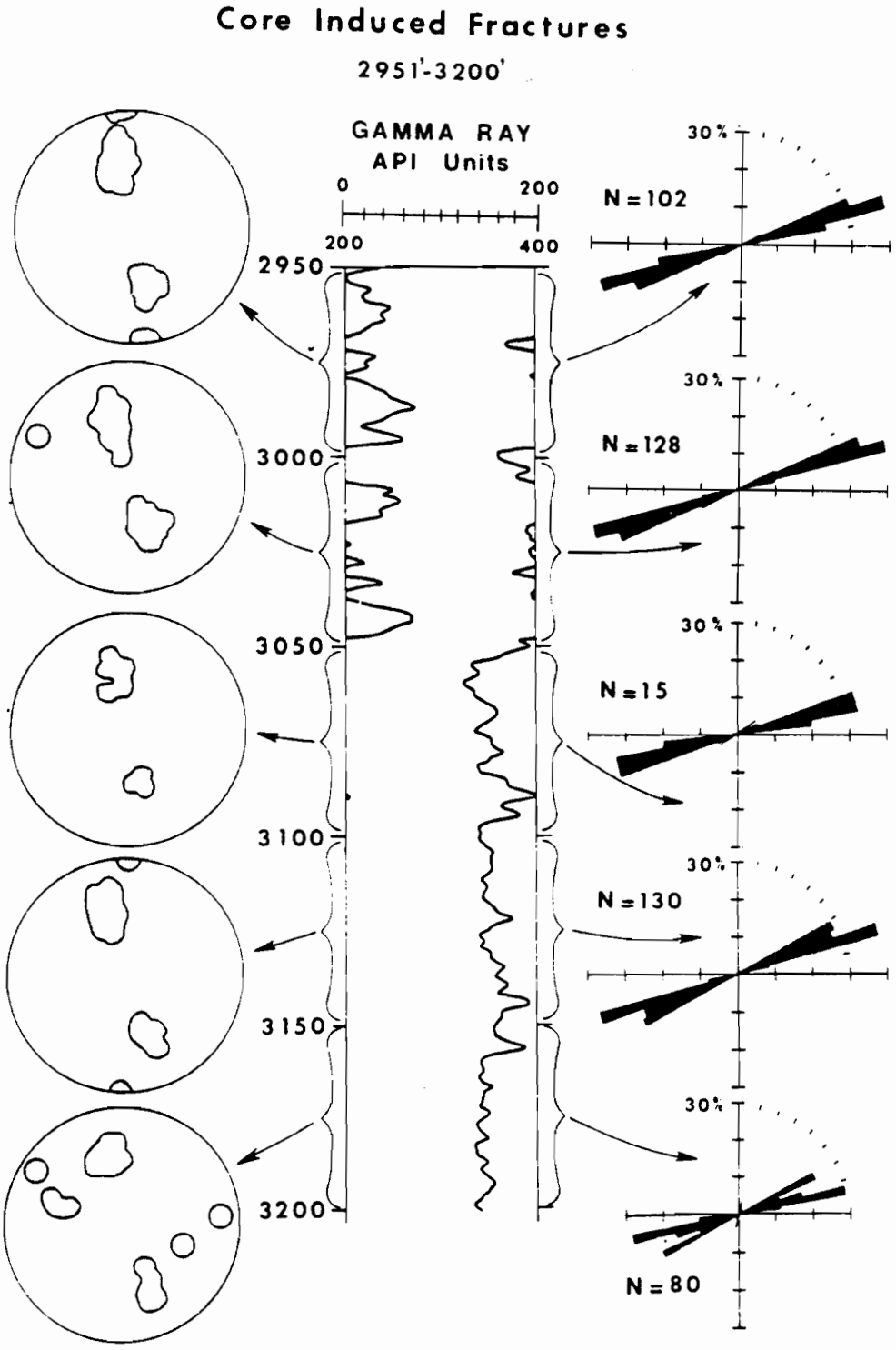
Core Induced Fractures
2951'-3200'
GAMMA RAY
API Units
0
200
200
400
2950
3000
3050
3100
3150
3200
30%
N = 102
N = 128
N = 15
N = 130
N = 80

Figure D-5.

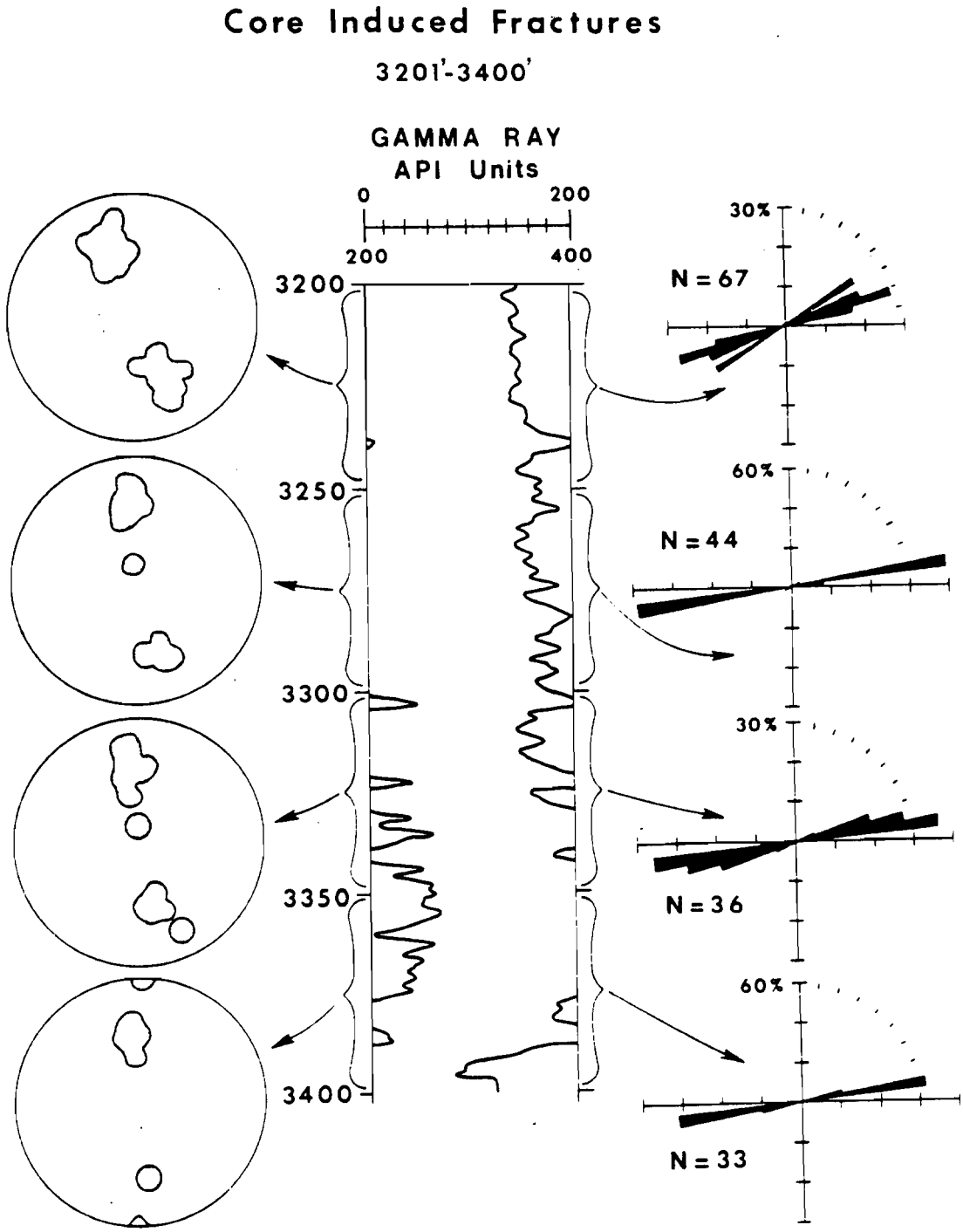
Core Induced Fractures
3201'-3400'
GAMMA RAY
API Units
0
200
200
400
3200
3250
3300
3350
3400
30%
N = 67
60%
N = 44
30%
N = 36
60%
N = 33

Figure D-6.

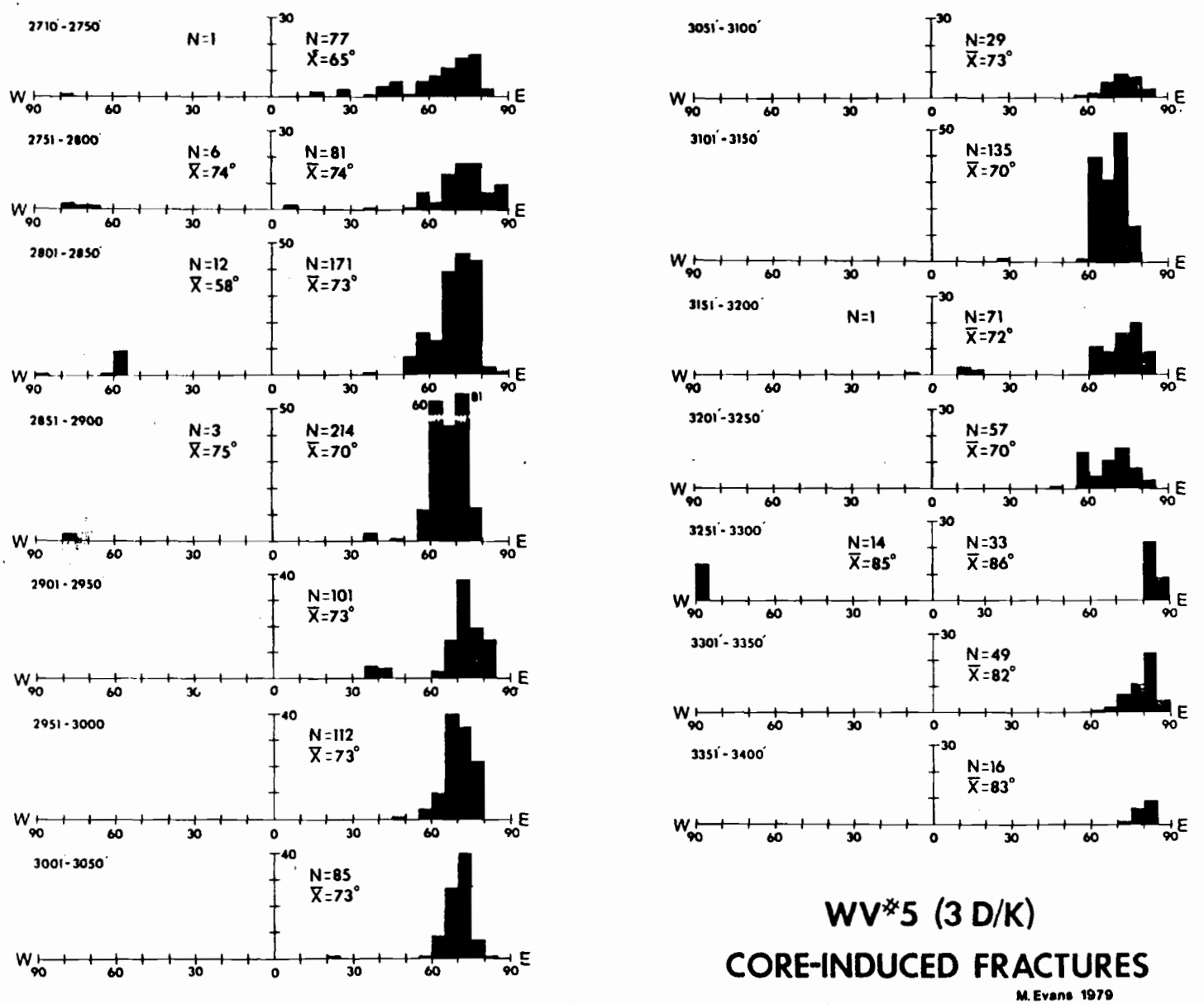

WV*5 (3 D/K)

CORE-INDUCED FRACTURES

M. Evans 1979

Figure D-7. Histograms of core-induced fracture orientations.

TABLE D-1

WV #5 (#3 D/K) INDUCED FRACTURES

Interval	N	VN	α
2710-2750	78		
		2.4324	≤ 0.10
2751-2800	87		
		2.1600	≤ 1.00
2801-2850	183		
		4.3652	≤ 0.01
2851-2900	217		
		3.6275	≤ 0.01
2901-2950	101		
		3.1441	≤ 0.01
2951-3000	112		
		1.6144	≤ 1.00
3001-3050	85		
		2.1934	≤ 1.00
3051-3100	29		
		1.8817	≤ 1.00
3101-3150	135		
		3.8419	≤ 0.01
3151-3200	72		
		2.5387	≤ 0.05
3201-3250	57		
		6.2031	≤ 0.01
3251-3300	47		
		2.9292	≤ 0.01
3301-3350	49		
		2.1173	≤ 1.00
3351-3400	16		

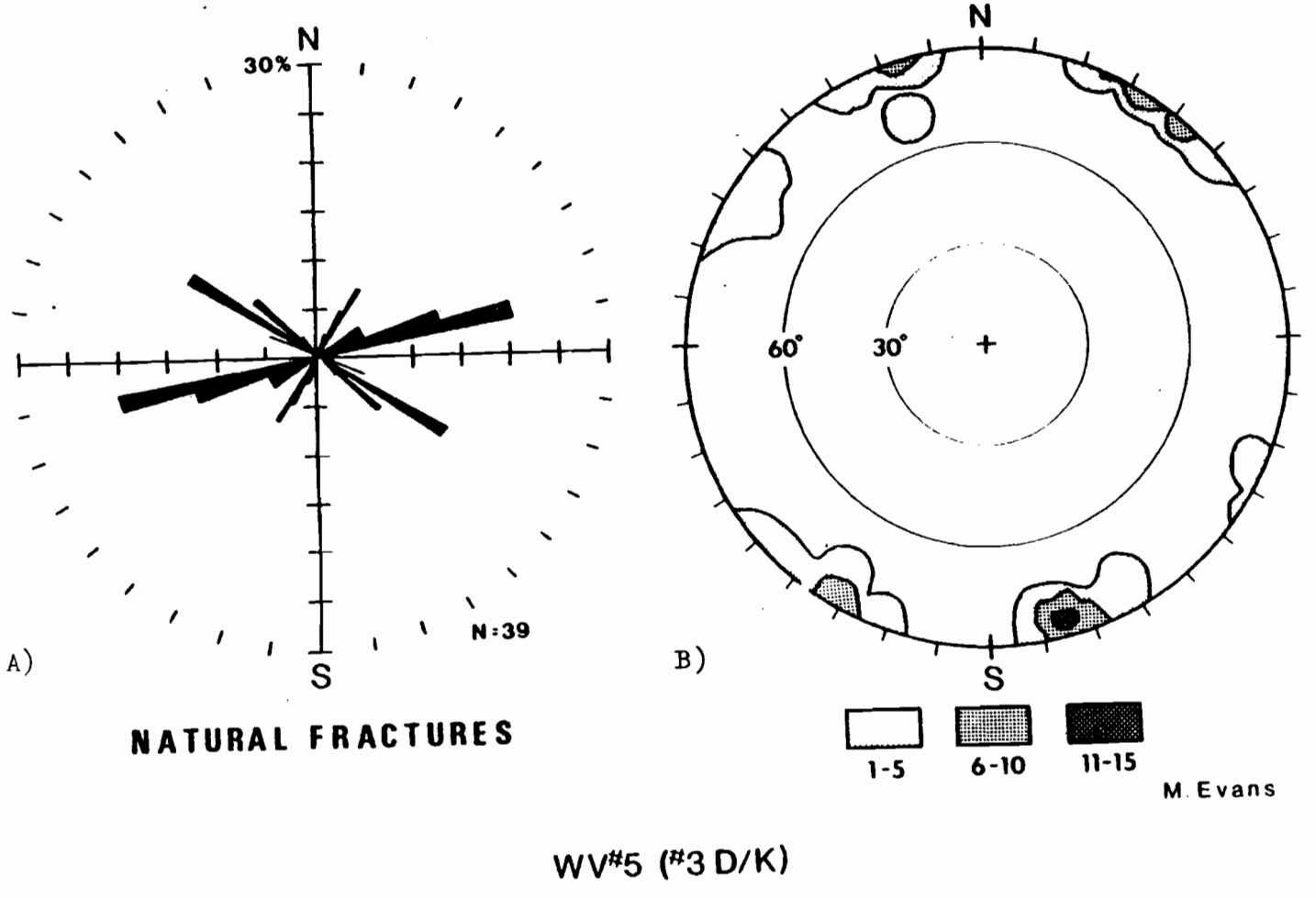

Figure D-8. (A) composite rose diagram of natural fracture strikes, and (B) equal area projection of poles to natural fracture surfaces

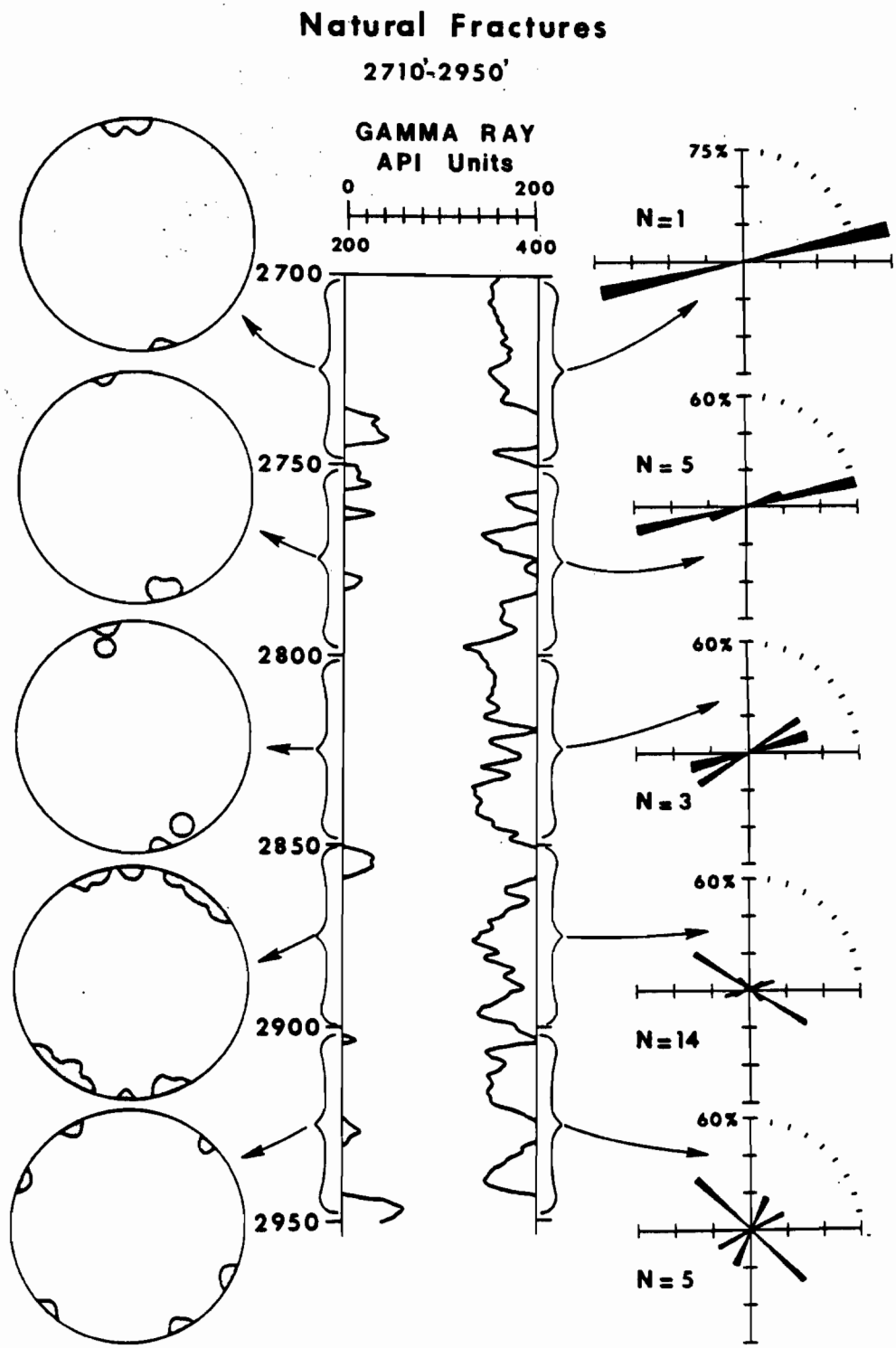

Figure D-9. Equal area projections of poles to natural fracture surfaces and rose diagrams of natural fracture strikes for approximately equal length intervals of the WV #5 (#3 D/K) core. Also figures D-10 and D-11.

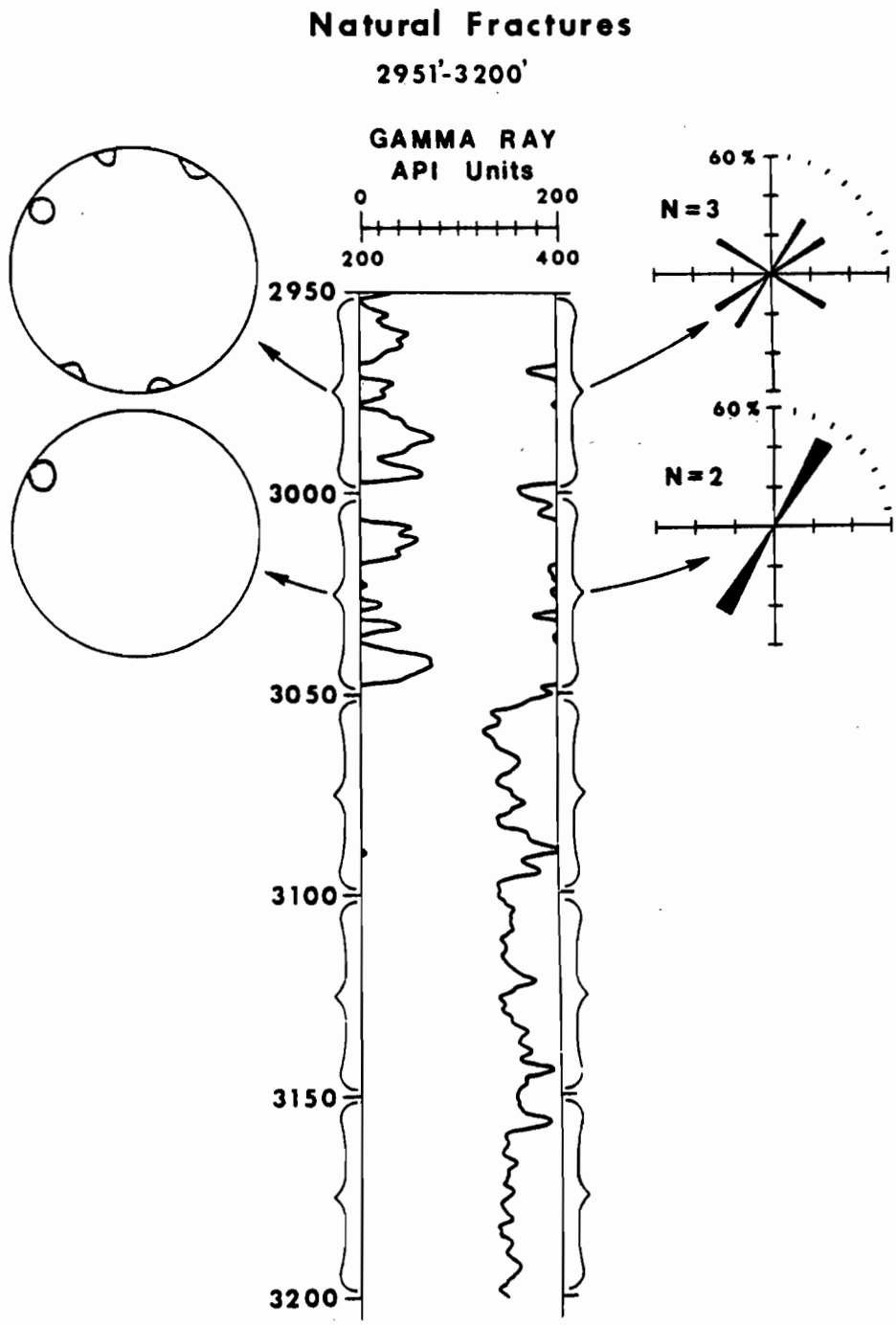
Natural Fractures
2951'-3200'
GAMMA RAY
API Units
0
200
200
400
2950
3000
3050
3100
3150
3200
60%
N=3
60%
N=2

Figure D-10.

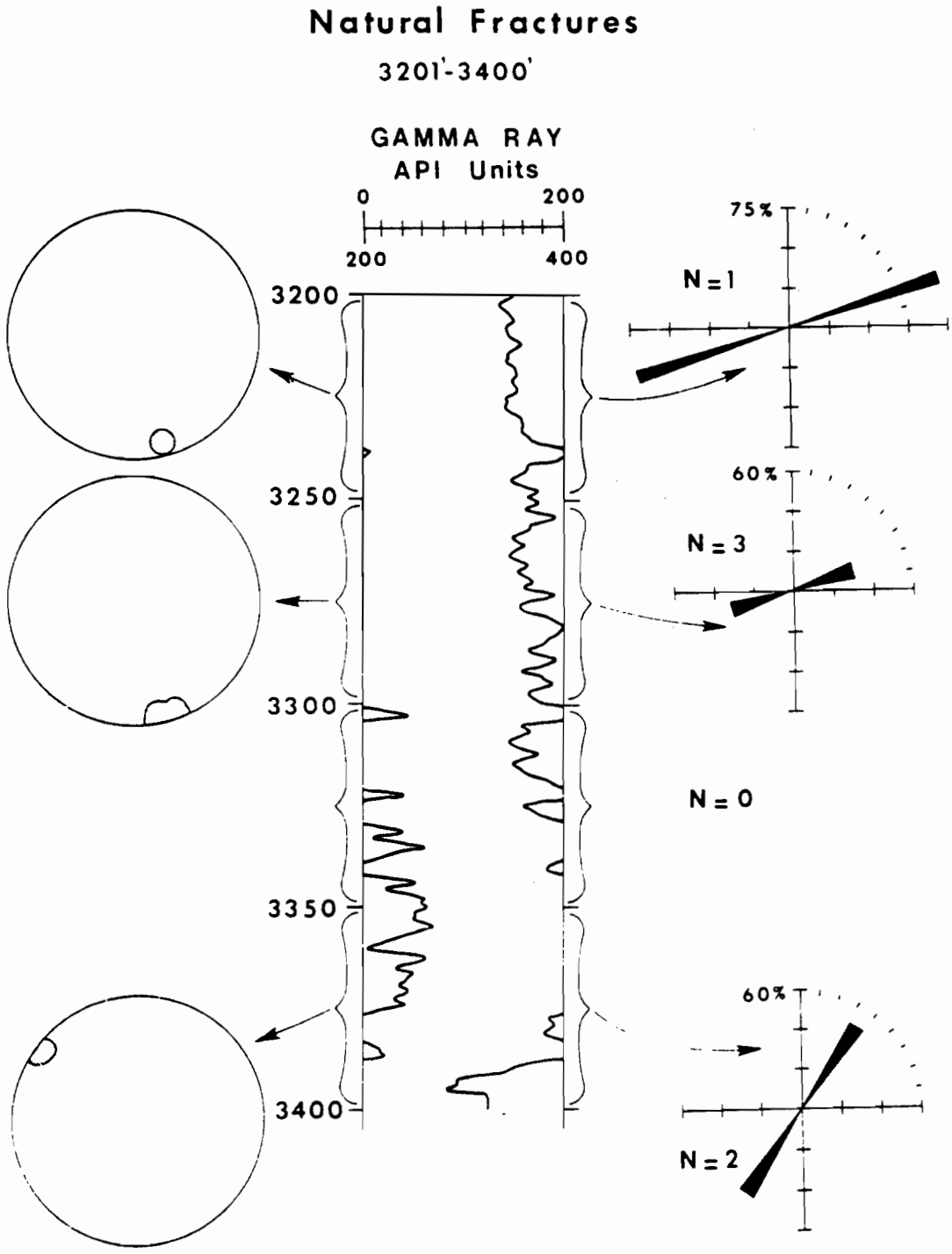
Natural Fractures
3201'-3400'
GAMMA RAY
API Units
0
200
200
400
3200
3250
3300
3350
3400
75%
N = 1
60%
N = 3
N = 0
60%
N = 2

Figure D-11.

Figure D-12. Natural fracture mineralized with euhedral calcite crystals - WV #5 (#3 D/K) core.

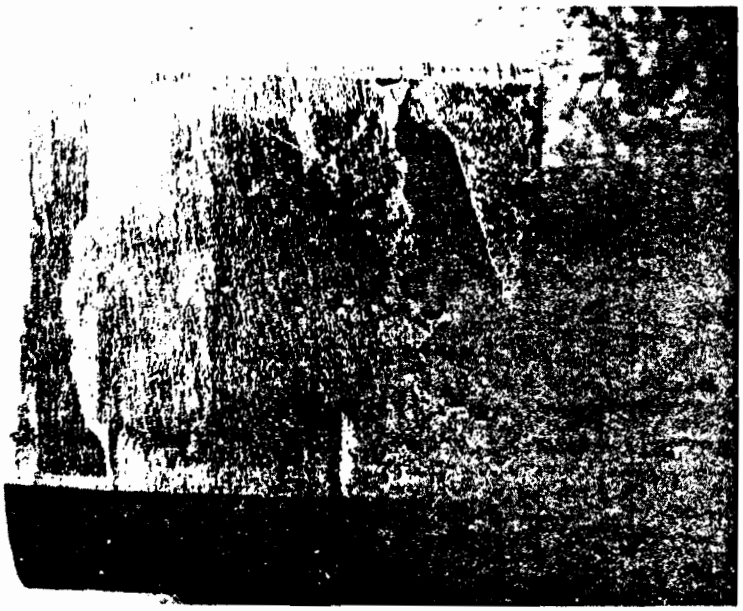

Figure D-13. Natural fracture mineralized with massive dolomite - WV #5 (#3 D/K) core.

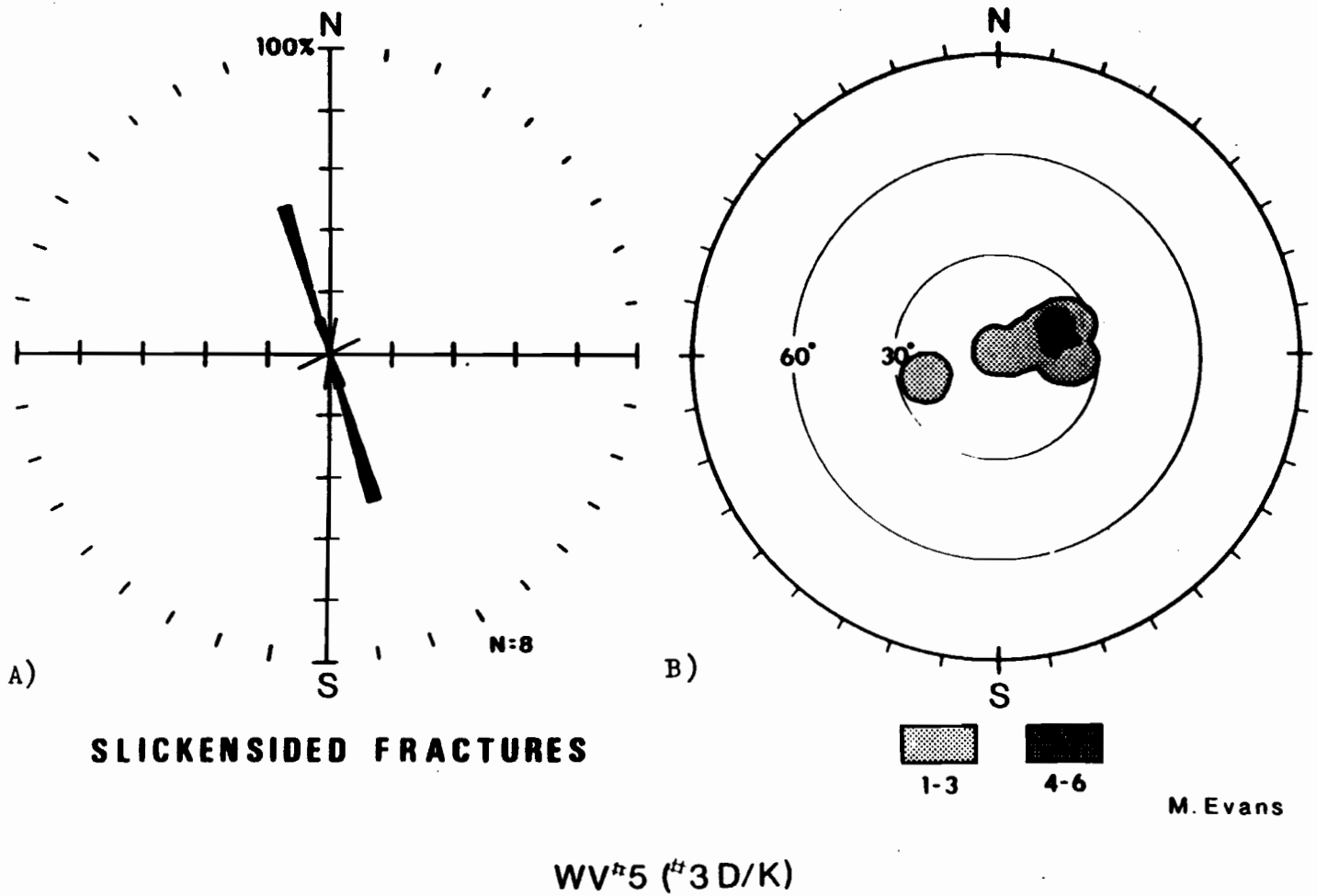

Figure D-14. (A) composite rose diagram of slickenside strikes, and (B) equal area projection of poles to slickensided surfaces

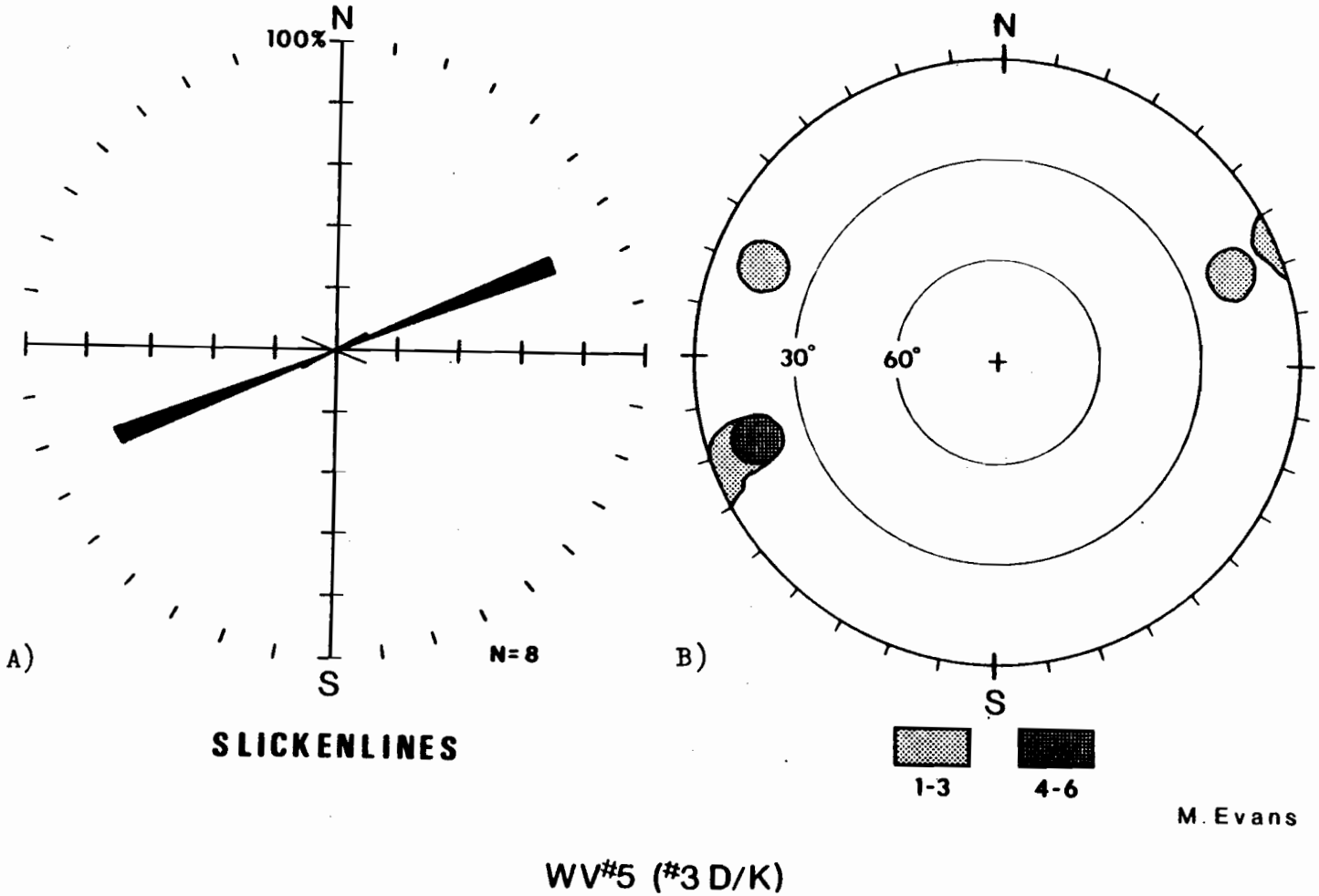

Figure D-15. (A) composite rose diagram of slickenline trends, and (B) equal area projection of slickenlines

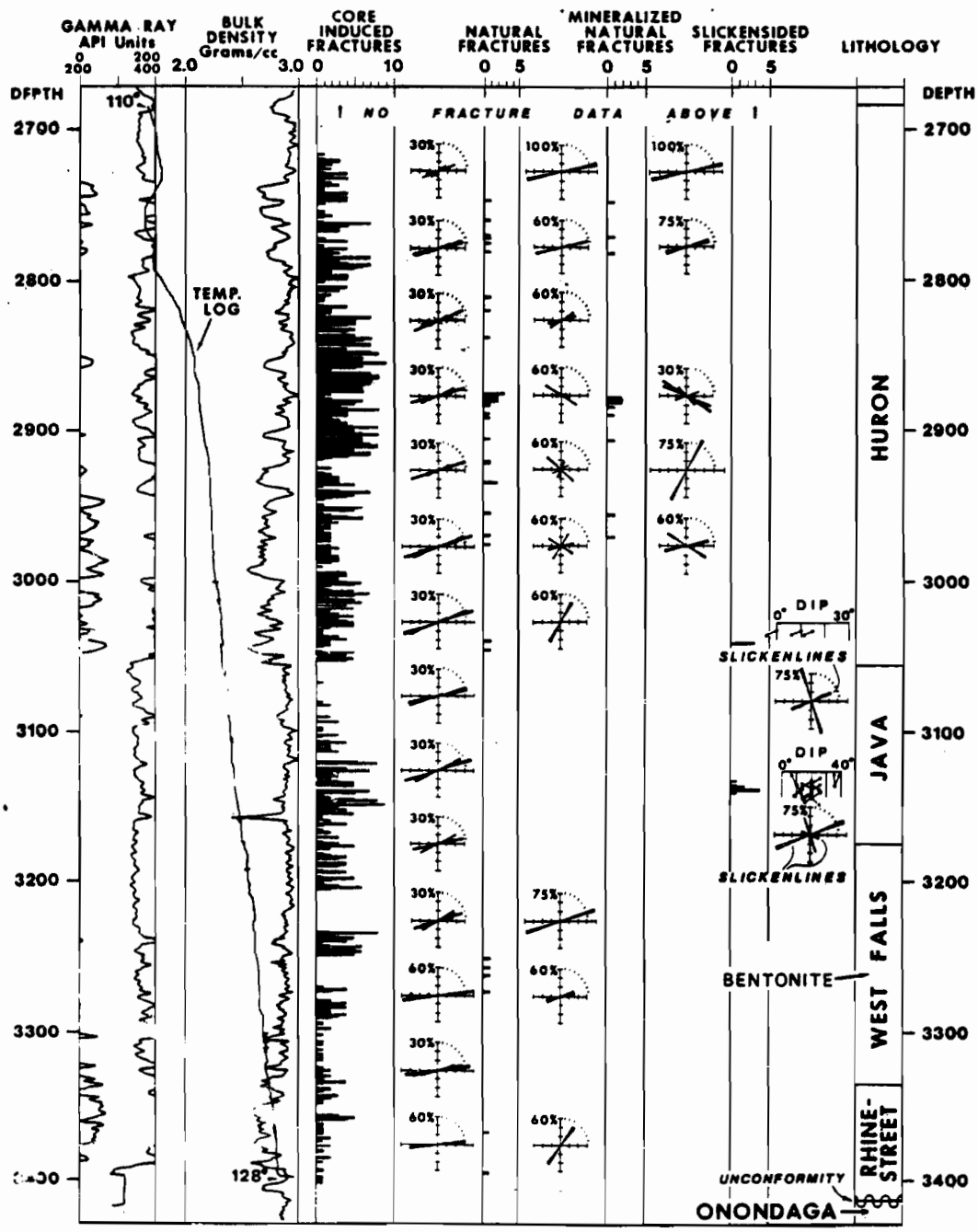

Figure D-16. Composite fracture data sheet of fracture frequencies and orientations for all fracture types in the WV #5 (#3 D/K) core.

APPENDIX E: WV #6 (MERC #1) CORE WELL

WV #6 (MERC #1) CORE WELL

Location

The WV #6 (MERC #1) core well is located in Monongalia County, West Virginia, approximately two miles north of the city of Morgantown (figures 1 and E-1, table 1). The wellsite is on the western flank of the Fayette Anticline, which is just west of the large N30°E trending Chestnut Ridge Anticline. A total of 352 feet of the Devonian was cored, from 7168'-7520' (figure E-2). Interval 7232'-7290' of the core could not be oriented because of a malfunction of the orienting camera. That interval was not used in this study to obtain fracture orientation data; however, fracture frequency data from this interval was recorded.

Production Data

The WV #6 (MERC #1) well had a show of gas from the Big Injun, Squaw, Gordon, 4th, 5th, Baynard, and Riley Sands, all of which are well above the cored interval. The only significant production from the Devonian shales was from the Burkett Member of the Harrell Shale. which produced 25 mcf/day after fracturing (Frone, 1978). This is immediately above the cored interval.

Core-induced Fractures

The only core-induced fractures in the core are torsion fractures and disc fractures. The lack of core-induced petal-centerline fractures may be related to the physical characteristics of the rock; which is generally a soft, fissile, black shale; or stress conditions present in the rock.

Natural Fractures

Unfortunately the Burkett Member was not cored. However, the Tully Limestone, just below the Burkett Member, was cored. The Tully Limestone and Marcellus Shale have the greatest number of natural fractures, while the Mahantango Formation has relatively few natural fractures (figure E-9). The natural fracture composite rose diagram (figure E-3) has two dominant peaks. There is a 1.0% chance that the peak at N83°E does not exist and a 5.0% chance that the peak at N67°W does not exist. One minor peak at N47°W is not statistically significant. The equal area projection of poles to natural fracture surfaces (figure E-3) has four peripheral clusters corresponding to the two dominant subvertical to vertical fracture sets. The natural fracture orientations show no pattern or systematic variation with depth or stratigraphy (figure E-4). Nearly all of the natural fractures are mineralized with calcite (crystalline or fibrous), barite, or pyrite. The mineral growth fibers are perpendicular to the fracture faces, implying that the principal acting tension during mineralization was horizontal. The type of mineralization shows no preference for fracture orientation, depth, or stratigraphy.

The N67°W fracture set is nearly orthogonal to the N30°E axial trend of the nearby Chestnut Ridge Anticline. The fractures in this set probably formed as extension fractures when tectonic compressive stresses were oriented approximately N60°-70°W during Alleghenian deformation. The N83°E set shows no relationship to any known nearby structures. However, these fractures may have formed as a result of the east to northeast trending maximum compressive stress present in

most of eastern North America (Sbar and Sykes, 1973).

Slickensides and Slickenlines

Slickensides are most abundant in the Tully Limestone and the lower portion of the Mahantango Formation through the base of the Marcellus Shale (figure E-9). The latter zone is vertically extensive, near a viscosity boundary (just above the Onondaga Limestone), and in a low viscosity unit; suggesting that it acted as a décollement zone. The slickenside composite rose diagram (figure E-5) has two significant peaks. There is a 5.0% chance that the peaks at N0°-30°E and N20°-30°W do not exist. The equal area projection of poles to slickensided surfaces (figure E-5) shows that slickensides are generally very low dipping (0°-30°) with an overall east to northeast dip. Although there is a great amount of scatter in slickenside orientations, a cluster pattern can be seen that matches that of the idealized shear zone model. The cluster in the center of the plot is the displacement shear cluster, the minor cluster dipping 20°NW is the Riedel shear cluster, and the cluster dipping 20°SE is the thrust shear cluster. R' shears are not present in this core. The wide scatter in slickenside orientations probably resulted strike measurements on low-dipping, undulating surfaces. Inclined slickenside orientations are quite variable but show no pattern or systematic variation with depth or stratigraphy (figure E-6).

The slickenline composite rose diagram (figure E-7) has one significant peak at N65°-75°W. There is a 1.0% chance that this peak does not exist. The equal area projection of slickenlines (figure E-7) has two peripheral clusters corresponding to the subhorizontal to

horizontal slickenlines. There is very little scatter in slickenline trend with depth or stratigraphy (figure E-8).

The N65°-75°W slickenline trend parallels the N67°W natural fracture set and is orthogonal to the N0°-30°E slickenside set. These three trends are related in that they all probably formed under the same N60°-70°W directed Alleghenian tectonic compressive stresses.

Many of the slickensides in this core are mineralized, usually with fibrous calcite in a layer which separates the fracture surfaces. The mineralization is found primarily on subhorizontal to horizontal slickensides. This is indicative of a very high fluid pressure in the bedding planes of the shales and a vertical principal acting tension during mineralization (Durney and Ramsay, 1973). Such abnormally pressured rocks are preferred sites for decollement because these rocks are probably less viscous than their normally pressured counterparts (Kehle, 1970). Fiber growth may have occured during or after décollement movement. The fibers are usually vertical but at times are curved indicating movement during fiber growth.

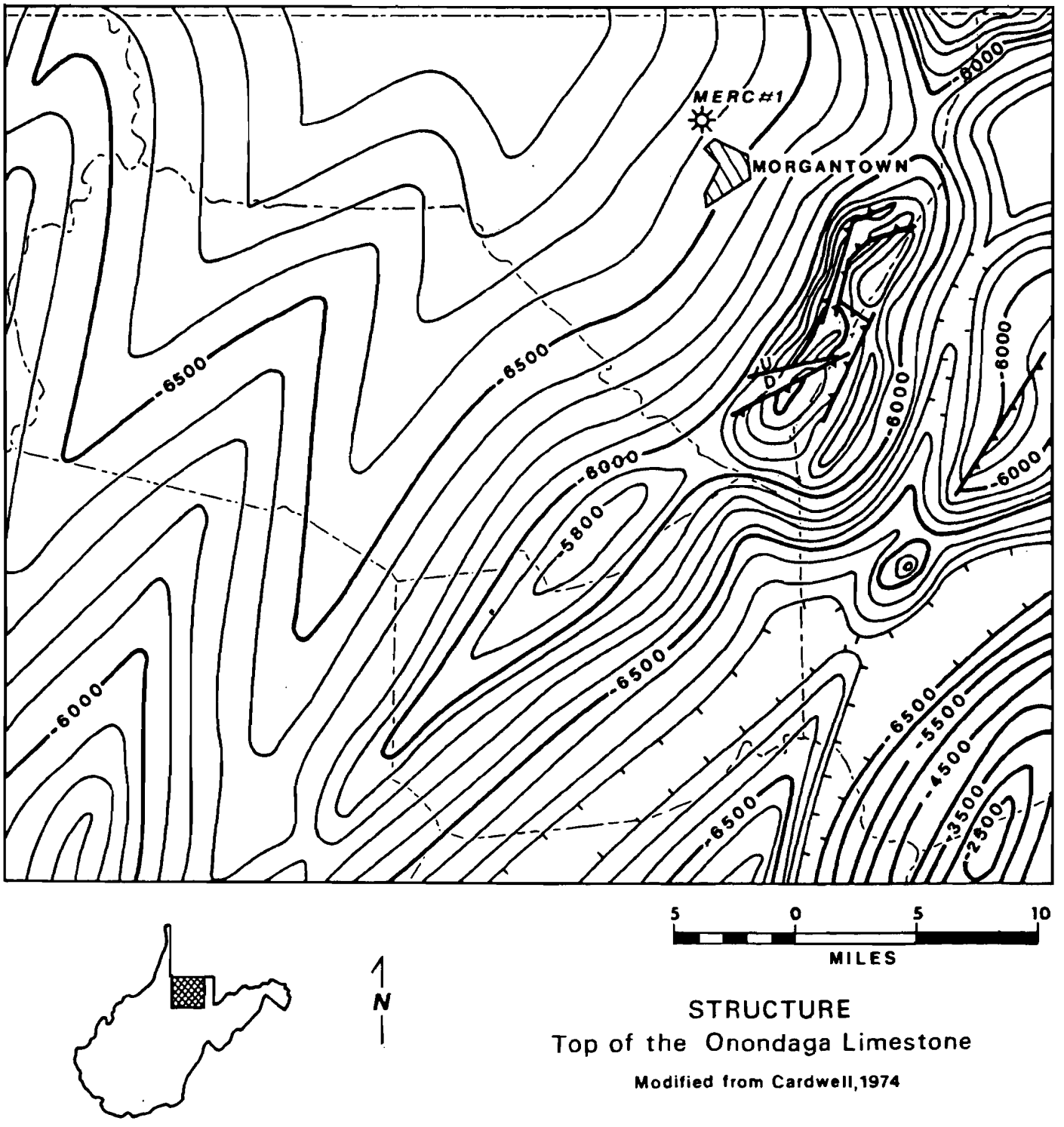

Figure E-1. Index map for the WV #6 (MERC #1) core well

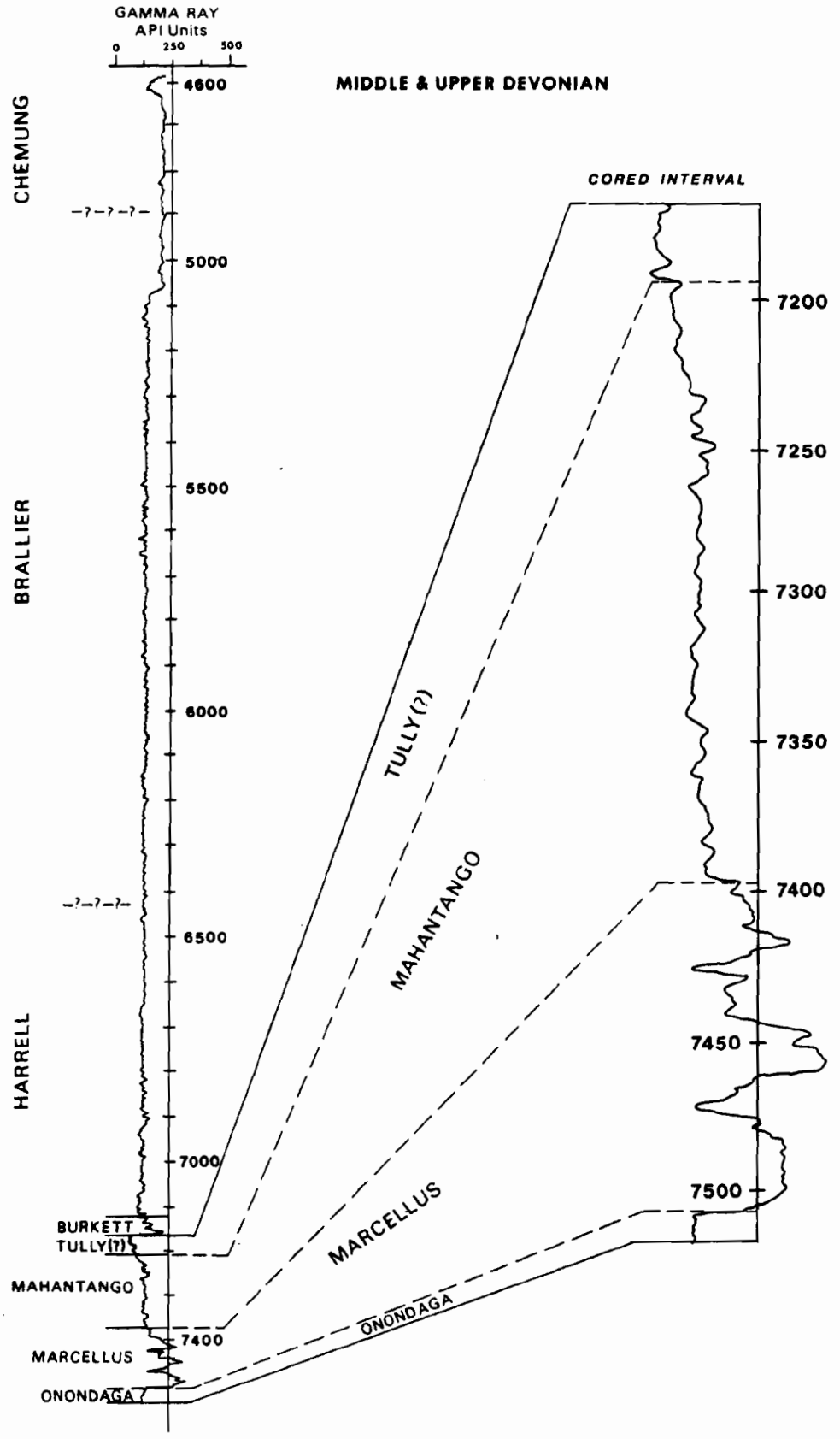

Figure E-2. Gamma-ray log, Middle and Upper Devonian - WV #6 (MERC #1) core well.

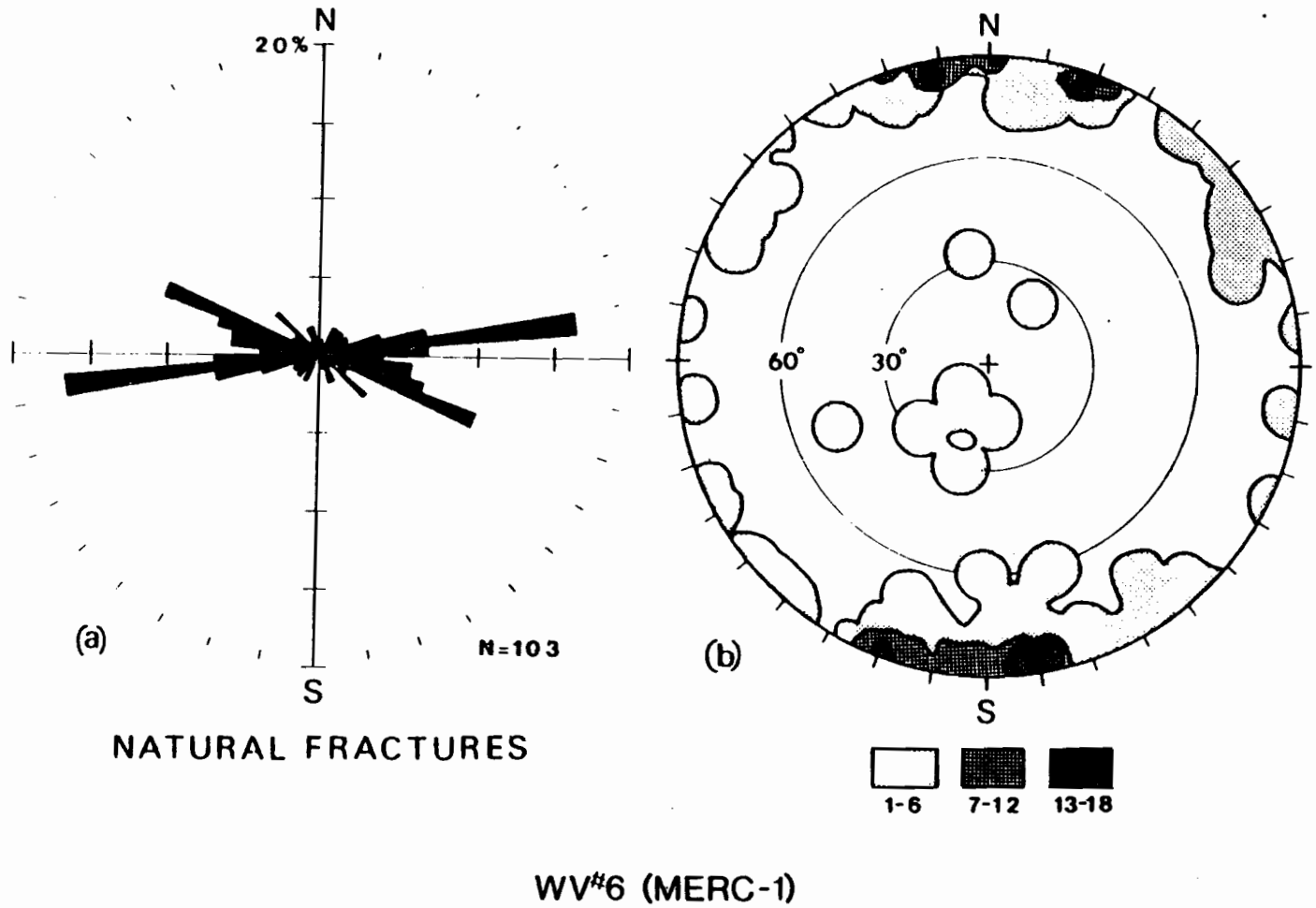

Figure E-3. (a) composite rose diagram of natural fracture strikes, and (b) equal area projection of poles to natural fracture surfaces

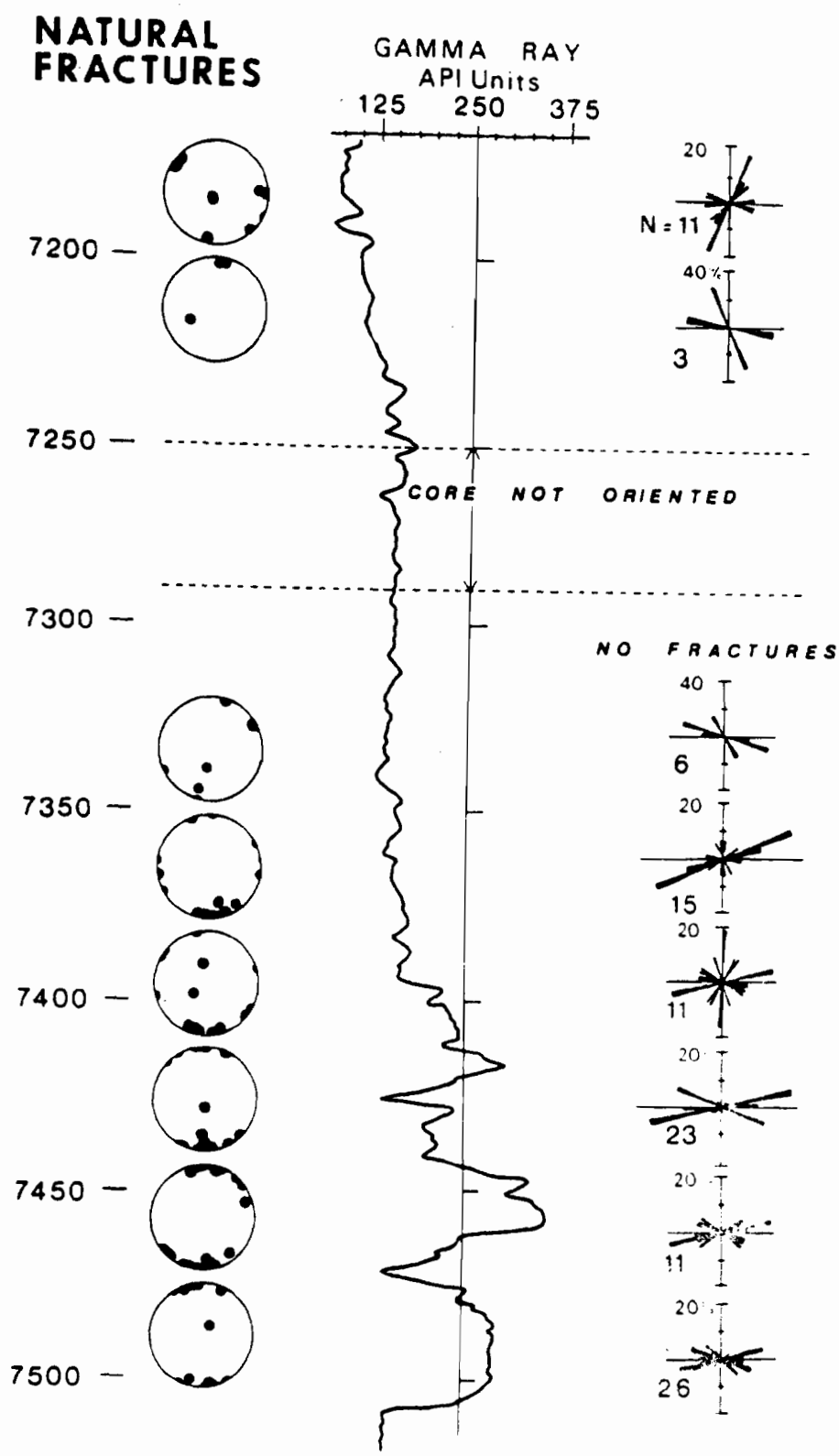

Figure E-4. Equal area projections of poles to natural fracture surfaces and rose diagrams of natural fracture strikes for approximately equal length intervals of the WV #6 (MERC #1) core.

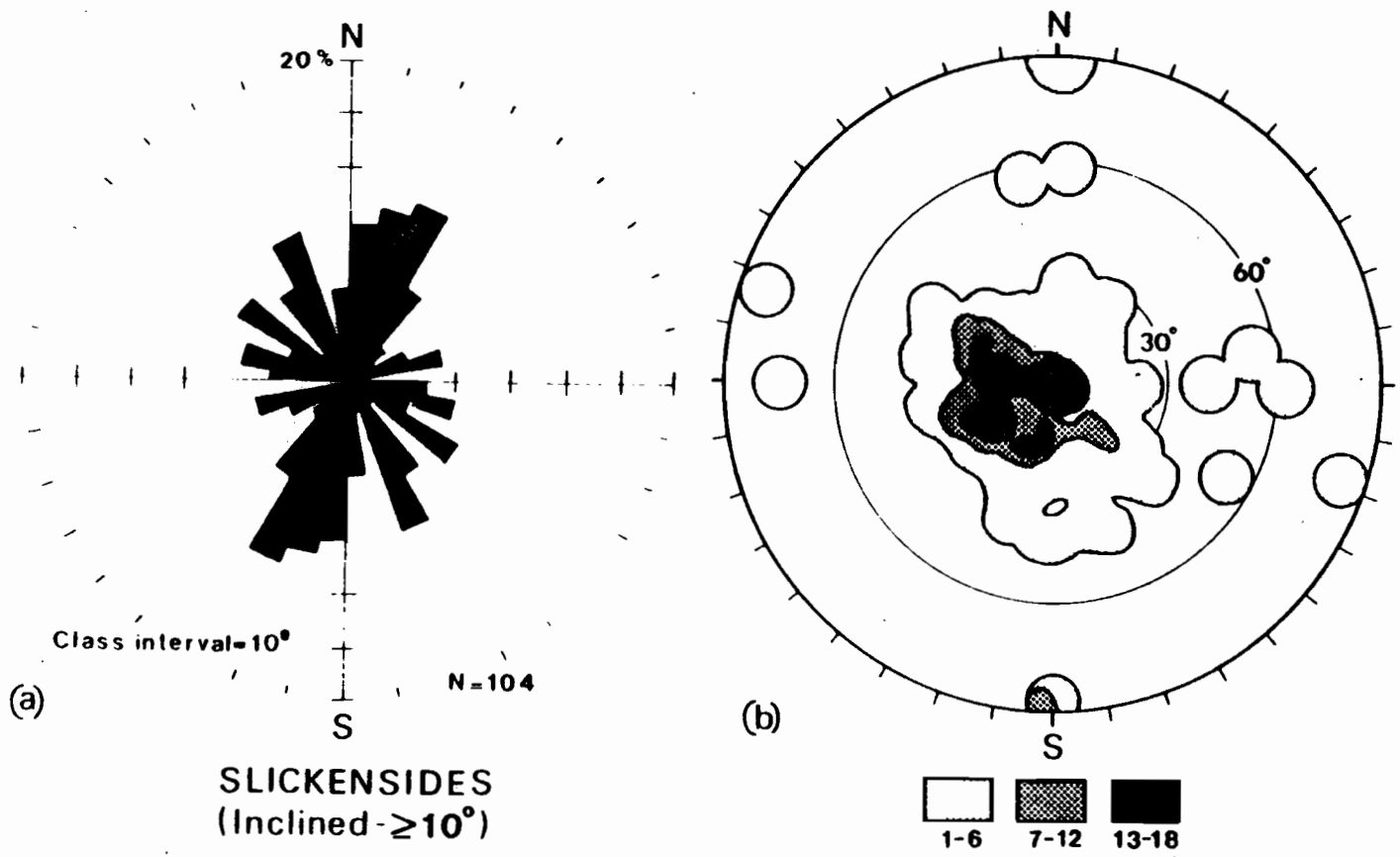

WV#6 (MERC-1)

Figure E-5. (a) composite rose diagram of slickenside strikes, and (b) equal area projection of poles to slickensided surfaces

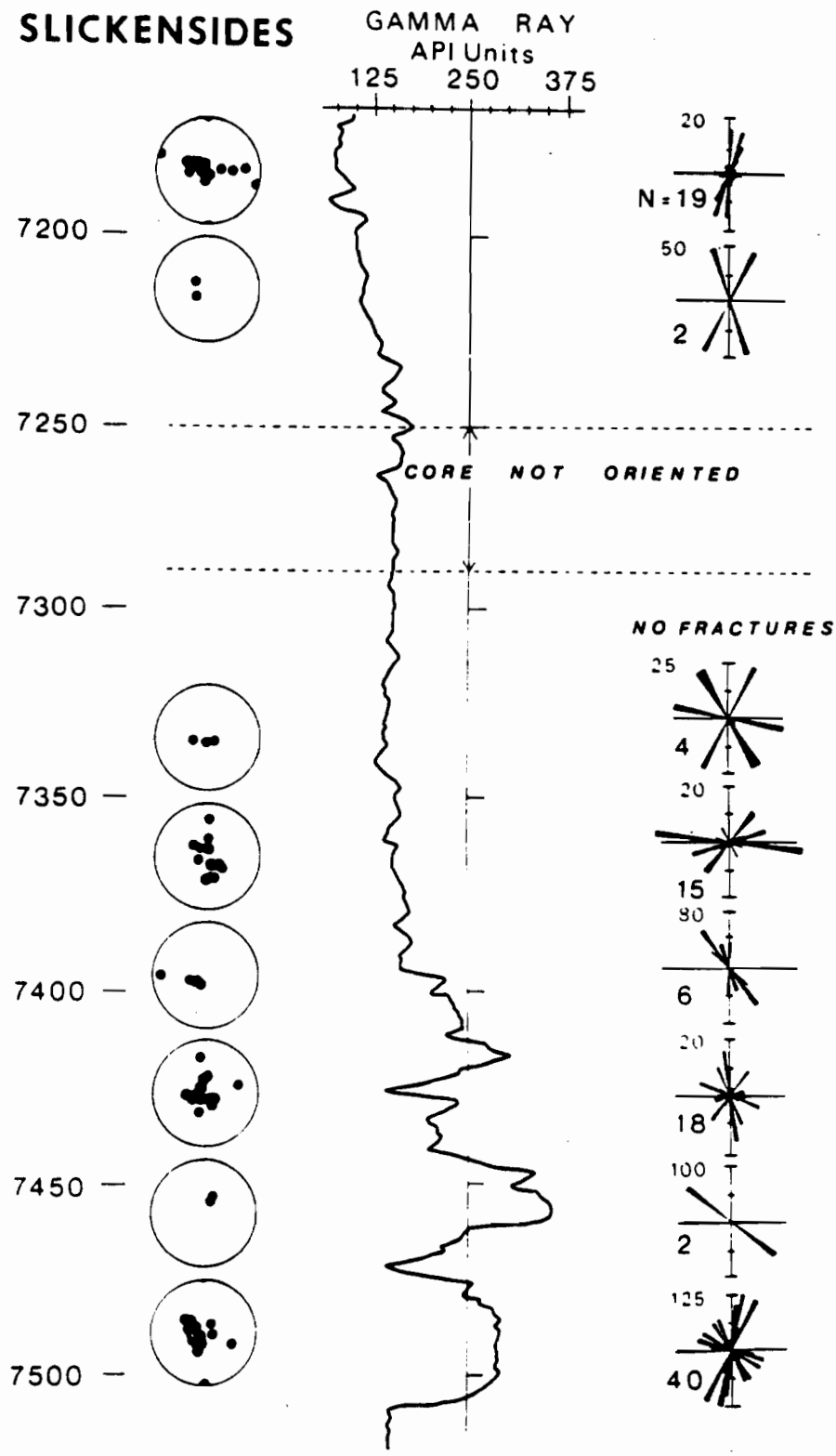

Figure E-6. Equal area projections of poles to slickensided surfaces and rose diagrams of slickenside strikes for approximately equal length intervals of the WV #6 (MERC #1) core.

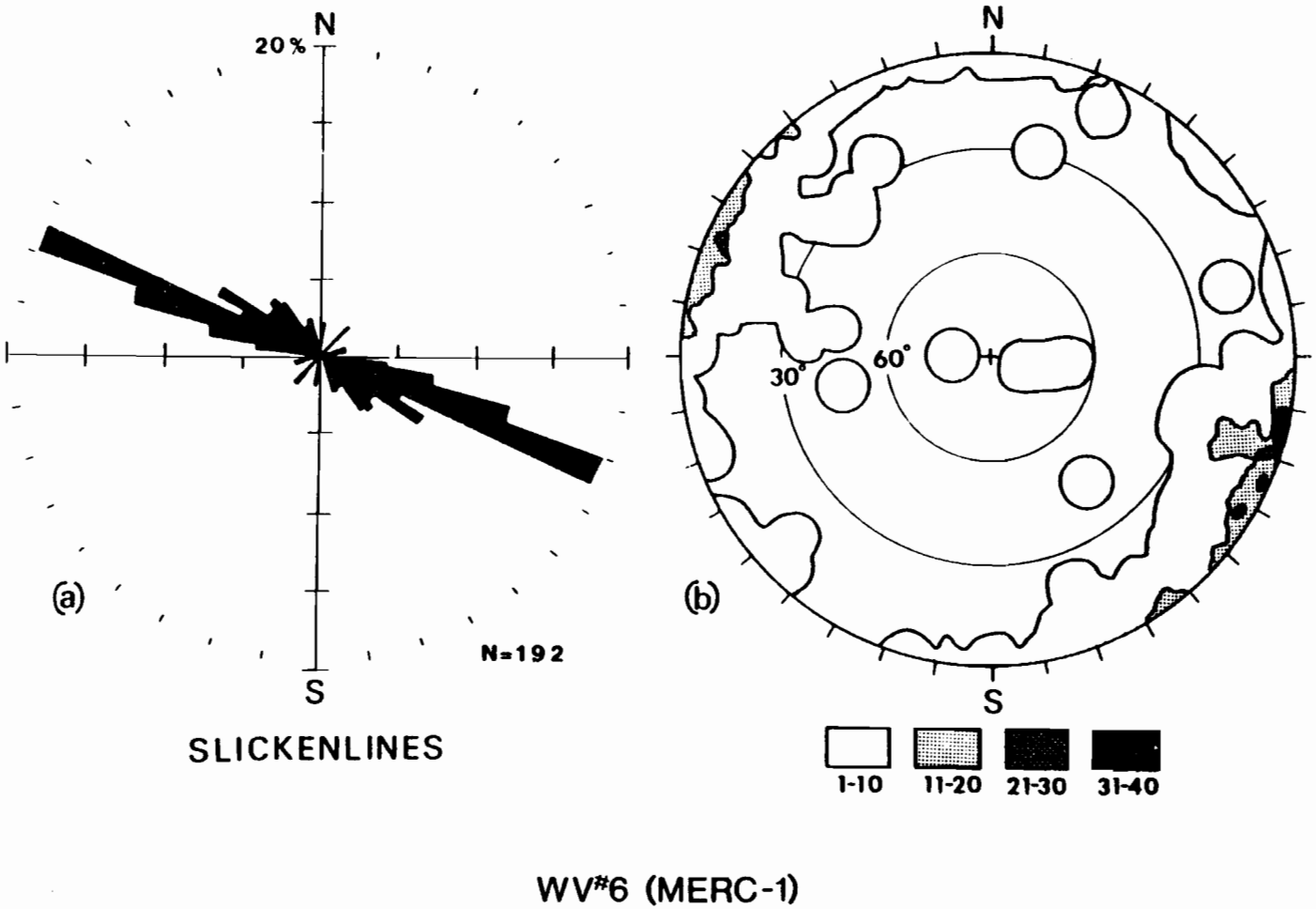

Figure E-7. (a) composite rose diagram of slickenline trends, and (b) equal area projection of slickenlines

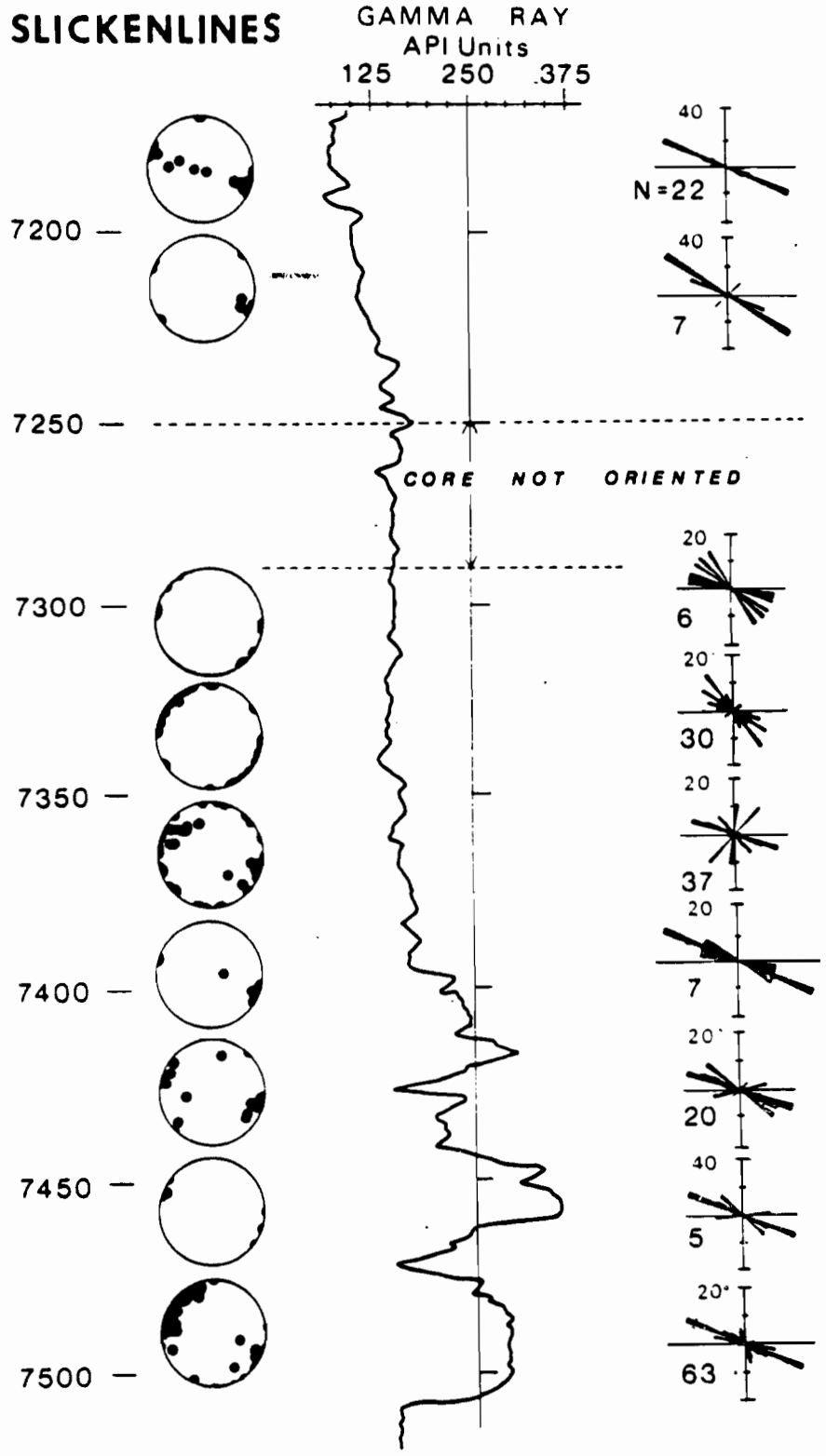

Figure E-8. Equal area projections of slickenlines and rose diagrams of slickenline trends for approximately equal length intervals of the WV #6 (MERC #1) core.

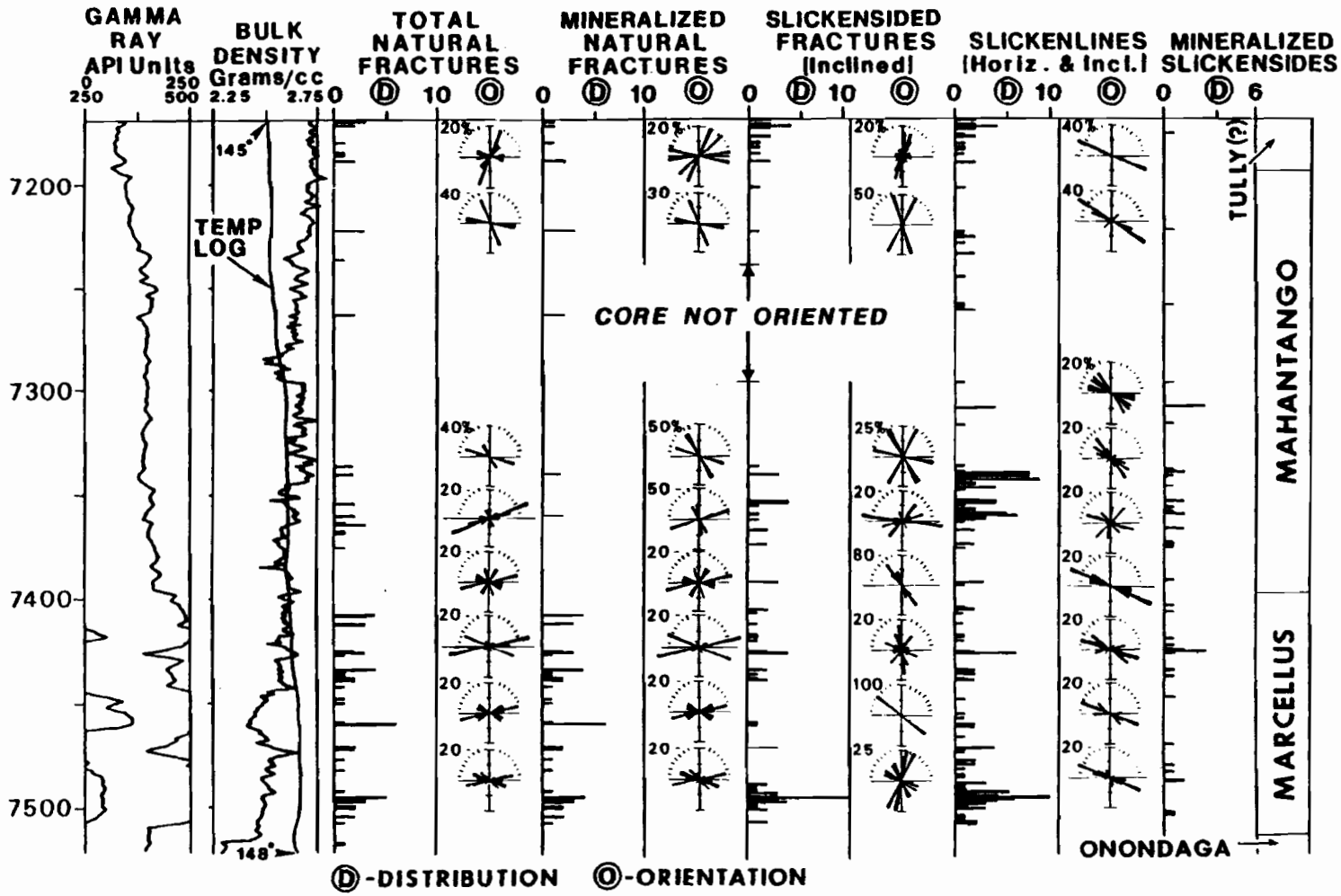

Figure E-9. Composite data sheet of fracture frequencies and orientations for all fracture types in the WV #6 (MERC #1) core

APPENDIX F: WV #7 (E-P #1) CORE WELL

WV #7 (E-P #1) CORE WELL

Location

The WV #7 (E-P #1) core well is located in Wetzel County, West Virginia, one mile northeast of the town of New Martinsville (figures 1 and F-1, table 1). The wellsite is near the crest of the northeast trending New Martinsville Anticline. Regional structure of the Devonian shales shows a monoclinal dip of less than 1° to the southeast. A total of 550 feet of the Devonian was cored, from 6100'-6650' (figure F-2).

Production Data

No production data was available.

Core-induced Fractures

Core-induced fractures in the WV #7 (E-P #1) core are primarily of the torsion and disc type with several petal-centerline fractures occurring only in the Sonyea Formation (figure F-11). The composite rose diagram of core-induced fracture strikes (figure F-3) has a single peak at $N67^{\circ}E$. There is a 1.0% chance that this peak does not exist. The equal area projection of poles to core-induced fracture surfaces (figure F-3) has two clusters corresponding to the opposing dips of the petals. Fracture orientations remain constant with depth (figure F-4) with the preference for the $N67^{\circ}E$ trend probably resulting from a stress or rock fabric anisotropy. This anisotropy may be related to the east to northeast trending maximum compressive stress present in most of eastern North America (Sbar and Sykes, 1973). The harder shales of the Sonyea Formation seem to be

the rock type best suited for the development of the anisotropy in the cored interval.

Natural Fractures

Natural fractures occur primarily in the Rhinestreet Shale, West River Shale, Geneseo Shale, and Marcellus Shale (figure F-11). The composite rose diagram (figure F-5) has two peaks. There is a 1.0% chance that the peak at N57°W does not exist and a 5.0% chance that the peak at N43°W does not exist. Fractures of both sets are found throughout the core. The equal area projection of poles to natural fracture surfaces (figure F-5) has four clusters corresponding to the two subvertical to vertical fracture sets. Natural fracture orientations are quite variable but show no pattern or systematic variation with depth or stratigraphy (figure F-6). Nearly all of the natural fractures in the WV #7 (E-P #1) core are mineralized with massive or crystalline calcite.

Both natural fracture sets are nearly orthogonal to the trend of local fold axes. They are probably extension fractures resulting from tectonic compressive stresses acting during Alleghenian deformation. The difference in strike between the two sets is probably a result of variable stresses in the décollement sheet.

Slickensides and Slickenlines

Slickensides are most abundant in the lower portion of the Rhinestreet Shale, Geneseo Shale, and Marcellus Shale (figure F-11). Each of these zones is either near or within a low-viscosity unit, suggesting that they acted as decollement zones. The Rhinestreet Shale is

a soft shale unit above the slightly stiffer Sonyea Formation, the Geneseo Shale is a soft shale unit above the stiffer Tully Limestone, and the Marcellus Shale is a soft shale unit above the Onondaga Limestone. The slickenside composite rose diagram (figure F-7) has two peaks. There is a 5.0% chance that the peak at N15°-30°E does not exist and a 10.0% chance that the peak at N43°W does not exist. Poles to slickensided surfaces form a girdle across the equal area projection (figure F-7). The pattern closely resembles that which would be expected from a shear zone. The 0° dipping cluster in the center is the displacement shear cluster, the Riedel shears are represented by the 25°NW dipping cluster, and the thrust shears are represented by the 25°SE dipping cluster. R' shears are not present in this core. Slickenside strikes show very little variability except for some scatter in the lower portion of the Rhinestreet Shale (figure F-8).

The slickenline composite rose diagram (figure F-9) has a single peak at N67°W. There is a 1.0% chance that this peak does not exist. The equal area projection of slickenlines (figure F-9) has two peripheral clusters which reflect the low-plunging slickenlines of the N67°W set. Two smaller clusters result from horizontal slickenlines trending N43°W and N83°W. There is some scatter in slickenline trend, mainly in the Rhinestreet Shale (figure F-10).

The N67°W slickenline trend is subparallel to the natural fracture trends and is orthogonal to the dominant slickenside trend. These fracture sets are related in that they all probably formed under the same Alleghenian tectonic compressive stresses.

Many of the slickensides in the core are mineralized, particularly those in the Geneseo Shale and Marcellus Shale. Calcite is the dominant mineral type and occurs as fibers between slickenside surfaces and as massive and crystalline coatings on the slickensided surfaces. The fibrous crystal growth is indicative of high fluid pressure in the bedding planes of the shales and a vertical principal acting tension during mineralization. Such abnormally pressured rocks are preferred sites for décollement because these rocks are probably less viscous than their normally pressured counterparts (Kehle, 1970).

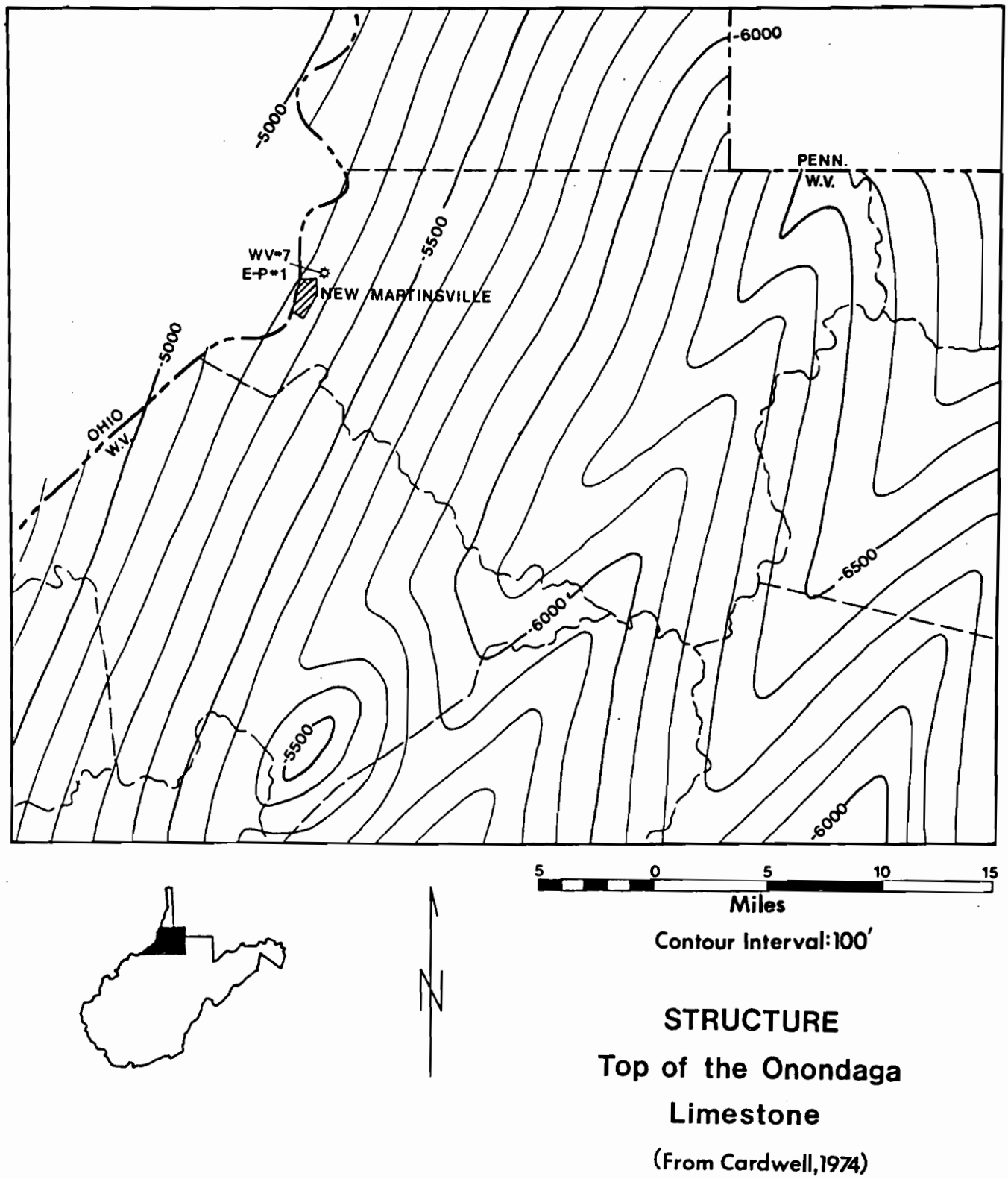

Figure F-1. Index map for the WV #7 (E-P #1) core well

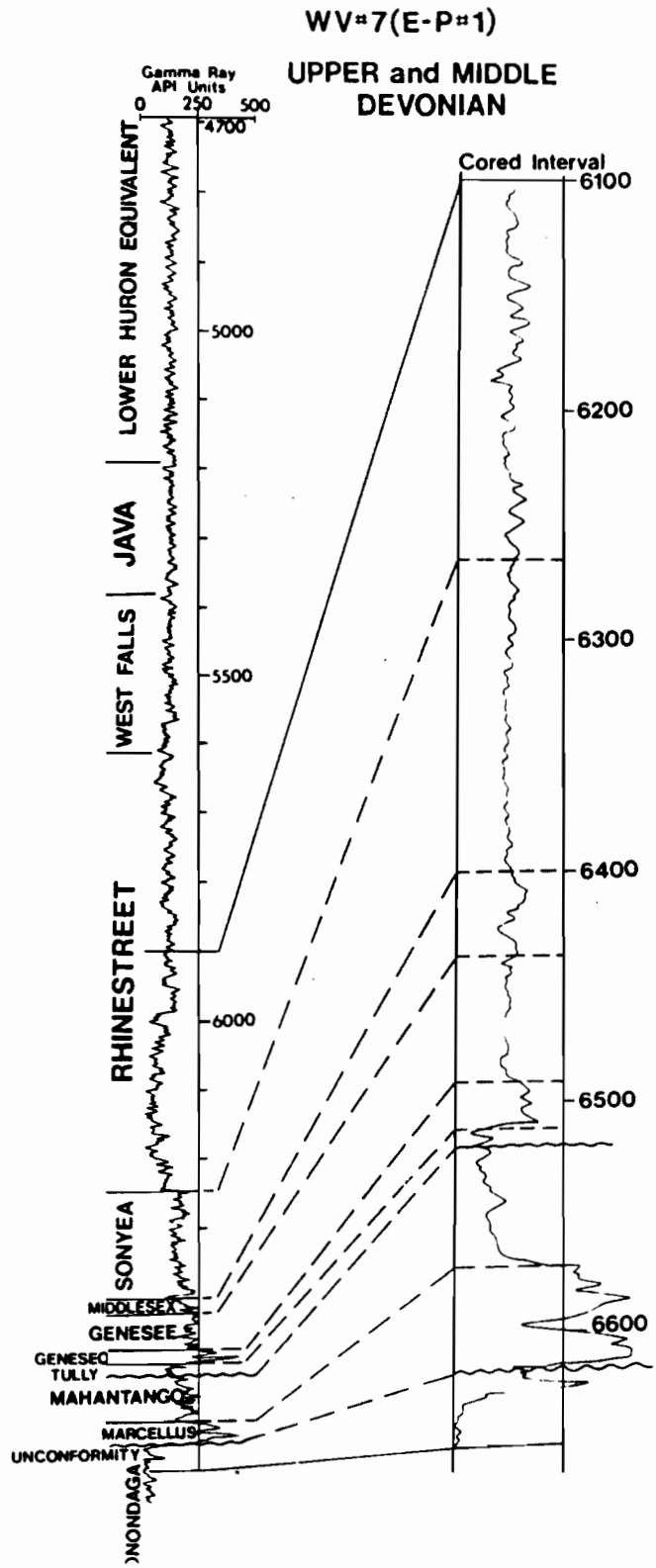

Figure F-2. Gamma-ray log, Middle and Upper Devonian.

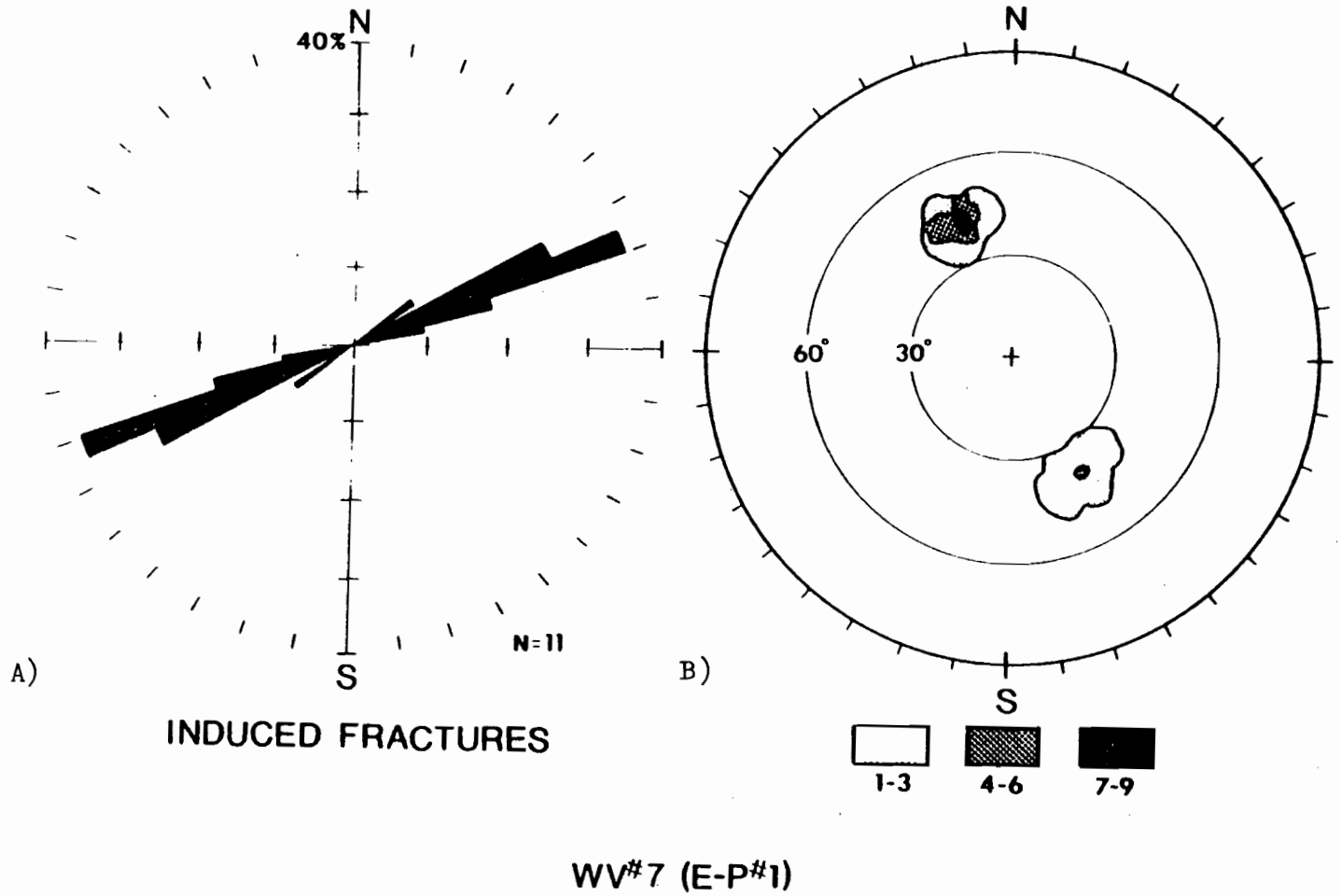

Figure F-3. (A) composite rose diagram of core-induced fracture strikes, and (B) equal area projection of poles to core-induced fracture surfaces

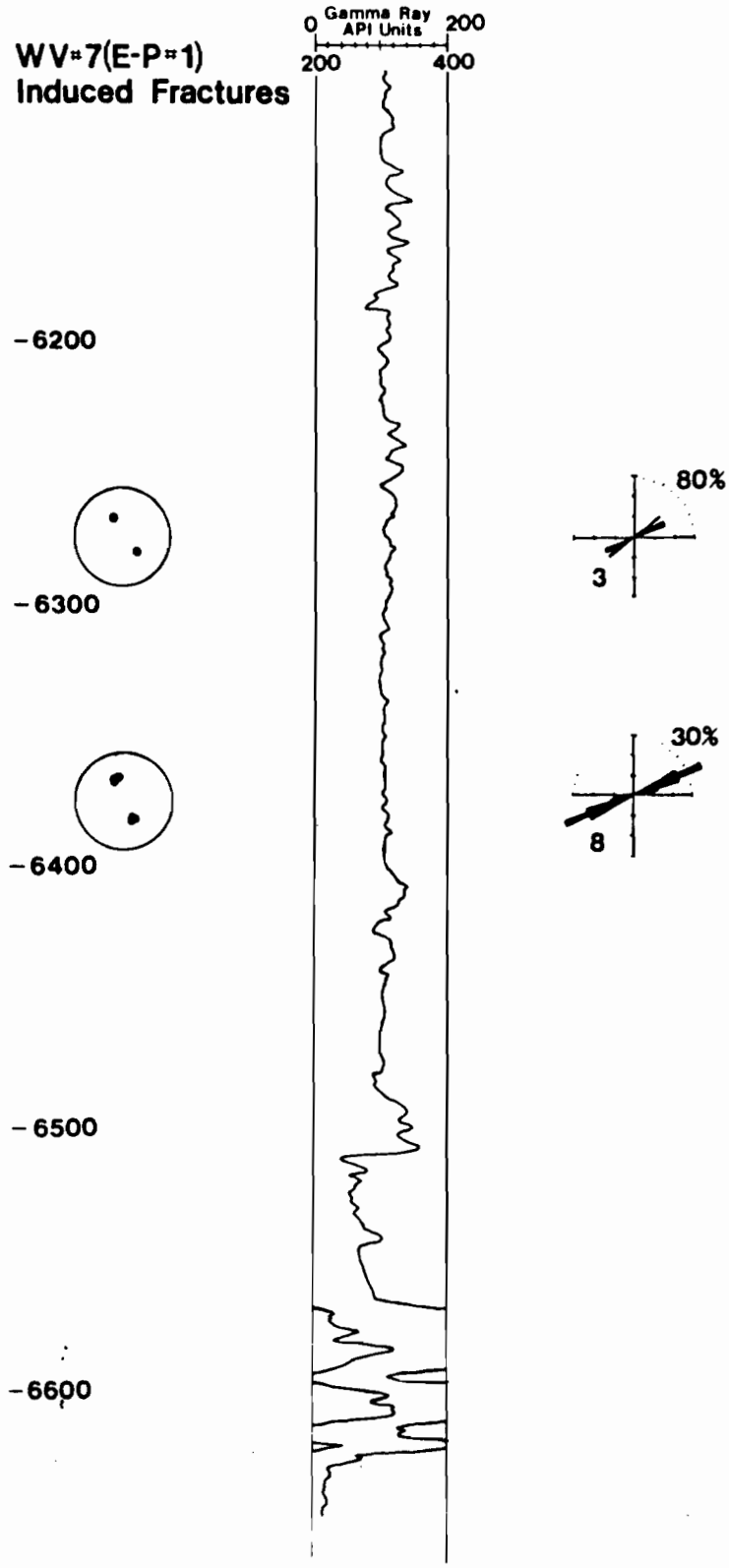

Figure F-4. Equal area projections of poles to core-induced fracture surfaces and rose diagrams of core-induced fracture strikes for approximately equal length intervals of the WV #7 (E-P #1) core.

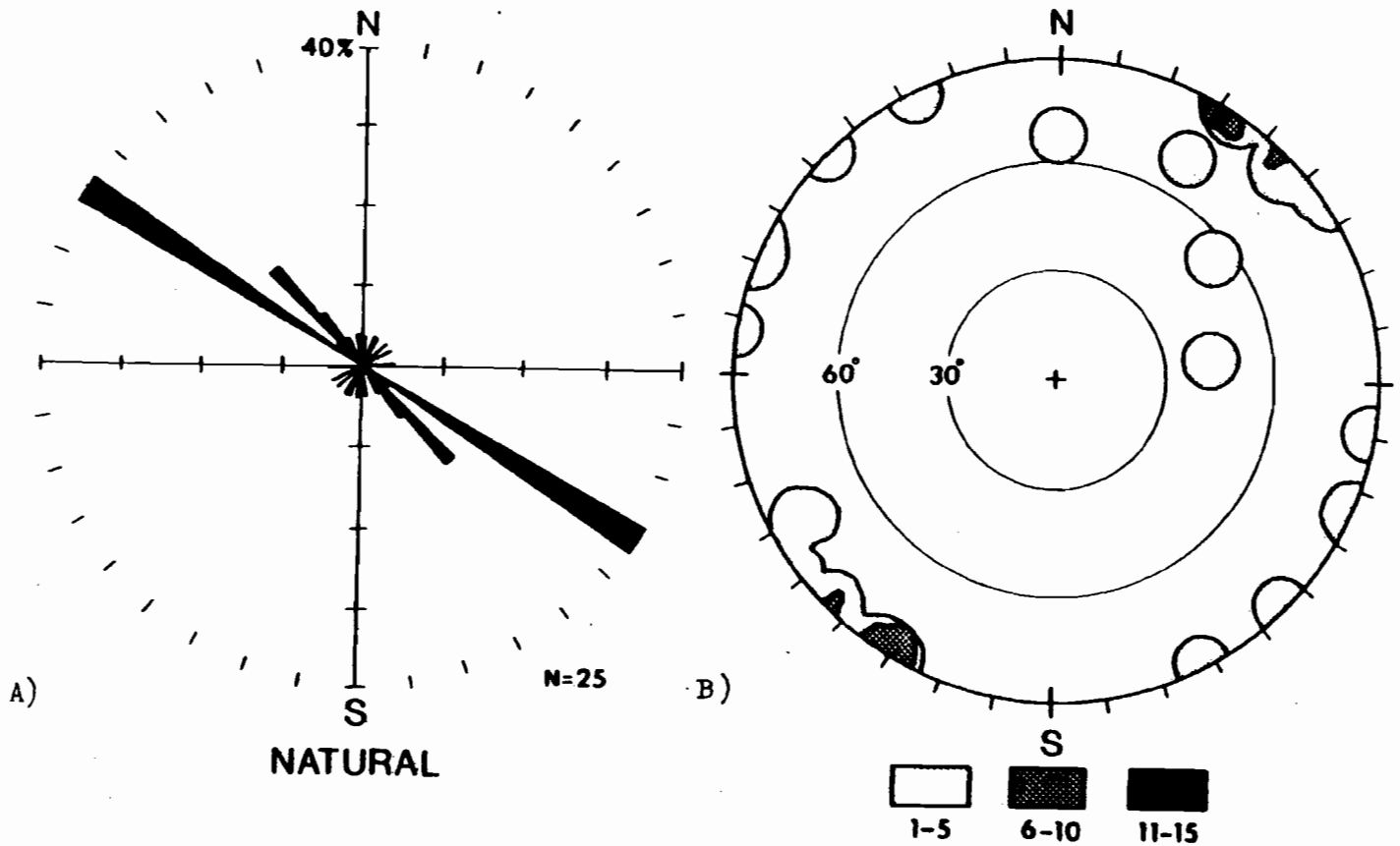

WV#7 (E-P#1)

Figure F-5. (A) composite rose diagram of natural fracture strikes, and (B) equal area projection of poles to natural fracture surfaces

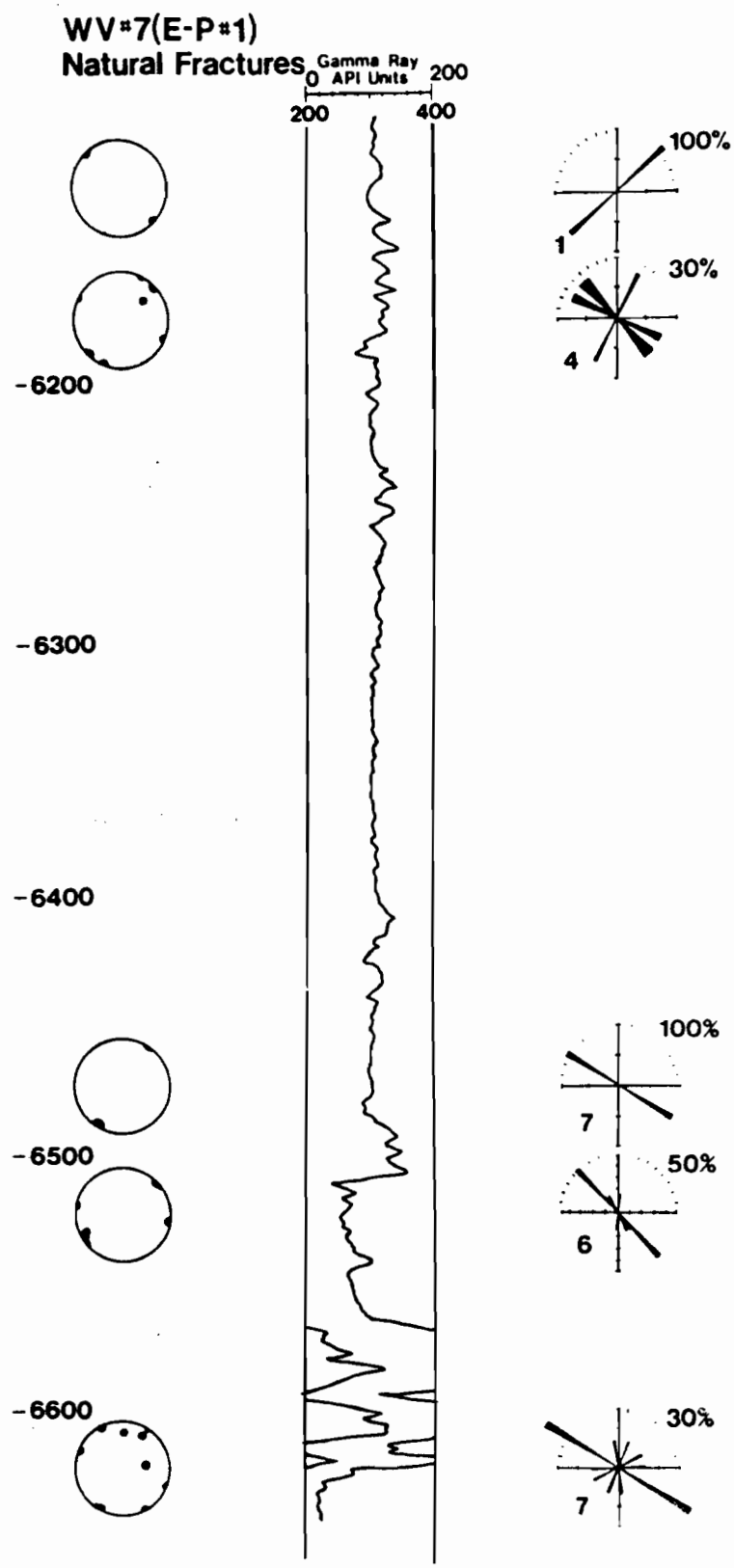

Figure F-6. Equal area projections of poles to natural fracture surfaces and rose diagrams of natural fracture strikes for approximately equal length intervals of the WV #7 (E-P #1) core.

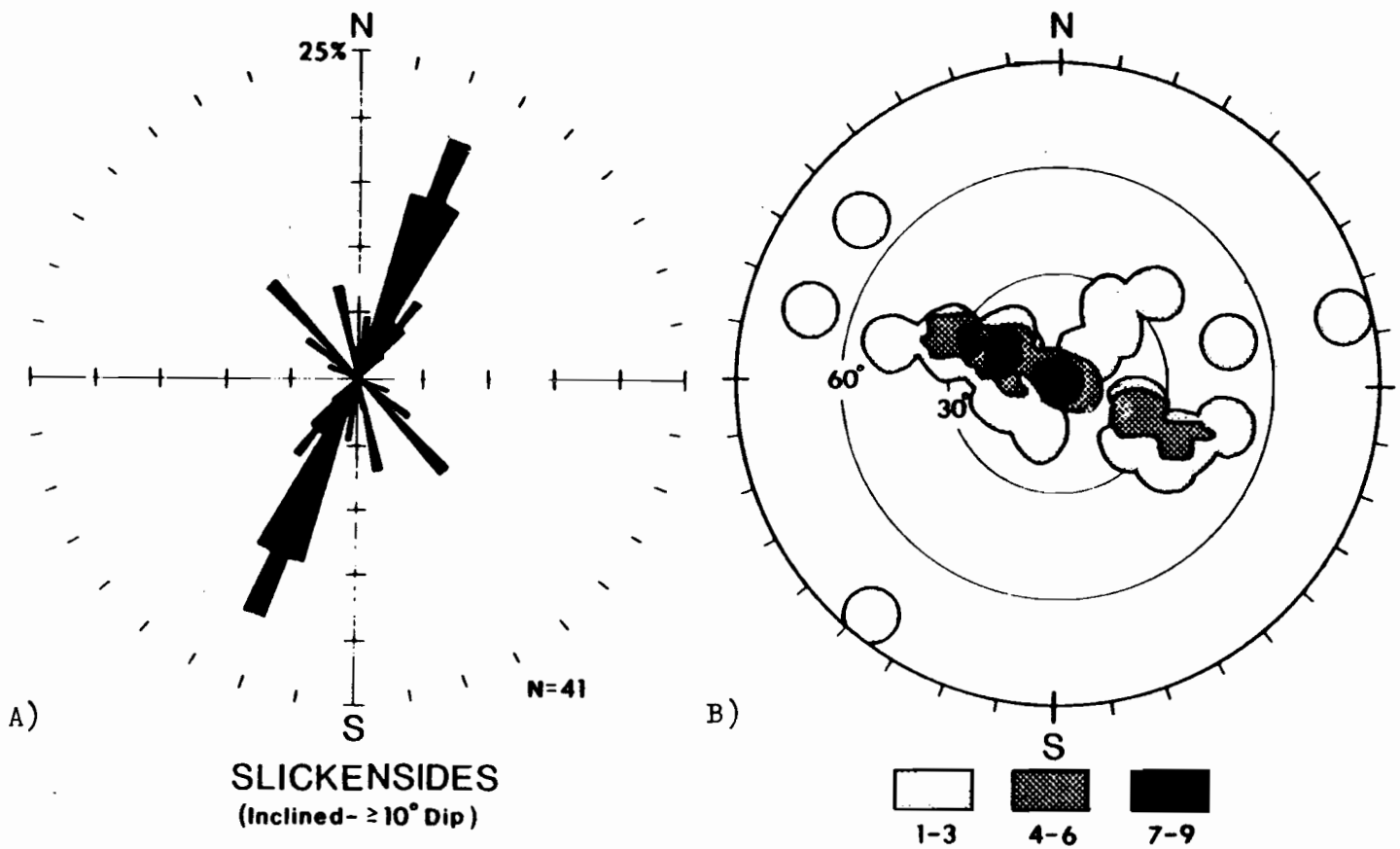

WV#7 (E-P#1)

Figure F-7. (A) composite rose diagram of slickenside strikes, and (B) equal area projection of poles to slickensided surfaces

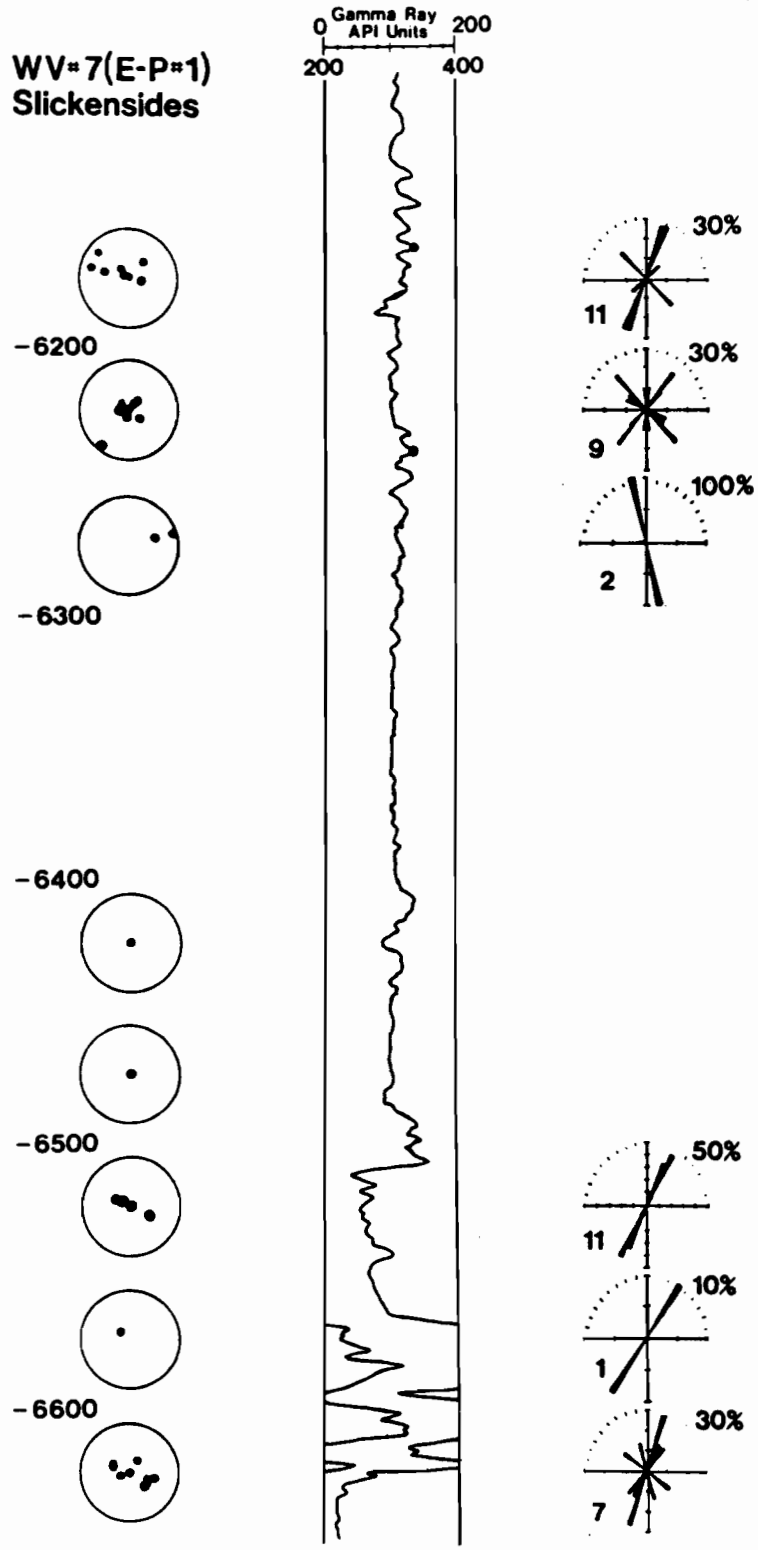

Figure F-8. Equal area projections of poles to slickensided surfaces and rose diagrams of slickenside strikes for approximately equal length intervals of the WV #7 (E-P #1) core.

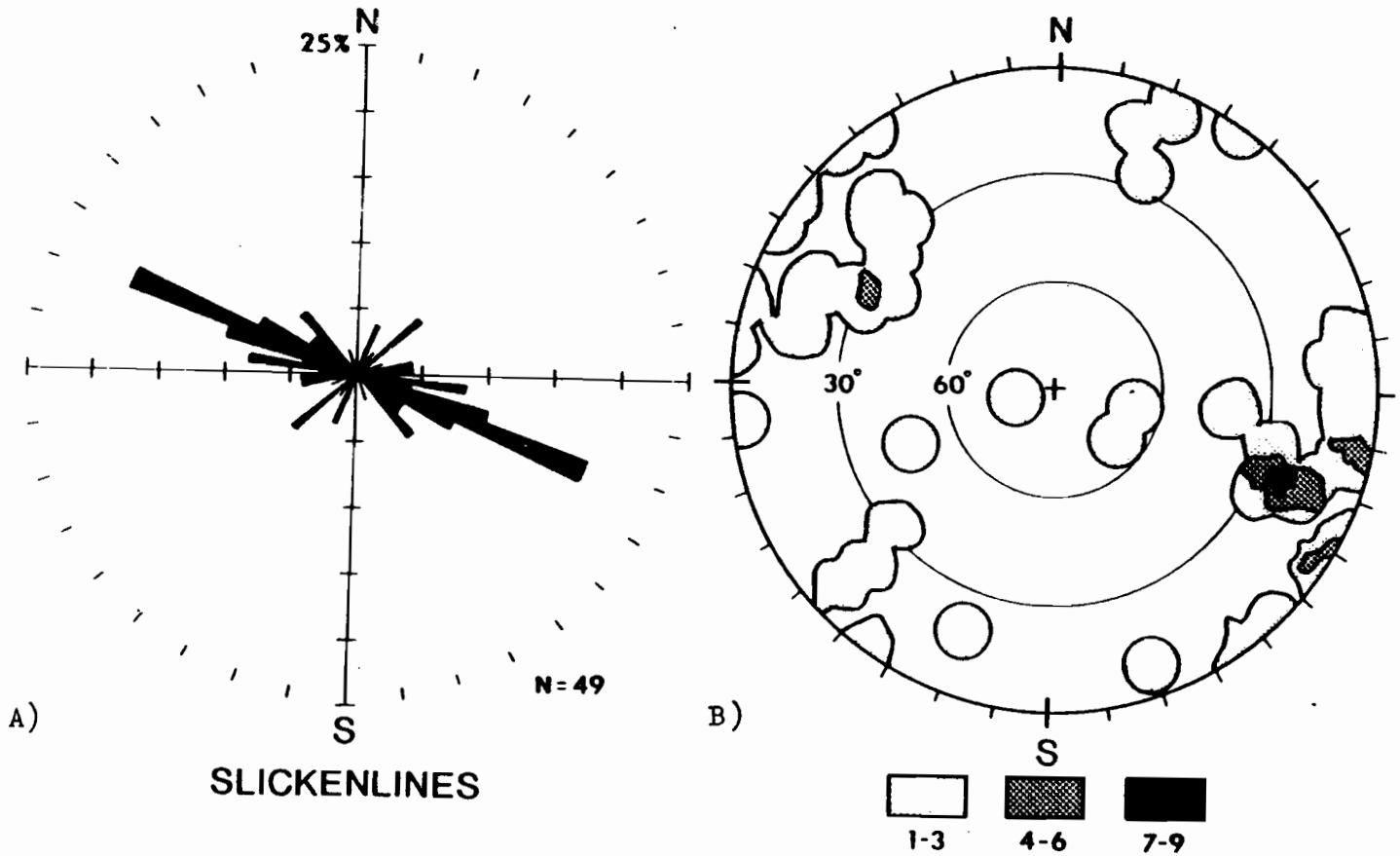

WV#7 (E-P#1)

Figure F-9. (A) composite rose diagram of slickenline trends, and (B) equal area projection of slickenlines

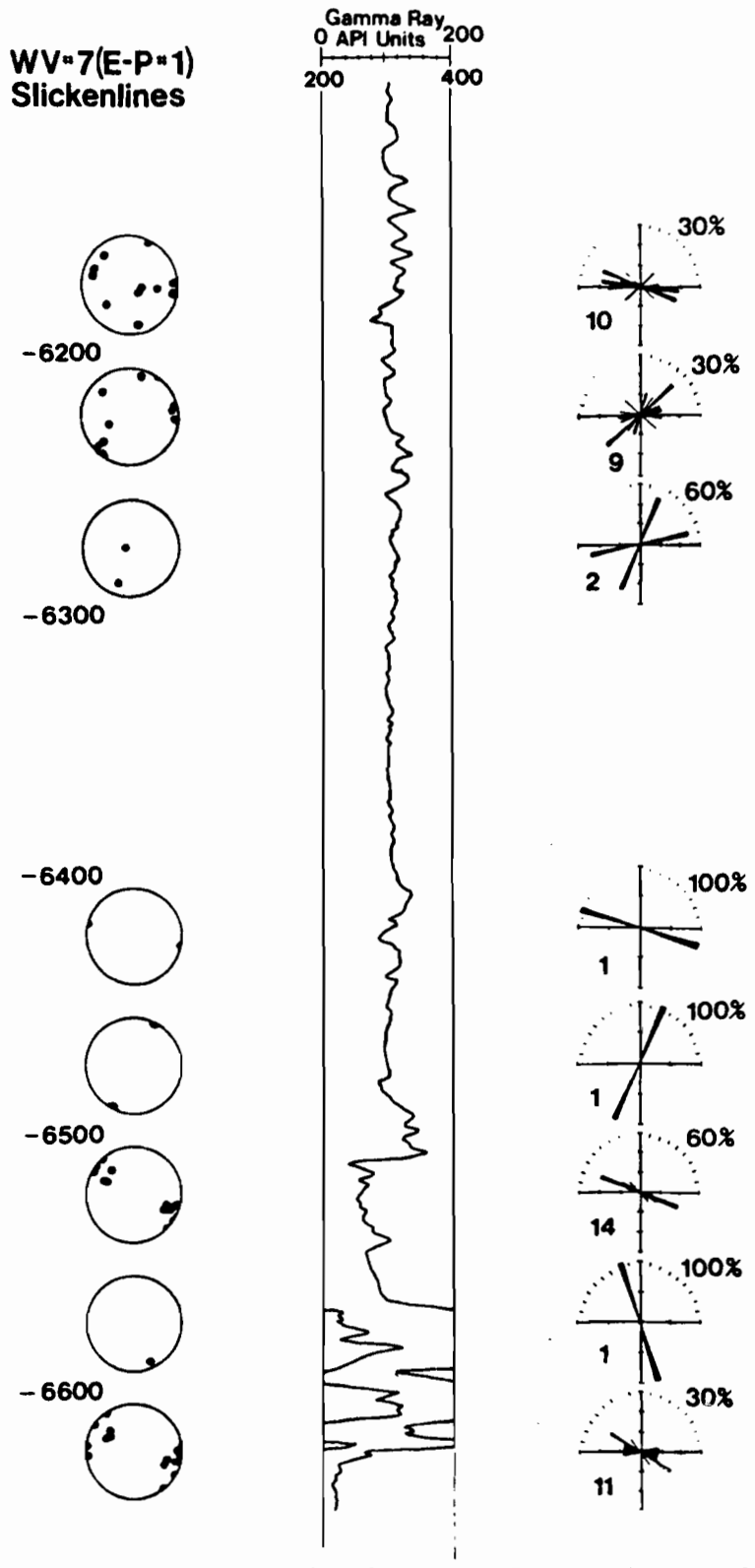

Figure F-10. Equal area projections of slickenlines and rose diagrams of slickenline trends for approximately equal length intervals of the WV #7 (E-P #1) core.

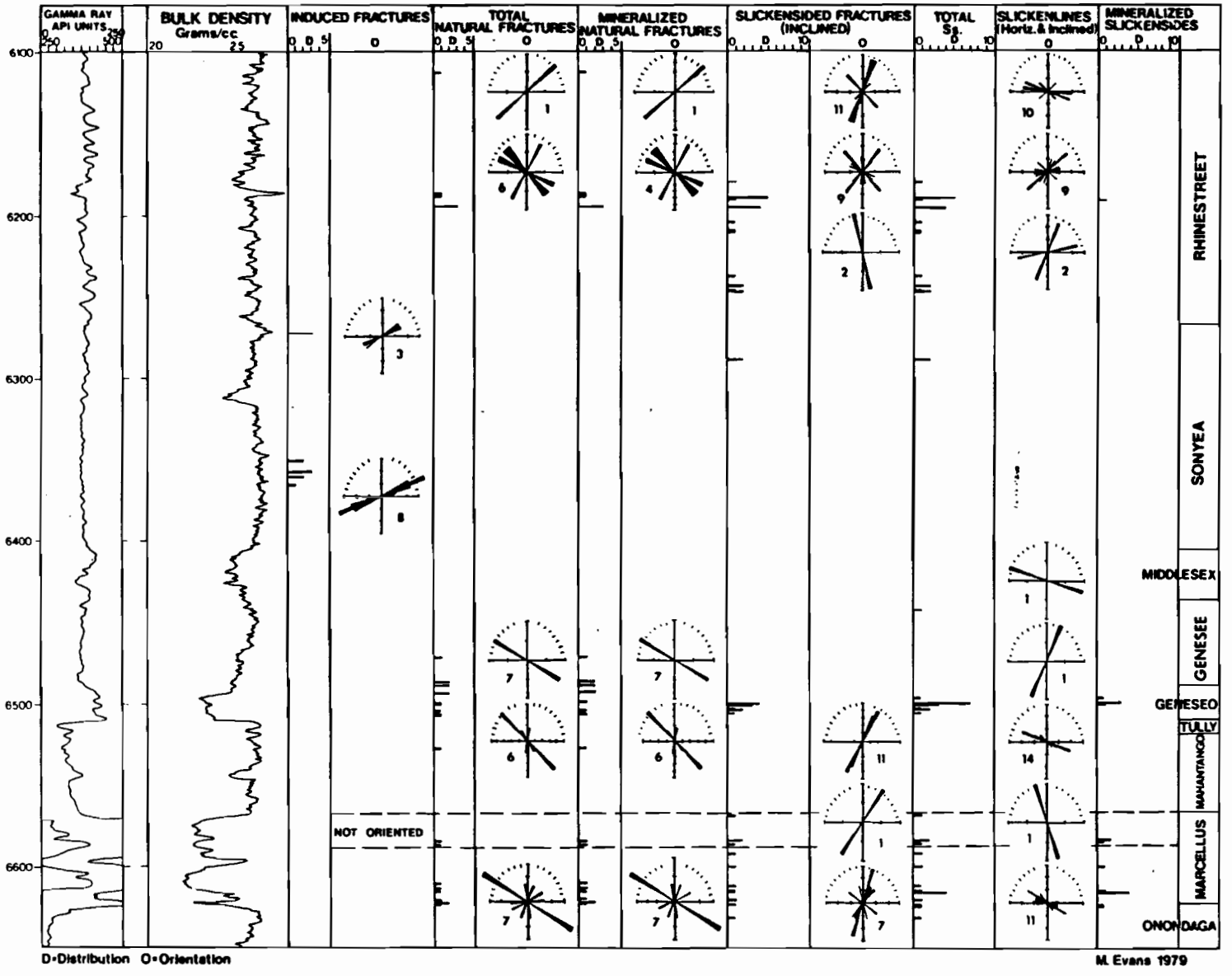

Figure F-11. Composite data sheet of fracture frequencies and orientations for all fracture types.

APPENDIX G: OH #1 (S-745) CORE WELL

OH #1 (S-745) CORE WELL

Location

The OH #1 (S-745) core well is located in Carroll County, Ohio, ten miles southeast of the city of Canton (figures 1 and G-1, table 1). Regional structure of the Devonian shales shows a monoclinal dip of less than 1° to the southeast. A total of 240 feet of the Devonian was cored in two separate sections, from 2080'-2200' in the Lower Huron Member of the Ohio Shale, and 3080'-3200' in the West Falls Formation.

Production Data

No production data was available for this well.

Undifferentiated Fractures

The core was oriented by Morgantown Energy Technology Center personnel with no distinction being made between core-induced fractures, natural fractures, and slickensided fractures. In this study they are all grouped under the catagory of undifferentiated fractures. Also, only fracture strikes were measured, no fracture dips (Byrer and Rhoads, 1976).

The composite rose diagram of undifferentiated fracture strikes (figure G-2) has a single statistically significant peak at $N25^{\circ}E$. There is a 5.0% chance that this peak does not exist. A smaller peak which is not statistically significant occurs at $N63^{\circ}W$. Fracture orientations show a great amount of variability (figures G-3 and G-4, table G-1). The Upper Huron Member of the Ohio Shale tends to show the most distinct fracture sets whereas the fractures in the West

Falls Formation show more scatter. Due to the fact that the fracture types are not known, nor fracture dips, no reliable interpretations can be made.

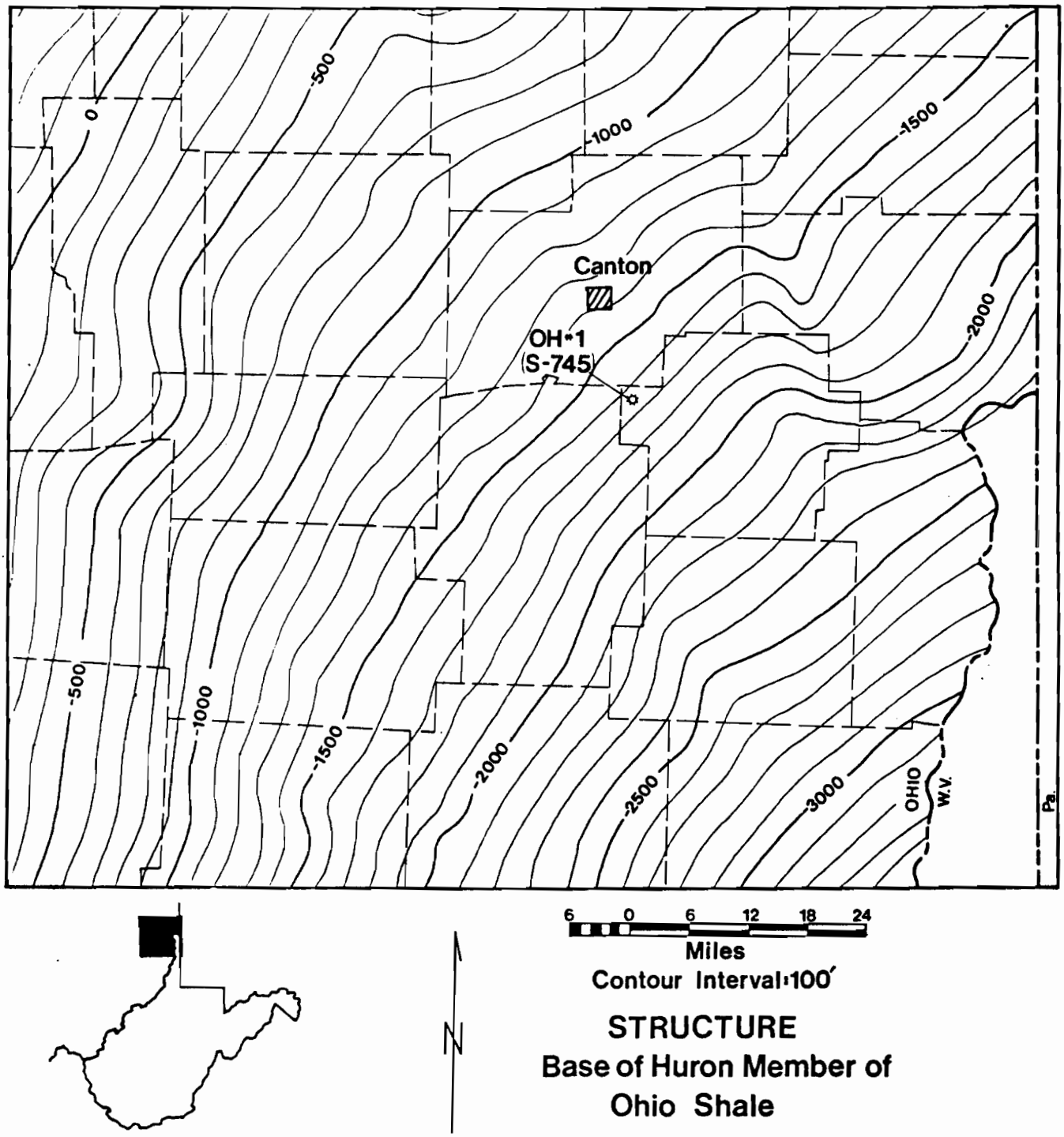

Figure G-1. Index map for the OH #1 (S-745) core well

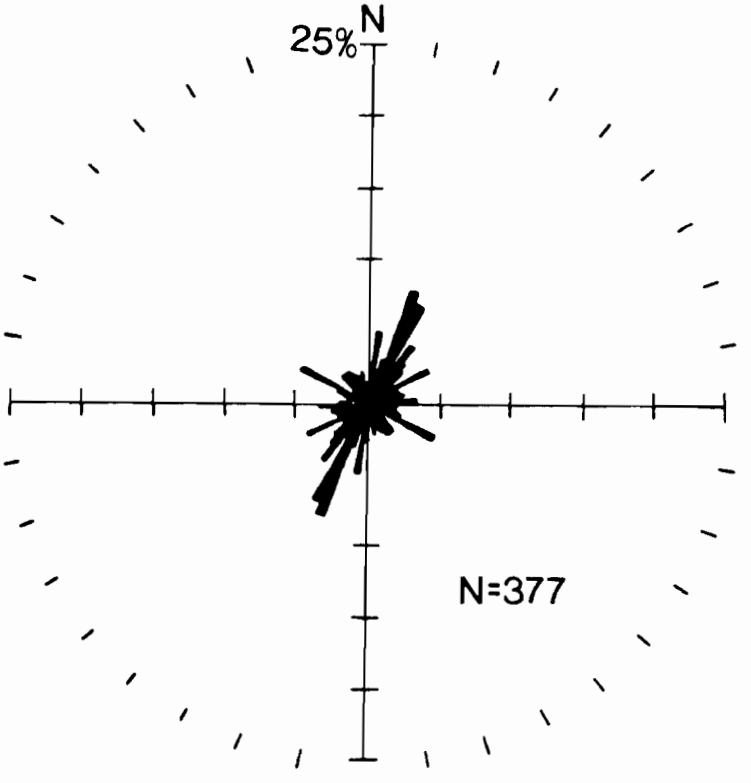

UNDIFFERENTIATED FRACTURES

OH*1 (S-745)

Figure G-2. Rose diagram of undifferentiated fracture strikes.

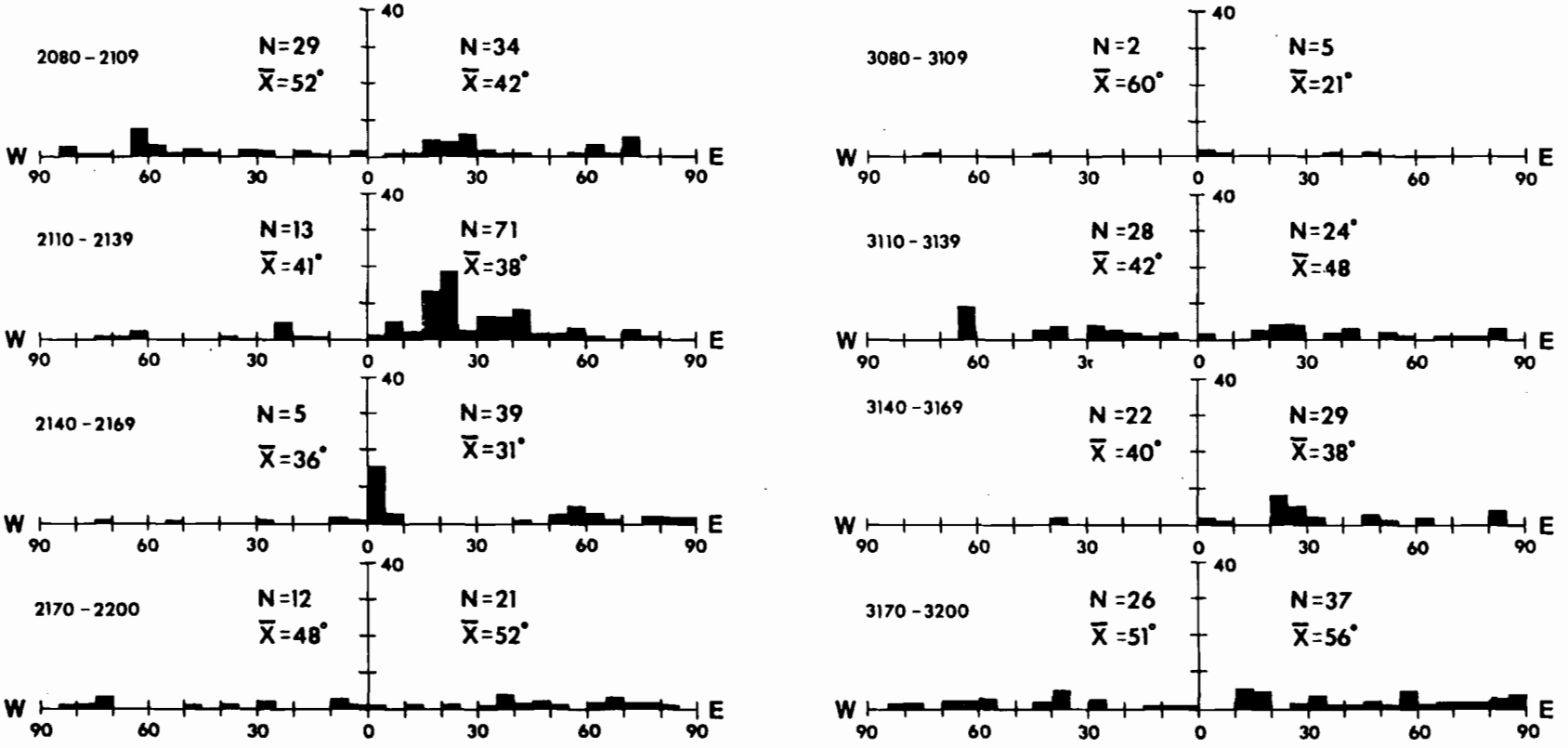

OH#1 (S-745) UNDIFFERENTIATED FRACTURES

Figure G-3. Histograms of undifferentiated fracture orientations.

TABLE G-1

OH #1 (S-745) UNDIFFERENTIATED FRACTURES

Interval	N	VN	α
2080-2109	63		
		3.9056	≤0.01
2110-2139	84		
		4.8242	≤0.01
2140-2169	44		
		2.5241	≤0.05
2170-2200	33		
		1.2484	≤1.00
3080-3109	7		
		1.2793	≤1.00
3110-3139	52		
		2.5628	≤0.05
3140-3169	31		
		2.1210	≤1.00
3170-3200	63		

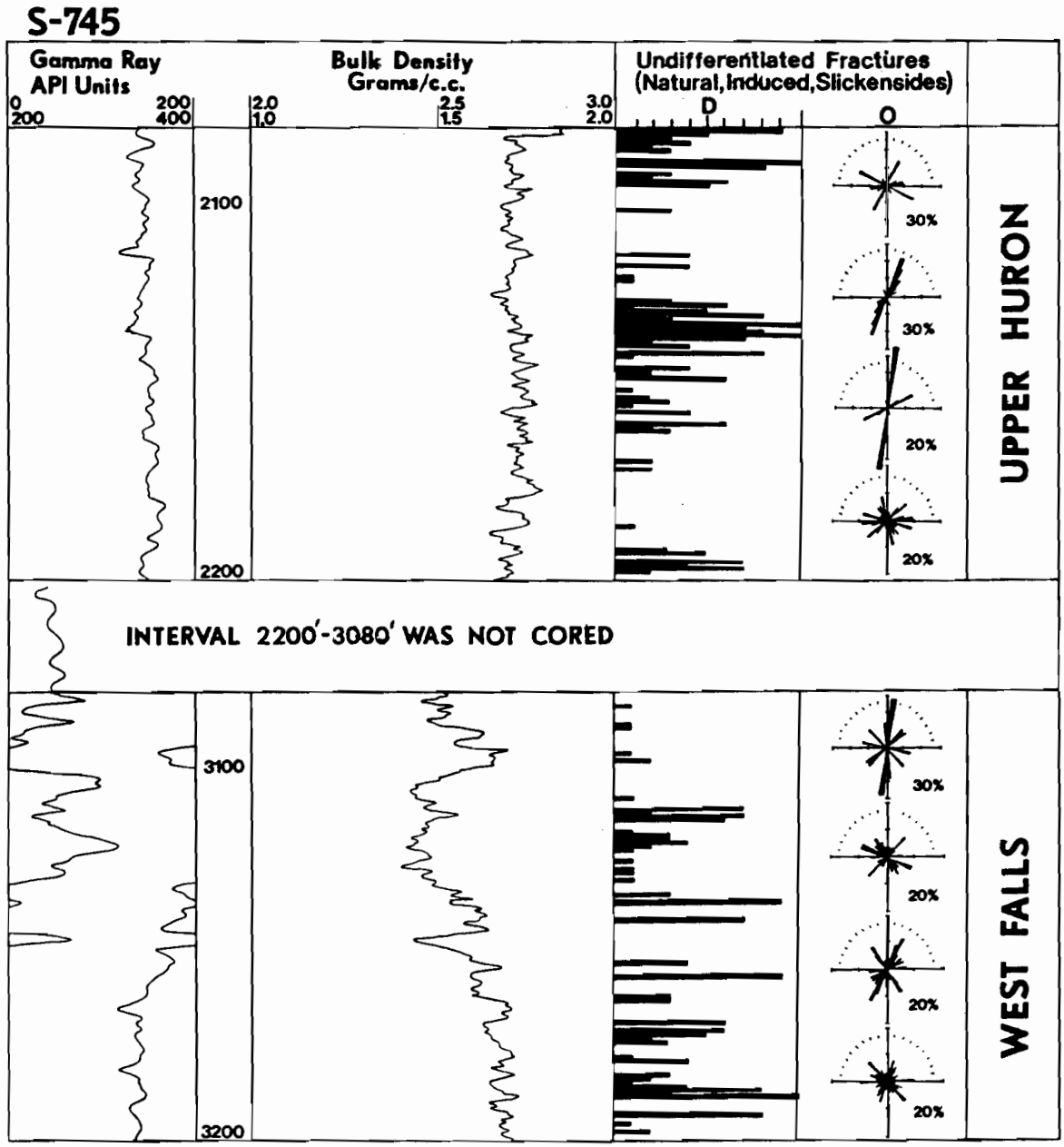

Figure G-4. Composite data sheet of undifferentiated fracture frequencies and orientations.

APPENDIX H: OH #2 (R-109) CORE WELL

OH #2 (R-109) CORE WELL

Location

The OH #2 (R-109) core well is located in Washington County, Ohio, along the Ohio River, approximately two miles northwest of the city of Parkersburg, West Virginia (figures 1 and H-1, table 1). The wellsite is on the northeast flank of the northwest trending Parkersburg-Lorain Syncline. Regional structure of the Devonian shales shows a monoclinal dip of less than 1° to the southeast. A total of 224 feet of the Devonian Lower Huron Member of the Ohio Shale was cored, from 3490'-3714' (figure H-2). The lower 59 feet of the core, interval 3655'-3714', could not be oriented due to a malfunction of the orienting camera. This interval was not used in this study.

Production Data

No production data was available for this well.

Undifferentiated Fractures

Core fracture orientations were measured by West Virginia Geologic and Economic Survey personnel with no distinction being made between core-induced fractures, natural fractures, and slickensided fractures. In this study they are all grouped together under the catagory of undifferentiated fractures. According to Vickers (1977, unpublished manuscript) a majority of the fractures logged in the core are core-induced fractures. He also states that slickensides are abundant below 3580' with none found above that point.

The rose diagram of undifferentiated fracture strikes (figure H-3) has a one statistically significant peak at $N60^{\circ}$-$75^{\circ}E$ with an average

strike of N65°E. There is a 1.0% chance that his peak does not exist. A very minor peak which is not statistically significant occurs at N20°W. Fractures in this set are found only in the interval 3574'-3601' (figures H-4 and H-6). The equal area projection of poles to undifferentiated fracture surfaces (figure H-3) has eight clusters; four corresponding to the inclined and vertical fractures of the N60° 75°E set, and four clusters corresponding to the inclined and vertical fractures of tne N20°W set. Fracture orientations exhibit a great amount of scatter in the interval 3490'-3517' (figures H-4 and H-5, table H-1), but are very consistent throughout the rest of the core. The consistent fracture orientations suggest the presence of a stress or rock fabric anisotropy. The dominant N60°-75°E strike may be related to the general east to northeast trending maximum compressive stress present in most of eastern North America (Sbar and Sykes, 1973). The N20°W set may be an anomalous core-induced fracture set caused by differential stresses in that particular interval, or possibly, a natural fracture set which formed as an extension fracture set under tectonic compressive stresses directed from the southeast during the formation of the southern Appalachians.

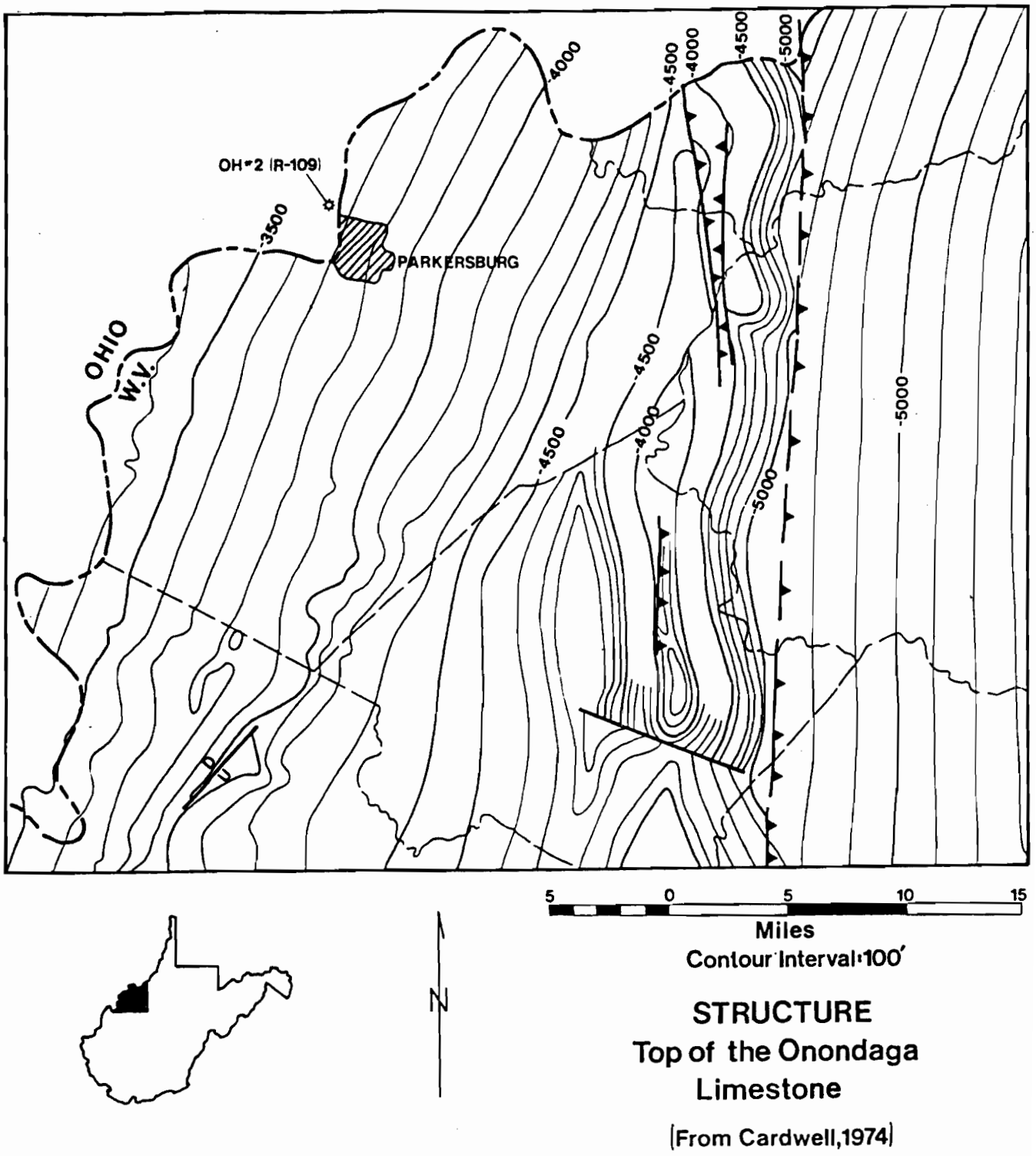

Figure H-1. Index map for the OH #2 (R-109) core well

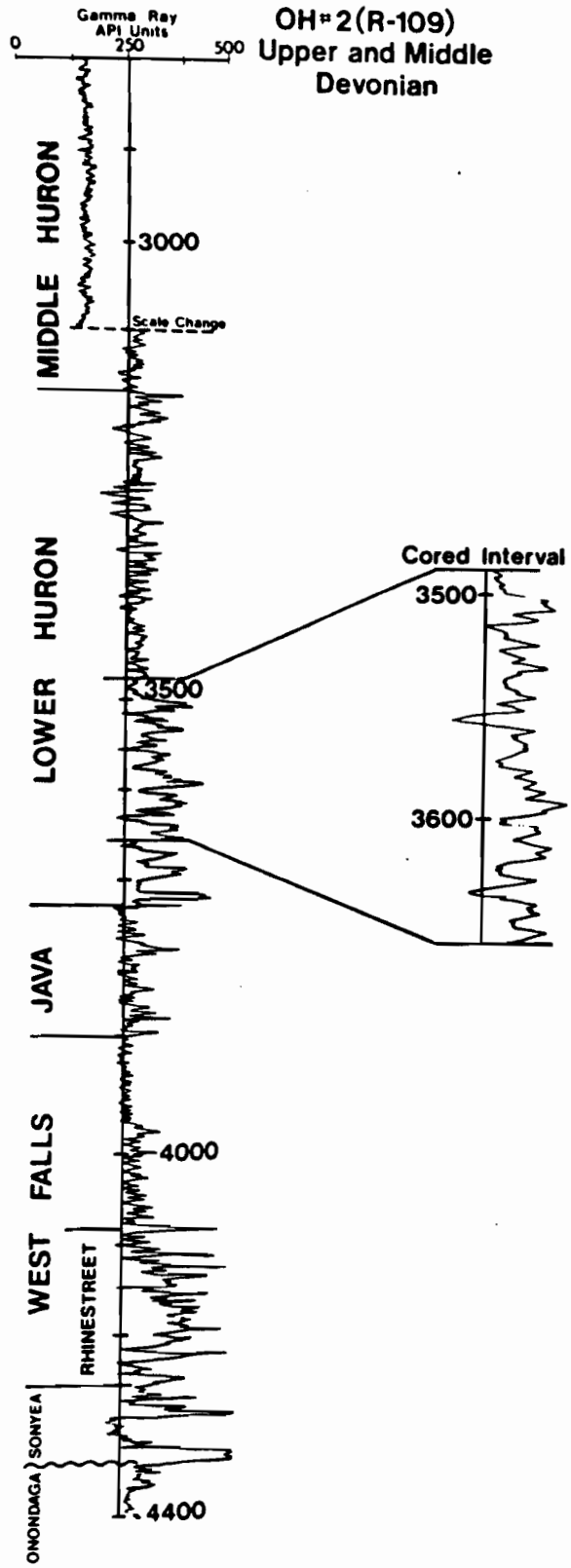

Figure H-2. Gamma-ray log, Middle and Upper Devonian.

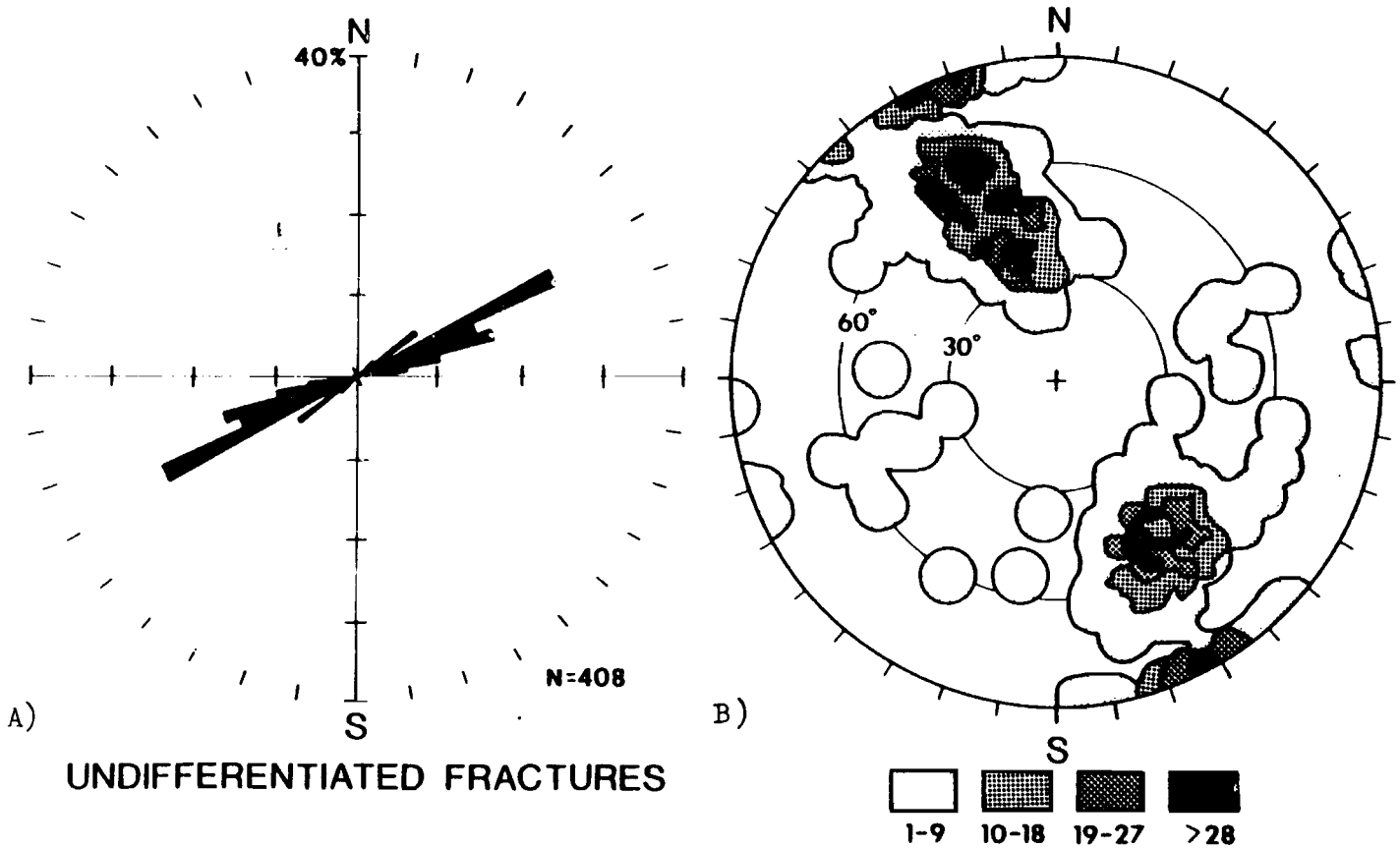

OH#2 (R-109)

Figure H-3. (A) composite rose diagram of undifferentiated fracture strikes, and (B) equal area projection of poles to undifferentiated fracture surfaces

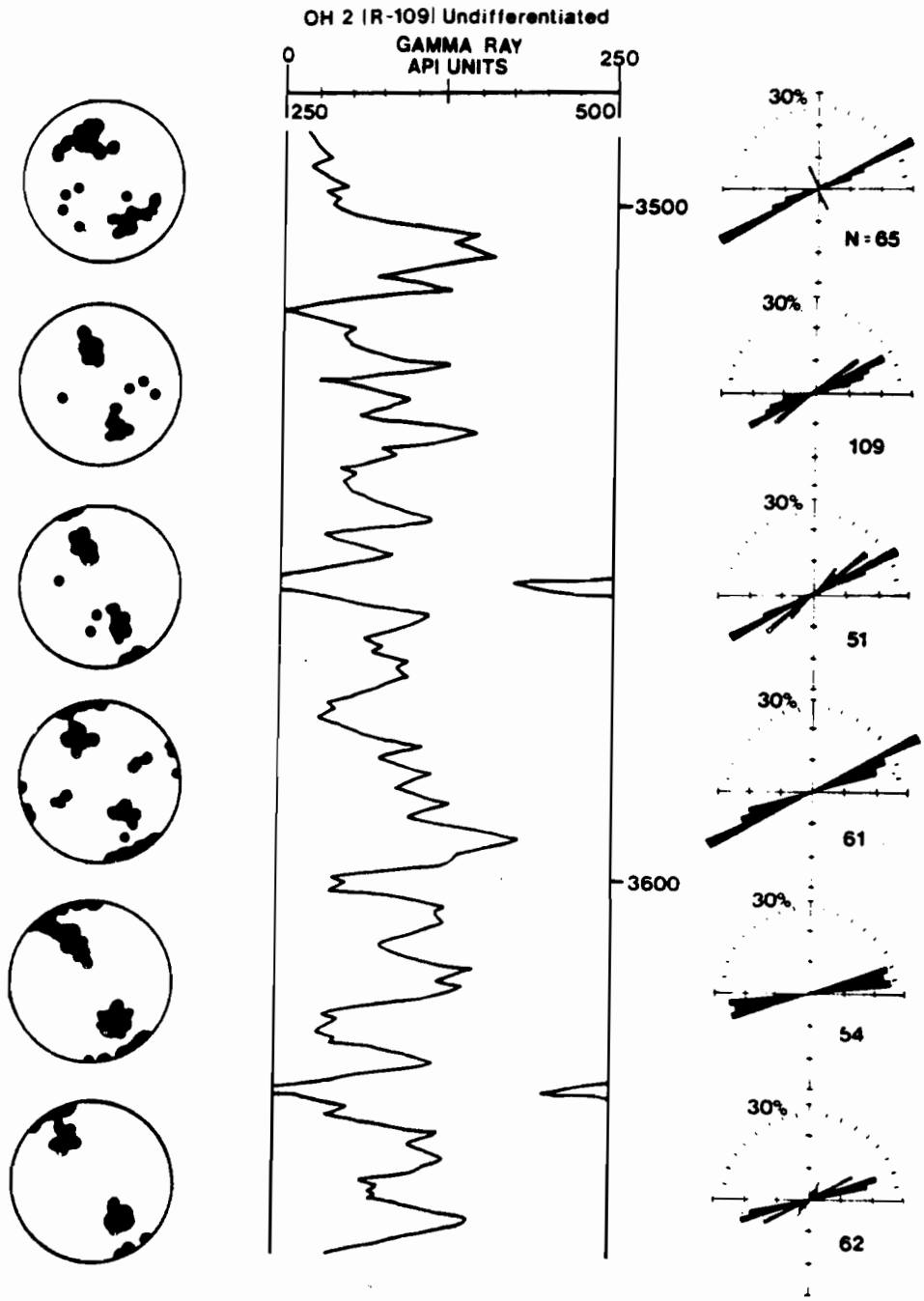

Figure H-4. Equal area projections of poles to undifferentiated fracture surfaces and rose diagrams of undifferentiated fracture strikes for approximately equal length intervals of the OH #2 (R-109) core.

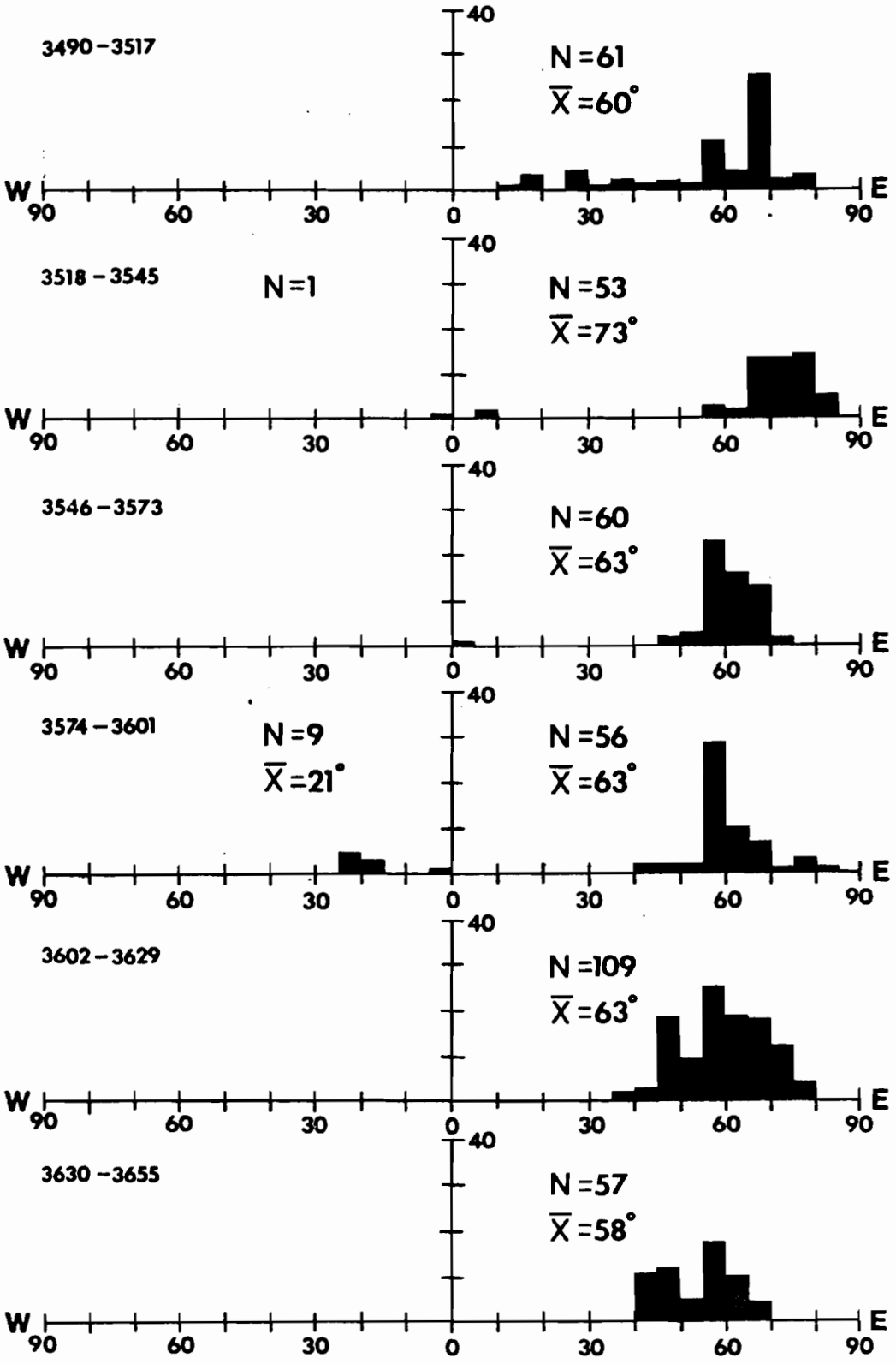

OH*2 (R-109) UNDIFFERENTIATED FRACTURES

Figure H-5. Histograms of undifferentiated fracture orientations.

TABLE H-1

OH #2 (R-109) UNDIFFERENTIATED FRACTURES

Interval	N	VN	α
3490-3517	61	3.0228	≤0.01
3518-3545	54	4.6357	≤0.01
3546-3573	61	1.6783	≤1.00
3574-3601	65	2.0506	≤1.00
3602-3629	109	2.5118	≤0.05
3630-3655	57		

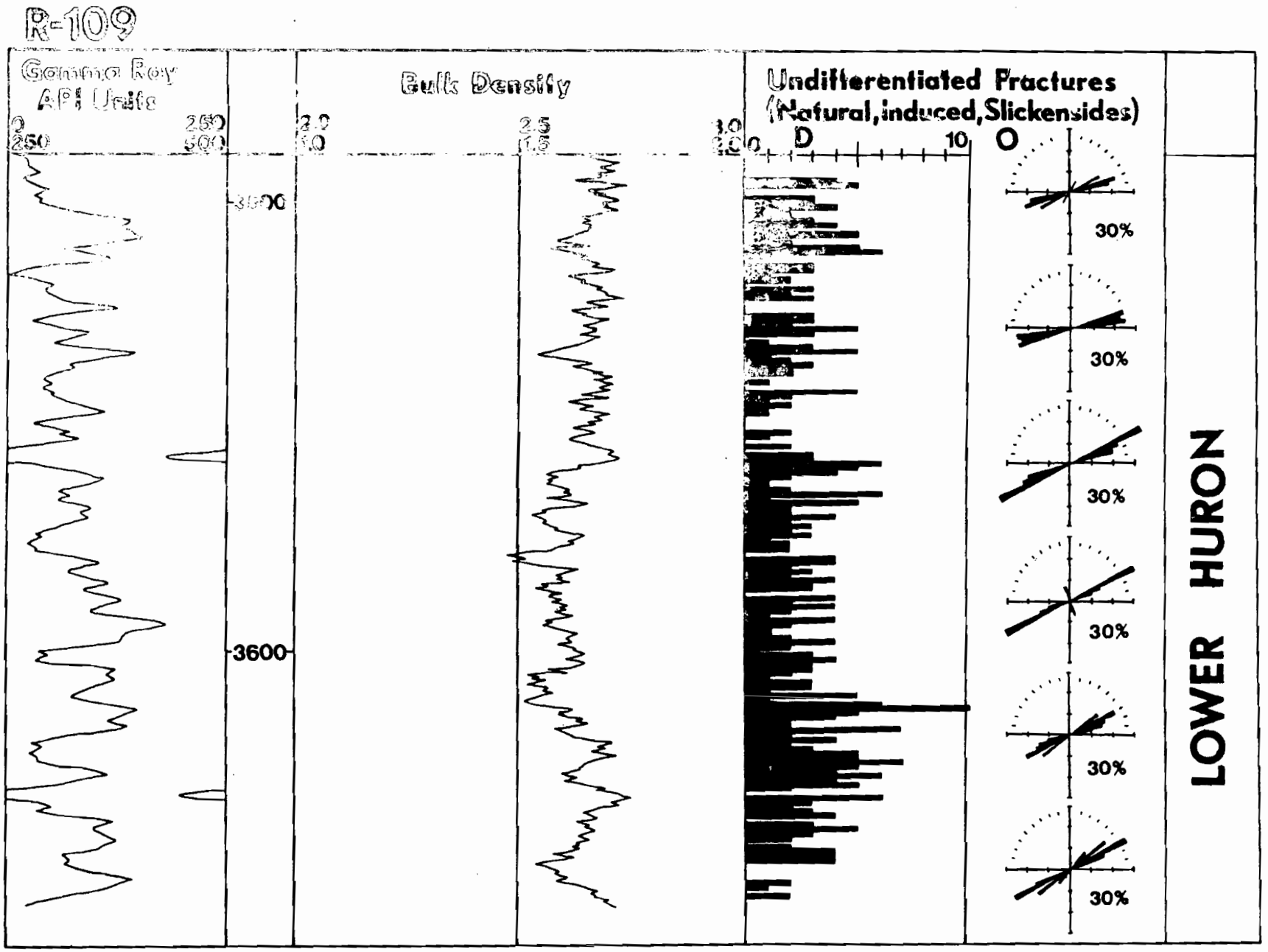

Figure H-6. Composite data sheet of undifferentiated fracture frequencies and orientations.

APPENDIX I: VA #1 (20338) CORE WELL

VA #1 (20338) CORE WELL

Location

The VA #1 (20338) core well is located in Wise County, Virginia, approximately ten miles southeast of the town of Whitesburg, Kentucky (figures 1 and I-1, table 1). The wellsite is near the center of the Millsboro Basin on the Pine Mountain overthrust sheet. A total of 380 feet of the Devonian was cored from two separate intervals, 4870'-4985' and 5210'-5475' (figure I-2).

Production Data

Two intervals of the well were stimulated by a cryogenic type treatment (gelled water and liquid CO_2). After stimulation, interval 4890'-4910', in the Cleveland Member of the Ohio Shale, had an initial open flow fluctuating between 54 mcf/day and 107 mcf/day; and interval 5450'-5480', in the Lower Huron Member of the Ohio Shale, had an initial open flow of 40 mcf/day (Komar, Frone, and Yost, 1978).

Core-induced Fractures

Core-induced fractures are the most common fracture type in the core. The Cleveland Member and the Three Lick Bed have the highest frequency of core-induced fractures whereas the Lower Huron Member has the lowest frequency (figure I-12). The core-induced fracture composite rose diagram (figure I-3) has a peak at N45°-70°E with an average strike of N57°E. There is a 1.0% chance that this peak does not exist. The equal area projection of poles to core-induced fracture surfaces (figure I-3) has two large clusters corresponding to the opposing dips of the N57°E fracture set, and two smaller clusters

corresponding to the opposing dips of a fracture set striking approximately N25°W. The N25°W set is not statistically significant. Core-induced fracture orientations show very little variability with depth. The greatest change occurs between the Cleveland Member, interval 4870'-4930', and the Three Lick Bed, interval 4931'-4985', where mean strikes are N62°E and N43°E respectively (figures I-4 and I-5, table I-1).

The dominant core-induced fracture oeientation, N45°-70°E, may be related to the east to northeast trending maximum compresssive stress which exists in most of eastern North America (Sbar and Sykes, 1973). The trend also parallels the Pine Mountain thrust. This suggests that the tectonic compressive stresses which formed the thrust and the resulting layer-parallel shortening, may have imposed a residual strain in the rocks in the form of an incipient cleavage (Engelder, 1979). This self-equilibrating recoverable strain may be responsible for the formation of the core-induced fractures, alone or in combination with the maximum compressive stress.

Natural Fractures

Natural fractures occur throughout the VA #1 (20338) core. The Lower Huron Member, however, has a greater frequency of natural fractures than other units in the core (figure I-12). The natural fracture composite rose diagram (figure I-6) has two significant peaks. There is a 1.0% chance that the peaks at N7°W and N37°W do not exist. Two peaks that are not statistically significant are found at N13°E and N83°W. The equal area projection of poles to natural fracture surfaces (figure I-6) has two clusters which correspond to the two major

subvertical natural fracture sets. The two smaller sets do not form definite clusters on the plot. Natural fracture orientations are quite variable and show no pattern or systematic variation with depth or stratigraphy (figure I-7). Surfaces of nearly all of the natural fractures are polished to some degree. However, since twist hackle and hackle plume can be distinguished on most of these fracture surfaces, displacement along the fracture probably took place during or after fracture formation.

The N37^{o}W natural fracture set is nearly orthogonal to the trace of the Pine Mountain thrust and probably formed as an extension fracture set under tectonic compressive stresses during formation of the thrust. The N7^{o}W set and the two smaller fracture sets parallel faults and fold axes on the thrust sheet. The transcurrent movement within the thrust sheet which formed these structures may also be responsible for the three fracture sets.

Slickensides and Slickenlines

Slickensides are found to be concentrated in two zones: an upper zone at the contact of the Cleveland Member with the Three Lick Bed; and a lower zone which includes the entire Lower Huron Member, a soft black shale unit (figure I-12). Slickensides are also scattered throughout the rest of the core. The two slickenside zones are vertically extensive and can be considered decollement zones. Lack of data between the two cored intervals inhibits determining whether the two slickenside zones are actually part of a single, much wider, decollement. Contours on blowout zones in the area (Young, 1957) fall near the top of the Lower Huron Member in the vicinity of this core

well. This agrees with the top of the lower décollement zone. The slickenside composite rose diagram (figure I-8) has a single peak at N40°-55°E with an average strike of N47°E. There is a 1.0% chance that this peak does not exist. A small peak that is not statistically significant is found at N27°E. Poles to slickensided surfaces form a girdle across the equal area projection (figure I-8). The pattern of clusters closely resembles the pattern of fracture dips which would be expected in a shear zone. The 0° dipping cluster in the center is the displacement shear cluster, the Riedel shear cluster dips 20°NW, and the thrust shear cluster dips 20°SE. R' shears may be present among the scatter in the southeast quadrant of the plot. In portions of the decollement zones the various sets of slip surfaces combine to divide the shear zone into numerous lenses. The lenses, usually bounded by Riedel and displacement shears, contain rock fragments so deformed as to be slickensided on all sides. Small fold and flow structures were also found in the lower décollement zone. Slickenside orientations show very little variability (figure I-9)

The slickenline composite rose diagram (figure I-10) has a single peak at N35°-55°W with an average trend of N45°W. There is a 1.0% chance that this peak does not exist. The equal area projection of slickenlines (figure I-10) has two peripheral clusters which correspond to the low dipping slickenlines. There is very little scatter in slickenline trend (figure I-11). Very few of the slickensides are mineralized. Massive barite on the slickensided surfaces is the most common type of mineralization.

The N40°-55°E slickenside trend parallels the trace of the Pine

Mountain thrust and the N35°-55°W trending slickenlines are orthogonal to it. Therefore, it can be assumed that these structures reflect movement of the Pine Mountain thrust sheet on décollement zones in the Devonian shales.

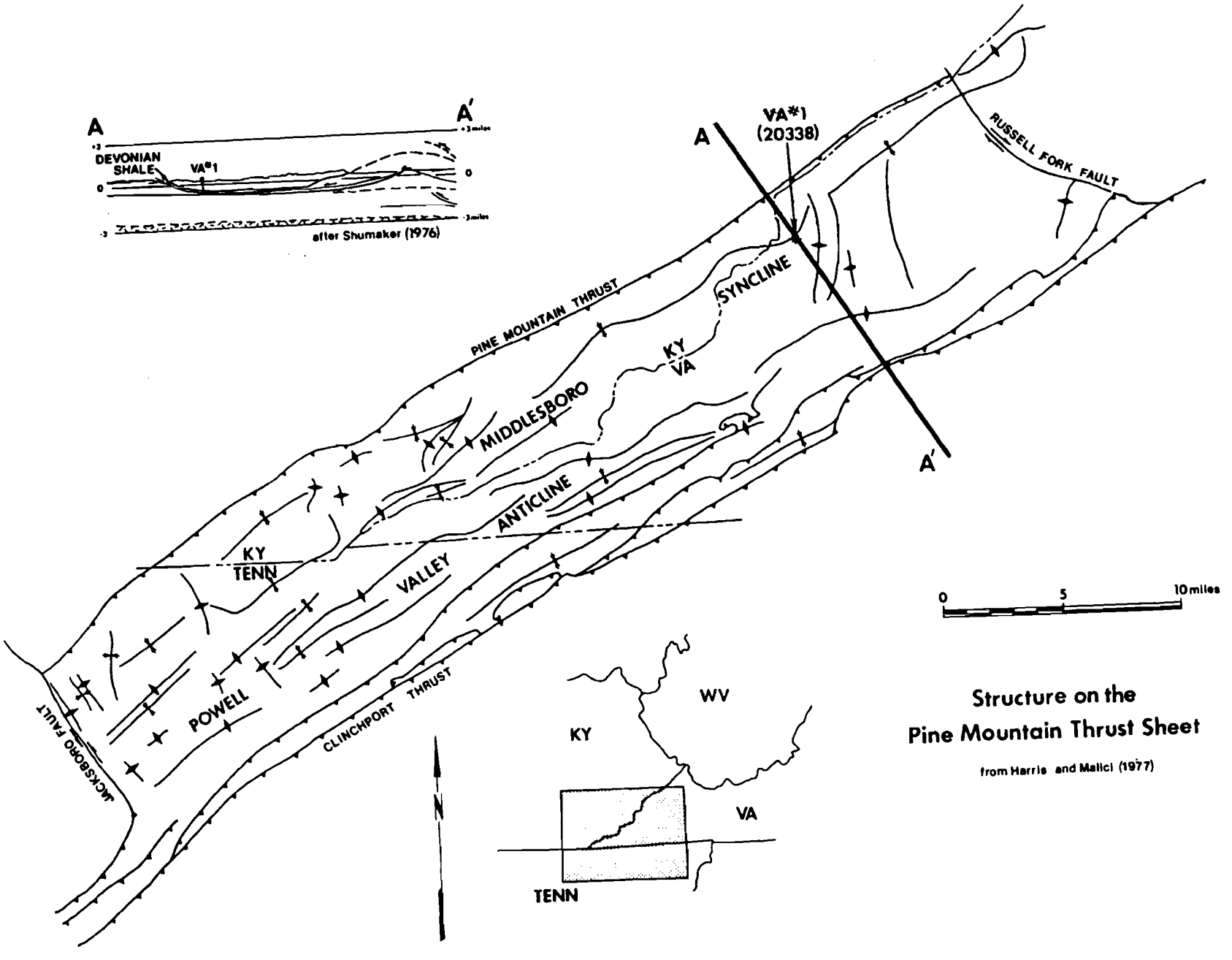

Figure I-1. Index map for the VA #1 (20338) core well showing surface structure on the Pine Mountain thrust sheet, and a cross section through the thrust sheet.

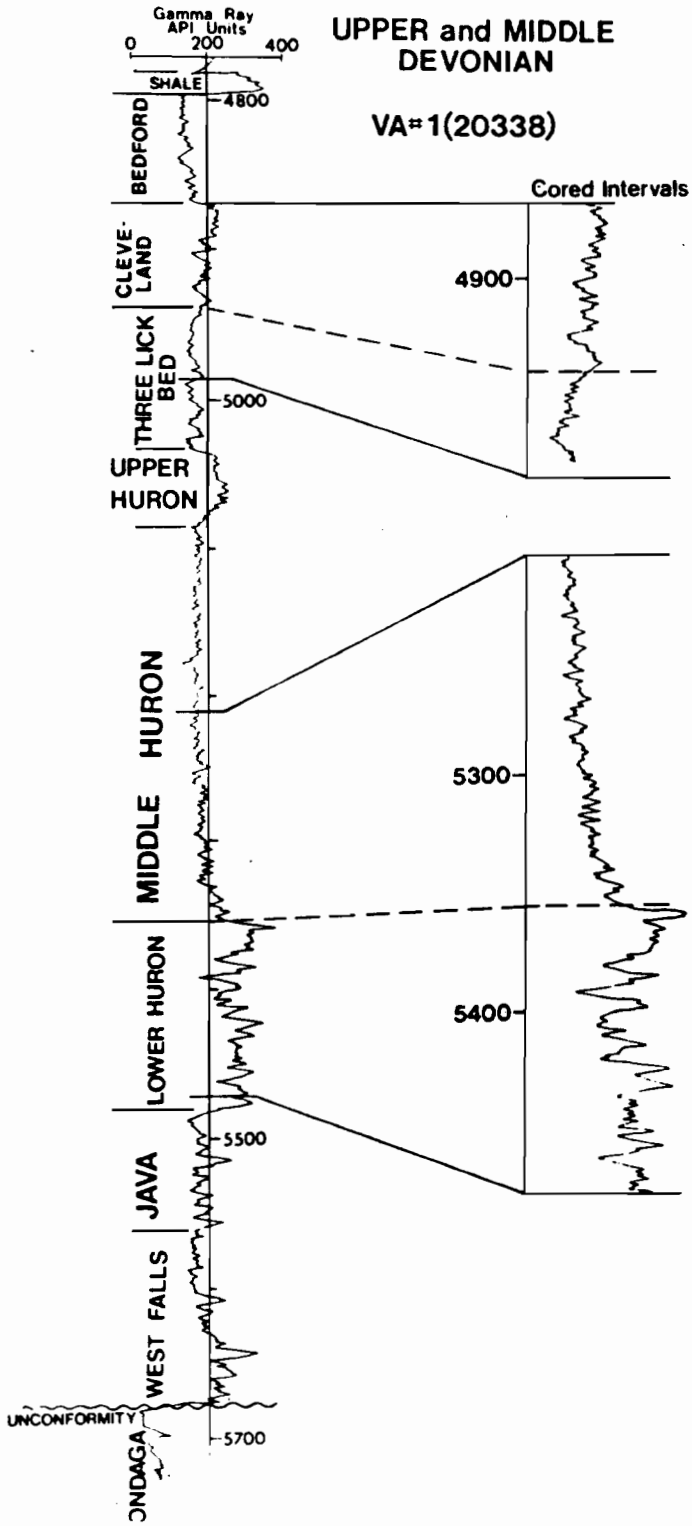

Figure I-2. Gamma -ray log, Upper and Middle Devonian.

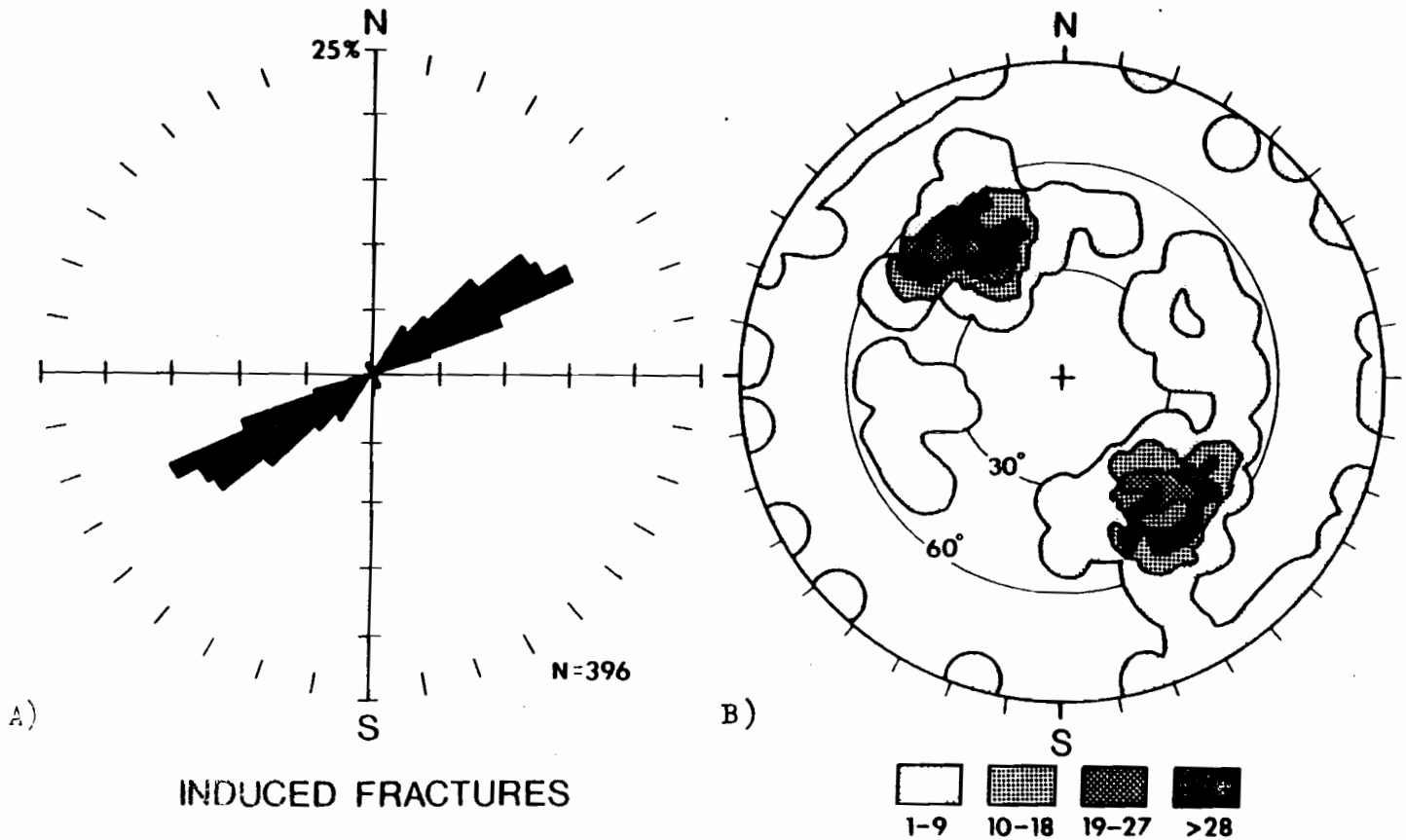

VA*1 (20338)

Figure I-3. (A) composite rose diagram of core-induced fracture strikes, and (B) equal area projection of poles to core-induced fracture surfaces

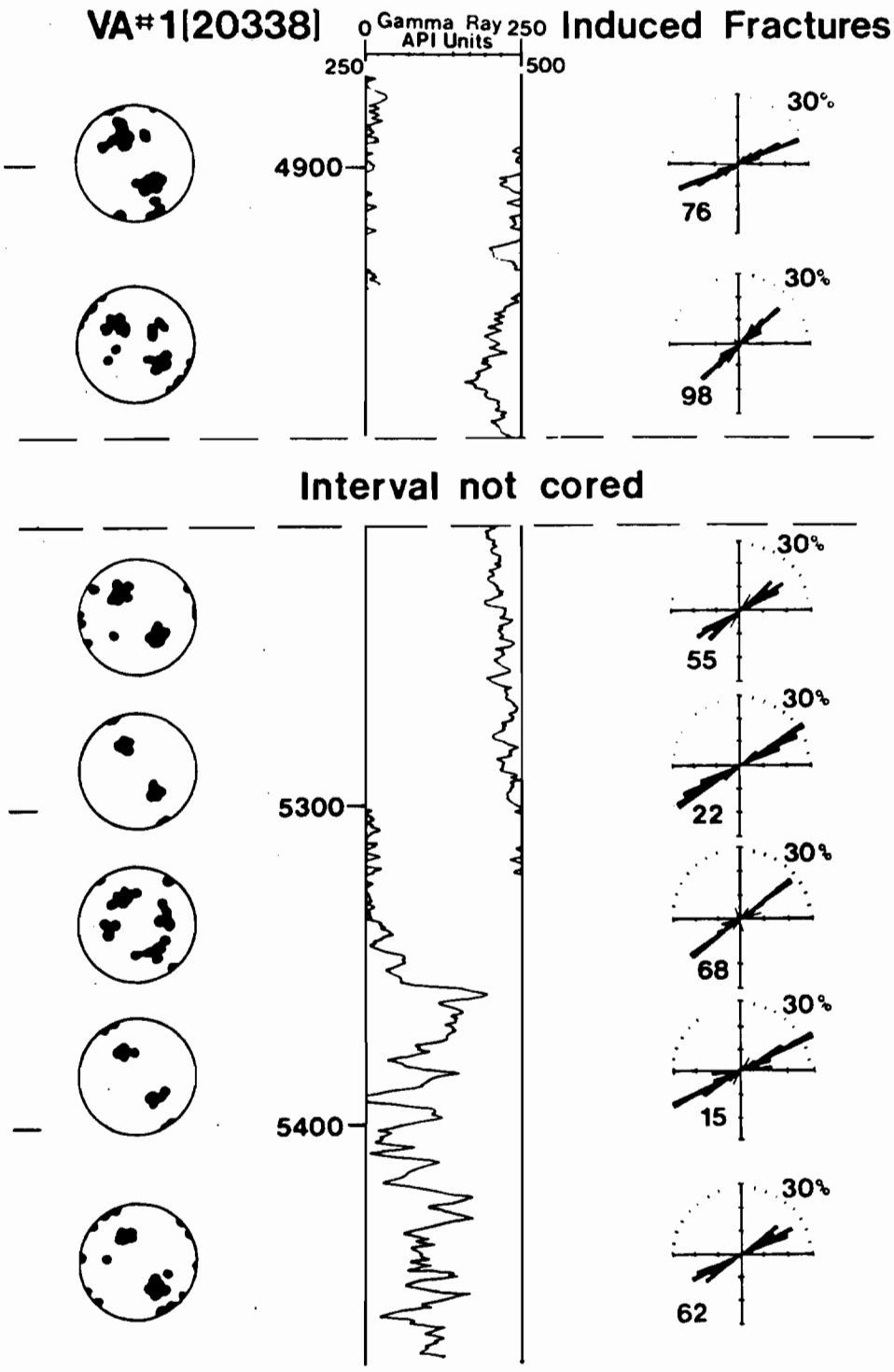

Figure I-4. Equal area projections of poles to core-induced fracture surfaces and rose diagrams of core-induced fracture strikes for approximately equal length intervals of the VA #1 (20338) core.

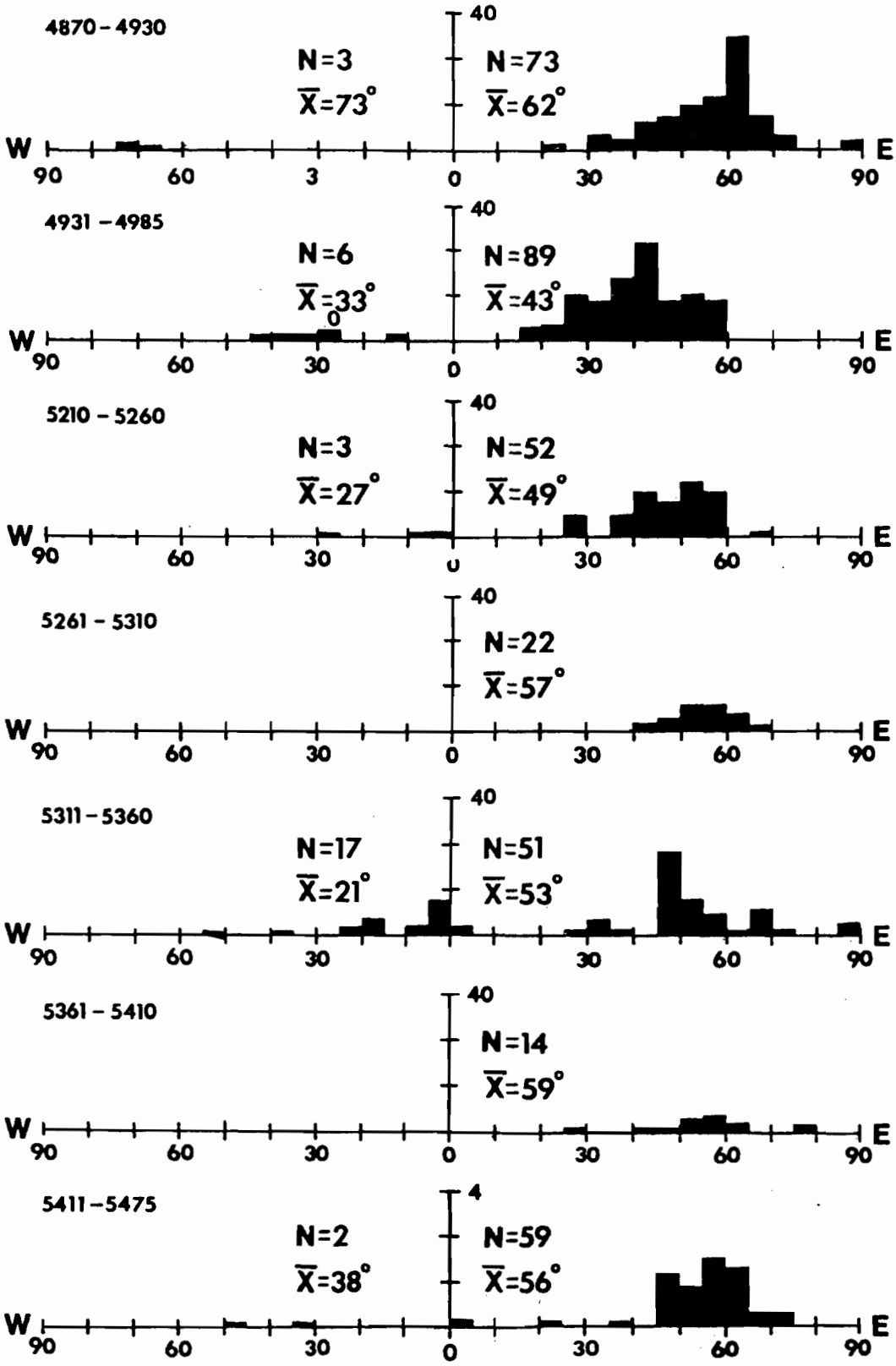

VA*1 (20338) CORE-INDUCED FRACTURES

Figure I-5. Histograms of core-induced fracture orientations.

TABLE I-1

VA #1 (20338) INDUCED FRACTURES

Interval	N	VN	α
4870-4930	76		
		4.9886	≤0.01
4931-4985	98		
		1.9194	≤1.00
5210-5260	55		
		1.8762	≤1.00
5261-5310	22		
		2.8030	≤0.01
5311-5360	68		
		1.9023	≤1.00
5361-5410	15		
		1.2952	≤1.00
5411-5475	62		

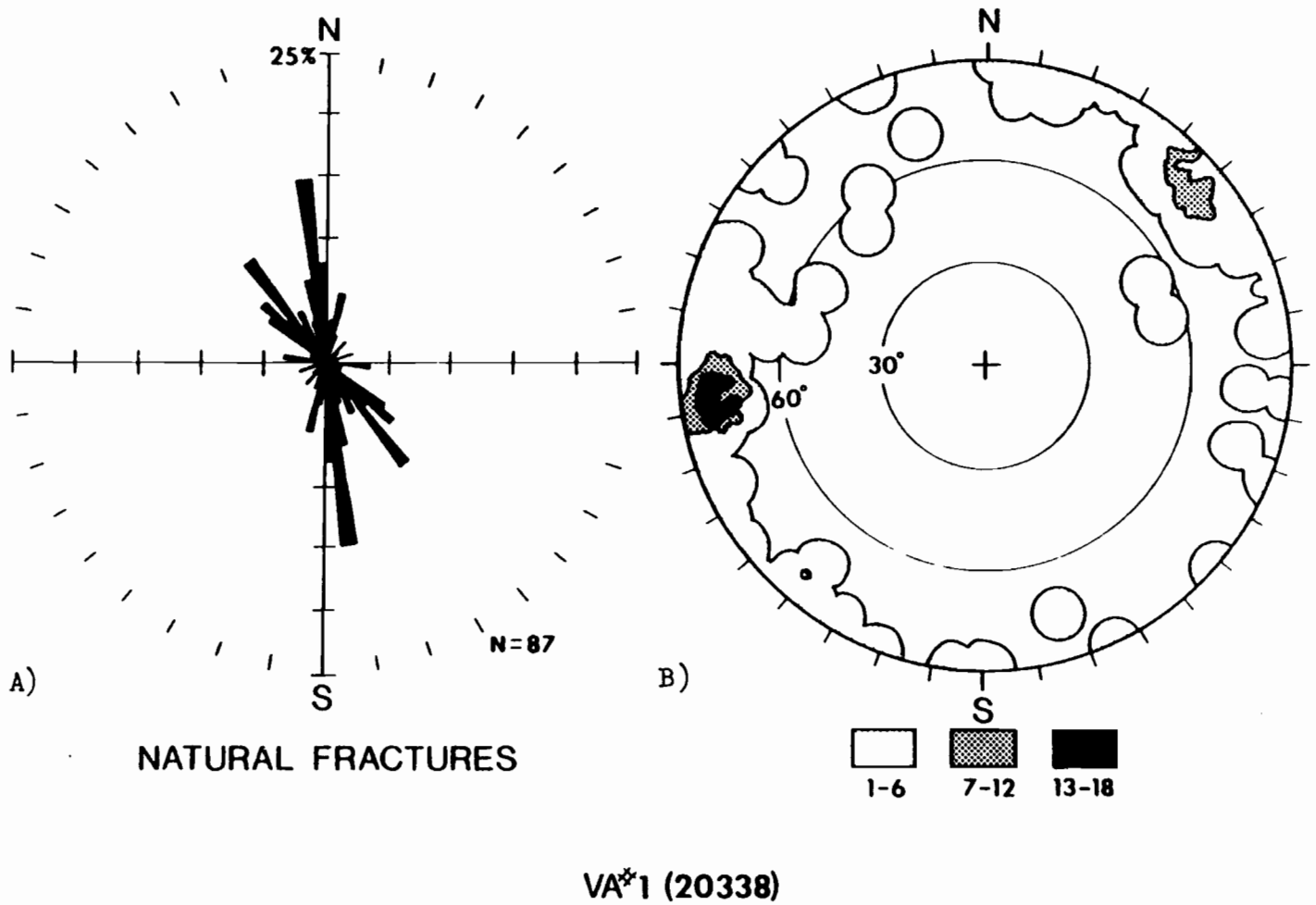

Figure I-6. (A) composite rose diagram of natural fracture strikes, and (B) equal area projection of poles to natural fracture surfaces

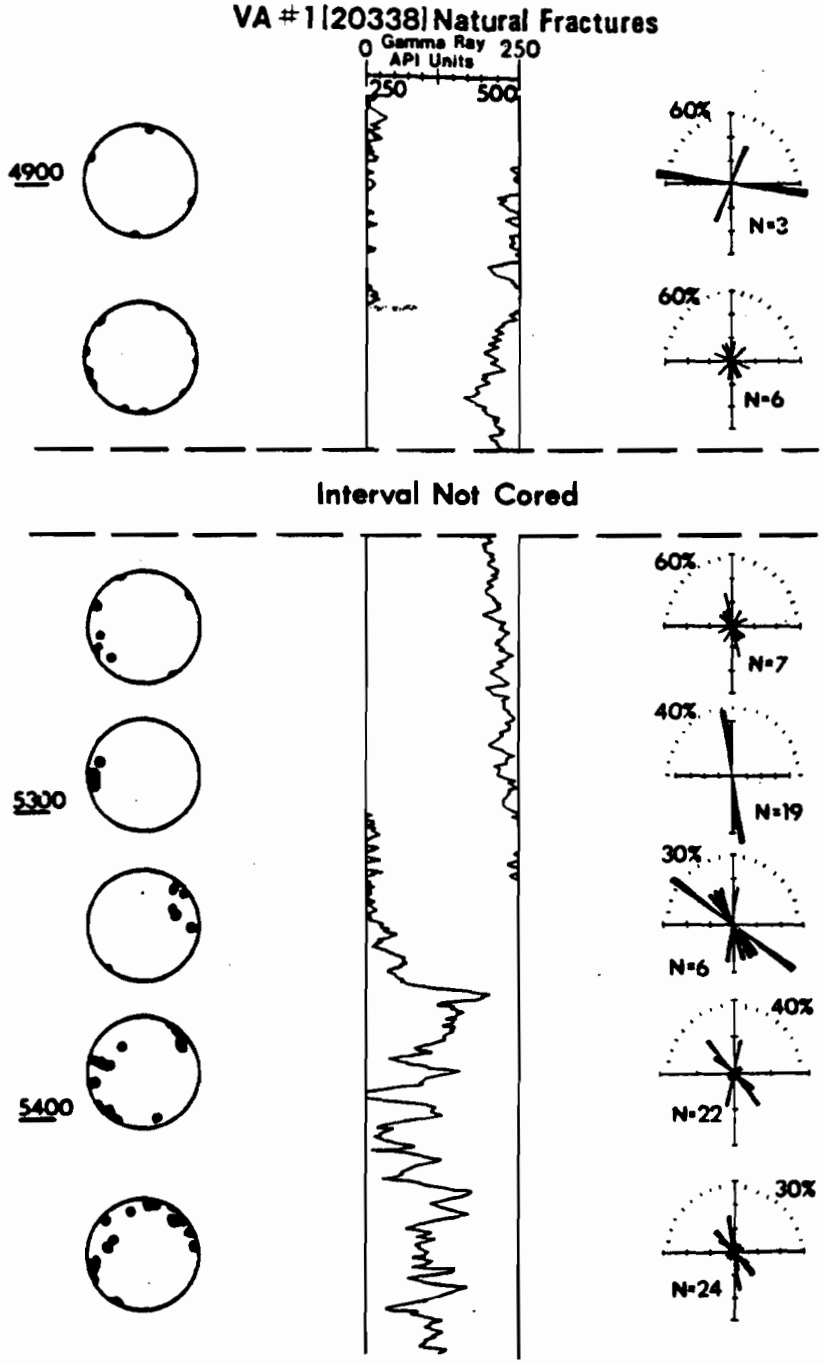

Figure I-7. Equal area projections of poles to natural fracture surfaces and rose diagrams of natural fracture strikes for approximately equal length intervals of the VA #1 (20338) core.

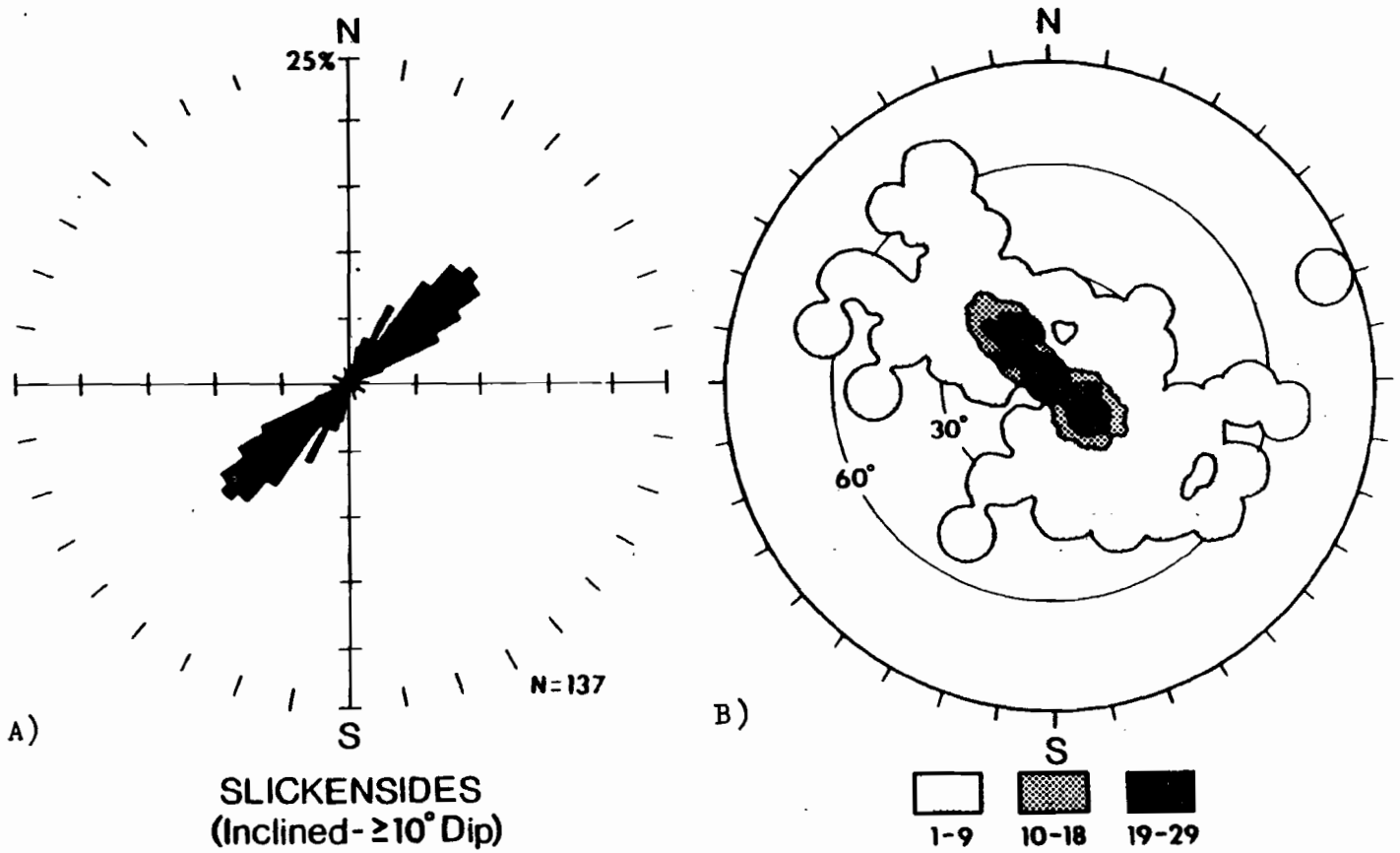

VA*1 (20338)

Figure I-8. (A) composite rose diagram of slickenside strikes, and (B) equal area projection of poles to slickensided surfaces

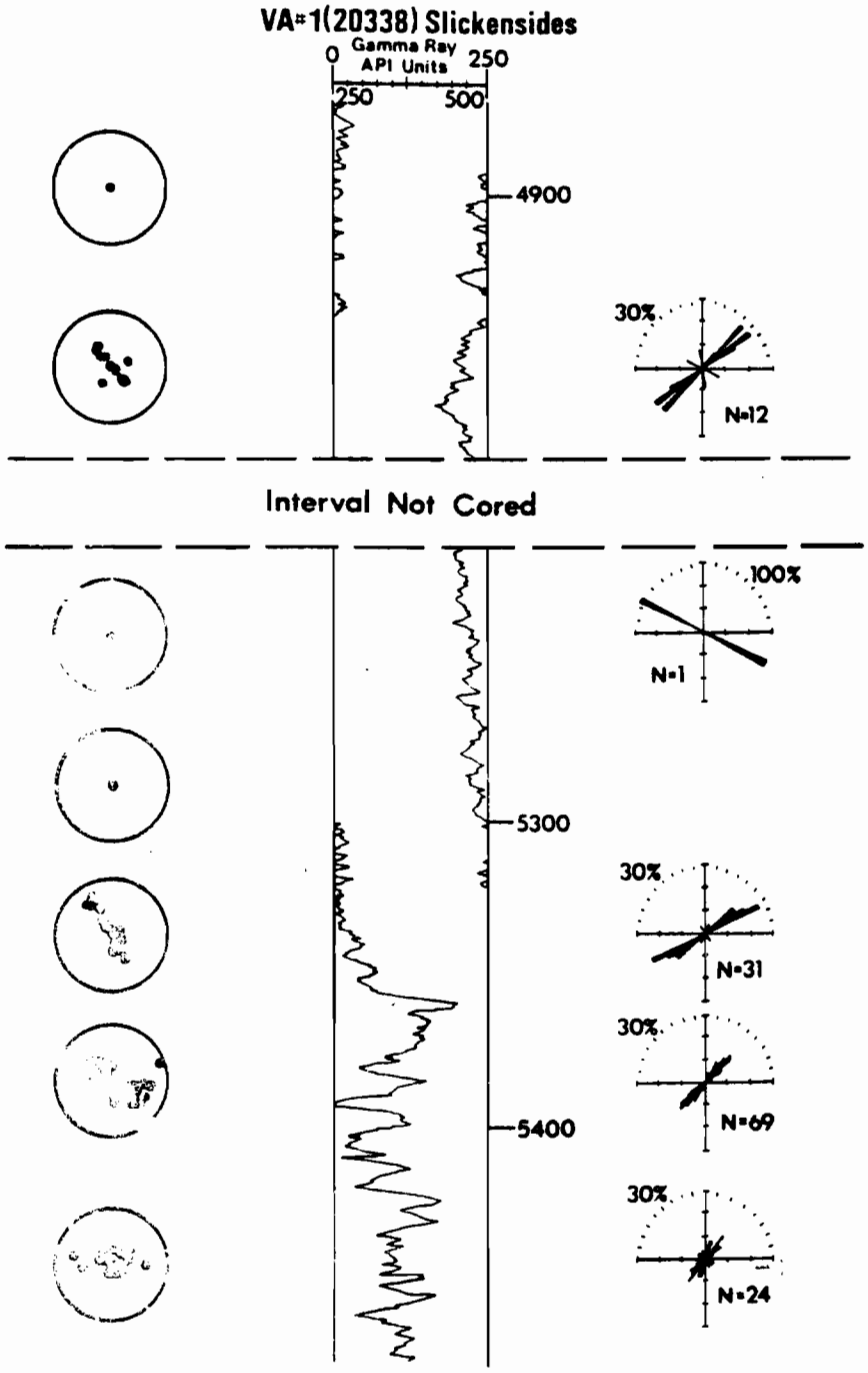

Figure I-9. Equal area projections of poles to slickensided surfaces and rose diagrams of slickenside strikes for approximately equal length intervals of the VA #1 (20338) core.

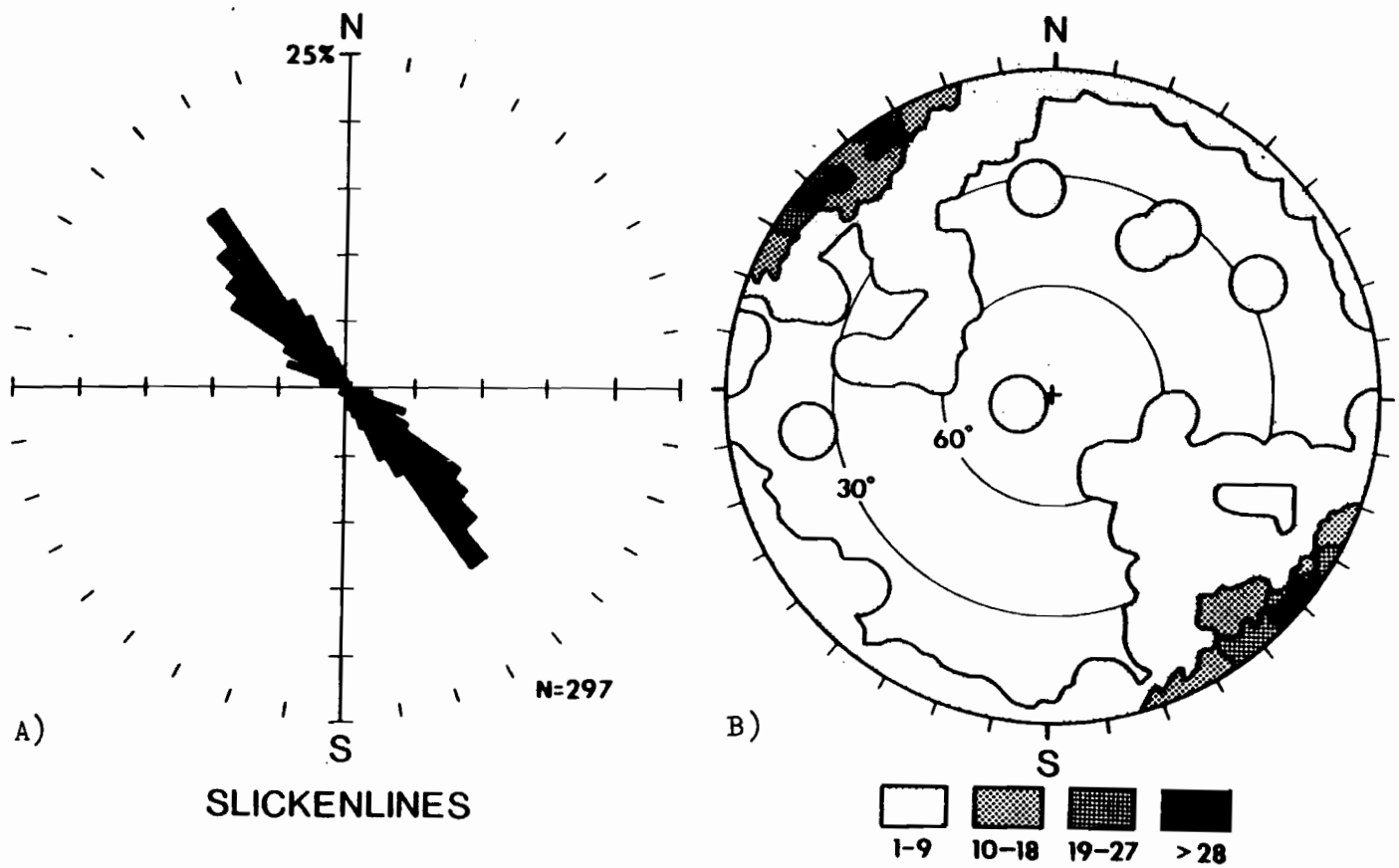

VA*1 (20338)

Figure I-10. (A) composite rose diagram of slickenline trends, and (B) equal area projection of slickenlines

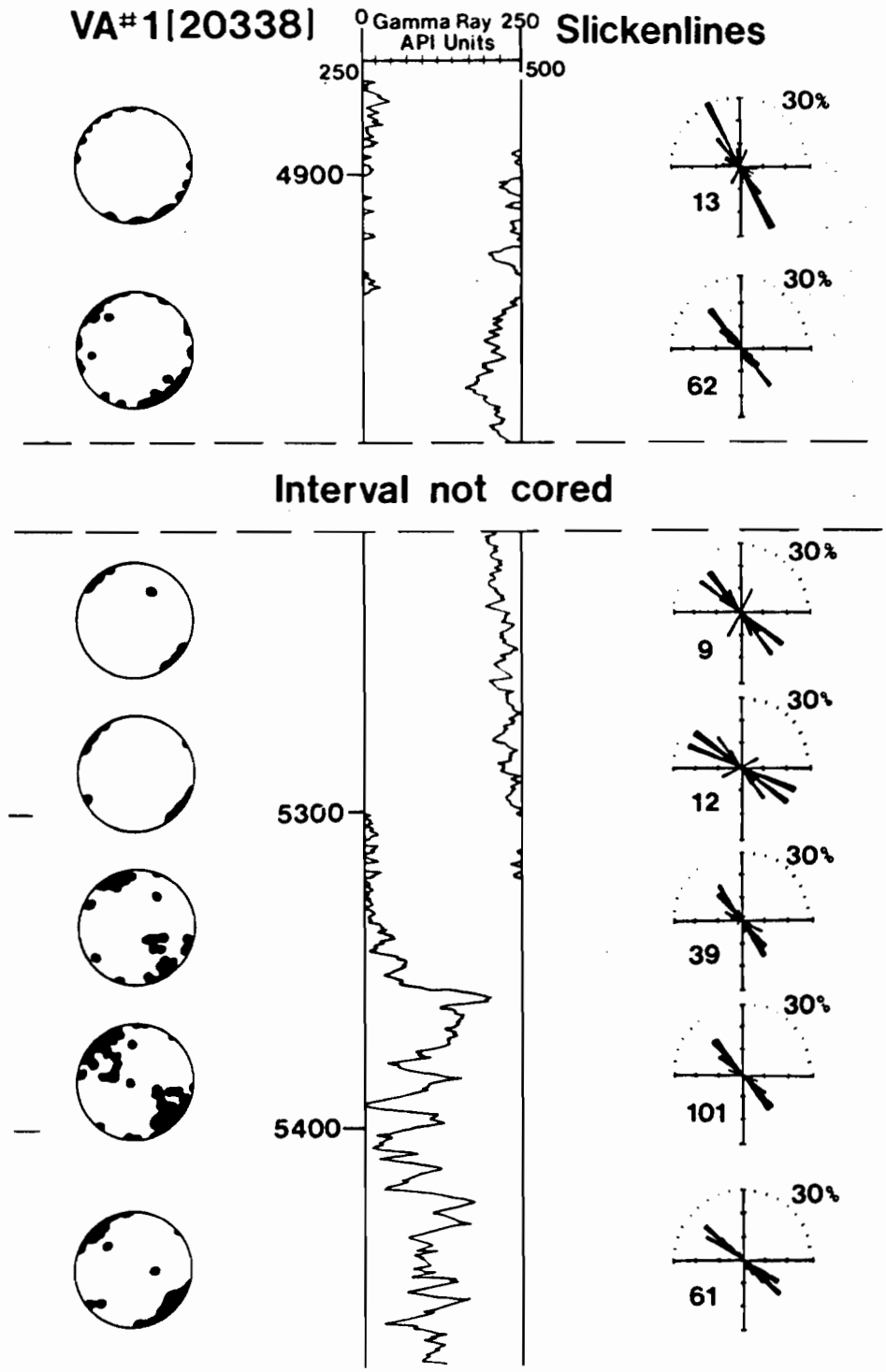

Figure I-11. Equal area projections of slickenlines and rose diagrams for approximately equal length intervals of the VA #1 (20338) core.

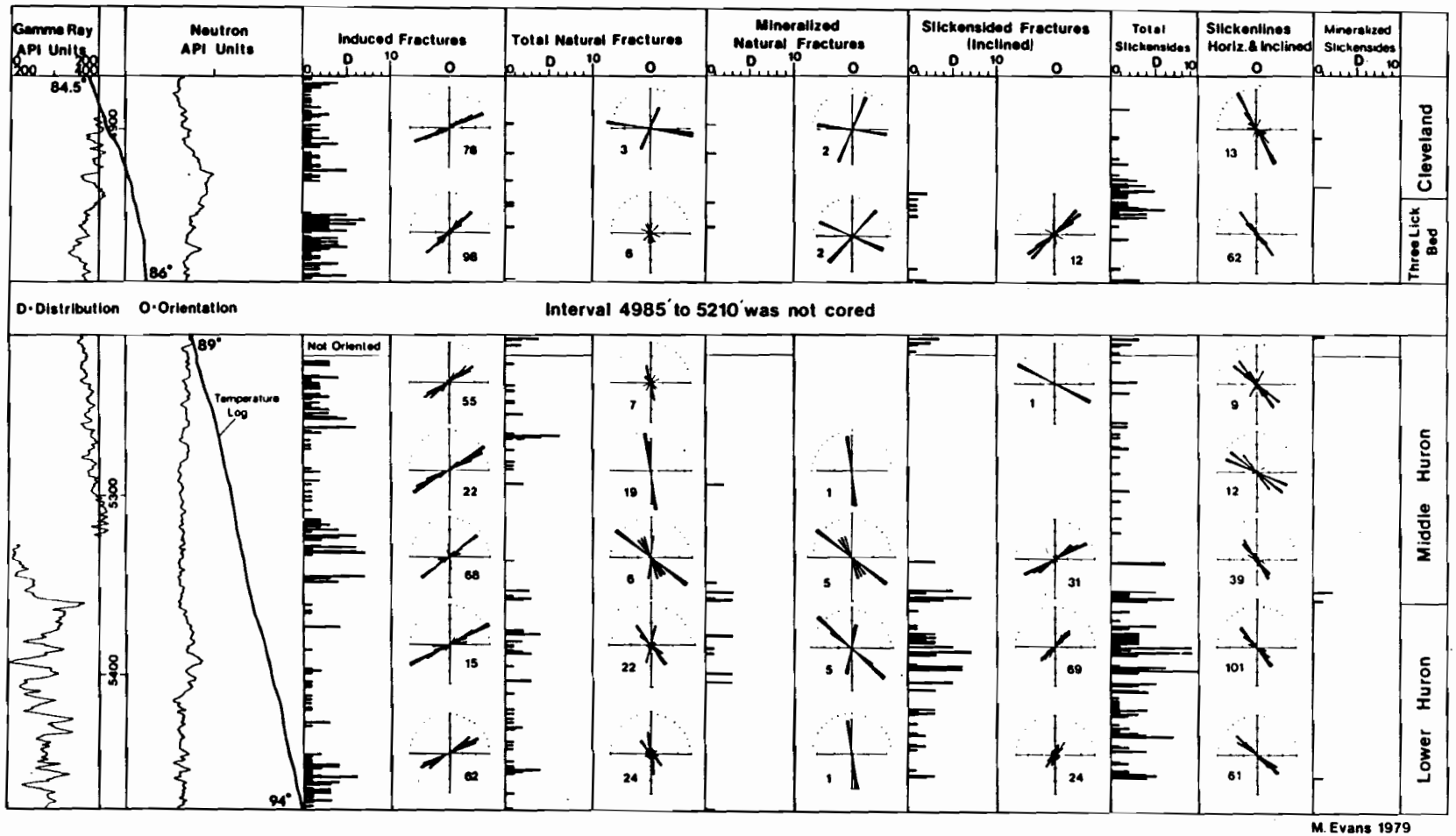

Figure I-12. Composite data sheet of fracture frequencies and orientations for all fracture types.

APPENDIX J: PA #2 (C.E.P.S. #1) CORE WELL

PA #2 (C.E.P.S. #1) CORE WELL

Location

The PA #2 (C.E.P.S. #1) core well is located in Allegheny County, Pennsylvania, one mile east of the town of Monongahela along the Monongahela River (figures 1 and J-1, table 1). The wellsite is on the southern border of a N70°W trending zone of structural discontinuity (Wagner and Lytle, 1976). It is also near what is believed to be a basement fault zone known as the Lat. 40°N Fault or the Transylvania Fault (Root and Hoskins, 1977) (figure J-1). The fault zone trends N70°W and is evidenced in the Plateau by aeromagnetic anamolies as well as the aforementioned zone of structural discontinuity where folds of the Appalachian trend are interrupted or terminated. The structural discontinuity also controls the distribution of oil and gas fields in the area (Wagner and Lytle, 1976). A total of 550 feet of the Devonian was cored, from 6950'-7500' (figure J-2).

Production Data

No production data was available for this core well.

Core-induced Fractures

The only core-induced fractures in the core are torsion and disc fractures. The lack of core-induced petal-centerline fractures may be related to the physical characteristics of the rock; which is generally a soft, fissile, black shale; or stress conditions in the rock.

Natural Fractures

Natural fractures are only found in three stratigraphic intervals

in this core: the Geneseo Shale, Tully Limestone, and Marcellus Shale (figure J-9). The West River Shale and the Mahantango Formation have no natural fractures. The natural fracture composite rose diagram has no statistically significant peaks (figure J-3). However, four dominant trends can be determined: N17°E, N37°E, N85°E, and N47°W. The equal area projection of poles to natural fracture surfaces (figure J-3) has six peripheral clusters which correspond to three of the four subvertical to vertical natural fracture sets. Natural fracture orientations are quite variable and show no pattern or systematic variation with depth or stratigraphy (figure J-4). Most of the natural fractures in the core are mineralized with fibrous or massive calcite. The mineral fibers are perpendicular to the fracture faces, implying that mineral growth has probably occured parallel to the principal acting tension as the fracture opened (Durney and Ramsay, 1973). The mineral fibers also suggest the existance of a high pore fluid pressure to open the fractures.

The proximity of the wellsite to the zone of structural discontinuity and proposed basement fault zone may account for the diversity of fracture trends in the core. Similar situations are reported by Kulander and Dean (1978) who found chaotic fracturing in coals above a basement fault zone in southwestern West Virginia, and Dixon (1979) who found that Devonian shales within a cross strike discontinuity were more intensely fractured than those outside of it. The N47°W fracture set is nearly orthogonal to the Appalachian trend in this area and probably formed as an extension fracture set under tectonic compressive stresses during Alleghenian deformation. The N17°E and

and N37°E fracture sets parallel portions of nearby folds and may have formed as release fractures when tectonic stresses were relaxed. The N85°E fracture set may be related to the general east to northeast trending maximum compressive stress present in most of eastern North America (Sbar and Sykes, 1973).

Slickensides and Slickenlines

Slickensides in the core are found primarily in the West River Shale, Tully Limestone, and Marcellus Shale (figure J-9). A very few slickensides are also found in the upper portion of the Geneseo Shale and Mahantango Formation. The West River slickenside zone occurs in a shale below the stiffer Sonyea Formation and above the Tully Limestone. The Marcellus Slickenside zone occurs in a soft shale unit above the much stiffer Onondaga Limestone. The West River and Marcellus zones are quite vertically extensive, suggesting that these two units acted as décollement zones. The slickenside composite rose diagram (figure J-5) has two peaks. There is a 1.0% chance that the peaks at N23°W and N47°E do not exist. Poles to slickensided surfaces form a girdle across the equal area projection (figure J-5). The pattern of clusters closely resembles the pattern of fracture dips which would be expected in a shear zone. The 0° dipping cluster in the center is the displacement shear cluster, the 30°NW dipping cluster is the Riedel shear cluster, and the 30°SE dipping cluster is the thrust shear cluster. R' shears are not present in this core. A 10°NE dipping cluster results from the low-dipping N23°W slickenside set. Slickenside orientations show a great amount of variation with depth. The West River Shale has a majority of northwest striking

slickensides whereas in the rest of the core they strike northeast (figure J-6).

The slickenline composite rose diagram (figure J-7) has a single peak at N40°-60°W with an average trend of N50°W. There is a 5.0% chance that this peak does not exist. The equal area projection of slickenlines (figure J-7) has two large peripheral clusters corresponding to the wide range in trends of low plunging slickenlines. There is very little variability in slickenline trend, except for those slickenlines in the upper portion of the Marcellus Shale which trend more to the north than those in the rest of the core (figure J-8).

The N40°-60°W slickenline trend parallels the N47°W natural fracture set and is nearly orthogonal to the N47°E slickenside set. These three sets are related in that they all probably formed under the same Alleghenian tectonic compressive stresses.

Several slickensides in the core are mineralized, particularly those in the West River Shale and in the lower portion of the Marcellus Shale. Mineralization generally consists of calcite fibers between slickensided surfaces, or massive or crystalline coatings on the slickensided surfaces. The fibrous crystal growth is indicative of high fluid pressure in the bedding planes of the shales, and a vertical principal acting tension during mineralization (Durney and Ramsay, 1973). Such abnormally pressured rocks are preferred sites for décollement because these rocks are probably less viscous than their normally pressured counterparts (Kehle, 1970).

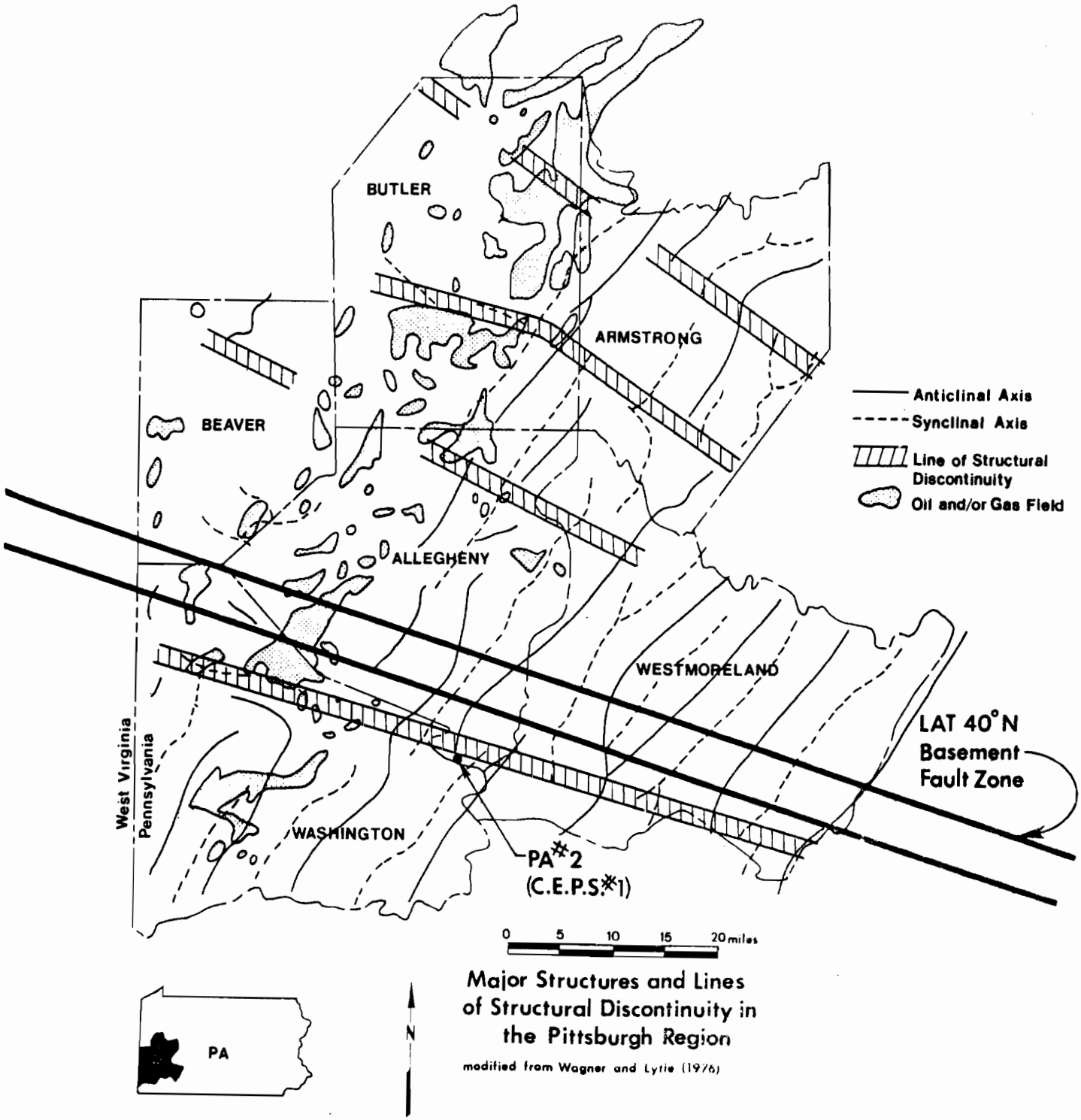

Figure J-1. Index map for the PA #2 (C.E.P.S. #1) core well with major structures and lines of structural discontinuity in the Pittsburgh, Pennsylvania, region. Also, the location of the proposed Lat 40°N Fault Zone.

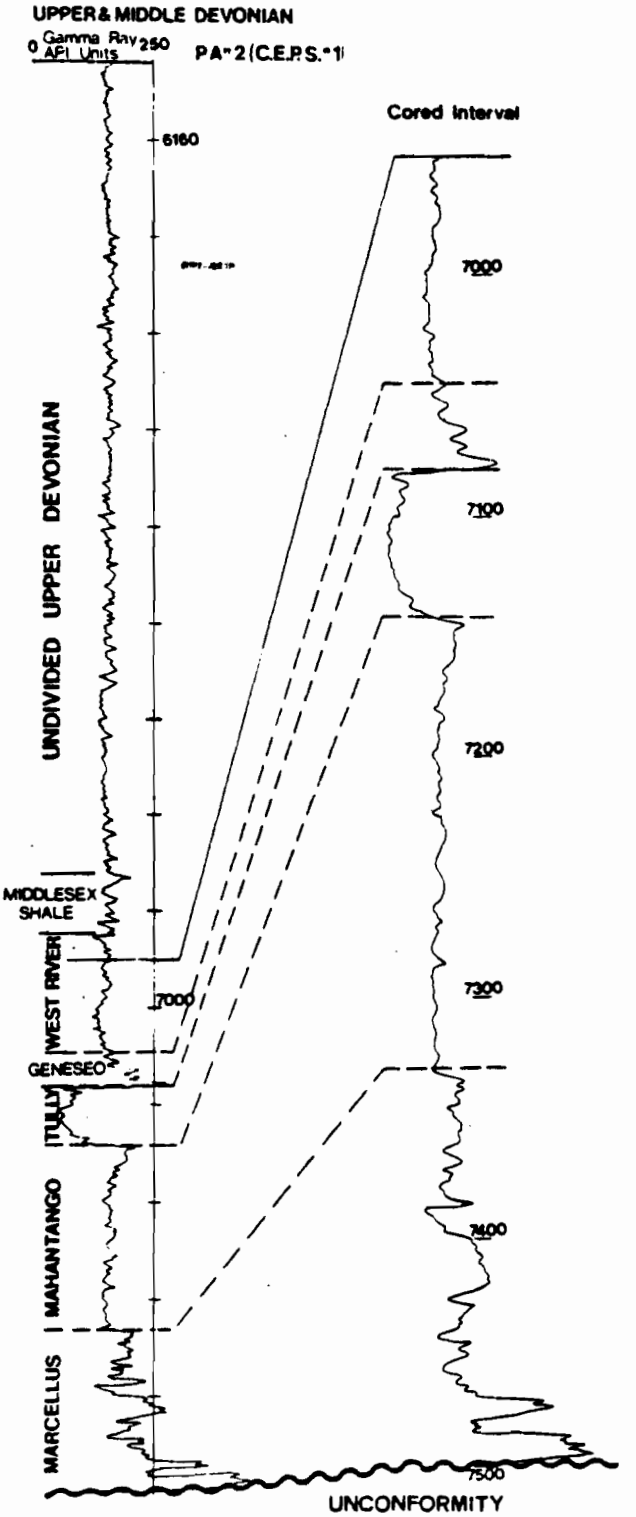

Figure J-2. Gamma-ray log, Middle and Upper Devonian

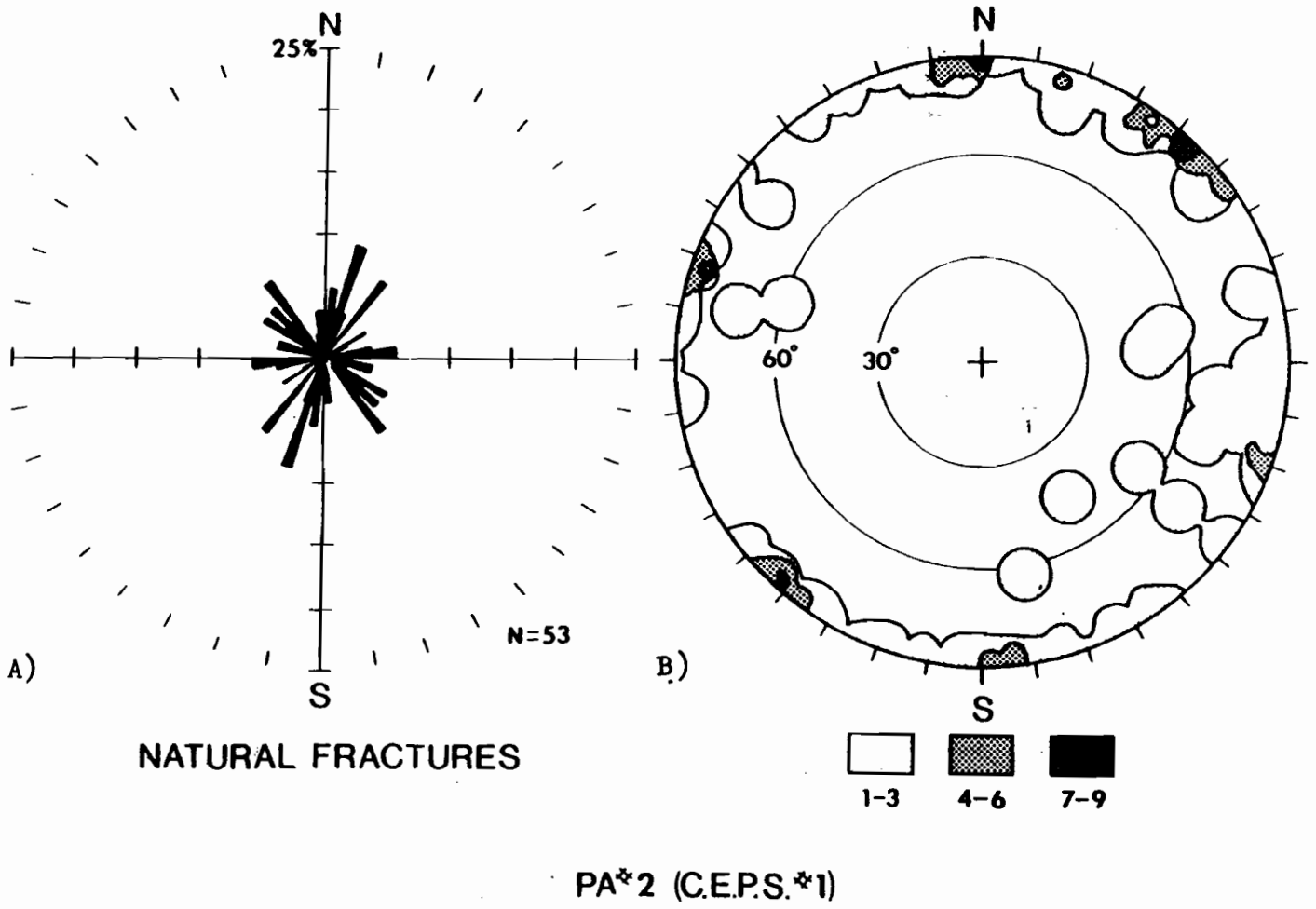

Figure J-3. (A) composite rose diagram of natural fracture strikes, and (B) equal area projection of poles to natural fracture surfaces

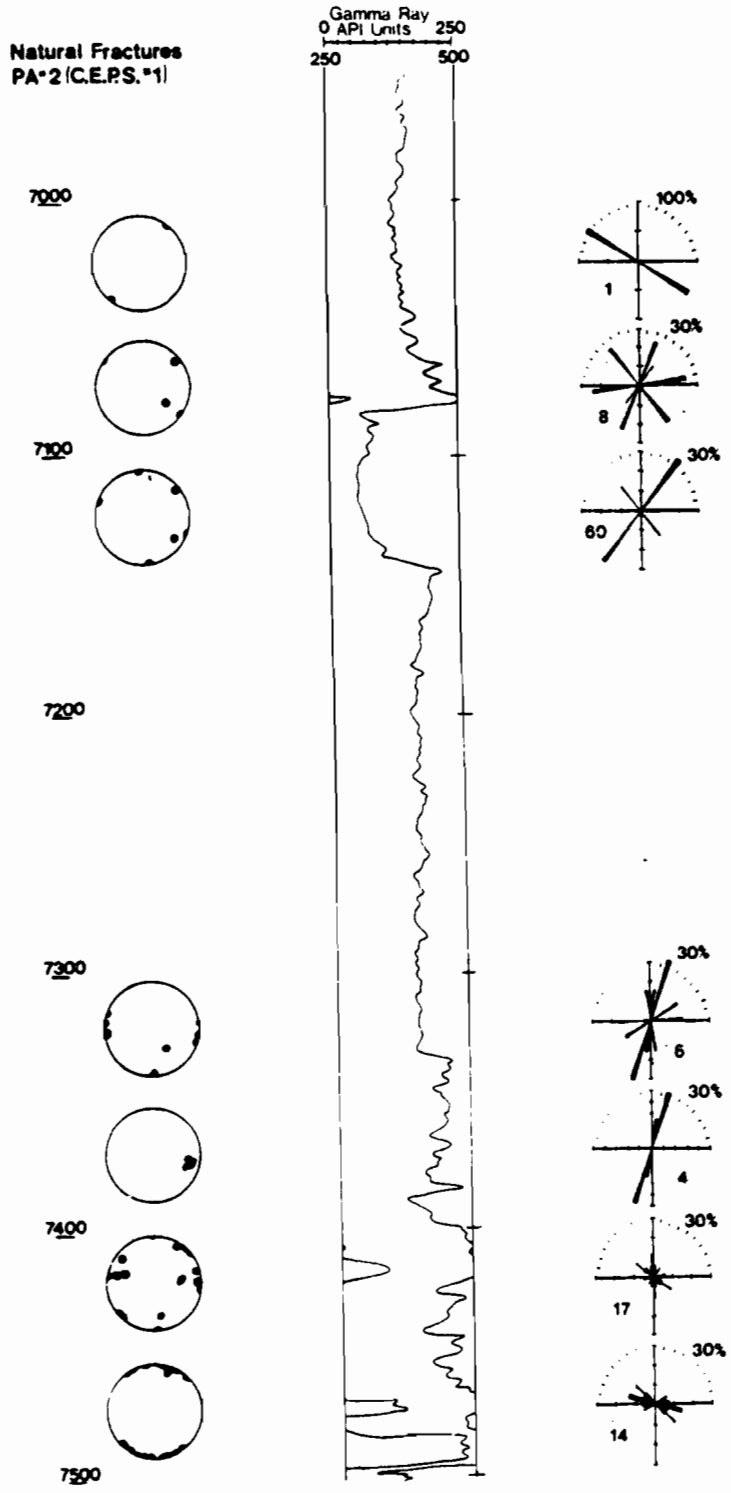

Figure J-4. Equal area projection of poles to natural fracture surfaces and rose diagrams of natural fracture strikes for approximately equal length intervals of the PA #2 (C.E.P.S. #1) core.

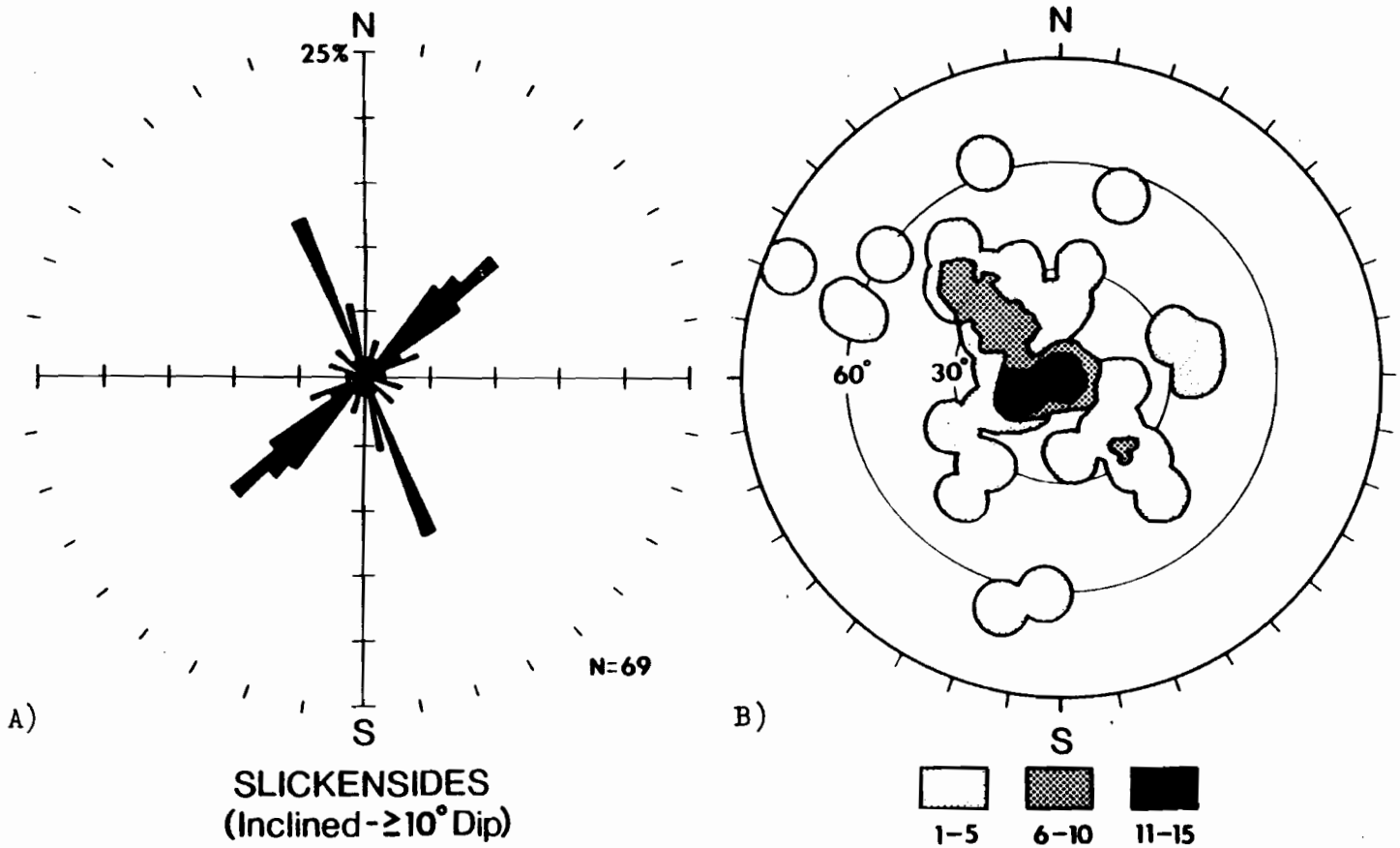

PA☆2 (C.E.P.S.☆1)

Figure J-5. (A) composite rose diagram of slickenside strikes, and (B) equal area projection of poles to slickensided surfaces

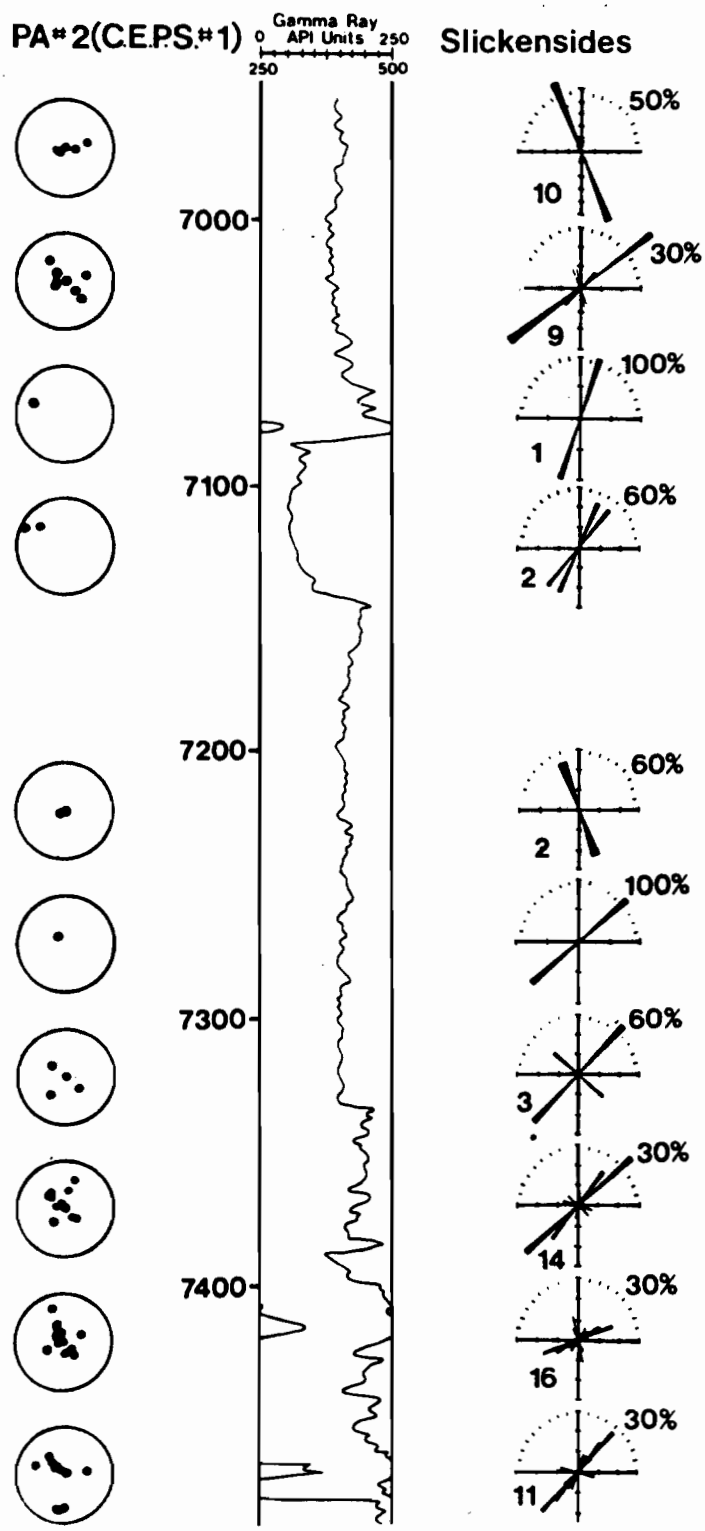

Figure J-6. Equal area projections of poles to slickensided surfaces and rose diagrams of slickenside strikes for approximately equal length intervals of the PA #2 (C.E.P.S. #1) core.

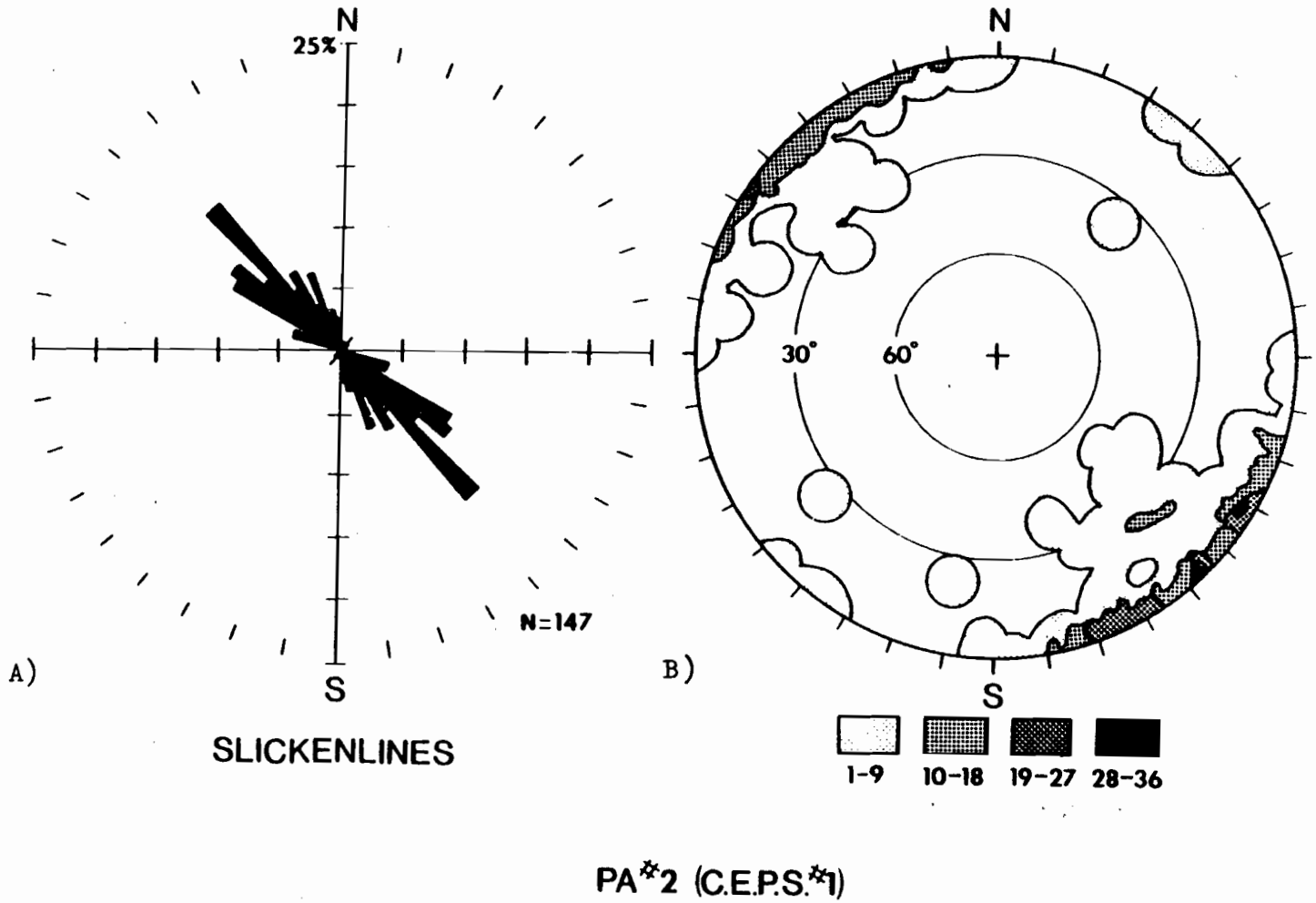

Figure J-7. (A) composite rose diagram of slickenline trends, and (B) equal area projection of slickenlines

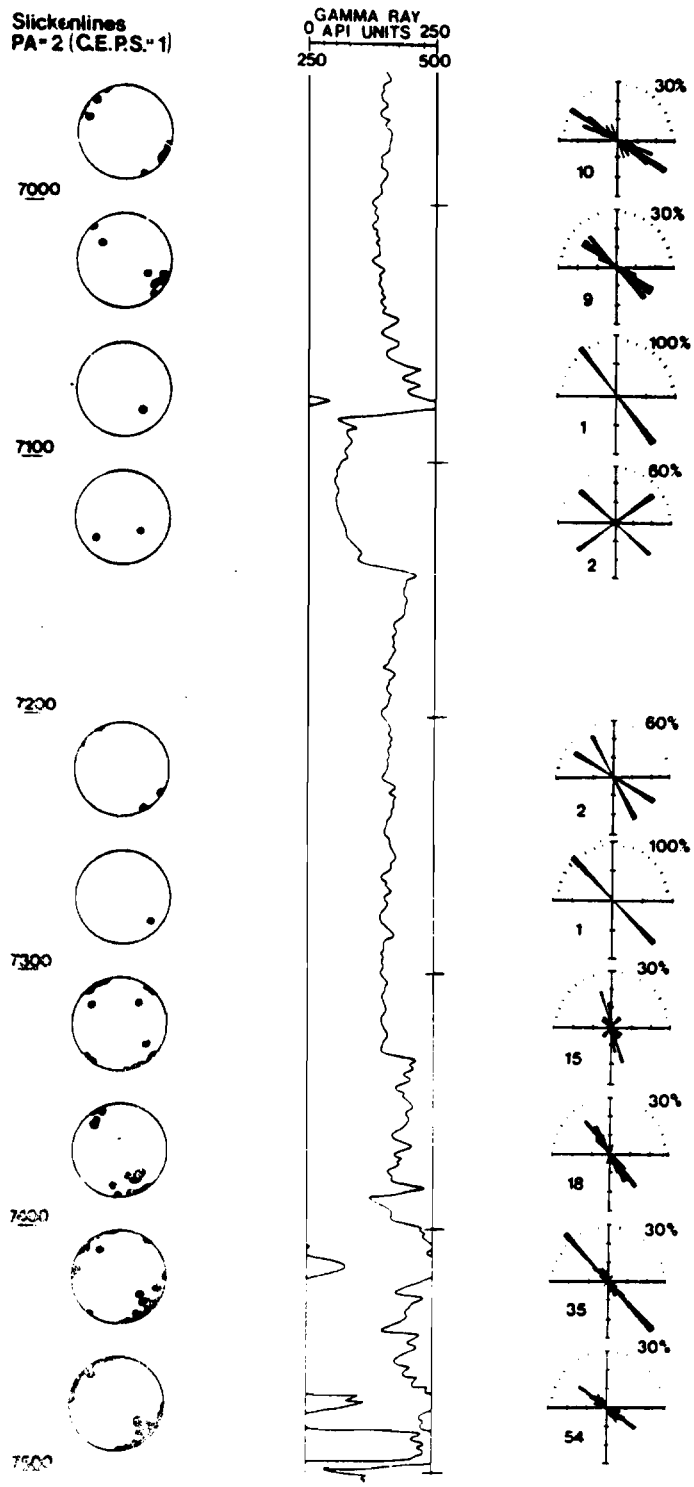

Figure J-8. Equal area projections of slickenlines and rose diagrams of slickenline trends for approximately equal length intervals of the PA #2 (C.E.P.S. #1) core.

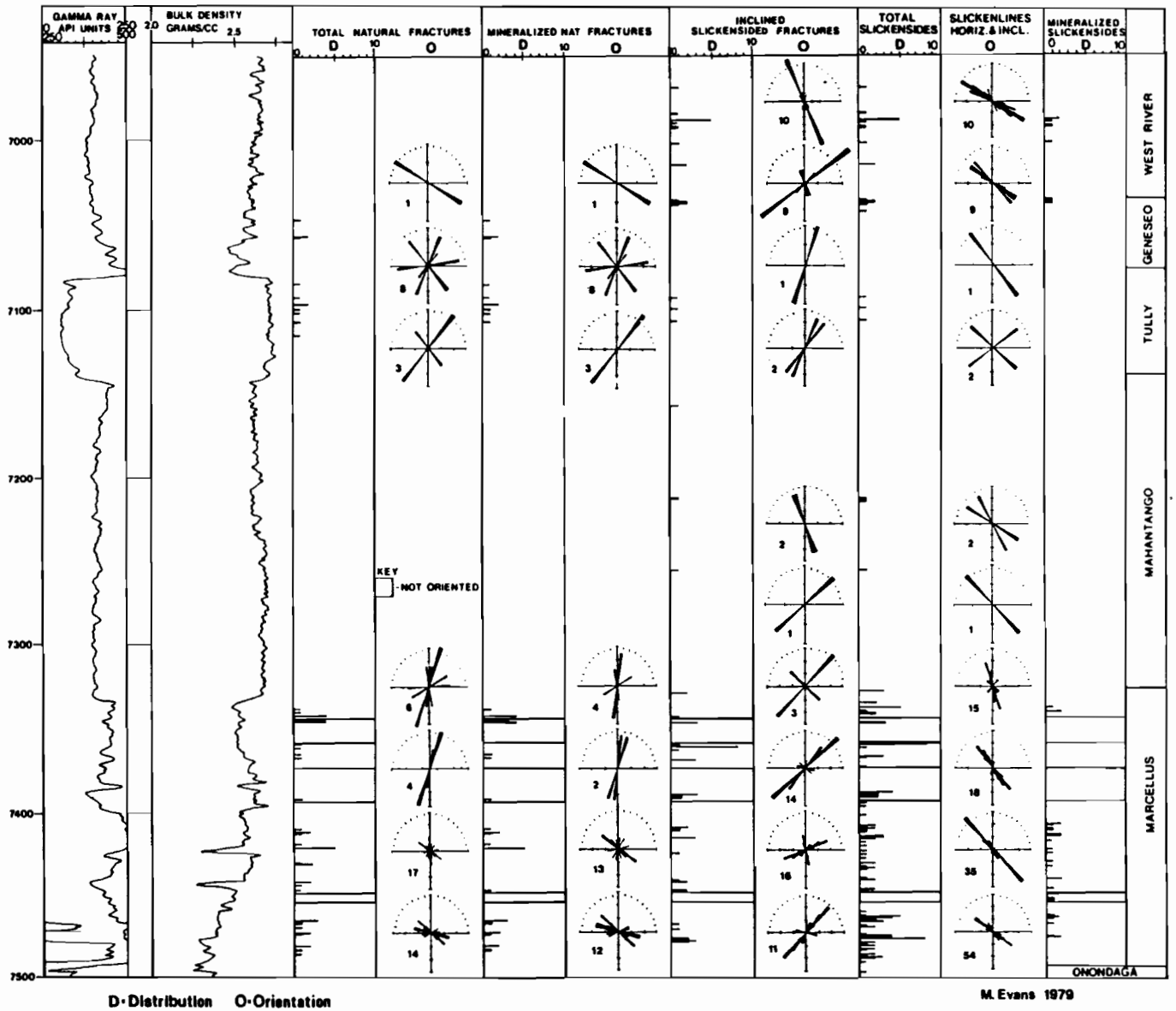

Figure J-9. Composite data sheet of fracture frequencies and orientations for all fracture types.

APPENDIX K: KY #1 (7239) CORE WELL

KY #1 (7239) CORE WELL

Location

The KY #1 (7239) core well is located in Perry County, Kentucky, twelve miles due north of the town of Hazard (figures 1 and K-1, table 1). The wellsite is between the Pine Mountain thrust, to the south, and the Irving-Paint Creek Fault, to the north. Regional structure of the Devonian shales shows a monoclinal dip of less than 1° to the southeast. A total of 339 feet of the Devonian was cored, from 2369'-2708'. In this study only two sections of the core were analyzed; a 52 foot section from 2374'-2426', and a 71 foot section from 2588'-2660' (figure K-2). This was done because the only reliable data available to the author for this core included only these sections. Within each of these two sections there is a small interval with no fracture data.

Production Data

Five intervals of the KY #1 (7239) well were stimulated by foam fracturing. After stimulation, interval 2326'-2675' had an initial open flow of 60 mcf/day, intervals 3174'-3180' and 3412'-3491' combined had an initial open flow of 450 mcf/day, and intervals 2560'-2580' and 2730'-2790' combined had an initial open flow of 103 mcf/day (Komar, Frone, and Yost, 1978).

Undifferentiated Fractures

The fractures in the two sections studied were previosly logged and analyzed by, and the results presented in, Kulander, Dean, and Barton (1977). No natural fractures were logged by Kulander, et.al.

(1977), but they stated that there is a "remote possibility" that some of the fractures they classified as core-induced fractures are actually pre-core (natural) fractures. The author is therefore placing all core-induced fractures as logged by Kulander, et. al. (1977) in the catagory of undifferentiated fractures. Kulander, et. al. (1977), however, did differentiate slickensided fractures, slickenlines, and horizontal mineral filled fractures.

Undifferentiated fractures were found to be distributed throughout the sections studied (figure K-10). The composite rose diagram of undifferentiated fracture strikes (figure K-3) has four peaks. There is a 5.0% chance that the peaks at N5°-15°W and N3°E do not exist, and a 10.0% chance that the peaks at N37°W and N33°E do not exist. The equal area projection of poles to undifferentiated fracture surfaces (figure K-3) has numerous clusters corresponding to the fractures which generally dip greater than 60°. Undifferentiated fracture orientations show significant changes with depth (figures K-4 and K-5, table K-1). Dominant orientations swing from N33°E in the Cleveland Member to N5°-15°W at the base of the Middle Huron Member and top of the Lower Huron Member, back to N33°E in interval 2614'-2638' and then to N37°W in interval 2639'-2669'. The various fracture sets, and their preference for certain intervals of the core, may be the result of the interaction of several stress fields; tensile stresses associated with faulting in the area, southern Appalachian tectonic compressive stresses, and the general east to northeast trending maximum compressive stress present in most of eastern North America (Sbar and Sykes, 1973).

Slickensides and Slickenlines

Slickensides are found in both sections of the core studied (figure K-10), and most are subhorizontal to horizontal. The only inclined slickensides occur in the Lower Huron Member (figure K-7). The slickenside composite rose diagram (figure K-6) has a single peak at N3°E. There is a 1.0% chance that this peak does not exist. The equal area projection of poles to slickensided surfaces (figure K-6) has two clusters; one, dipping 0°, corresponding to the numerous horizontal slickensides; and one, dipping 60°W corresponding to the inclined N3°W striking slickensides.

The slickenline composite rose diagram (figure K-8) has four significant peaks. There is a 1.0% chance that the peaks at N87°W, N27°E, and N83°E do not exist, and a 5.0% chance that the peak at N33°W does not exist. The equal area projection of slickenlines (figure K-8) has several peripheral clusters corresponding to the horizontal slickenlines, and a cluster dipping 60°W, corresponding to the slickenlines on the N3°E striking slickensides. The N33°W set occurs primarily in the Cleveland Member, and the N87°W and N83°E sets occur primarily in the Lower Huron Member (figure K-9).

Tectonic compressive stress directed from the southeast may be responsible for the N33°W trending slickenlines. The N27°E, N83°E, and N87°W sets may be related directly to local fault movement, or to compaction and settling of the rock after fault movement. The N83°E trending, and 60°W dipping slickenlines may indicate the presence of a north-south trending normal fault to the west. Some of the scatter in slickenline orientations may be due to local movements on the flanks

of low-amplitude, short-wavelength, discontinuous, shale folds (Kulander, et. al., 1977).

Numerous mineral filled fractures were found throughout the two sections studied; most of these are horizontal. Fibrous and non-fibrous calcite is the predominant mineral filling. The fibrous mineral growth is indicative of high fluid pressure in the bedding planes of the shales, and a vertical principal acting tension during mineralization (Durney and Ramsay, 1973). such abnormally pressured rocks are preferred sites for decollement because these rocks are probably less viscous than their normally pressured counterparts (Kehle, 1970). It is possible that the shales penetrated by this core acted as a poorly developed decollement zone.

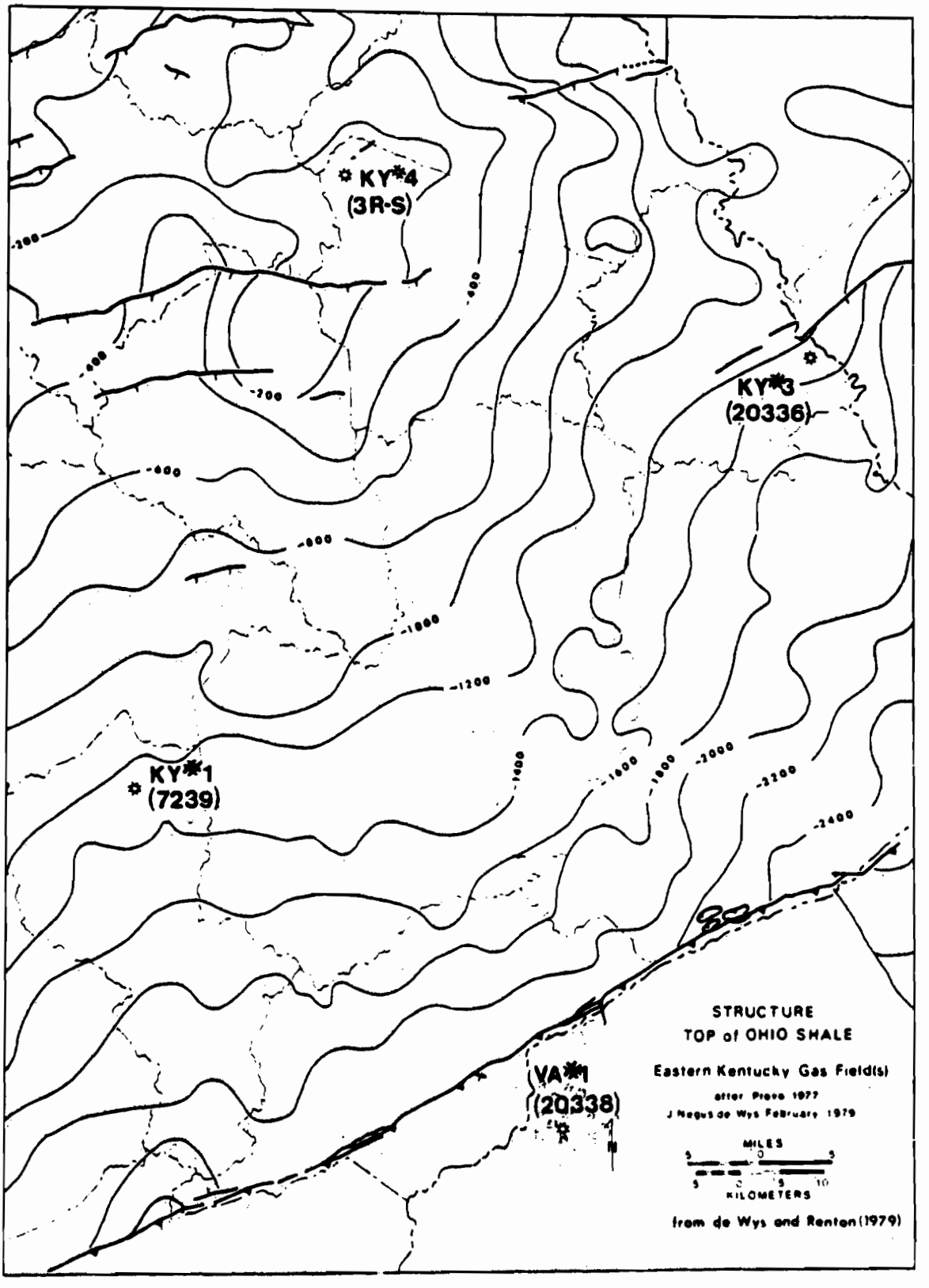

Figure K-1. Index map for the KY #1 (7239) core well

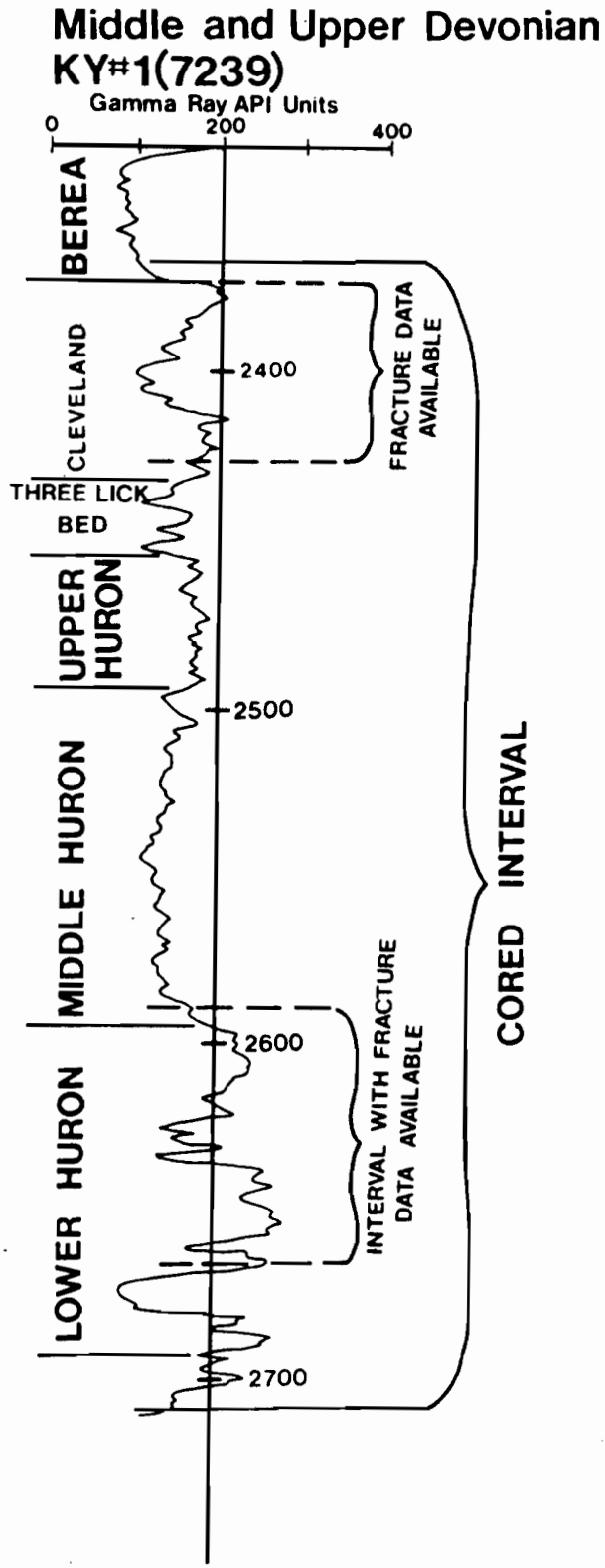

Figure K-2. Gamma-ray log, Upper and Middle Devonian.

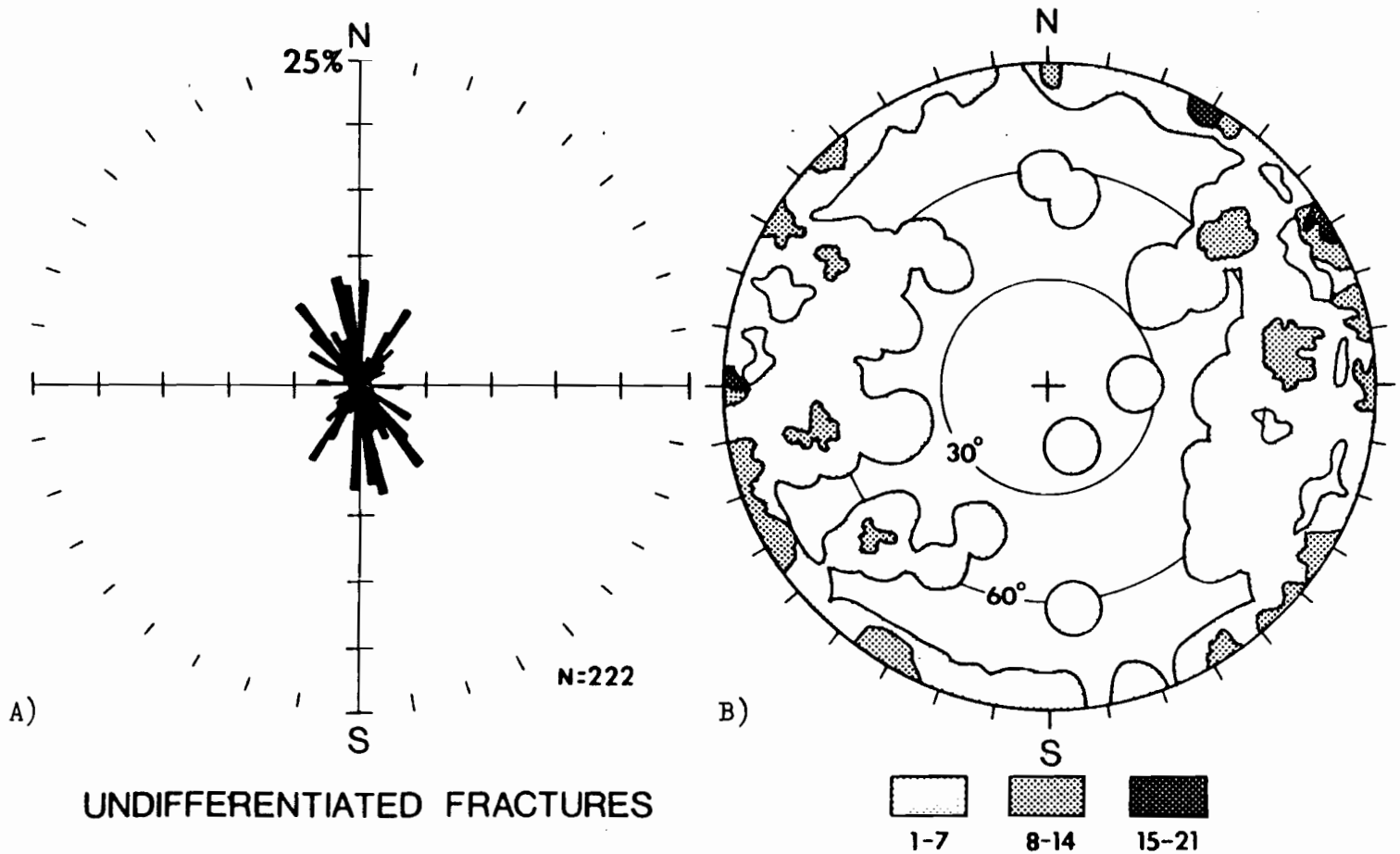

UNDIFFERENTIATED FRACTURES

KY*1 (7239)

Figure K-3. (A) composite rose diagram of undifferentiated fracture strikes, and (B) equal area projection of poles to undifferentiated fracture surfaces.

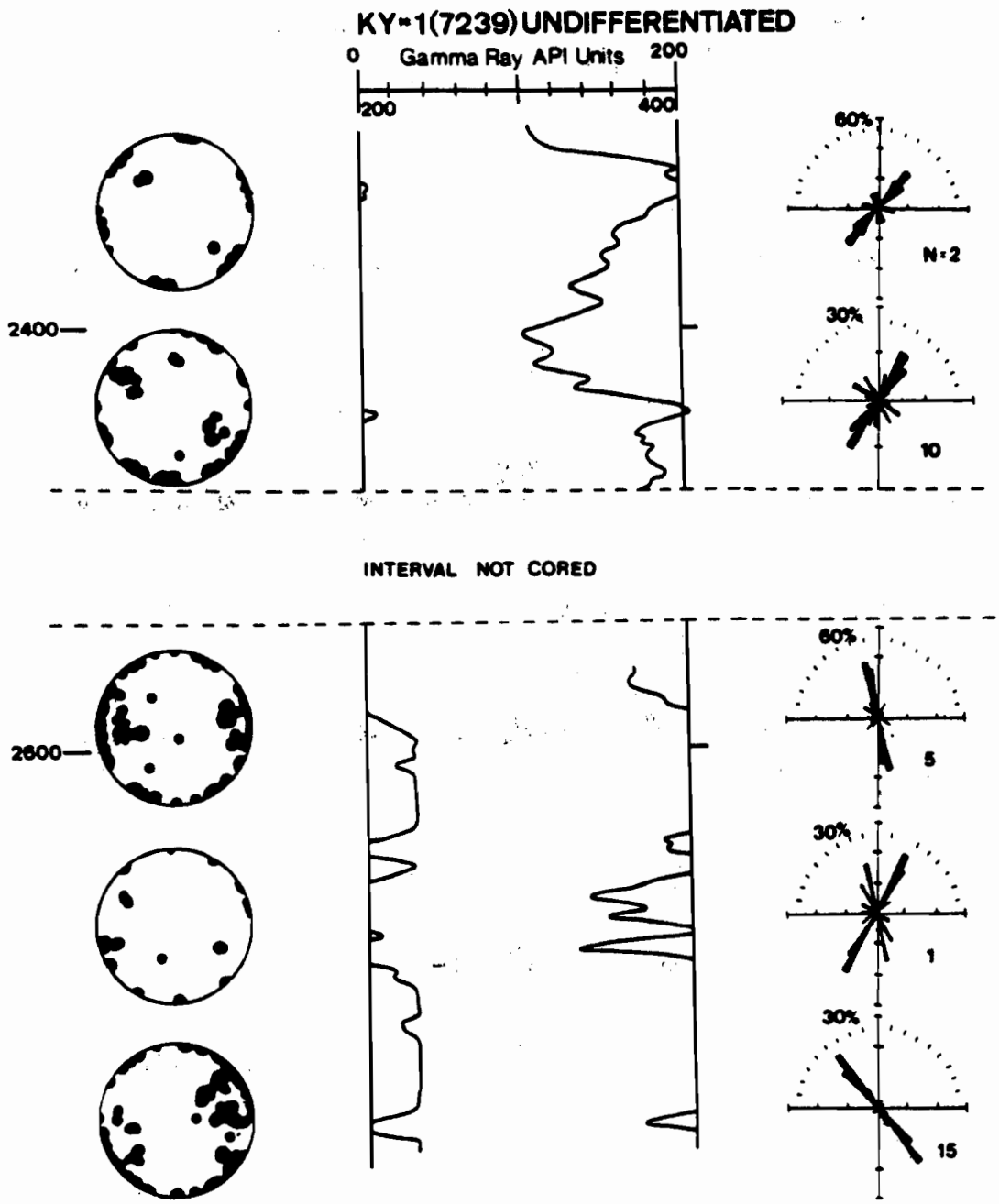

Figure K-4. Equal area projections of poles to undifferentiated fracture surfaces and rose diagrams of undifferentiated fracture strikes for approximately equal length intervals of the KY #1 (7239) core.

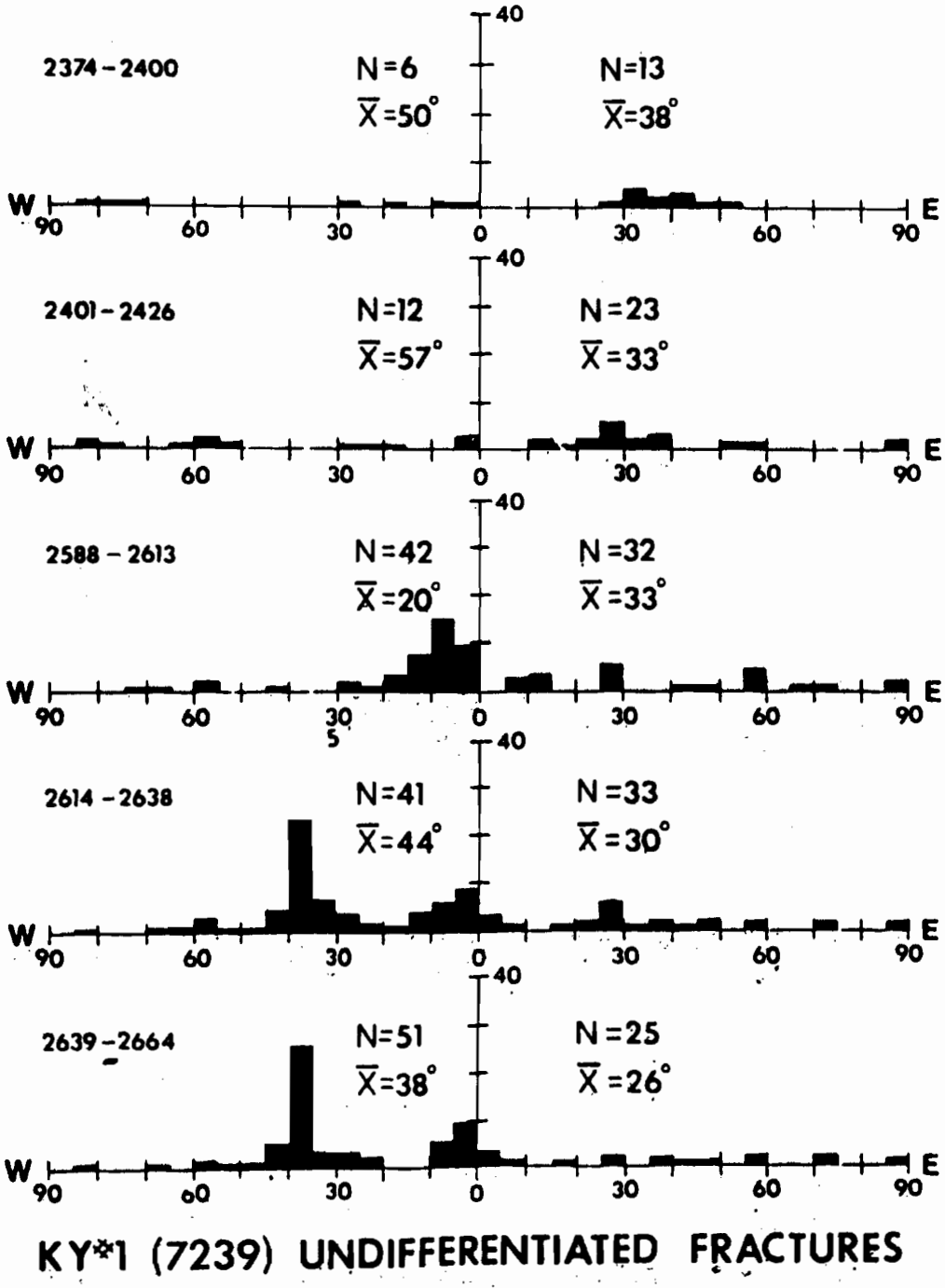

Figure K-5. Histograms of undifferentiated fracture strikes.

TABLE K-1

KY #1 (7239) UNDIFFERENTIATED FRACTURES

Interval	N	VN	α
2374-2400	19		
		1.8812	≤1.00
2401-2426	35		
		2.9215	≤0.01
2588-2613	74		
		3.3860	≤0.01
2614-2638	94		
		2.1111	≤1.00
2639-2664	76		

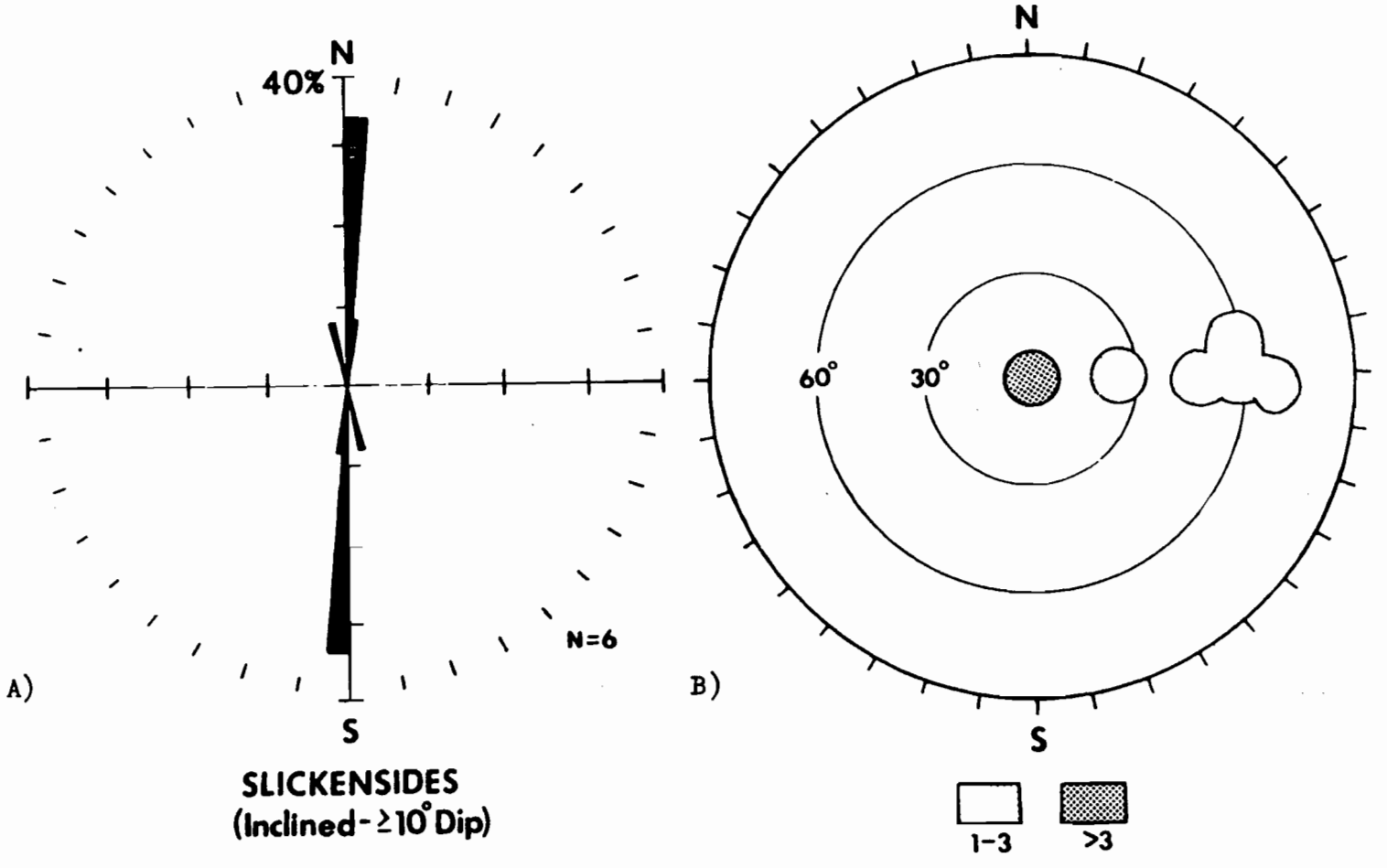

KY*1 (7239)

Figure K-6. (A) composite rose diagram of slickenside strikes, and (B) equal area projection of poles to slickensided surfaces.

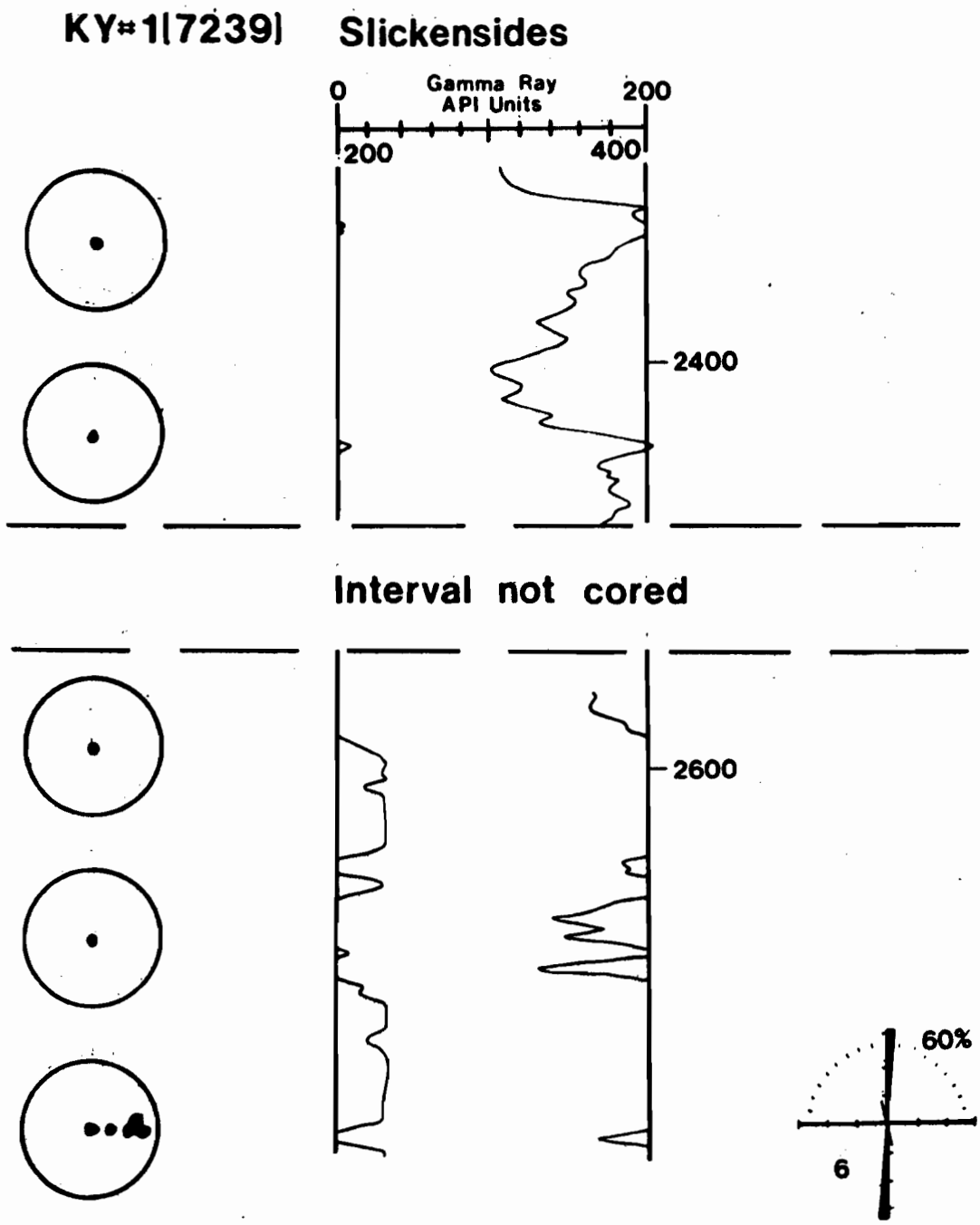

Figure K-7. Equal area projections of poles to slickensided surfaces and rose diagrams of slickenside strikes for approximately equal length intervals of the KY #1 (7239) core.

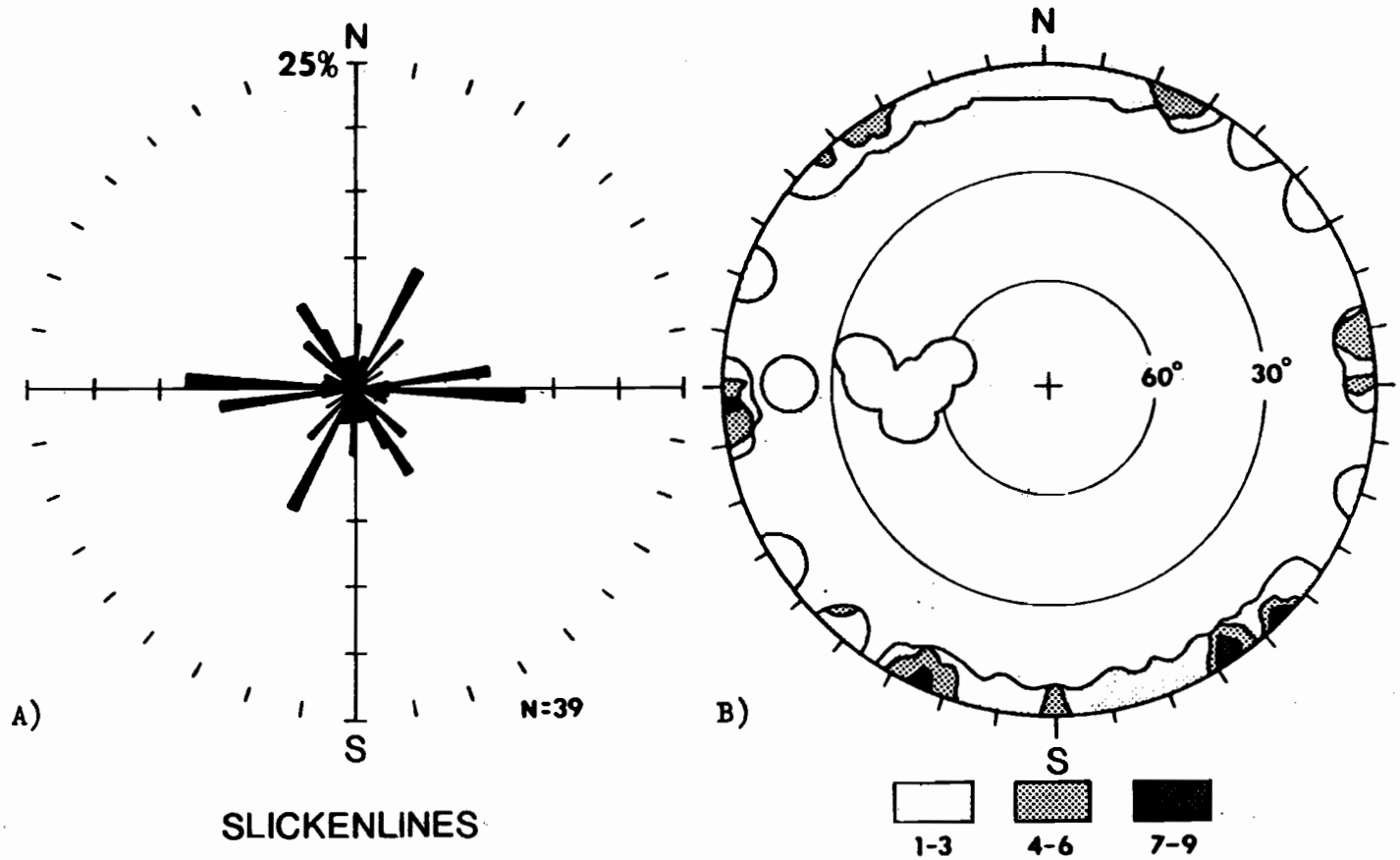

KY*1 (7239)

Figure K-8. (A) composite rose diagram of slickenline trends, and (B) equal area projection of slickenlines.

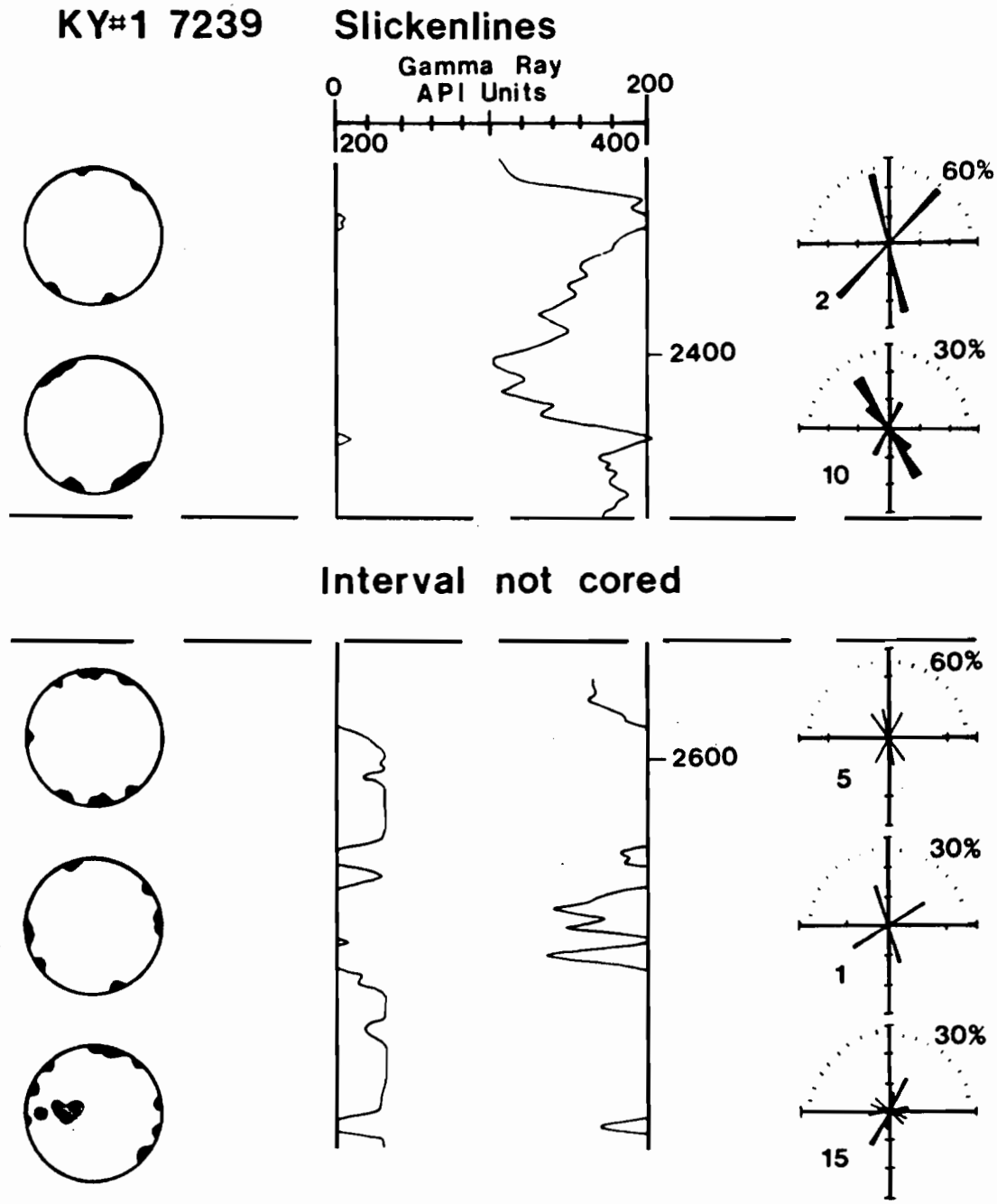

Figure K-9. Equal area projections of slickenlines and rose diagrams of slickenline trends for approximately equal length intervals of the KY #1 (7239) core.

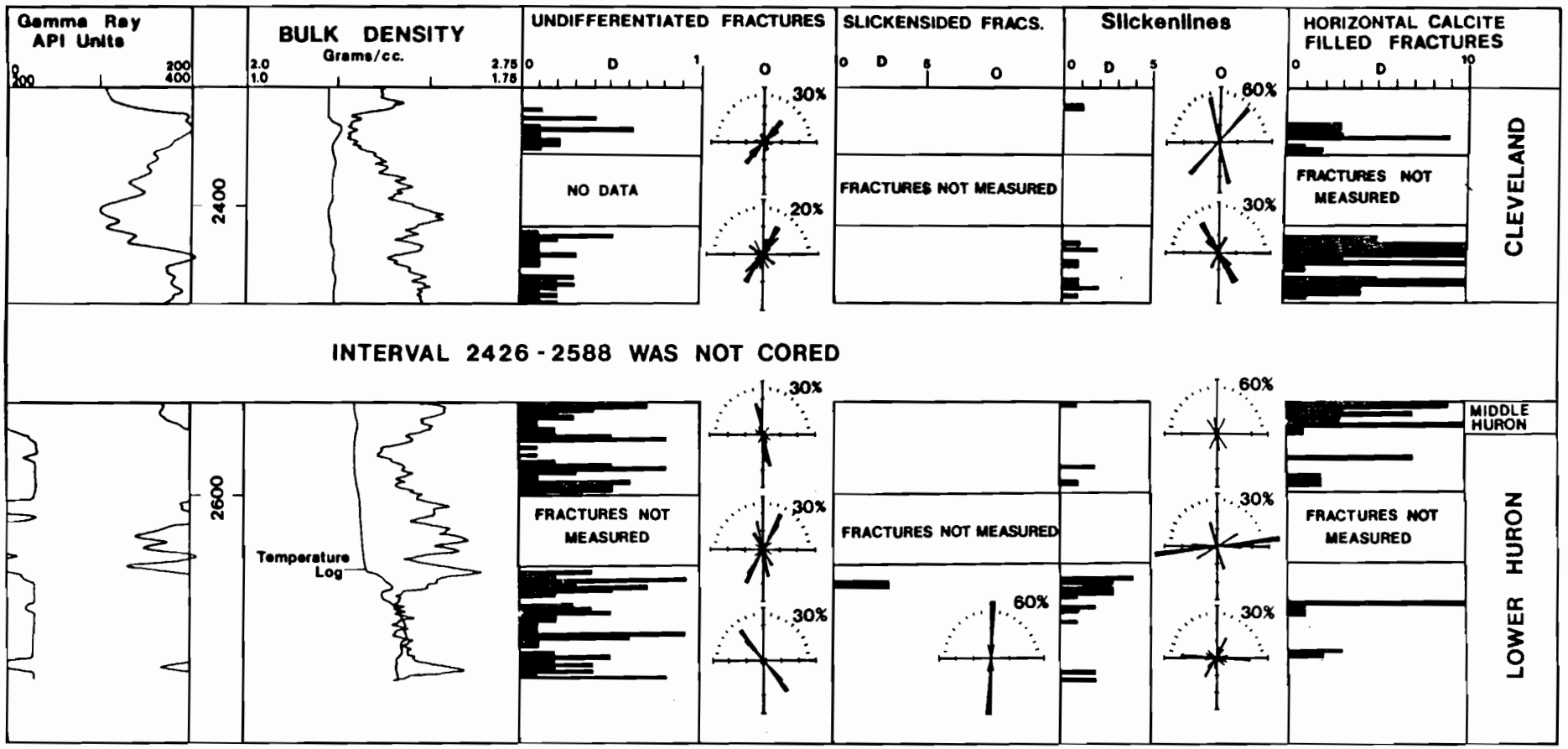

Figure K-10. Composite data sheet of fracture frequencies and orientations for all fracture types.

APPENDIX L: KY #3 (20336) CORE WELL

KY #3 (20336) CORE WELL

Location

The KY #3 (20336) core well is located in Martin County, Kentucky, approximately three miles south of the town of Warfield, near the Warfield Fault (figures 1 and L-1, table 1). A total of 982 feet of the Devonian was cored, from 2429'-3411' (figure L-2). Intervals 2429'-2486' and 3404'-3411' were not oriented, and are therefore not used in this study.

Production Data

Two intervals of the well were stimulated; 2666'-2712', in the Upper Huron Member, which produced an initial open flow of 250 mcf/day after stimulation; and 2968'-3122', in the Lower Huron Member, which had an initial open flow of 370 mcf/day after stimulation (Yost, 1979, written communication).

Core-induced Fractures

Core-induced fractures are the most common fracture type in the core and are well distributed throughout (figure L-12). The core-induced fracture composite rose diagram (figure L-3) has three peaks. There is a 1.0% chance that the peaks at N40°-55°E, N63°E, and N33°E do not exist. The equal area projection of poles to core-induced fracture surfaces (figure L-3) has four large clusters corresponding to the vertical and inclined, opposite dipping fractures in the three merged sets. Scattered poles are also found in the northwest and southeast quadrants. Most of the scatter occurs in interval 2487'-2550'. In general, core-induced fracture orientations show a gradual

swing to the north down the core (figures L-4 and L-5, table L-1).

The N33°E and N63°E fracture sets parallel the core-induced fractures in the WV #4 (20402) and WV #3 (20403) cores, respectively, which are located to the northeast. The largest peak, N40°-55°E, bisects the two smaller peaks, and probably represents a merging of the two trends. The consistent core-induced fracture orientations suggest the presence of a stress or rock fabric anisotropy. This anisotropy may be related to the general east to northeast trending maximum compressive stress present in most of eastern North America (Sbar and Sykes, 1973).

Natural Fractures

Natural fractures are found throughout the core (figure L-12). The natural fracture composite rose diagram (figure L-6) shows the great variability in natural fracture orientations. There are no statistically significant peaks. However, three dominant trends are present: N67°W, N47°W, and N37°E. The equal area projection of poles to natural fracture surfaces (figure L-6) has two clusters corresponding to the vertical fractures of the N67°W and N47°W sets, and two clusters corresponding to the subvertical to vertical fractures of the N37°E set. Natural fractures generally strike northeast in and above the Middle Huron Member, and northwest below (figure L-7).

The N37°E natural fracture set parallels the N33°E core-induced fracture set, and may be related to the same stress or rock fabric anisotropy responsible for the core-induced fractures. The two northwest striking natural fracture sets show no relationship to any known nearby structures. However, the great variation in fracture orientation may be the result of the interaction of stress fields associated

with nearby faulting.

Slickensides and Slickenlines

Slickensides are found in and below the Middle Huron Member, with a majority occurring in the West Falls Formation (figure L-12). The slickenside composite rose diagram (figure L-8) has three peaks. There is a 5.0% chance that the peaks at N17°W, N47°E, and N83°E do not exist. The equal area projection of poles to slickensided surfaces (figure L-8) has several clusters; one, dipping 25°SW, corresponds to the N17°W set; two clusters, dipping 40°SE and 60°SE, correspond to the N83°E set; and one, dipping 30°SE, corresponds to the N47°E set. The N83°E set occurs only in the Lower Huron Member and below, whereas the other two sets are scattered throughout the core (figure L-9). Very few slickensides in the WV #3 (20336) core are mineralized.

The slickenline composite rose diagram (figure L-10) has two statistically significant peaks. There is a 1.0% chance that the peak at N5°W does not exist, and a 10.0% chance that the peak at N73°E does not exist. A smaller peak which is not statistically significant occurs at N43°W. The equal area projection of slickenlines (figure L-10) has three clusters: N73°E/65°SW, N5°W/40°SE, and N43°W/0°SE. The N43°W trend is generally found in the Middle Huron Member, and the N5°W and N73°E sets are found in the Lower Huron Member and below (figure L-11).

All three slickenside sets parallel mapped or proposed normal faults in the area, suggesting that they developed through actual fault movement, or compaction and settling of the rock after fault movement.

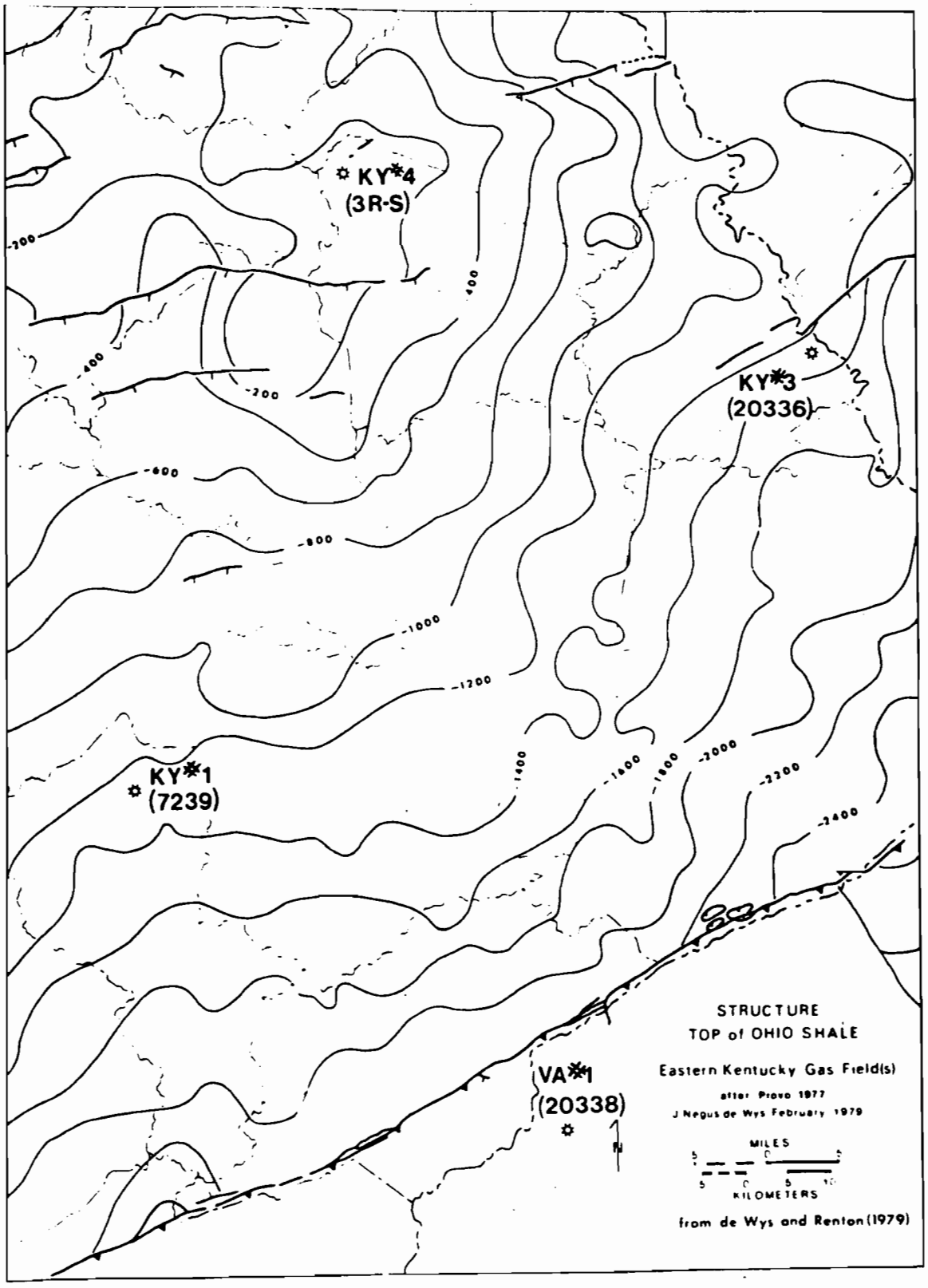

Figure L-1. Index map for the KY #3 (20336) core well

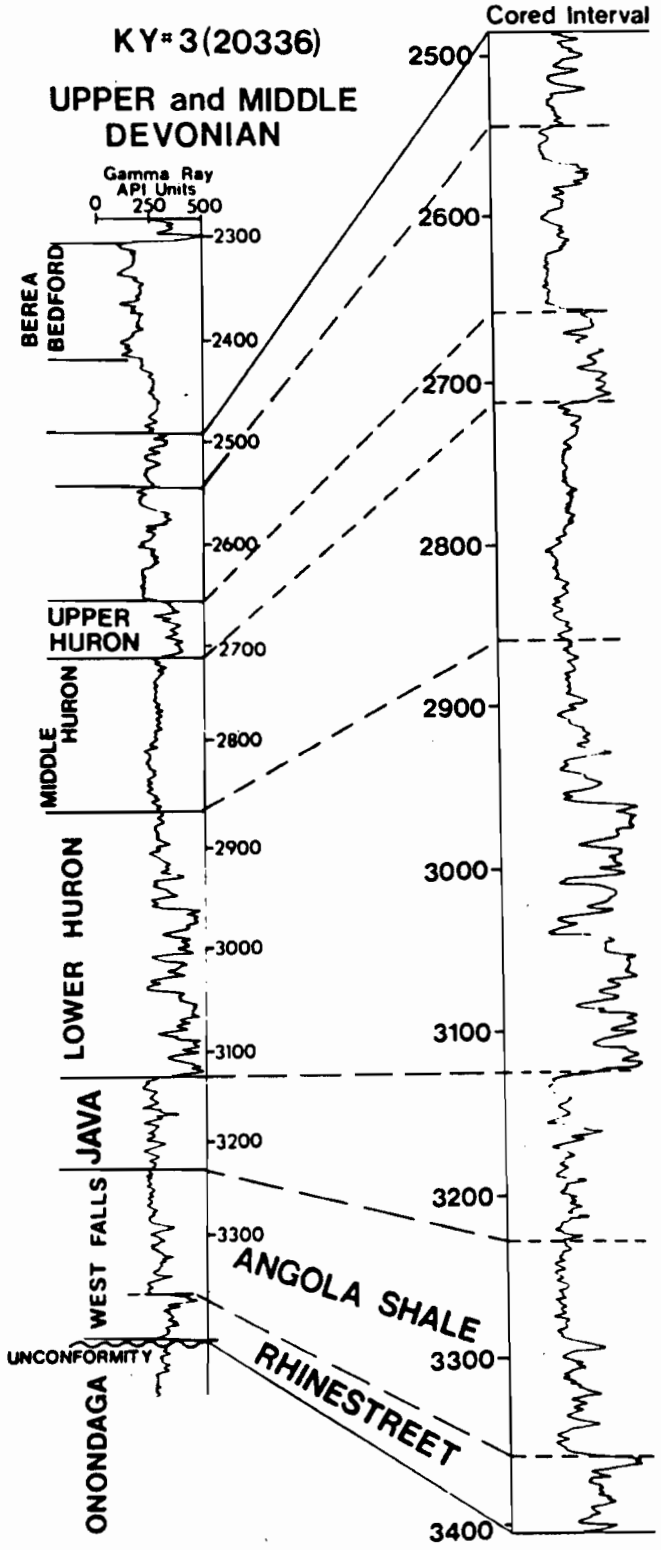

Figure L-2. Gamma-ray log, Upper and Middle Devonian.

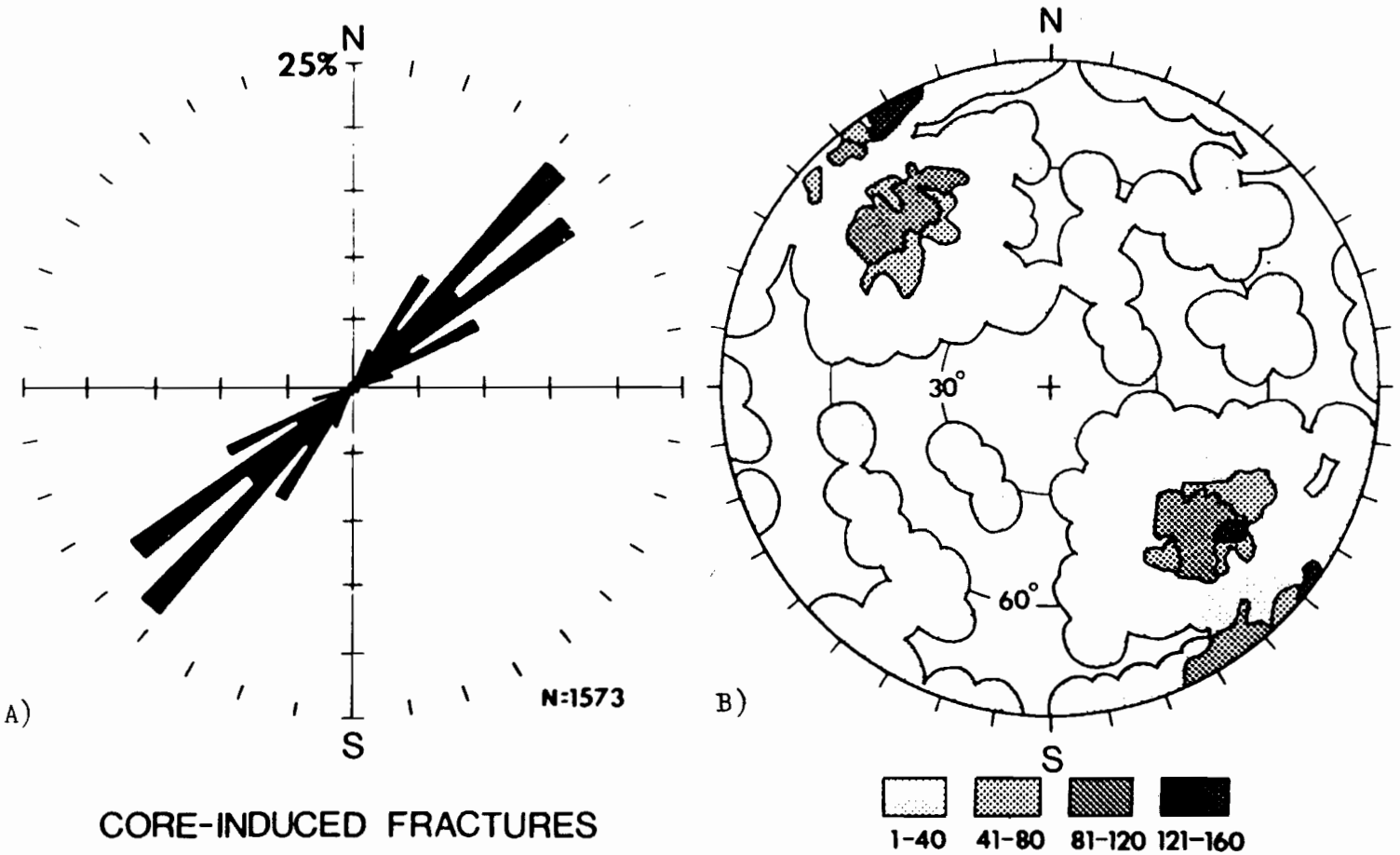

KY*3 (20336)

Figure L-3. (A) composite rose diagram of core-induced fracture strikes, and (B) equal area projection of poles to core-induced fracture surfaces.

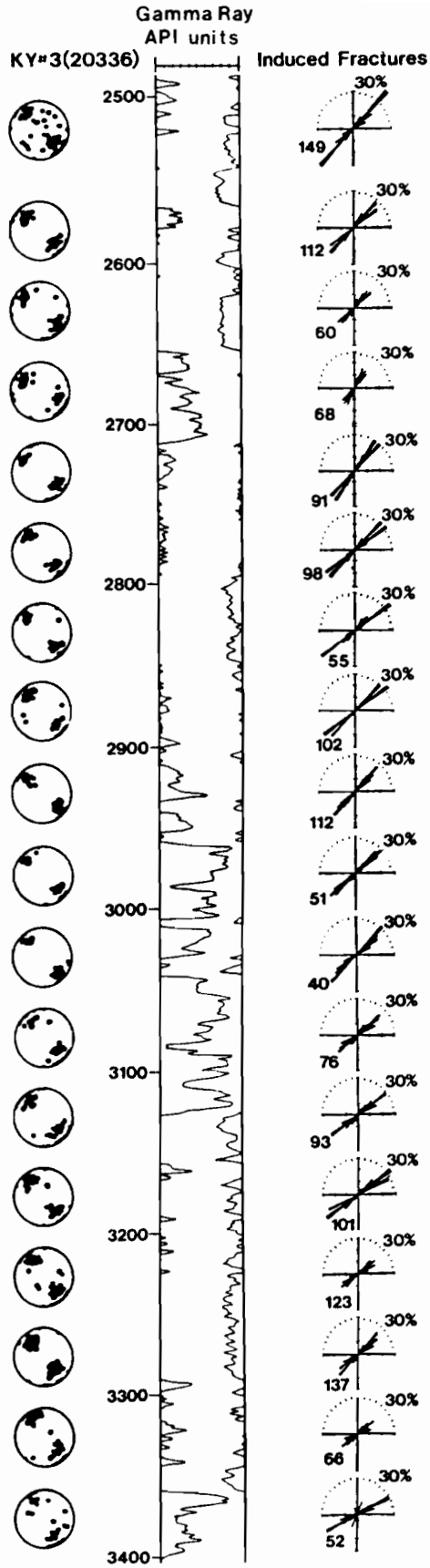

Figure L-4. Equal area projections of poles to core-induced fracture surfaces and rose diagrams of core-induced fracture strikes for approximately equal length intervals of the KY #3 (20336) core.

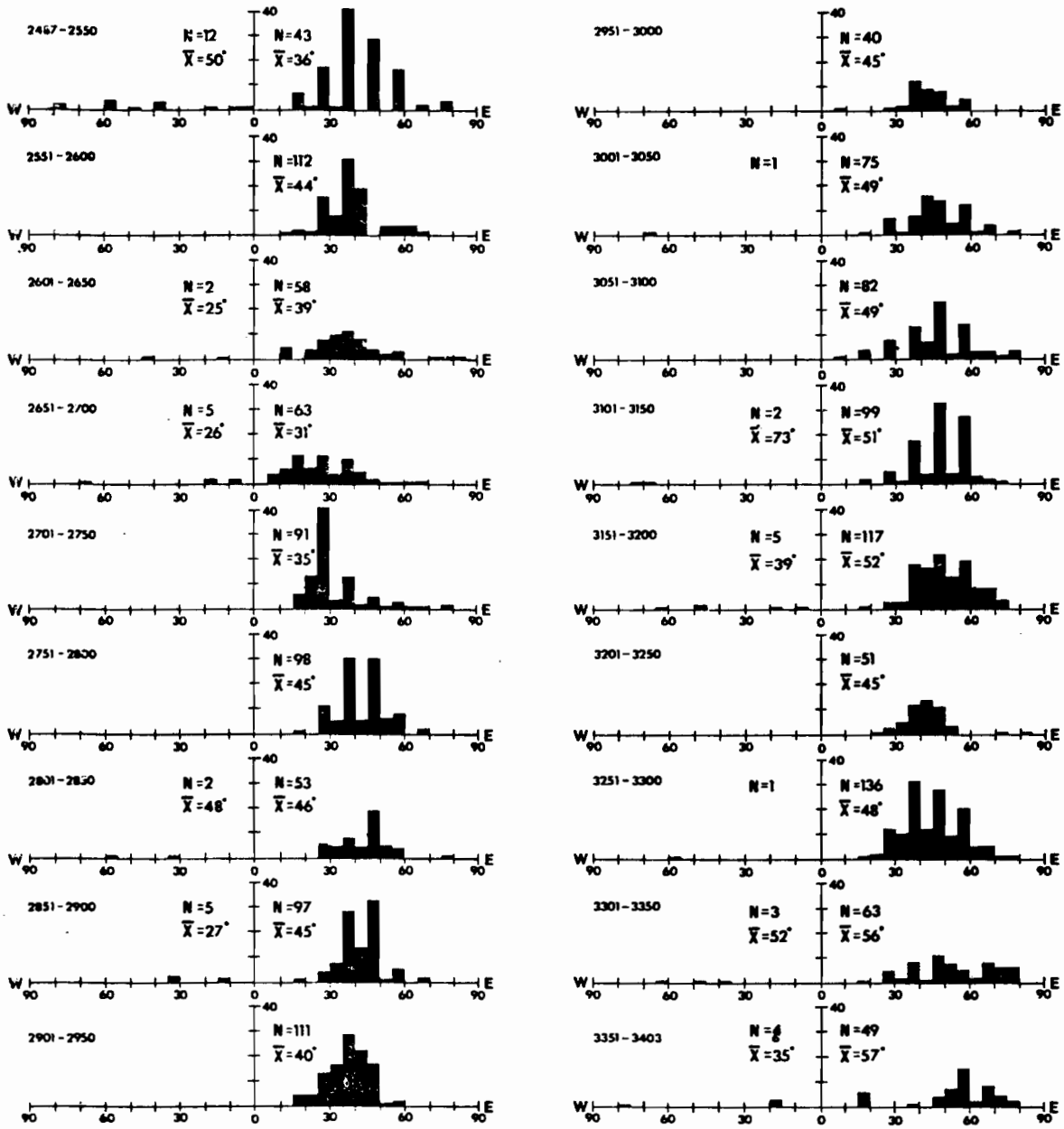

KY#3 (20336) CORE-INDUCED FRACTURES

Figure L-5. Histograms of core-induced fracture orientations.

TABLE L-1

KY #3 (20336) INDUCED FRACTURES

Interval	N	VN	α
2487-2550	148		
		2.5078	≤ 0.05
2551-2600	112		
		2.8125	≤ 0.01
2601-2650	60		
		2.4605	≤ 0.10
2651-2700	68		
		2.7931	≤ 0.05
2701-2750	91		
		3.9011	≤ 0.01
2751-2800	98		
		1.6649	≤ 1.00
2801-2850	55		
		1.8706	≤ 1.00
2851-2900	102		
		2.7600	≤ 0.05
2901-2950	112		
		1.5528	≤ 1.00
2951-3000	51		
		0.7906	≤ 1.00
3001-3050	40		
		2.1553	≤ 1.00
3051-3100	76		
		1.3983	≤ 1.00
3101-3150	84		
		2.2127	≤ 1.00
3151-3200	100		
		2.2098	≤ 1.00
3201-3250	122		
		2.3420	≤ 0.10
3251-3300	137		
		2.6681	≤ 0.05
3301-3350	65		
		2.1911	≤ 1.00
3351-3403	52		

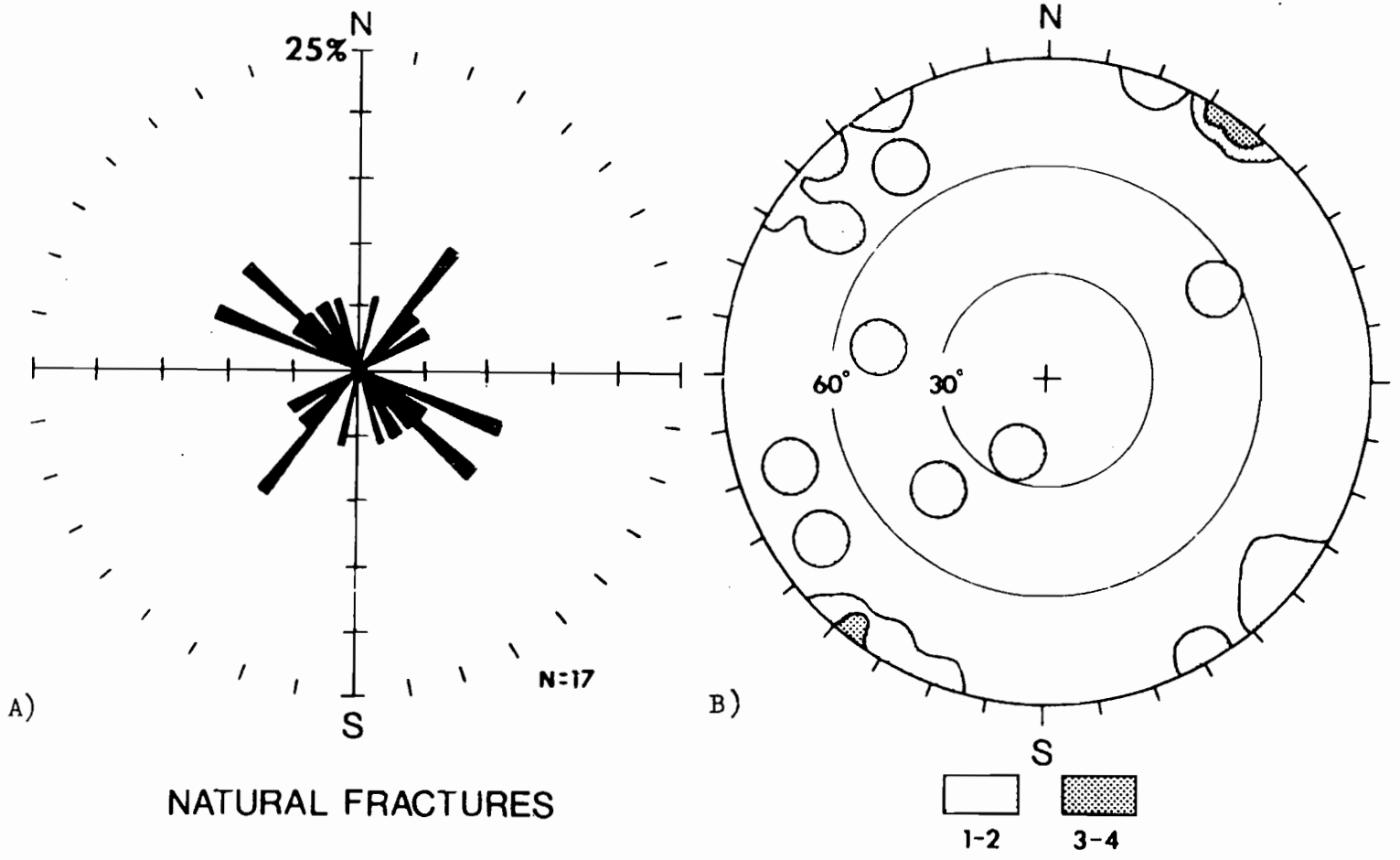

KY*3 (20336)

Figure L-6. (A) composite rose diagram of natural fracture strikes, and (B) equal area projection of poles to natural fracture surfaces.

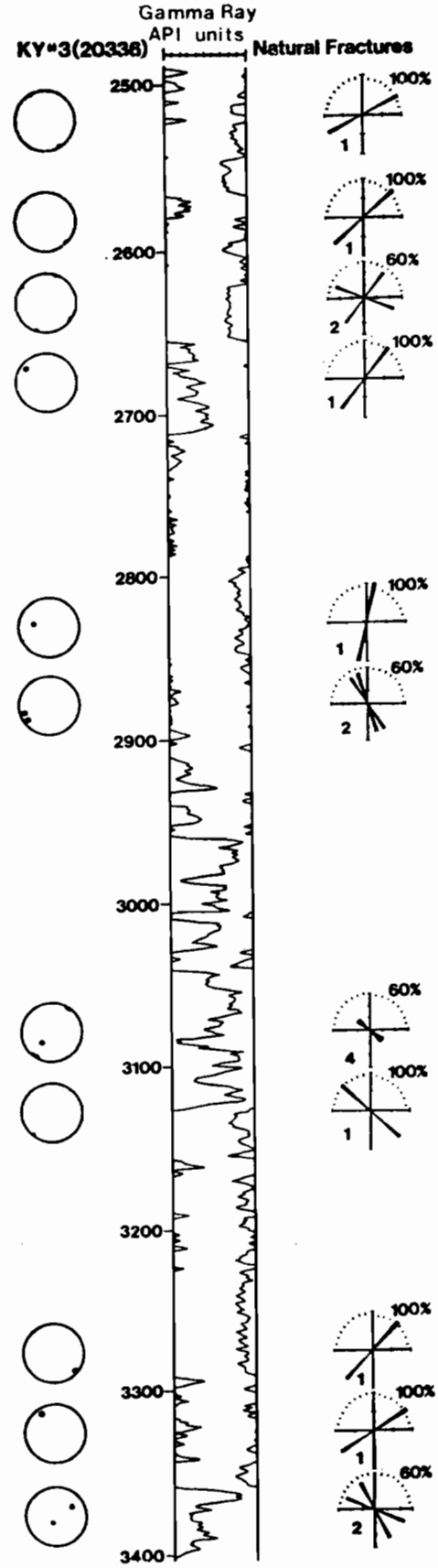

Figure L-7. Equal area projections of poles to natural fracture surfaces and rose diagrams of natural fracture strikes for approximately equal length intervals of the KY #3 (20336) core.

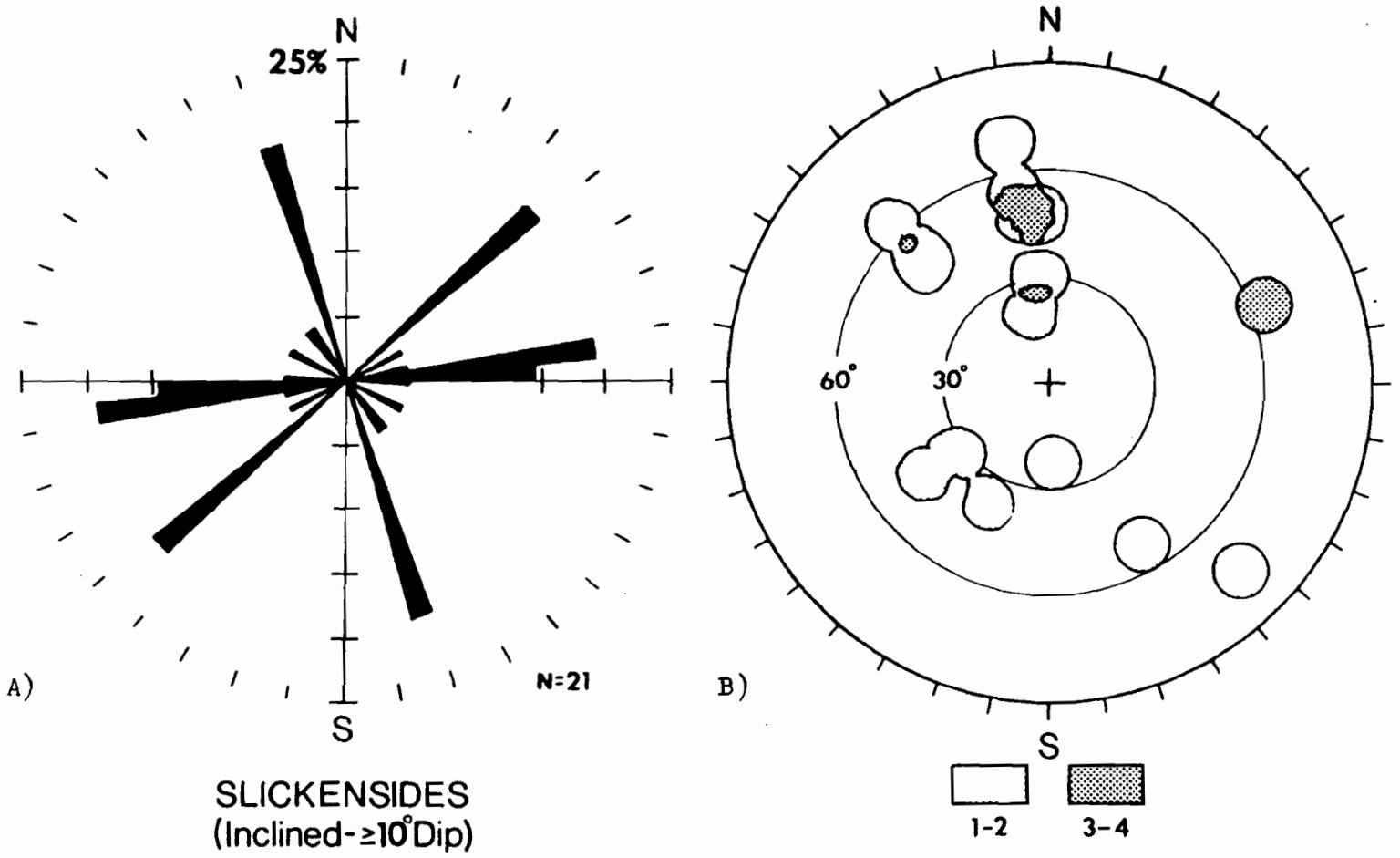

KY*3 (20336)

Figure L-8. (A) composite rose diagram of slickenside strikes, and (B) equal area projection of poles to slickensided surfaces.

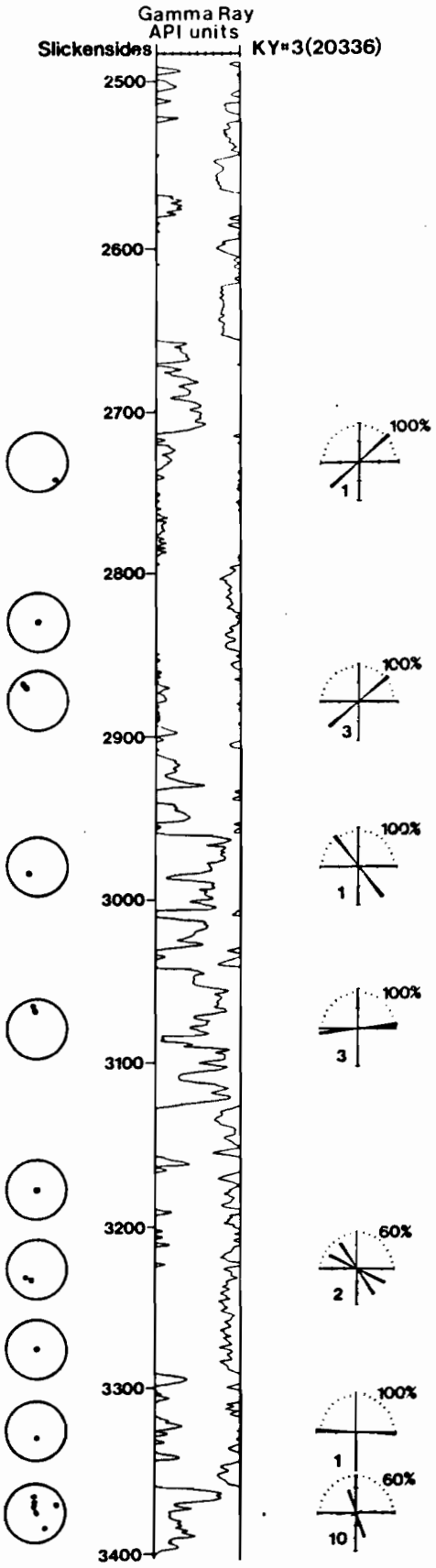

Figure L-9. Equal area projections of poles to slickensided surfaces and rose diagrams of slickenside strikes for approximately equal length intervals of the KY #3 (20336) core.

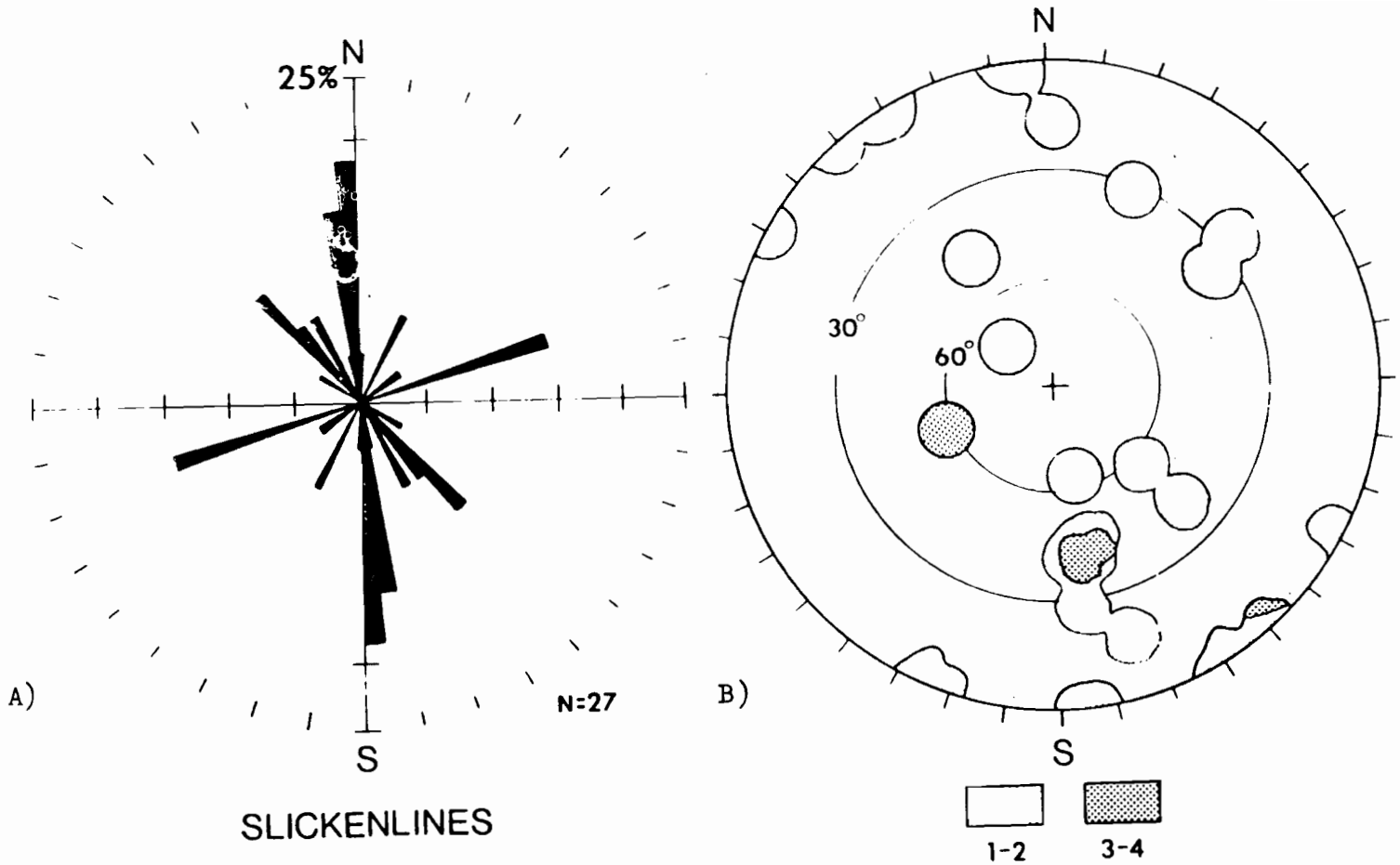

KY#3 (20336)

Figure L-10. (A) composite rose diagram of slickenline trends, and (B) equal area projection of slickenlines.

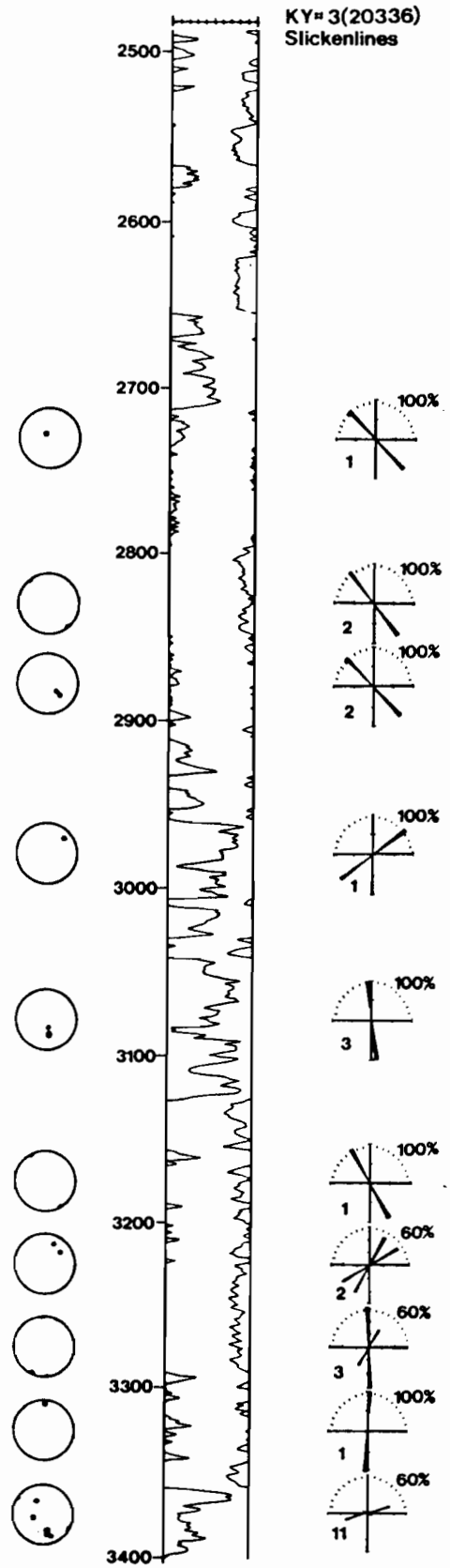

Figure L-11. Equal area projections of slickenlines and rose diagrams of slickenlines trends for approximately equal length intervals of the KY #3 (20336) core.

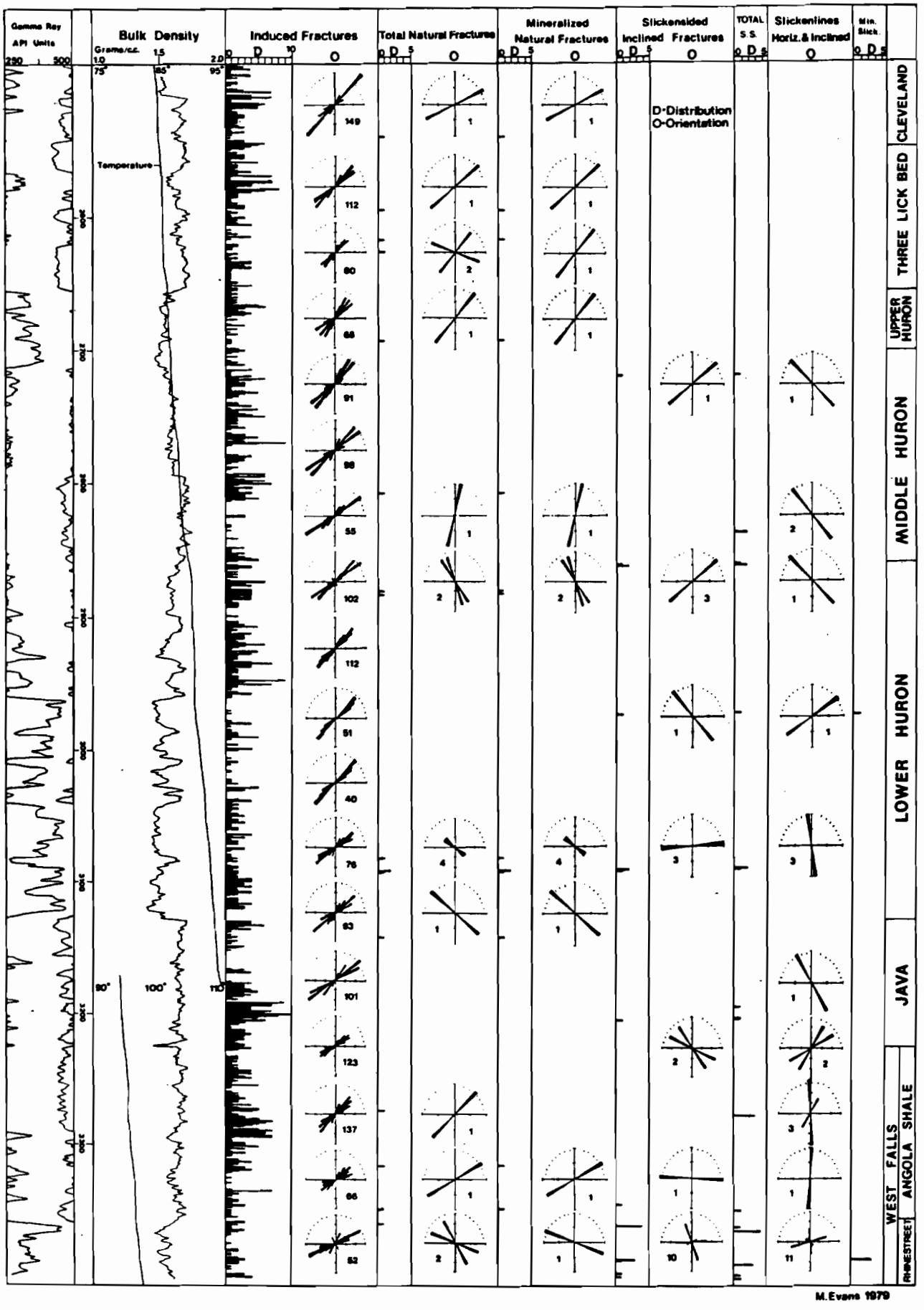

Figure L-12. Composite data sheet of fracture frequencies and orientations for all fracture types.

APPENDIX M: KY #4 (#3 R-S) CORE WELL

KY #4 (#3 R-S) CORE WELL

Location

The KY #4 (#3 R-S) core well is located in Johnson County, Kentucky, approximately 13 miles northwest of the town of Paintsville (figures 1 and M-1, table 1). The wellsite is in the Eastern Kentucky Fault System, about seven miles north of the east-west trending Irving-Paint Creek Fault. A total of 550 feet of the Devonian was cored, from 950'-1500' (figure M-12).

Production Data

A gas show, illustrated by a deviation of the temperature log (figure M-12), occurs in a zone of inclined unmineralized fractures at 1307'-1310'. Two intervals of the well were stimulated; 1294'-1382', in the Lower Huron Member, which had an initial open flow of 33 mcf/day after stimulation; and 1010'-1120', in the Cleveland Member and Three Lick Bed, which had an initial open flow of 52 mcf/day after stimulation (Yost, 1979, written communication).

Core-induced Fractures

Core-induced fractures are not common in this core, with only three petal fractures recorded in the Upper Huron Member (figure M-12). Disc fractures and torsion fractures are present, but rare. The core-induced fracture composite rose diagram (figure M-2) has two peaks. There is a 1.0% chance that the peaks at N55°-65°E and N77°E do not exist. The equal area projection of poles to core-induced fracture surfaces (figure M-2) has a single cluster corresponding to the northwest dipping petals. Although the sample is small (3) it

may still indicate the presence of a stress or rock fabric anisotropy in the rock around the KY #4 (#3R-S) well. This anisotropy may be related to the east to northeast trending maximum compressive stress present in most of eastern North America (Sbar and Sykes, 1973). The restriction of petal fractures to the Upper Huron Member may be related to the physical characteristics of the rock. No significant changes in orientation with depth can be determined (figure M-3).

Natural Fractures

Natural fractures in this core fall into two classes: 1) vertical, calcite filled fractures which probably formed before rock lithification, possibly as dessication cracks (figure M-4); and 2) inclined unmineralized fractures (figure M-5). Fractures of class 1 have a most unexpectedly consistent orientation, and occur only in the Cleveland Member and Middle Huron Member. Fractures in class 2 occur only in the Berea Sandstone and Lower Huron Member (figure M-12). Both fracture types have the same general northeast strike. The natural fracture composite rose diagram (figure M-6) has two peaks. There is a 1.0% chance that the peak at N60°-70°E does not exist, and a 10.0% chance that the peak at 47° E does not exist. The equal area projection of poles to natural fracture surfaces (figure M-6) has five clusters; four peripheral clusters corresponding to the vertical fractures in the two sets, and a cluster dipping 50°SW corresponding to the inclined fractures in the N60°-70°E set. Fracture orientations vary very little with depth or stratigraphy (figure M-7).

The two natural fracture sets parallel nearby faults. The prelithification (class 1) fractures may have formed in relation to

faulting in the area which stressed the sediments, thus producing oriented cracks that later filled with calcite. As lithification continued, the sediment and fractures were compacted, deforming the fracture and filling. The inclined fractures (class 2) may have also formed in relation to local faulting, or they may have formed under the same stresses which formed the core-induced fractures.

Slickensides and Slickenlines

Most of the slickensides in the core occur near the contact of the Berea Sandstone and the Cleveland Member (figure M-12); a few also occur near the base of the Lower Huron Member. The slickenside composite rose diagram (figure M-8) has no statistically significant peaks. A predominant N50°-90°E strike can be determined, however. The equal area projection of poles to slickensided surfaces (figure M-8) has three questionable clusters dipping 0°, 45°S, and 45°NW. Poles to slickensided surfaces tend to form a girdle across the plot, suggesting that the contact of the Berea Sandstone and Cleveland Member may be a poorly developed shear zone. In general, slickenside orientations are quite variable with depth (figure M-9).

The slickenline composite rose diagram (figure M-10) also shows a wide variety of trends. However, clusters on the equal area projection of slickenlines (figure M-10) tends to show three dominant trends; N40°W (two clusters, dipping 40°NW and 35°SE), N85°E (two clusters, dipping 0°W and 0°-50°E), and N5°W (cluster dipping 40°SW). The N40°W trending slickenlines are nearly orthogonal to the southern Appalachian trend and may have formed under tectonic compressive stresses directed from the southeast. The N5°W and N85°E sets are

orthogonal to nearby faults and probably formed as a result of compaction and adjustment of the rock after fault movement. The N40°W set occurs only in the Berea Sandstone and Cleveland Member, the N5°W set occurs only in the Berea Sandstone and Lower Huron Member, and the N85°E set occurs only in the Berea Sandstone (figure M-11).

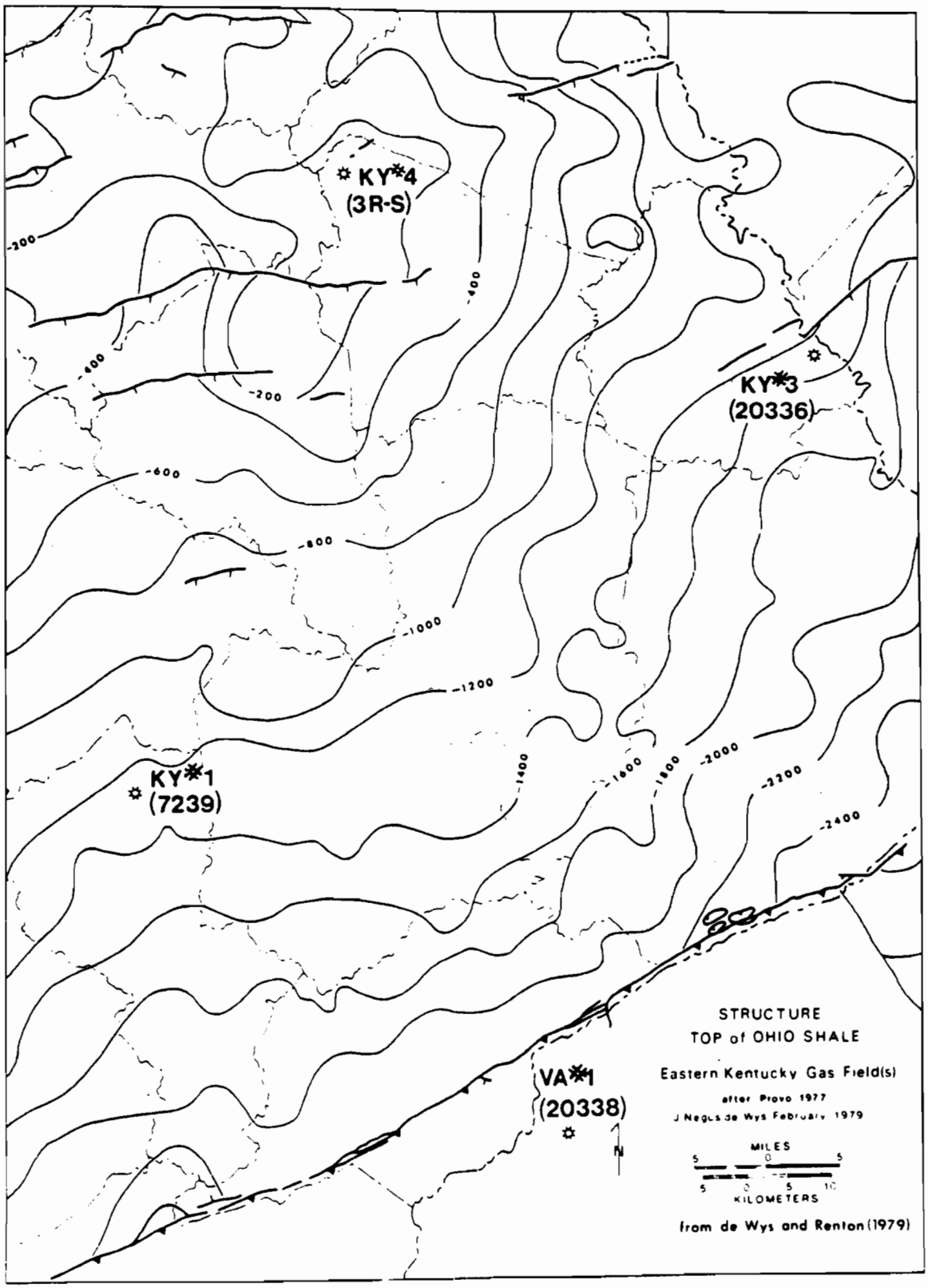

Figure M-1. Index map for the KY #4 (#3 R-S) core well

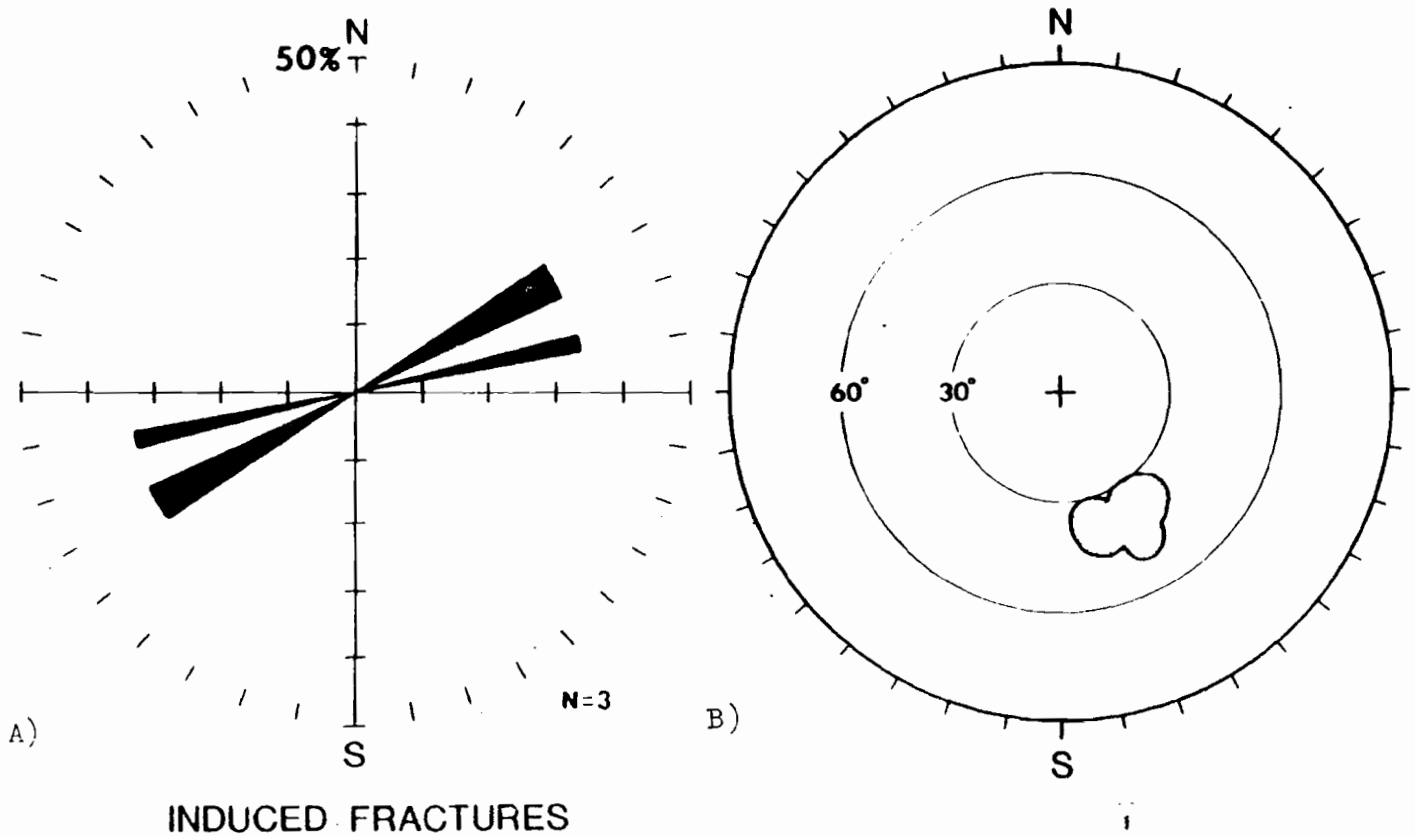

KY*4 (3R-S)

Figure M-2. (A) composite rose diagram of core-induced fracture strikes, and (B) equal area projection of poles to core-induced fracture surfaces

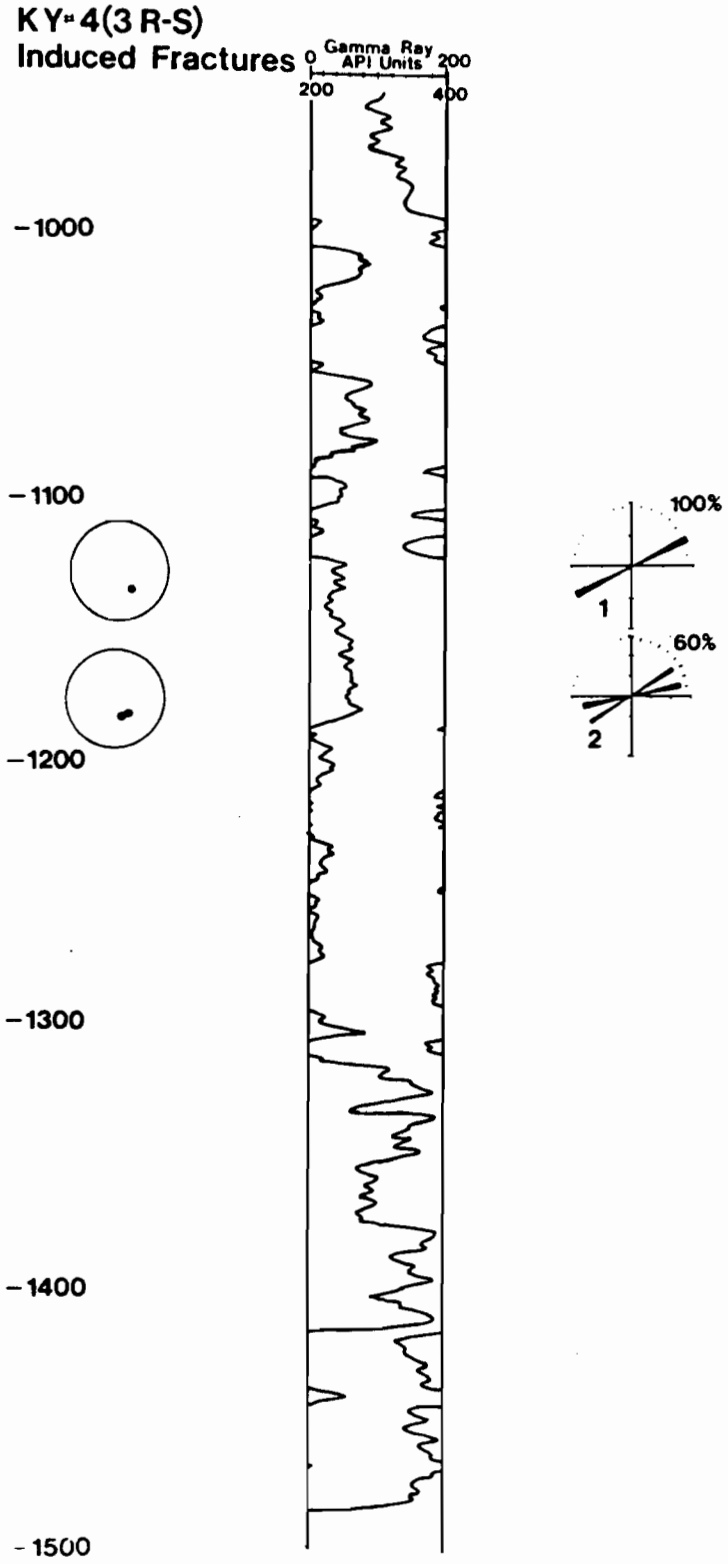

Figure M-3. Equal area projections of poles to core-induced fracture surfaces and rose diagrams of core-induced fracture strikes for approximately equal length intervals of the KY #4 (#3 R-S) core.

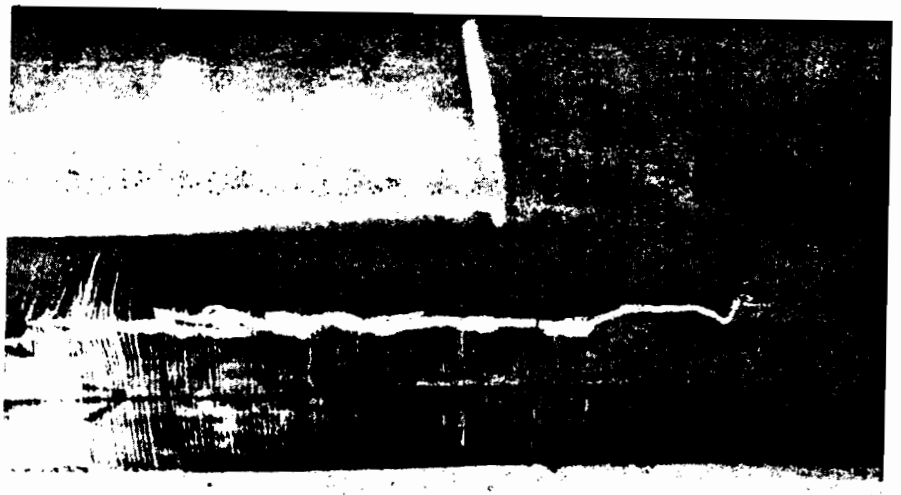

Figure M-4. Class 1 fracture - KY #4 (#3 R-S) core.

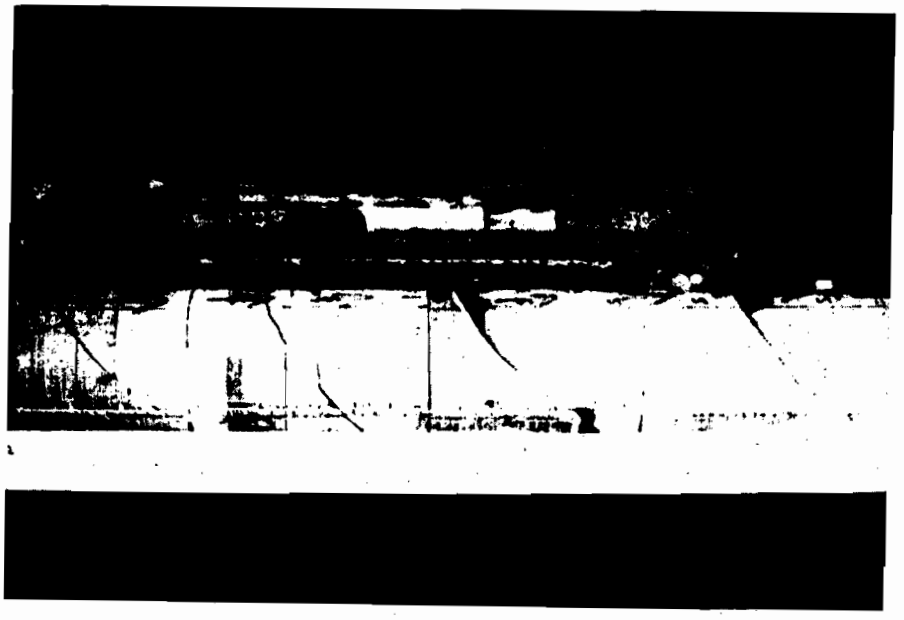

Figure M-5. Class 2 fracture - KY #4 (#3 R-S) core.

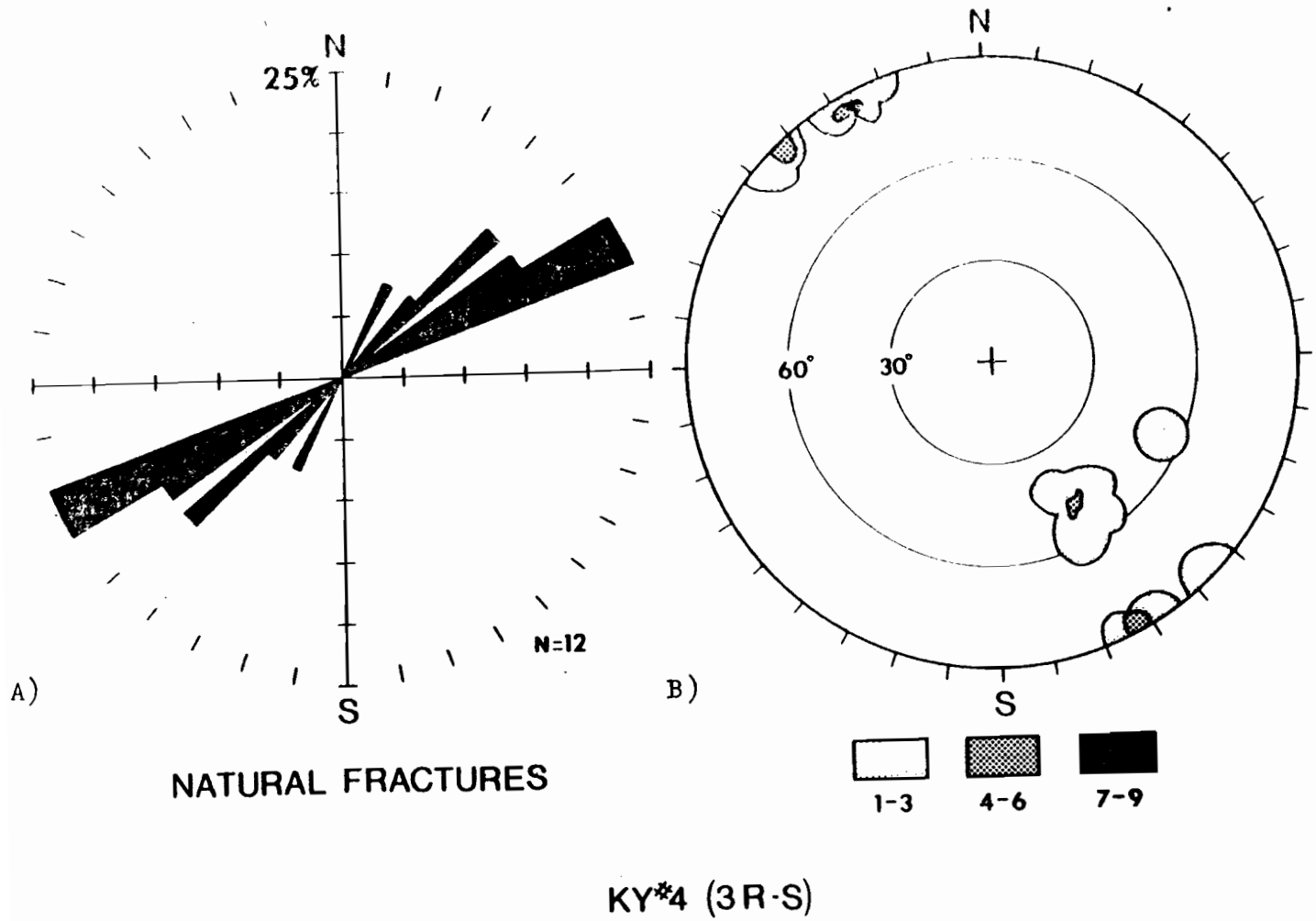

Figure M-6. (A) composite rose diagram of natural fracture strikes, and (B) equal area projection of poles to natural fracture surfaces

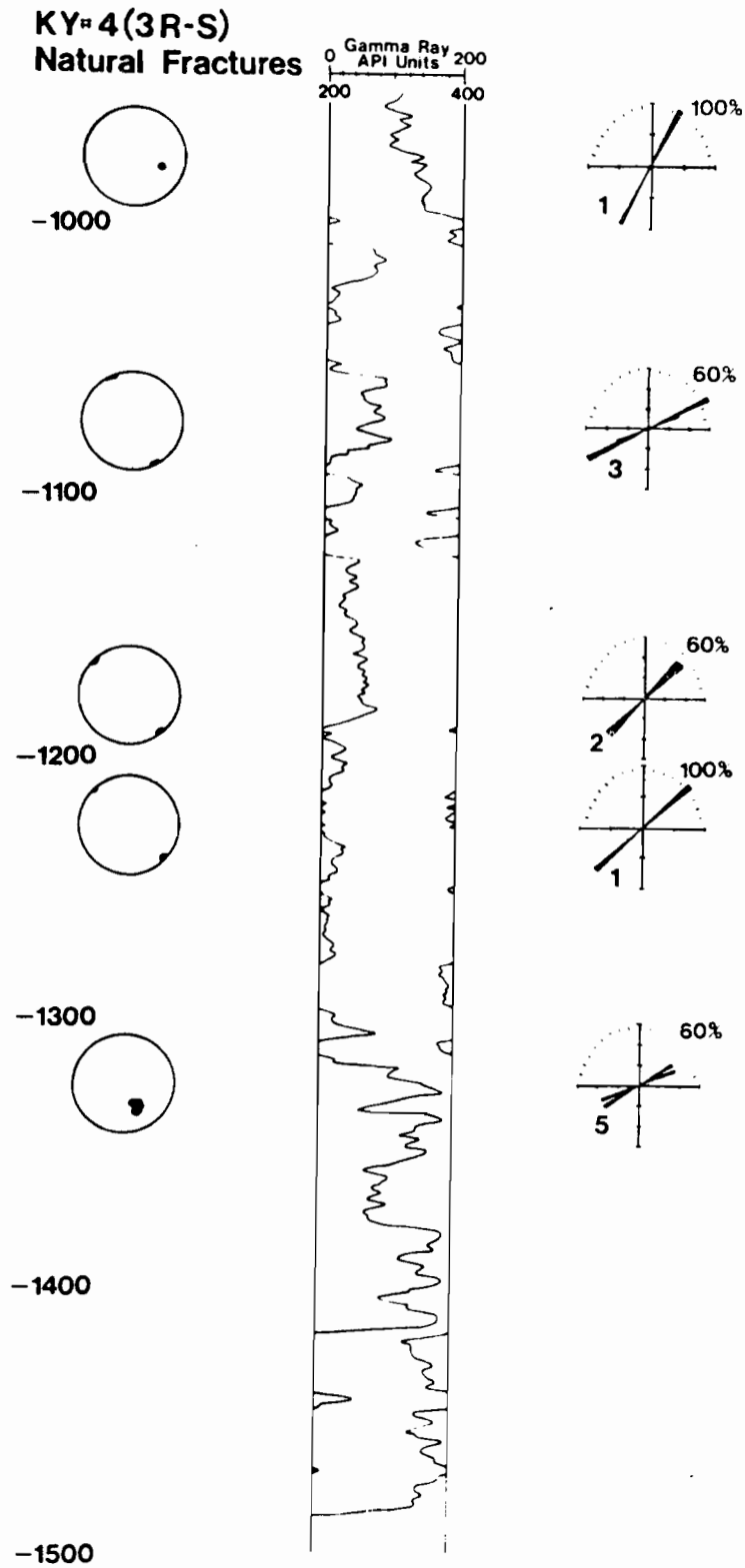

Figure M-7. Equal area projections of poles to natural fracture surfaces and rose diagrams of natural fracture strikes for approximately equal length intervals of the KY #4 (#3 R-S) core.

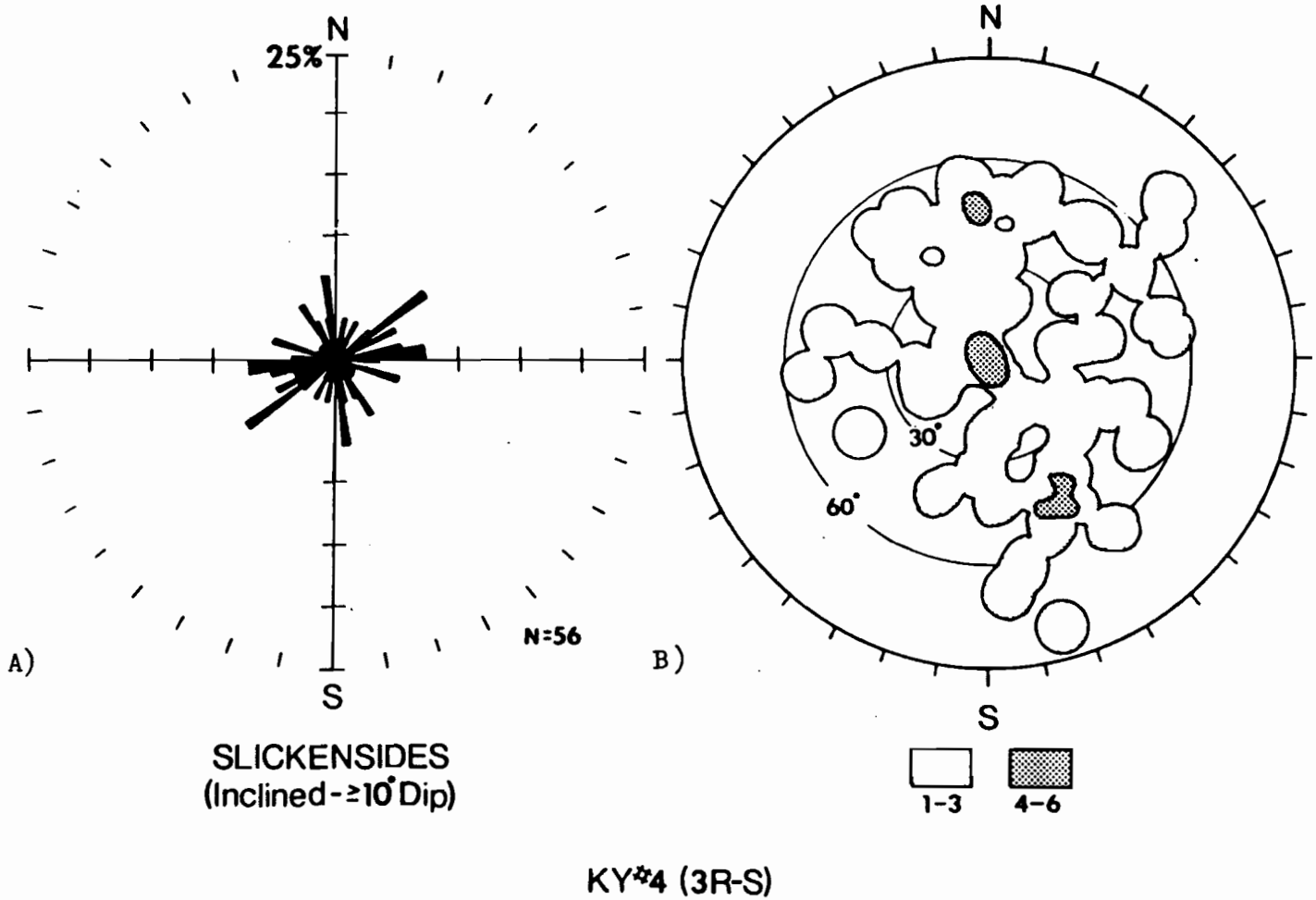

Figure M-8. (A) composite rose diagram of slickenside strikes, and (B) equal area projection of poles to slickensided surfaces.

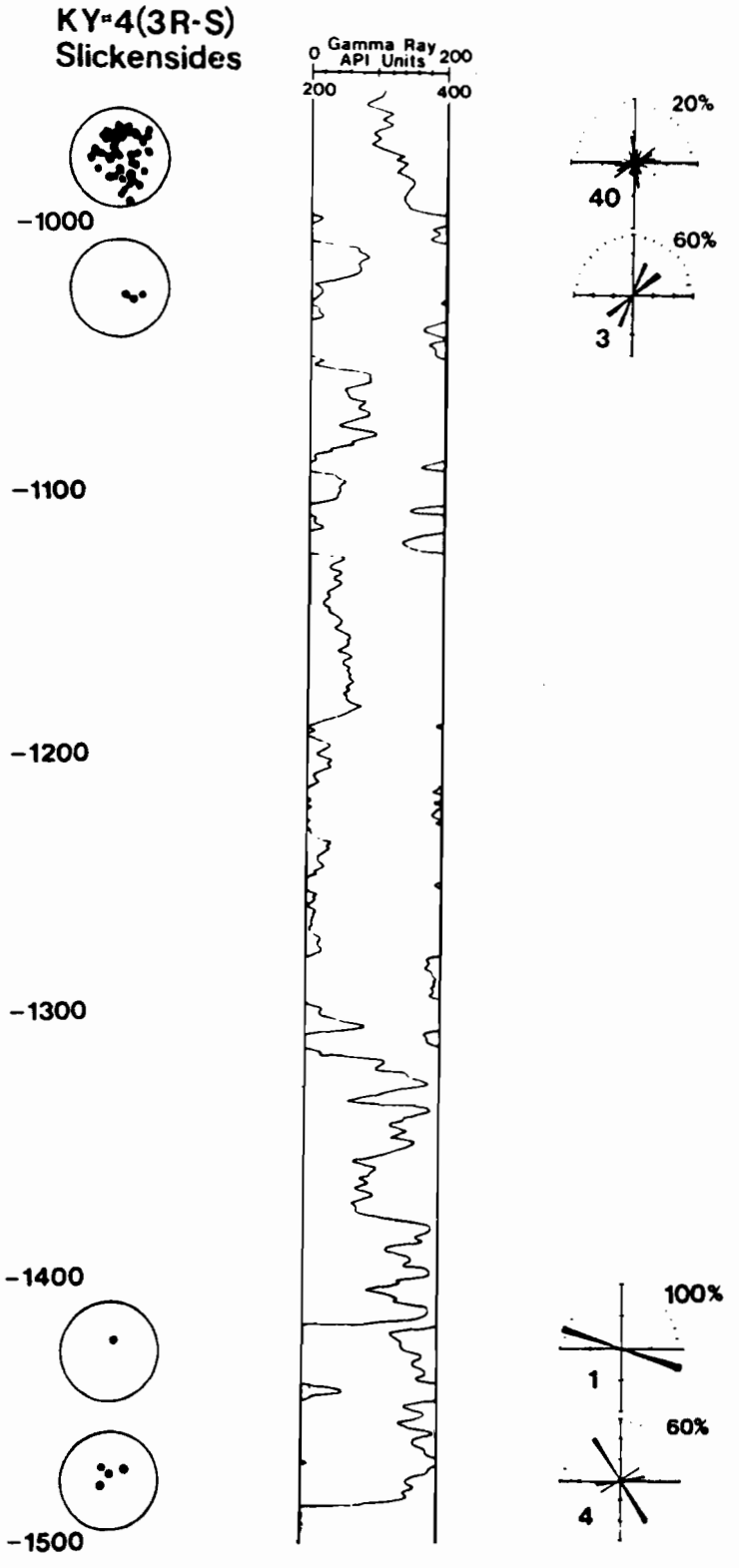

Figure M-9. Equal area projections of poles to slickensided surfaces and rose diagrams of slickenside strikes for approximately equal length intervals of the KY #4 (#3 R-S) core.

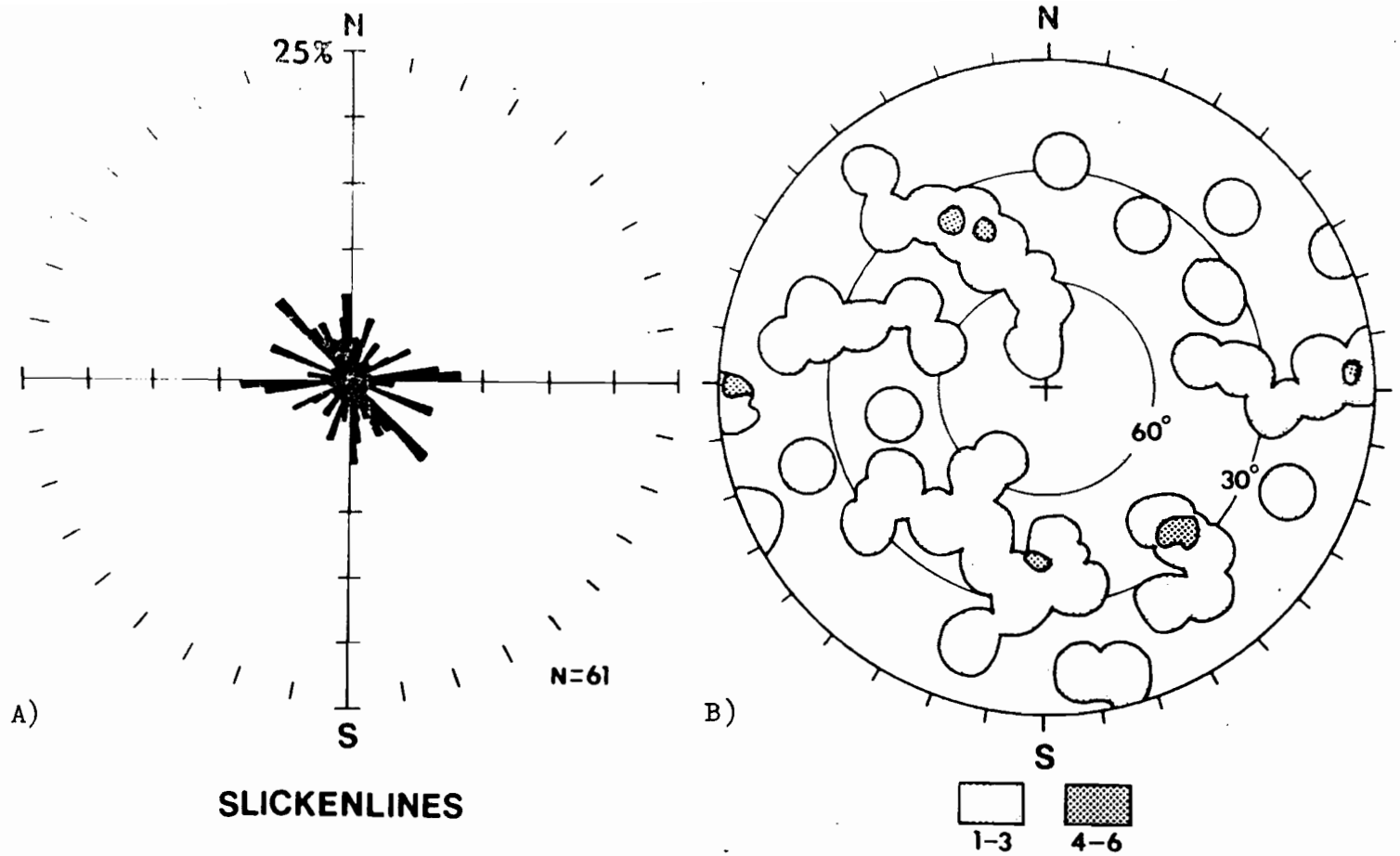

KY*4 (3R-S)

Figure M-10. (A) composite rose diagram of slickenline trends, and (B) equal area projection of slickenlines.

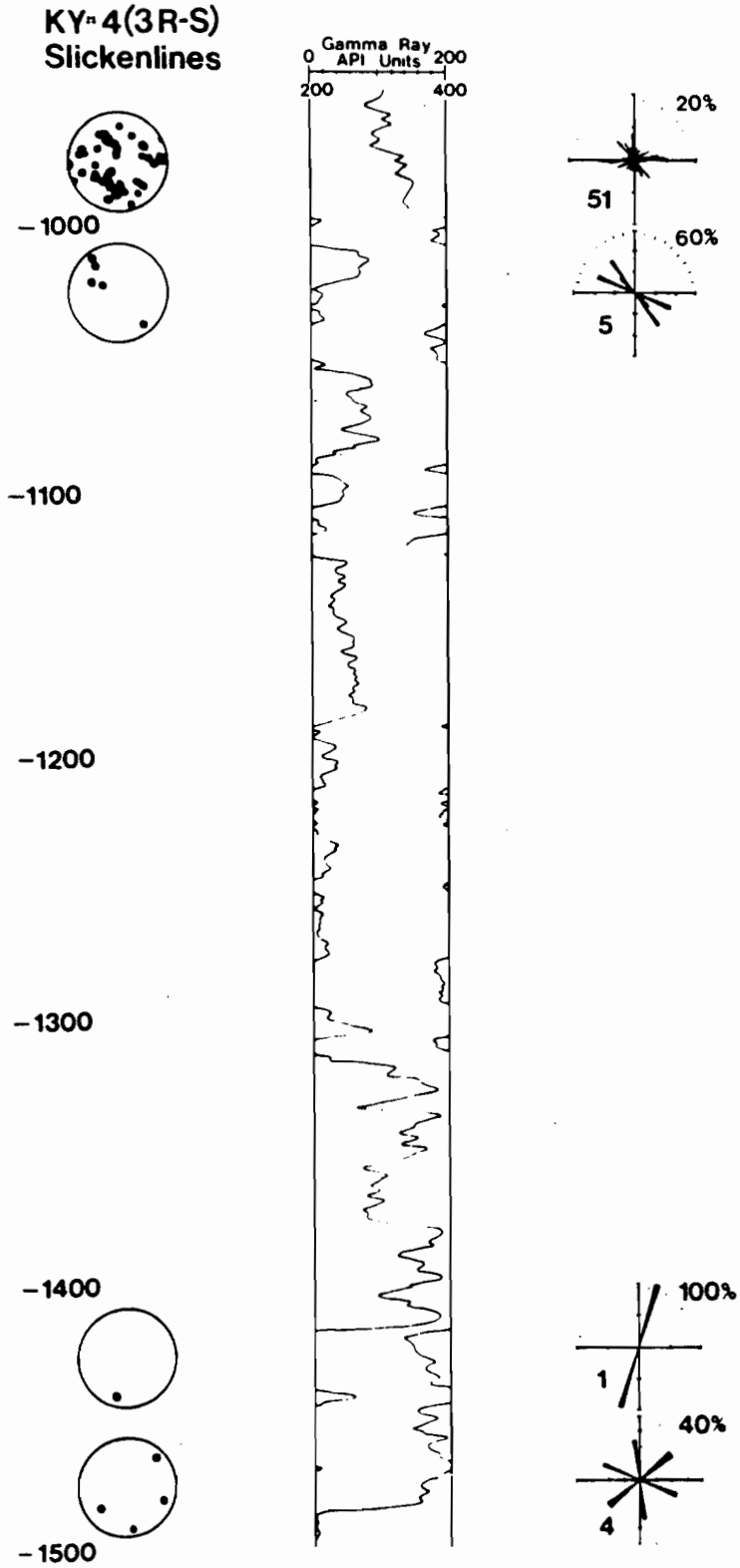

Figure M-11. Equal area projection of slickenlines and rose diagrams of slickenline trends for approximately equal length intervals of the KY #4 (#3 R-S) core.

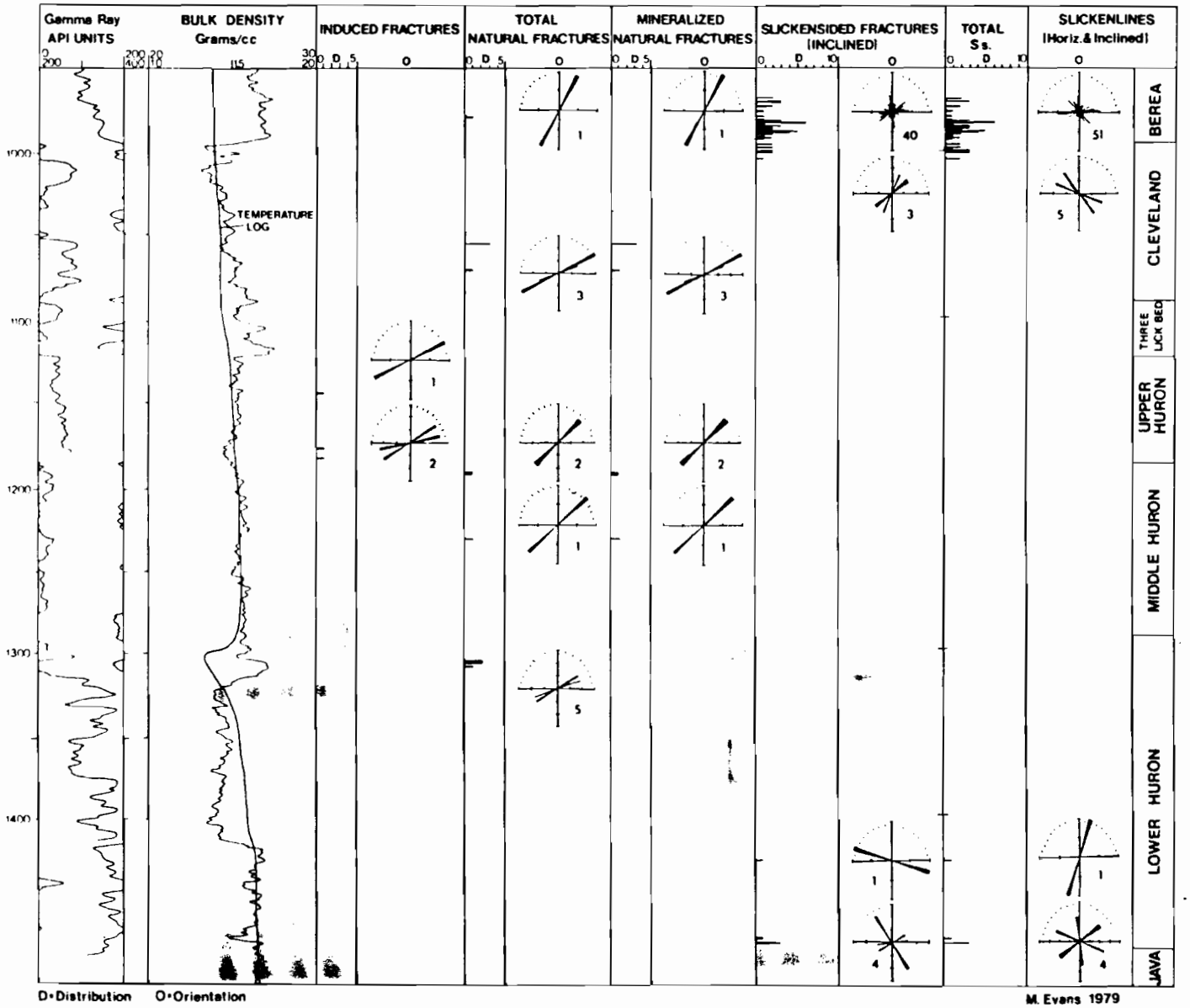

Figure M-12. Composite data sheet of fracture frequencies and orientations for all fracture types.

☆ U.S. GOVERNMENT PRINTING OFFICE: 1983-646-069/773